Atto-09 Home
Int'l Committee
Local Committee
Registration
Invited Talks
General Program
Scientific Program
Posters
Deadlines
Travel
Accommodations
Sponsors
Atto-07 (Dresden)
JRM Home

All Posters by Session

Thursday | Friday | Saturday

There is also a list of the short oral presentations, or you may search the posters.
This list is also available as an Acrobat *(pdf)* document.

Thursday

T01: "Streaking of shake-up ionization in helium"
Johannes Feist, Andreas Kaltenbäck, Stefan Nagele, Renate Pazourek, Emil Persson, Barry I. Schneider, Lee A. Collins, Joachim Burgdörfer

T02: "Elliptically polarized high-order harmonics from aligned molecules within the strong-field approximation"
Adam Etches, Christian Bruun Madsen, Lars Bojer Madsen

T03: "High harmonics generation using long wavelengths: scaling and scaled systems"
Gilles Doumy, Anne Marie March, Erik Power, Jonathan Wheeler, Chris Roedig, Emily Sistrunk, Fabrice Catoire, Karl Krushelnick, Pierre Agostini, Louis DiMauro

T04: "Modeling Attosecond Pulse Formation in Strongly Ionized Gaseous Media"
V. Tosa,1, K. Kovacs, R. Velotta, C. Altucci, K. T. Kim, and C. H. Nam

T05: "Benchmark experiment on H3+ in intense ultrashort laser pulses"
J. McKenna, A. M. Sayler, B. Gaire, Nora G. Johnson, K. D. Carnes, B. D. Esry and I. Ben-Itzhak

T06: "Ultrafast high-harmonic imaging of a chemical reaction"
H. J. W¨orner, J. B. Bertrand, P. B. Corkum and D. M. Villeneuve

T07: "Attosecond Electron Interferometry"
K. Klünder, M. Swoboda, M. Gisselbrecht, M. J. Dahlström, P. Johnsson, T. Remetter, J. Mauritsson, A. L'Huillier

T08: "Electron Wavepacket Interferences pointing to Holographic Imaging with Few Cycle Laser Pulses"
R. Gopal, A. Rudenko, K. Simeonidis, K.-U. Kühnel, M. Kurka, C. D Schröter, O. Herrwerth, Th.Uphues, M. Schultze, E. Goulielmakis, M. Uiberacker, D. Bauer, M. Lezius, R. Moshammer, M. F. Kling, J. Ullrich

T09: "Asymmetric dissociation of H2 and D2 by a two-color laser field"
D. Ray, S. De, H. Mashiko, I. Znakovskaya, F. He, U. Thumm, G.G.Paulus, M. Kling, I. Litvinyuk, and C.L. Cocke

T10: "Intensity dependence of strong field double ionization mechanisms of diatomic molecules: from field-assisted electron recollision to recollision-assisted field ionization"
Agapi Emmanouilidou

T11: "Time-resolved core-hole decay and sideband structure in laser-assisted photoemission from metal surfaces"
C.-H. Zhang, U. Thumm

T12: "Time-resolved Coulomb explosion imaging of CO ultrafast dynamics using fewcycle IR and EUV laser pulses"
A. S. Alnaser, I. Bocharova, K. Singh, C. Wei, M. Kling, C. L. Cocke, I. V. Litvinyuk

T13: "Ultrashort IR-visible- and VUV-pulse generation for attosecond pump-probe experiments on atoms and molecules using a reaction microscope"
K. Simeonidis, R. Gopal, H. Rietz, A. Sperl and J. Ullrich

T14: "Magnetic-bottle electron energy spectrometer for measuring 25 as pulses"
Kun Zhao, Chao Wang, Ximao Feng, Steve Gilbertson, Sabih D. Khan, and Zenghu Chang

T15: "Interferometric Delay Control in Attosecond Streaking Experiments"
Michael Chini, He Wang, Hiroki Mashiko, Shouyuan Chen, Chenxia Yun, Steve Gilbertson, Zenghu Chang

T16: "Ab Initio Modeling of Attosecond Streaking Measurements"
M. Korbman, Y. Komninos, T. Mercouris, C.A. Nicolaides, F. Krausz, V.S. Yakovlev

T17 O08: "Attosecond Hard X-Ray Scattering Spectroscopy"
G. L. Yudin, D. I. Bondar, S. Patchkovskii, P. B. Corkum, A. D. Bandrauk

T18: "Phase-matching of high-order harmonic generation in a semi-infinite gas cell geometry"
Daniel S. Steingrube, Tobias Vockerodt, Emilia Schulz, Uwe Morgner, and Milutin Kovacev

T19: "Wavelength Scaling of High Harmonic Generation Efficiency"
A. D. Shiner, C. Trallero-Herrero, N. Kajumba, H.-C Bandulet, D. Comtois, F. Légaré, M. Gigèure, J-C. Kieffer, P. B. Corkum, D. M. Villeneuve

T20: "Femtosecond enhancement cavities for high repetition rate HHG"
D. C. Yost, Jun Ye

T21: "Highly stable, few-cycle, 2.2-μm optical parametric chirped pulse amplifier"
Shu-Wei Huang, Jeffrey Moses, Kyung-Han Hong, Edilson L. Falcão-Filho, Andrew Benedick, Jeremy Bolger, Benjamin Eggleton, Franz X. Kärtner

T22: "Temperature feedback control for long-term carrier-envelope phase locking"
Shouyuan Chen, Chenxia Yun, He Wang, Michael Chini, and Zenghu Chang

T23: "Fractional Instability of a Phase Stabilized Carbon Nanotube Fiber Laser Frequency Comb"
Jinkang Lim, Kevin Knabe, Yishan Wang, Rodrigo Amezcua-Correa, François Couny, Philip S. Light, Fetah Benabid, Jonathan C. Knight, Kristan L. Corwin, Jeffrey W. Nicholson, Brian R. Washburn

T24: "Coupling between Energy and Carrier-Envelope Phase in Hollow-Core Fiber based f-to-2f Interferometers"
He Wang, Michael Chini, Eric Moon, Hiroki Mashiko, and Zenghu Chang

T25: "An isolated short attosecond pulse produced by using intense few-cycle chirped laser and an ultraviolet attosecond pulse"
Xiao-Xin Zhou, Song-Feng Zhao, Peng-Cheng Li, Zhangjin Chen

T26: "Multiple Ionic Channel Formulation for Strong Field Single Ionization of Multielectron Targets"
Michael Spanner, Serguei Patchkovskii, Julien Bertrand, and Hans Jakob Worner

T27: "Ultrafast Molecular Dynamics Probed Using Strong Field Ionization"
Wen Li; Vandana Sharma; Craig Hogle; Agnieszka Jaron-Becker; Andreas Becker; Henry Kapteyn, Margaret Murnane

T28: "Single Molecule Laser Induced Nuclear Fusion, LINF, In Superintense Laser Fields"
Andre D. Bandrauk, Gennady K. Paramonov

T29 O06: "Counterintuitive angular shifts in the photoelectron momentum distribution for atoms in strong few-cycle circularly laser pulses"
C. P. J. Martiny, M. Abu-samha, L. B. Madsen

T30: "Manipulating the torsion of molecules by strong laser pulses"
C. B. Madsen, L. B. Madsen, S. S. Viftrup, M. P. Johansson, T. B. Poulsen, L. Holmegaard, V. Kumarappan, K. A. Jørgensen, H. Stapelfeldt

T31: "The onset of asymmetry in electron angular distributions for dissociative photoionization of H2 by ultrashort xuv laser pulses"
J. F. Perez-Torres, F. Morales, J. L. Sanz-Vicario and F. Martýn

T32: "Electron localization following attosecond molecular photionization"
F. Kelkensberg, G. Sansone, M.F. Kling, W. Siu, O. Ghafur, P. Johnsson, M. Swoboda, E. Benedetti, F. Ferrari, F. Lépine, S. Zherebtsov, I. Znakovskaya, M. Yu. Ivanov, J.F. Pérez, F. Morales, J.L. Sanz-Vicario, F. Martin, M. Nisoli, M.J.J. Vrakking

T33: "Time-Resolved Molecular Fragmentation at FLASH"
Jiang, Rudenko, Kurka, Kühnel, Toppin, Herrwerth, Lezius, Kling, Foucar, Schöffler, Cole, Ullrich, Neumann, Dörner, Pérez-Torres, Plésiat, Martín, Cassimi, Düsterer, Treusch, Gensch, Schröter, Moshammer, Ullrich

T34: "Intense-Field Ionization of Cyclic Hydrocarbon Molecules Measured with Spatial Resolution of Focal Ion Distributions"
Tim Scarborough, James Strohaber, David Foote, and Cornelis Uiterwaal

T35 O09: "Electron localization in molecular fragmentation with CEP stabilized laser pulses"
Bettina Fischer, Manuel Kremer, Bernold Feuerstein, Vitor L.B. de Jesus, Artem Rudenko, Claus Dieter Schröter, Robert Moshammer, Joachim Ullrich

T36: "Vibrationally cold CO2+ probed by intense femtosecond laser pulses"
J. McKenna, A. M. Sayler, B. Gaire, Nora G. Johnson, M. Zohrabi, F. Anis, U. Lev, K. D. Carnes, B. D. Esry, and I. Ben-Itzhak

T37: "Electron release dynamics in double ionization of Ar and Ne by elliptically polarized laser pulses"
Adrian Pfeiffer, C. Cirelli, M. Smolarski, R. Dörner, U. Keller

T38 O03: "Auger decay in krypton induced by attosecond pulse trains and twin pulses"
Christian Buth, Kenneth J. Schafer

T39: "Photoelectron emission from atoms by ultra-short pulses: Impulse Coulomb-Volkov description"
M.S. Gravielle, D.G. Arbó, J.E. Miraglia

T40: "Electron emission from metal surfaces by ultra-short pulses"
M. N. Faraggi, I. Aldazabal, M. S. Gravielle, A. Arnau, V. M. Silkin

T41: "Interference effects in laser assisted photo-ionization of atoms"
Pablo A. Macri, Denise Bendersky

T42: "Acceleration of neutral atoms in intense short laser"
U. Eichmann, T. Nubbemeyer, H. Rottke , and W. Sandner

Friday

F01: "Extending upper limit of laser pulse duration for generating single attosecond pulses"
Ximao Feng, Steve Gilbertson, Hiroki Mashiko, He Wang, Sabih D. Khan, Michael Chini, Zenghu Chang

F02: "Electron Localization and Multiple Ionization Bursts in H2+ within a Half Cycle of Near-Infrared Laser Light"
Norio Takemoto, Andreas Becker

F03: "Wavelength Scaling in High Harmonic Tomographic Imaging"
Jonathan A. Wheeler,Gilles Doumy,Terry Miller,Pierre Agostini,Louis F. DiMauro

F04: "Femtosecond Dynamics and Multiphoton Ionization driven with an Intense High Order Harmonic Source"
J. van Tilborg, T. K. Allison, T. W. Wright, M. P. Hertlein, Y. Liu, H. Merdji, R. W. Falcone, A. Belkacem

F05: "High Harmonic Generation from Multiple Orbitals in N2"
Brian K. McFarland, Joseph P. Farrell, Philip H. Bucksbaum, and Markus Gühr

F06: "High accuracy, real time, single-shot measurement of absolute carrier-envelope phase and pulse duration for few-cycle laser pulses"
A. Max Sayler, T. Rathje, J.V. Hernandez, W. Müller, B.D. Esry, and G.G. Paulus

F07: "Analytic Formulas for High-Order Harmonic Generation"
M.V. Frolov, N.L. Manakov, T.S. Sarantseva, Anthony F. Starace

F08: "Zero Photon Dissociation of H2+ in Few Cycle Pulses"
B. Gaire, J. McKenna, A. M. Sayler, M. Zohrabi, Nora G. Johnson, F. Anis, J.J. Hua, K.D. Carnes, B.D. Esry, and I. Ben-Itzhak

F09: "Theoretical study of Carrier-envelope phase effects from three-dimensional momentum distribution of H2+ dissociation by ultrashort laser pulses"
Fatima Anis, B. D. Esry

F10: "Two-source double-slit interference in angle-resolved high-energy above-threshold ionization spectra of diatoms"
M. Okunishi, R. Itaya, K. Shimada, G. Prumper, K. Ueda, M. Busuladzic, A. Gazibegovi Busuladzic, D. B. Milosevic, W. Becker

F11: "Ultrafast Science and Development at the Astra-Artemis Facility"
Turcu, Springate, Froud, Collier, Marangos, Tisch, La Porte, Siegel, El-Taha, Kajumba, Brugnera, Procino, Newell, Williams, Greenwood, Calvert, Bryan, Cavalleri, Dhesi, Underwood, Mercer, Gabrielsen, Cogdell, Poletto, Villoresi, Frassetto, Bonora, Roper

F12: "Inner and Outer Ionization of Atomic Clusters by an Intense Attosecond Laser Pulse"
A.V. Gets and V.P. Krainov

F13: "Long-term CEP stabilization of a high-power femtosecond laser by the direct locking method"
Jae-hwan Lee, Yong Soo Lee, Juyun Park, Tae Jun Yu, Chang Hee Nam

F14: "Attosecond control of electron dynamics in enhanced nanolocalized fields"
S. Zherebtsov, I. Znakovskaya, I. Ahmad, A. Wirth, O. Herrwerth, S. Trushin, V. Pervak, S. Karsch, M. Stockman, F. Krausz, M.F. Kling, J. Plenge, E. Antonsson, B. Langer, C. Graf, E. Rühl, M.J.J. Vrakking, Th. Fennel

F15: "10 kHz Accuracy Spectroscopy in Acetylene-filled Hollow-core Kagome Fiber as Measured with

Optical Frequency Combs"
Kevin Knabe, Andrew Jones, Jinkang Lim, Rajesh Thapa, Karl A. Tillman, Shun Wu, François Couny, Phillip S. Light, Natalie Wheeler, Fetah Benabid, Jeffrey W. Nicholson, Brian R. Washburn, and Kristan L. Corwin

F16 O01: "Controlling the Carrier-Envelope Phase of Single-Cycle Waveforms Synthesized from Raman Generated Frequency Combs"
Zhi-Ming Hsieh, Chien-Jen Lai, Han-Sung Chan, Sih-Ying Wu, Chao-Kuei Lee, Wei-Jan Chen, Ci-Ling Pan, Fu-Goul Yee, A. H. Kung

F17: "Generation of 3.7-fs, 1.2-mJ pulses using a hollow-fiber pulse compressor"
Juyun Park, Jae-hwan Lee, Luu Tran Trung, Chang Hee Nam

F18 O04: "Generation of high-order harmonics with ultra-short pulses from filamentation"
E. Schulz, D. S. Steingrube, T. Vockerodt, U. Morgner, and M. Kovacev

F19: "Reflective and Diffractive Optics for Coherent Ultrafast Radiation at Extreme Ultraviolet and Soft X-Ray Wavelengths"
Yanwei Liu, Andrew L. Aquila, Farhad Salmassi, Anne Sakdinawat, Eric Gullikson

F20: "The Robustness of Attosecond Streaking Measurements"
Justin Gagnon, Vladislav S. Yakovlev

F21: "Strong-Field Modulated Diffraction Effects in the Correlated Electron-Nuclear Motion in Dissociating H+"
Feng He, Andreas Beckery, Uwe Thumm

F22: "Retrieval of target photorecombination cross sections from high-order harmonics generated in a macroscopic medium"
Cheng Jin, Anh-Thu Le, C. D. Lin

F23: "Accurate Retrieval of Structural Information of Atoms and Molecules from Laser-Induced Photoelectron and High-Order Harmonic Spectra by Intense Laser Pulses"
Toru Morishita, Toshihito Umegaki, Shinichi Watanabe, Oleg.I. Tolstikhin, Anh-Thu Le, Zhangjin Chen, C.-D. Lin

F24: "High-order harmonic generation in fullerenes"
A. Jaron-Becker, M. F. Ciappina, and A. Becker

F25: "Extreme ultraviolet (XUV) pulse shaping with aligned molecules"
Zhinan Zeng, Ruxin Li, Zhizhan Xu

F26: "Strong field dynamics with ultrashort electron wave packet replicas"
P. Riviere, O. Uhden, U. Saalmann and J.-M. Rost

F27: "Secondary electron cascade in attosecond photoelectron spectroscopy from metals"
Jan Conrad Baggesen and Lars Bojer Madsen

F28: "Monte Carlo wave packet theory of dissociative double ionization"
Henriette Astrup Leth, Lars Bojer Madsen and Klaus Mlmer

F29: "Analytic Theory of Few-Cycle XUV Attosecond Pulse Photoionization of Atoms"
E.A. Pronin, M.V. Frolov, N.L. Manakov, Anthony F. Starace

F30: "Angle-resolved high-order above-threshold ionization spectra of inert gases in the low-frequency approximation"
D. B. Milosevic, A. Cerkic, B. Fetic, E. Hasovic, and W. Becker

F31: "Amplitude and phase spectroscopy of attosecond electron wave packets"
Kyung Taec Kim, Dong Hyuk Ko, Juyun Park, Chang Hee Nam and Jongmin Lee

F32: "Polarization Characterization of High Harmonic Generation from Transiently Aligned Molecules"
Xibin Zhou, Robynne Lock, Henry Kapteyn, and Margaret Murnane

F33: "Angular distribution of high-order harmonic generation from aligned molecules"
Peng Liu, Zhinan Zeng, Pengfei Yu, Ruxin Li , Zhizhan Xu

F34: "A new test of optical tunnel ionization"
L Arissian, C Smeenk, C Trallero, P B Corkum

F35: "Angular dependence of the strong-field ionization in randomly oriented hydrogen molecules"
Maia Magrakvelidze, Feng He, Sankar De, Irina Bocharova, Dipanwita Ray,Uwe Thumm and I.V. Litvinyuk

F36 O05: "Towards Disentangling High Harmonic Generation: Multiple Active Electrons in Strong Field Ionization of Polyatomic Molecules"
Arjan Gijsbertsen, Andrey E. Boguslavskiy, Jochen Mikosch, Michael Spanner, Niklas Gador, Marc J. J. Vrakking, Olga Smirnova, Serguei Patchkovskii, Misha Y. Ivanov, and Albert Stolow

F37: "High-Harmonic Generation in Polyatomic Molecules"
M. C. H. Wong, J.-P. Brichta, V. R. Bhardwaj

F38: "Effects of laser pulse duration and intensity on Coulomb explosion of CO2: signatures of charge-resonance enhanced ionization"
Igor V. Litvinyuk, Irina Bocharova, Joseph Sanderson, Jean-Paul Brichta, Jean-Claude Kieffer, François Légaré

F39: "Dynamic field-free orientation of polar molecules by intense two-color femtosecond laser pulses"
Sankar De, Dipanwita Ray, Irina Znakovskaya, Fatima Anis, Nora G. Johnson, Irina Bocharova, Maia Magrakvelidze, B. D. Esry, C. L. Cocke, Matthias F. Kling and Igor V. Litvinyuk

F40: "Controlling Asymmetric Coulomb Explosion Using 2-Color Fields"
K. J. Betsch, D. W. Pinkham, R. R. Jones

F41: "Time-resolved laser Coulomb explosion imaging of ultrafast molecular dynamics induced in N2, O2 and CO by interaction with intense laser field"
Irina Bocharova, Sankar De, Dipanwita Ray, Maia Magrakvelidze, Uwe Thumm, Lew Cocke, Ali Alnaser, Igor V Litvinyuk

F42: "Molecular Frame High Harmonic Dipole Amplitude and Phase Measurements"
Julien B. Bertrand, Hans Jakob Wörner, David M. Villeneuve, Paul B. Corkum

F43 O07: "Attosecond Transient Absorption of High Order Harmonics in Helium"
Mirko Holler, Florian Schapper, Johan Mauritsson, Kenneth J. Schafer, Lukas Gallmann and Ursula Keller

F44 O02: "Ultrafast electronic dynamics in Helium nanodroplets studied by femtosecond time-resolved EUV photoelectron imaging"
Oliver Gessner, Oleg Kornilov, Stephen R. Leone, and Daniel M. Neumark

F45: "Direct Determination of Spatial Electric Field Variations"
Steve Gilbertson, Ximao Feng, Sabih Khan, Michael Chini, He Wang, Hiroki Mashiko, and Zenghu Chang

F46: "Carrier-envelope phase control and stabilization by an acousto-optic programmable dispersive filter"
N. Forget, L. Canova, X. Chen , A. Jullien and R. Lopez-Martens

F47: "Carrier-envelope phase stabilization of a high-power regenerative amplifier"
Fraser Turner, Andrei Naumov, Chengquan Li, Alan Fry

Saturday

S01: "A robust all-non-optical method for the complete characterization of single-shot few-cycle laser pulses"
Zhangjin Chen, T. Wittmanny, C. D. Lin

S02: "Chirp-controlled polarization gating for isolated attosecond pulse generation"
Florian Schapper, Mirko Holler, Lukas Gallmann, Ursula Keller

S03: "Generation of continuum harmonic spectrum using multi-cycle two-color infrared laser fields"
Eiji J. Takahashi, Pengfei Lan, and Katsumi Midorikawa

S04: "Control of Electron Localization Using XUV and IR pulses"
Kamal P. Singh, W. Cao , P. Ranitovic, S. De, D. Ray, H. Mashiko, S. Chen, F. He, A. Becker, U. Thumm, I. Litvinyuk, C. L. Cocke

S05: "High Harmonic Generation seeded by a XUV pulse train"
F. Kelkensberg, G. Gademann, W. Siu, P. Johnsson, M.J.J. Vrakking

S06: "Mapping attosecond electron wavepacket motion in a molecule by using two-color laser pulses"
Hiromichi Niikura, D. M. Villeneuve, and P. B. Corkum

S07: "Attosecond chirp-encoded dynamics of light nuclei"
S. Haessler, W. Boutu, S. Weber, J. Caillat, R. Taieb, A. Maquet, P. Brege, B .Carre, P. Salieres

S08: "Atomic wavefunctions probed through strong field light-matter interactions"
D. Shafir, Y. Mairesse, J. Higuet, B. Fabre, E. Mével, E. Constant, D. M. Villeneuve, P. B. Corkum, N. Dudovich

S09: "High order harmonic generation with mid-infrared driven pulses"
Han Xu, Hui Xiong, Yuxi Fu, Jinping Yao, Bin Zeng, Wei Chu, Ya Cheng, Zhizhan Xu

S10: "High Harmonic Generation using 1425 nm sub-3 cycles laser pulses"
F. Légaré, B. E. Schmidt, A. D. Shiner, C. Trallero, H. Worner, M. Giguère, P. B. Corkum, J-C. Kieffer, D. M. Villeneuve

S11: "Quantum phase- and population-control in a vibrational wavepacket"
W. A. Bryan, C. R. Calvert, R. B. King, J. Nemeth, J. B. Greenwood, J. D. Alexander, E. L. Springate, C. A. Froud, I. C. E. Turcu, I. D. Williams, W. R. Newell

S13: "Generation of continuum XUV radiation by CE-phase stabilized 5-fs laser pulse"
H. Teng, C.X. Yun, H.H. Han, J.F. Zhu, X. Zhong, Z.Y. Wei

S14: "Statistical Noise in Attosecond Pulse Retrieval"
Sabih D. Khan, Michael Chini, He Wang, Steve Gilbertson, Ximao Feng, Zenghu Chang

S15: "Generation of XUV continuum in the plateau region of high-order harmonics driven with 7fs/800nm laser pulses"
Yinghui Zheng, Zhinan Zeng, Hui Xiong, Yan Peng, Xuan Yang, Heping Zeng, Ruxin Li, Zhizhan Xu

S16: "Practical Issues of Retrieving Isolated Attosecond Pulse from CRAB"
He Wang, Michael Chini, Sabih D. Khan, and Zenghu Chang

S17: "Accurate Retrieval of Satellite Pulses of Single Isolated Attosecond Pulses"
Michael Chini, He Wang, Sabih D. Khan, Shouyuan Chen, Zenghu Chang

S18: "Strong-field Below Threshold Harmonics"
Jennifer Tate, Kenneth Schafer, Mette Gaarde

S19: "Carrier-Envelop Offset Frequency Linewidth Narrowing Using an Intracavity Spatial Filter"
Karl A. Tillman, Brian R. Washburn, and Kristan L. Corwin

S20: "Conversion efficiency and scaling for high harmonic generation: an analytical approach"
Edilson L. Falcão-Filho, V. M. Gkortsas, Ariel Gordon and Franz X. Kärtner

S21: "Generation of CE Phase Stabilized 5 fs, 0.5 mJ, Pulses from Adaptive Phase Modulator"
He Wang, Yi Wu, Michael Chini, Hiroki Mashiko and Zenghu Chang

S22 O10: "Probing Doubly Excited Helium with Isolated Attosecond Pulses"
Steve Gilbertson, Ximao Feng, Sabih Khan, Michael Chini, He Wang, and Zenghu Chang

S23: "Double Ionization of Helium Atom in Combined Near-infrared and XUV Pulses"
Shaohao Chen, Andreas Becker

S24: "Multi-color attosecond control of single ionization"
J. V. Hernandez, B. D. Esry

S25: "Attosecond photoionization of a coherent superposition of bound and dissociative molecular states: effect of nuclear motion"
Szczepan Chelkowski, Andre D Bandrauk, Paul B Corkum, Jorn Manz, Gennady L Yudin

S26: "Tomographic measurement of 3D ion velocity distributions from rotationally cold molecules using a kHz VMI spectrometer"
Xiaoming Ren, Varun Makhija, Vinod Kumarappan

S27: "Controlling the Double Photoionization Dynamics of Li Atoms by Optical Pumping"
G. Zhu, J. Steinmann, M. Schuricke, J. Albrecht, A. Dorn, I. Ben-Itzhak, T.J.M. Zouros, J. Colgan, M.S. Pindzola, J. Ullrich

S28: "Controlling the Vibrational and Dissociation Dynamics of the Hydrogen Molecular Ion with Intense Infrared Laser Pulses."
T. Niederhausen, U. Thumm, and F. Martín

S29: "Two-center interference and nuclear motion effects in molecular harmonic generation"
Ciprian C. Chirila, Manfred Lein

S30: "Highlighting the role of dipole matrix elements in strong field molecular dissociation: vibrational suppression in H2+"
M. Zohrabi, F. Anis, J. McKenna, B. Gaire, Nora G. Johnson, K. D. Carnes, B. D. Esry and I. Ben-Itzhak

S31: "Strong-field dynamics of a one-dimensional H+2 /H2 model molecule"
C. B. Madsen, F. Anis, J. J. Hua, B. D. Esry

S32: "Strong-field ionization of aligned molecules"
M. Abu-samha and L. B. Madsen

S33: "Ionization, dissociation, and Coulomb explosion of H2 in intense laser fields: A theoretical study based on moving-grid approach in phase space"
Zhongyuan Zhou, Shih-I Chu

S34: "Dynamic Stark effect and the Coulomb-Volkov approximation"
V D Rodriguez and M G Bustamante

S35: "Multiple orbital contribution in multiphoton ionization of H2O in intense ultrafast laser fields"
Sang-Kil Son and Shih-I Chu

S36: "The Magnus expansion for laser-matter interaction"
Darko Dimitrovski, Morten Foerre, Michael Klaiber, Lars B. Madsen and John S. Briggs

S37: "Strong field double ionization of H2 : The phase space perspective"
F. Mauger, C. Chandre, T. Uzerc

S38: "Unitary model for the ionization of atoms of hydrogen by an intense laser pulse"
V D Rodriguez and M G Bustamante

S39: "Tomographic reconstruction of the 3D momentum distribution in velocity map imaging experiments"
C Smeenk, L Arissian, A Staudte, D M Villeneuve, P B Corkum

S40: "Strong-field electron spectra of rare gas atoms in the rescattering region: channel closing and a simulation of the experiment"
D. B. Milosevic, W. Becker, M. Okunishi, G. Prumper, K. Shimada, and K. Ueda

S41: "Attosecond soft X-ray pulses : From XUV attosecond pulse control by aperiodic multilayer optics to localized surface plasmon field dynamics"
Michael Hofstetter, Casey Chew, Jingquan Lin, Nils Weber, Matthias Escher, Michael Merkel, Ulf Kleineberg

S42: "White light generation under laser driven avalanche breakdown of air"
Updesh Verma, A. K. Sharma

S43: "Tunable THz Generation by Short Laser Pulses"
Anil K Malik, Hitendra K Malik

S44: "Collinear generation of few-cycle UV and XUV laser pulses for probing and controlling ultrafast electron dynamics at solid interfaces"
Agustin Schiffrin, Elisabeth Bothschafter, Ulrich Graf, Eleftherios Goulielmakis, Ralph Ernstorfer, Reinhard Kienberger, Ferenc Krausz

S45: "Photoelectron Angular Distributions at the Ionization of Atoms by Intense Sub-one-cycle Laser Pulses"
V.S. Rastunkov, V.P. Krainov

Thursday | **Friday** | **Saturday**

116 Cardwell Hall
Kansas State University
Manhattan, KS, USA
66506-2604
Voice: 785-532-6786
Fax: 785-532-6806
atto-09@phys.ksu.edu

Streaking of shake-up ionization in helium

Johannes Feist[*,1], **Andreas Kaltenbäck**[*], **Stefan Nagele**[*], **Renate Pazourek**[*], **Emil Persson**[*], **Barry I. Schneider**[†,§], **Lee A. Collins**[¶], **Joachim Burgdörfer**[*]

[*]Institute for Theoretical Physics, Vienna University of Technology, 1040 Vienna, Austria, EU
[†]Physics Division, National Science Foundation, Arlington, Virginia 22230, USA
[§]Electron and Atomic Physics Division, National Institute of Standards and Technology, Gaithersburg, Maryland 20899, USA
[¶]Theoretical Division, Los Alamos National Laboratory, Los Alamos, New Mexico 87545, USA

Synopsis We investigate whether an apparent "time delay" between electrons ionized by an attosecond XUV pulse with and without shake-up excitation of the remaining ion can be extracted using XUV-IR streaking setups. To do so, we solve the full Schrödinger equation for the helium atom including all correlation effects. We discuss whether a time delay extracted from the streaking spectra corresponds to a "real" time delay or is induced by other effects, such as the influence of the IR field on the ionization process.

The question whether there is a time delay between electrons liberated from an atom with or without shake-up excitation of the remaining ion has recently become a topic of interest. Such time delays can be measured in streaking experiments, which for example have shown an apparent time delay between electrons ionized from the conduction band and from core states in condensed matter systems [1].

In a streaking setup, an attosecond XUV pulse is used to free electrons from the target, which then acquire additional momentum from the IR pulse. This allows one to map the release time of the electron to the final momentum. A physical time delay between electrons produced in different processes results in a shift between the streaking curves (Fig. 1) with respect to each other.

One fundamental problem is the time delay between the electrons liberated from an atom with or without excitation (shake-up) of the remaining ion. An XUV pulse of high enough energy can either leave the ion in its ground state or promote it to an excited state through electron-electron interaction. We investigate this problem for the helium atom, for which it is possible to solve the full six-dimensional time-dependent Schrödinger equation ab initio [2].

The interpretation of any *apparent* "delay" extracted from simulations requires great care. In particular, the ionization and shake-up process itself can be influenced by the IR field, leading to additional momentum shifts on the electron which are not related to any time delay. In our contribution, we will address these questions and investigate whether a time delay between electrons ejected with and without shake-up can be unambiguously extracted.

Work supported by the FWF-Austria, grant SFB016, and NSF, TeraGrid grant TG-PHY090031.

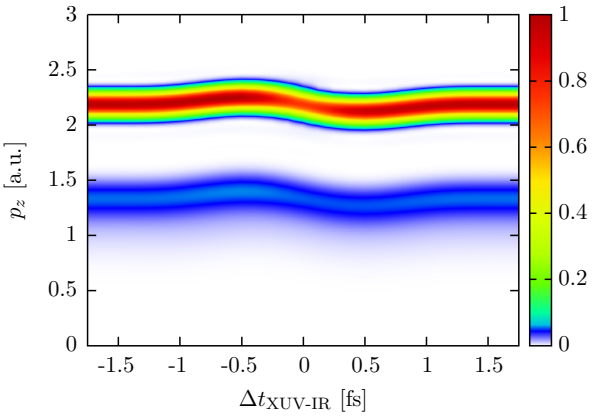

Fig. 1. Streaking image (electron spectrum in polarization direction vs. time delay) for ionization of a He atom by an 90 eV XUV pulse, synchronized with a single-cycle IR pulse. The upper line ($p_z \approx 2.2$ au) corresponds to ionization leaving the He^+ ion in the ground state, while the lower line corresponds to ionization leaving the ion in an excited state (primarily $2s$ and $2p$).

References

[1] A. L. Cavalieri et al., Nature **449**, 1029 (2007).

[2] J. Feist et al., Phys. Rev. A **77**, 043420 (2008).

[1]E-mail: johannes.feist@tuwien.ac.at

Elliptically polarized high-order harmonics from aligned molecules within the strong-field approximation

Adam Etches[1], **Christian Bruun Madsen**[2], **Lars Bojer Madsen**[3]

The Lundbeck Foundation Theoretical Center for Quantum System Research
Department of Physics and Astronomy, Aarhus University, 8000 Aarhus C, Denmark.

Synopsis A correction term is introduced in the stationary-point analysis on high-order harmonic generation (HHG) from aligned molecules. Arising from a multi-centre expansion of the electron wave function, this term brings our numerical calculations of the Lewenstein model into qualitative agreement with recent experiments [1].

Within the field of HHG there is currently a large deal of interest in the ellipticity of high-order harmonics from aligned molecules. Experimental results, such as those presented in [1], have challenged the validity of standard theoretical models. These models are extensions of the Lewenstein model to molecules and have the appeal of allowing qualitative predictions of experiment based on a few well-known approximations.

The process of HHG is typically split into three steps: *i)* Ionization of the outer electron *ii)* Propagation of the free electron in the laser field *iii)* Recombination of the electron to the ground state followed by emission of radiation. A standard treatment of step two is to perform a stationary-point analysis on the fast varying phase factors yielding the instantaneous free-electron momentum

$$\mathbf{k}_{st}(t) = -\frac{1}{t-t'}\int_{t'}^{t}\mathbf{A}(t'')\mathrm{d}t'',$$

where t' is the ionization time and $\mathbf{A}$ the vector potential of the laser field. However, if the molecular orbital is written explicitly in a multi-centre expansion it can easily be seen that the momentum is

$$\mathbf{k}_{st}(t) = -\frac{1}{t-t'}\int_{t'}^{t}\mathbf{A}(t'')\mathrm{d}t'' + \frac{1}{t-t'}\left(\mathbf{R}_f - \mathbf{R}_i\right),$$

where $\mathbf{R}_i$ ($\mathbf{R}_f$) is the ionization (recombination) site [2]. Depending on the orientation of the molecule, the extra term allows a non-zero component of the emitted harmonics polarized perpendicular to the driving laser.

The spectrum in Fig. 1 was calculated according to the Lewenstein model for molecules using the laser parameters from [1] and incorporating the additional term in the electron momentum. This term is responsible for the perpendicular component, which becomes comparable to the parallel component near the 21st harmonic.

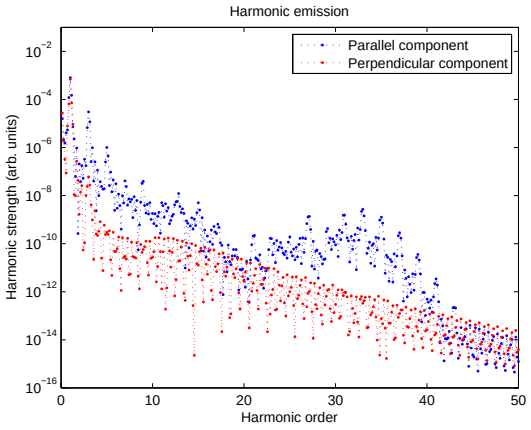

Fig. 1. Spectrum of N_2 HOMO at Euler angle $\phi = 55, \theta = 90, \chi = 0$.

References

[1] Xibin Zhou *et al.*, Phys. Rev. Lett. **102**, 073902 (2009).

[2] C. C. Chirilă and M. Lein, Phys. Rev. A. **73**, 023410 (2006)

[1]E-mail: etches@phys.au.dk
[2]E-mail: cbm@phys.au.dk
[3]E-mail: bojer@phys.au.dk

High harmonics generation using long wavelengths: Scaling and scaled systems

Gilles Doumy*[,1], Anne Marie March*, Erik Power[†,2], Jonathan Wheeler*, Chris Roedig*, Emily Sistrunk*, Fabrice Catoire*, Karl Krushelnick[†], Pierre Agostini* and Louis DiMauro*

[*] Department of Physics, The Ohios State University, Columbus, OH, 43210, USA
[†] Center for Ultrafast Optical Science, University of Michigan, Ann Arbor, MI, 48109, USA

Synopsis: Long wavelength lasers have started to become ubiquitous in studies of high harmonics generation, due to their attractive scaling properties (cutoff extension, better synchronization for shorter pulses). They also enable studies where the whole interaction is scaled compared to the usual situation using 800nm light. I will present both results that verified the wavelength scaling and a complete temporal characterization of the emission in a scaled Cesium\3.6mm system using Cross-correlation frequency resolved optical gating (XFROG).

High harmonics generation from gas targets has lead to the advent of attosecond physics, by being able to coherently produce photons across a large bandwidth in the extreme UV [1]. It has accompanied the development of ultrashort, femtosecond lasers, by bringing continuous improvements such as the extension of the generation cutoff or the generation of isolated attosecond pulses.

However, all this tremendous progress has been realized using what had become the workhorse of strong field physics, the Ti:Sapphire systems, operating at a wavelength around 800nm. Experimental progress was accompanied by a very successful theoretical description that indicated how the ponderomotive energy (average quiver energy of an electron in the strong field of the laser pulse) U_p was the main parameter to consider.

Following that reasoning, the attractive qualities of using longer wavelengths were obvious: cutoff extension as λ^2, harmonic synchronization improving as λ^{-1}. And since ultrashort intense sources have started to appear thanks to the development of Optical Parametric Amplifiers (OPA), it has become possible to test those predictions [2]. I will show some of those results, obtained by studying the interaction of noble gases with 50fs pulses up to a wavelength of 2 microns [3]. An example is illustrated in Fig.1.

Another very interesting new angle introduced by those longer wavelengths sources lies in the capability of completing the understanding of the interaction responsible for the generation. Indeed, following Keldysh's treatment [4] of the strong field interaction, noble gases at 800nm should behave very similarly to alkali atoms in the mid-infrared (~4μm). For example, HHG is observed in the interaction of cesium and 3.6 μm light. One remarkable property of those harmonics is that a good number of them lie in the visible\near UV, where it is still possible to use standard pulse characterization techniques, such as Frequency resolved optical gating. I will present results of a cross-correlation FROG measurement, which yielded the full temporal characterization of the pulse train obtained in those conditions. Most of the harmonics in that study had energies below the ionization threshold of cesium, which corresponds to a scantily studied region of the harmonic spectra.

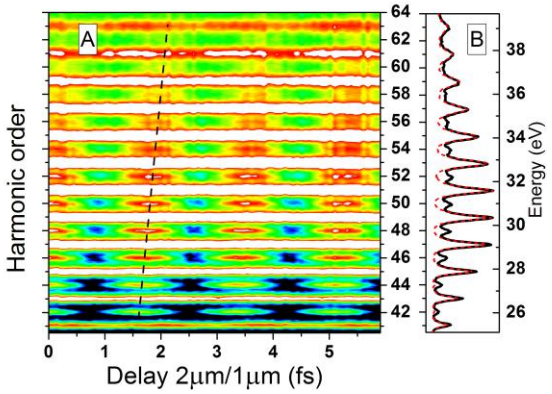

Fig. 1. Measure of the attochirp at 2 micron [3]

References

[1] Krausz, F. & Ivanov, M. Rev. Mod. Phys. 81, 163 (2009).
[2] Colosimo, P. et al. Nat Phys 4, 386-389(2008).
[3] Doumy, G. et al. Phys. Rev. Lett. 102, 093002 (2009).
[4] Keldysh, L. V. Sov. Phys. JETP 20, 1945 (1964).

[1] E-mail: doumv.1@osu.edu
[2] E-mail: eppower@umich.edu

Modeling Attosecond Pulse Formation in Strongly Ionized Gaseous Media

V. Tosa*[,1], K. Kovacs[*], R. Velotta[+], C. Altucci[+], K. T. Kim[**], and C. H. Nam[**]

[*]National Institute for R&D Isotopic and Molecular Technologies, 400293 Cluj-Napoca, Romania
[+]Dipartimento Scienze Fisiche, Universita Federico II, M. Santangelo, 80126 Napoli, Italia
[**]Korean Advanced Institute for Science and Technology, 305-701 Daejeon, Korea

Synopsis: We present the results obtained in modeling single attosecond pulse (SAP) as well as attosecond pulse trains (APT) formation as a result of femtosecond laser pulse interaction with rare gas atoms. A non-adiabatic model is used for solving the laser and harmonic field propagation, while strong field approximation is used to calculate the single dipole response. Quantum trajectories of the electron are generated and their phases are used in a time-dependent phase matching analysis. The role of the propagation can be beneficial in SAP generation as it contributes to the elimination of spurious bursts. APT characteristics will bear the signature of the distorted laser field, which will generate less, shorter and shifted to earlier time wagons.

High-order harmonic generation (HHG) is taking place when an atom/molecule is ionized by a high intensity laser field, and, after acceleration in the laser field, the electron recombines with the core to emit a harmonic burst of radiation [1]. Depending on experimental conditions the radiation is emitted either in a single attosecond pulse (SAP) or in successive bursts developing an attosecond pulse train (APT) synchronized with the optical cycle of the laser pulse.

In performing this study we first had in mind that HHG is most frequently investigated from the perspective of the single atom effect, while it is intrinsically a macroscopic process. For example the formation of the attosecond pulses in a gas jet/cell can be viewed as a coherent sum of many individual transient phenomena *i.e.* the atomic dipole bursts. As dipoles emit all over the interaction region with different amplitudes, durations and phases, it is essential to understand the role of single atom response and the role of collective effects in building the macroscopic signal which, in the end, is available from experiments.

In line with the above, we recently investigated the mechanism of formation of APT and SAP in strongly ionized gases by using a three dimensional non-adiabatic model [2] in which the propagation equation for the laser and the harmonic field are solved numerically by using the Fourier transform method and the strong field approximation for the single dipole response. A classical trajectory calculation was also used to study the phase matching and APT formation in the far field. The present results are obtained by generating the quantum trajectories of the electron using the saddle point equations.

In studying SAP formation we show that the atomic dipole emission (ADE) developed during laser-atom interaction is quite different from the final harmonic field. In particular, in the polarization gate schemes studied by us [3] ADE is composed of three or more bursts of radiation. We found that phase matching and three-dimensional (3D) propagation effects contribute to cleaning the total harmonic emission so that SAP can occur in the macroscopic medium.

For longer laser pulses ADE is depending on the optical cycle in which the process takes place, as the driving intensity is changing from cycle to cycle. Moreover, not only the dipole emissions but also the phase matching conditions are different for different optical cycles and depend on the spatial position, so that the intensity and emission properties of the resultant harmonic field are different for different pulses in the APT and for different locations in the interaction region. In these conditions, the process of APT formation is found to be the result of an interlace among the driving laser field, single atom response, phase matching effects in the near field and burst interference in the far field. The computed results compare very well with the FROG measurements. This enables us to understand better the underlying physics and to draw useful conclusions concerning the optimization control of the spectral, temporal and intensity characteristics of the APT.

References

[1] P.B. Corkum, Phys. Rev. Lett. **71**, 1994 (1993).
[2] V. Tosa, K.T. Kim, C.H. Nam, Phys. Rev. A **79**, 043828 (2009)
[3] C. Altucci, R. Esposito, V. Tosa, R. Velotta, Opt. Lett. **33**, 2943 (2008)

[1] E-mail: tosa@itim-cj.ro

Benchmark experiment on H_3^+ in intense ultrashort laser pulses

J. McKenna, A. M. Sayler, B. Gaire, Nora G. Johnson, K. D. Carnes, B. D. Esry and I. Ben-Itzhak [1]

J. R. Macdonald Laboratory, Physics Department, Kansas State University, Manhattan, Kansas 66506, USA

Synopsis Using coincidence 3D momentum imaging we have probed, for the first time, the fragmentation dynamics of H_3^+ and its isotopologues in intense ultrashort laser pulses. As the simplest polyatomic molecule, these measurements on H_3^+ can serve as a benchmark for future theoretical calculations.

The two-electron H_3^+ ion is the simplest stable polyatomic molecule. The H_3^+ nuclei are arranged in a unique triangular configuration, which provides a fundamentally new system for theoretical development of calculating strong laser-field phenomena. Currently, however, H_3^+ is a serious challenge to theorists since it is at the boundary of present capabilities. Thus, appropriate simplifying assumptions are needed and experiments can provide the necessary guidance to find them.

Unfortunately neither H_3^+, nor H_3, exist naturally in the laboratory, despite their central role in interstellar chemistry. Thus, to perform experiments on H_3^+ requires their production in an ion source. This necessitates the use of the more demanding ion beam targets. Nonetheless, many previous attempts have been made to study H_3^+ in an intense laser field without any success.

Seemingly the biggest factor in these failings has been the low rate of H_3^+ fragmentation, even at intensities up to 10^{16} W/cm^2. Consequently, in parallel with work on diatomic molecules [1, 2], we have developed a coincidence 3D momentum-imaging method [1] that allows for the efficient detection of all fragments, both from two-body and three-body breakup of H_3^+ — see illustration in Fig. 1.

At this conference we present extensive measurements from dissociation and ionization of a few keV D_3^+ beam target and contrast them with measurements on H_3^+ and D_2H^+, where interestingly we find isotopic effects in the latter. We use 790 nm, 7-40 fs, 1 kHz (linearly polarized) laser pulses that span $10^{14} - 10^{16}$ W/cm^2 in our measurements.

Some of the interesting questions we address involve the competition between two-body and three-body dissociation, and single ionization. Moreover, the three-body breakup channels particularly provide insight on the alignment and orientation preference of fragmentation of the H_3^+ triangle relative to the laser polarization.

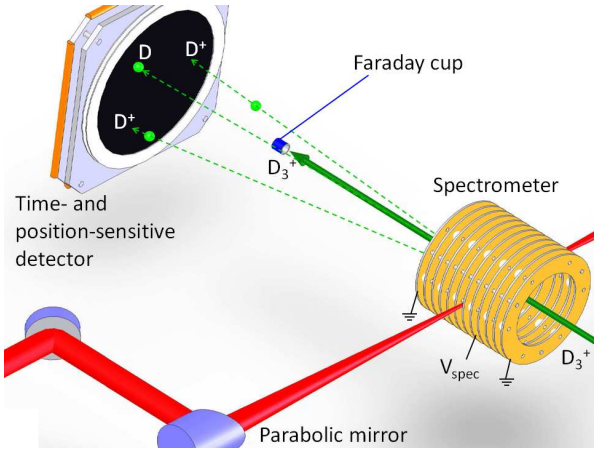

Fig. 1. Schematic of the experimental setup where all fragments from D_3^+ breakup are imaged in coincidence.

This work was supported by the Chemical Sciences, Geosciences, and Biosciences Division, Office of Basic Energy Sciences, Office of Science, U.S. Department of Energy.

References

[1] I. Ben-Itzhak *et al.* Phys. Rev. Lett. **95**, 073002 (2005)

[2] J. McKenna *et al.* Phys. Rev. Lett. **100**, 133001 (2008)

[1] E-mail: ibi@phys.ksu.edu

Ultrafast high-harmonic imaging of a chemical reaction

H. J. Wörner, J. B. Bertrand, P. B. Corkum and D. M. Villeneuve

Joint laboratory for attosecond science,
National Research Council of Canada and University of Ottawa,
100, Sussex Drive, Ottawa, ON, Canada K1A0R6

Synopsis High-harmonic generation in aligned molecules provides information about their electronic structure and ionization continuum within a fraction of a laser cycle. We exploit the ultrahigh time resolution to experimentally observe a chemical reaction of fixed-in-space molecules. We non-adiabatically align Br_2 molecules, launch a photodissociation wave packet and measure the high harmonic yield as a function of time delay and angle between the molecular axis and the polarization of the generating laser field. We develop an interferometric technique to extract the harmonic dipole and phase of the excited state along the photodissociation coordinate. This provides the complete information required for the dynamic tomographic imaging of the chemical reaction.

When a molecule is exposed to a strong laser field, the tunnel-ionized electron wave packet can recombine with the parent ion to emit high-harmonic radiation. The amplitude and phase of the emitted radiation characterizes the electronic structure of the atoms or molecules subjected to this process. This property has been used to image the highest occupied molecular orbital of nitrogen (N_2) using a tomographic procedure [1]. In fact, not only the bound state is characterized by the high-harmonic radiation but also the ionization continuum [2, 3, 4]. This perspective combined with the ultrafast time scale of the process opens exciting perspectives for imaging the electrons in molecules undergoing a chemical reaction [5].

We exploit the ultrahigh time resolution that can be achieved in high harmonic generation to extract high harmonic dipole amplitudes and phases of a molecule undergoing a chemical reaction. Our experiment proceeds in three steps: non-adiabatic alignment, impulsive excitation and high-harmonic generation. We use the photodissociation of Br_2 in a proof-of-principle experiment. The major difficulty is the separation of signals from the dominant ground state population from the excited state. Both coherently related states emit harmonics and interfere on the attosecond time scale. The transient interference of the two states results in a high visibility of the photodissociation process on the femtosecond time scale. The variation of the observed signal with harmonic order provides dynamic information on the attosecond time scale. We develop a homodyne technique that enables us to extract the harmonic amplitude and phase of the excited state undergoing dynamics. Molecular frame information on the evolution of the electronic structure along the dissociation coordinate and the associated ionization continuum is thereby obtained. The results indicate that the coherence of the atomic fragments manifests itself up to very large internuclear separations. These experiments pave the way towards dynamic orbital tomography - a movie of the molecular orbitals undergoing a chemical reaction.

References

[1] J. Itatani, J. Levesque, D. Zeidler, H. Niikura, H. Pépin, J. C. Kieffer, P. B. Corkum, and D. M. Villeneuve *Nature*, **432**, 867 (2004).

[2] T. Morishita, A.-T. Le, Z. Chen, and C. D. Lin *Phys. Rev. Lett.*, **100**, 013903 (2008).

[3] H. J. Wörner, H. Niikura, J. B. Bertrand, P. B. Corkum, and D. M. Villeneuve *Phys. Rev. Lett.*, **102**, 103902 (2008).

[4] A. T. Le, R. R. Lucchese, S. Tonzani, T. Morishita and C. D. Lin *arXiv*, **0903.5354v1** (2009).

[5] V.-H. Le, A.-T. Le, R.-H. Xie, and C. D. Lin *Phys. Rev. A*, **76**, 013414 (2007).

Attosecond Electron Interferometry

***K. Klünder*[*], *M. Swoboda*[*], *M. Gisselbrecht*[*], *M. J. Dahlström*[*], *P. Johnsson*[*], *T. Remetter*[*], *J. Mauritsson*[*], *A. L'Huillier*[*]**

[*]Department of Physics, Lund University, P. O. Box 118, SE-221 00 Lund, Sweden

Synopsis: We present two different interferometric pump-probe experiments aiming to access state specific phase information after attosecond pulse excitation. The common idea is that when creating the wave packet we introduce simultaneously a reference that allows us to measure the phase evolution. In the first experiment we use isolated attosecond pulses to characterize ultrafast bound electron dynamics. While in the second we apply attosecond pulse trains in a RABITT measurement to access the phase induced by a resonant bound state in a two-photon-ionization process.

Attosecond science aims to measure electron dynamics on their natural time scale. The pulse durations required are in the range of only a few hundred attoseconds. Both experiments make use of the broad coherent bandwidth linked to theses short pulse durations.

In the first experiment, which was done in Milan in collaboration with AMOLF, LSU, MPQ etc [1], we use an isolated attosecond pulse with sufficient photon energy and bandwidth to simultaneously excite and ionize Helium. As shown in Figure 1 this leads to a coherent excitation of the *p*-states in Helium and a fraction of the continuum, which will act as a reference. The excited bound wave packet is later ionized by a 7 fs infrared (IR) laser field with a locked phase-relation. From the observed interference between the different ionization pathways we show that it is possible to extract the amplitude and phase evolutions and reconstruct the excited bound state wave packet.

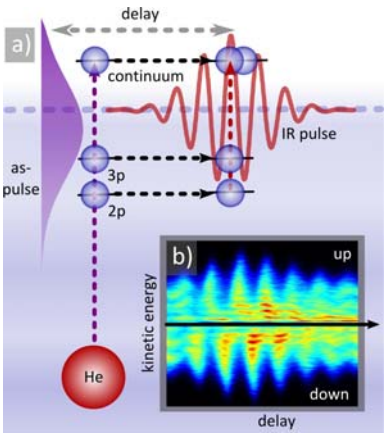

Fig. 1. a) An isolated attosecond pulse is used to excite and ionize Helium; at a later time the trapped portion of the wave packet is ionized by a few cycle IR pulse, which is locked in phase to the attosecond pulse. b) Experimentally observed interference fringes in the photoelectron spectra as a function of delay between the two pulses.

In a second experiment we use an attosecond pulse train for excitation. The photoelectron spectrum consists of a comb of energies, corresponding to the odd harmonics of the fundamental laser field. An additional IR field introduces sidebands through a two-photon process, which allows us to measure the relative phase variation over the harmonic spectrum from a delay-dependent scan (RABITT) [2]. As depicted in Fig. 2 harmonic 15 resonantly excites the 3p state in Helium.

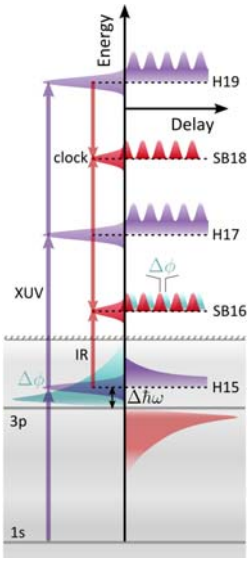

Fig. 2. Influence of a resonant bound state in a RABITT measurement.

The resonance acts as a phase-modulator on the sideband 16 for the two-photon transition, where the phase modulation depends on the detuning of harmonic 15 from the resonance. Referencing SB16 with SB18, we can detect this phase difference. By tuning the laser frequency, we are then able to map out the phase pattern resulting from the presence of the bound state. Having obtained this phase map, we can use it to track the binding energy of the 3p state in Helium when influenced by a strong external laser field (AC-Stark shift).

References

[1] T. Remetter, K. J. Schafer, O. Ghafur, F. Kelkensberg, W. Siu, M. J. J. Vrakking, I. Znakovskaya, T. Uphues, S. Zherebtsov, M.F. Kling, F. Lépine, E. Benedetti, F. Ferrari, G. Sansone, M. Nisoli.

[2] P. M. Paul et al., Science 292, 1689 (2001).

[1] E-mail: Kathrin.Klunder@fysik.lth.se

Electron Wavepacket Interferences pointing to Holographic Imaging with Few Cycle Laser Pulses

R. Gopal[*,1], A. Rudenko[‡], K. Simeonidis[*], K.-U. Kühnel[*], M. Kurka[*], C. D Schröter[*], O. Herrwerth[†], Th.Uphues[†], M. Schultze[†], E. Goulielmakis[†], M. Uiberacker[†], D. Bauer[1], M. Lezius[†], R. Moshammer[*], M. F. Kling[†] and J. Ullrich[*]

[*] Max-Planck-Institut für Kernphysik, 69117 Heidelberg, Germany
[‡] Max-Planck Advanced Study Group at CFEL, 22607 Hamburg, Germany
[†] Max-Planck-Institut für Quantenoptik, 85748 Garching, Germany

Synopsis: Three-dimensional (3D) electron (and ion) momentum (**P**) spectra have been recorded for carrier-envelope-phase (CEP) stabilized few-cycle (~5 fs), intense (~0.4 PW/cm^2) laser pulses (740 nm) impinging on He using a reaction microscope. Preferential emission of low-energy electrons (E_e < 15 eV) to either hemisphere is observed as a function of the CEP. Clear interference patterns emerge in **P**-space at CEPs with maximum asymmetry, interpreted as holographic images of re-scattered electron wavepackets by means of a simple model and in line with previous theoretical predictions.

Interferometry with coherent electron wavepackets (EWPs), modulated through ultrafast processes (10^{-18}-10^{-15} s) in atoms and molecules, opens new possibilities to enhance our understanding of these dynamics. In recent experiments EWPs generated by attosecond pulse trains and steered by an infrared laser pulse have been demonstrated to image the coherent scattering of electrons from the parent ion [1]. In this contribution we present an alternative scheme for EWP interferences, manifested in the photoelectron spectra of single ionization in atoms with Carrier Envelope Phase (CEP)-stabilized few-cycle (~5 fs) laser pulses, investigated by a 'reaction microscope' [2].

In the experiment, linearly-polarized CEP stabilized 5 fs pulses at 740 nm (repetition rate: 3 kHz) were obtained at the attosecond beamline at Max-Planck-Institut für Quantenoptik, Garching. The laser beam, with intensities up to 0.4 PW/cm^2 at the focus was crossed with a supersonic, cold He jet (~10^{11} atoms/cm^2) in the ultra-high vacuum chamber (~10^{-10} mbar) of the reaction microscope.

2D electron momentum spectra (Fig. 1) at certain fixed CEP reveal in addition to enhanced emission into one **P**-hemisphere, regular interference stripes, parallel to the transverse momentum axis in the corresponding hemisphere and radial structures in the opposite hemisphere, in good qualitative agreement with theoretical predictions [3] and TDSE calculations. The spacing between the peaks, significantly smaller than the multi-photon peak structure previously observed for longer pulses, agrees with those calculated in a simple Strong Field Approximation (SFA)-based model. This model, invoking the interference of two quantum paths leading to the same final drift momentum, captures the basic mechanism of holographic imaging via the superposition of a re-scattered, modulated EWP on an unaffected, directly launched 'reference' EWP (of the same electron!)[3].

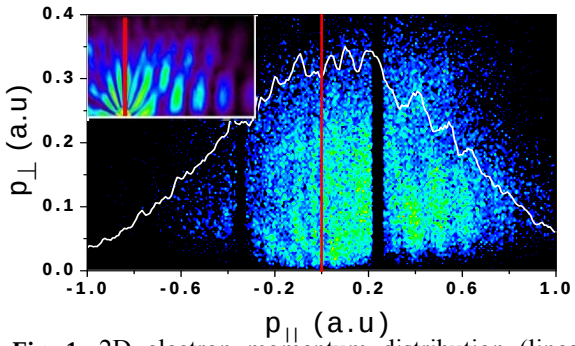

Fig. 1: 2D electron momentum distribution (linear scale) for a CEP with maximum asymmetry. The x-axis is the longitudinal momentum; the y-axis is the momentum transverse to the laser polarization axis. The red line indicates the position of $p_{||}$ = 0. The projection onto the $p_{||}$ -axis is indicated as a white line. Inset: TDSE calculations for a gaussian pulse (740 nm) with I_0 = 0.3 PW/cm^2, FWHM ~ 2.7 fs.

We believe that holographic imaging through EWPs has the potential to obtain unprecedented information on ultra-fast correlated electron dynamics, for example, the details of the (time dependent) scattering potential in atoms and molecules

References

[1] Mauritsson J *et al.* 2008 *Phys. Rev. Lett.* **100** 073003.
[2] Ullrich J *et al.* 2003 *Rep. Prog. Phys.* **66** 1463.
[3] Arbó D *et al.* 2006 *Phys. Rev. A.* **74** 063407.

[1]E-mail: Ram.Gopal@mpi-hd.mpg.de

Asymmetric dissociation of H_2 and D_2 by a two-color laser field

D. Ray*[,1], S. De*, H. Mashiko* , I. Znakovskaya[†], F. He*, U. Thumm*, G.G.Paulus[††], M. Kling[†], I. Litvinyuk*, and C.L. Cocke*

[*] Department of Physics, Kansas State University, Manhattan, KS 66506, USA
[†]Max-Planck Institut für Quantenoptik, D-85748 Garching, Germany
[††] Institute of Optics and Quantum Electronics, 07743, Jena, Germany

Synopsis: Two-color (800 nm and 400 nm) short (45 fs) linearly polarized pulses are used to ionize and dissociate $H_2(D_2)$ into a neutral hydrogen (deuterium) atom and a proton(deuteron). The yields and energies of the ions are measured left and right along the polarization vector. As the relative phase of the two colors is varied, strong yield asymmetries are found in the ion energy regions corresponding to bond softening, above-threshold dissociation and rescattering. A model based on the dynamic coupling by the laser field of the gerade and ungerade states in the molecular ion accounts for many of the observed features.

It is known that few-cycle carrier-envelope-phase-stabilized laser pulses can be used to control electron localization in the dissociation of the hydrogen molecular ion [1], resulting is left-right asymmetry of the ion emission. Here we report experiments which demonstrate a similar control achieved by scanning the relative phase between two-color (800 and 400nm) many-cycle pulses. The superposition of the two colors generates, in an easily reproducible and robust manner, the required asymmetric light-field. A neutral $D_2(H_2)$ gas is ionized and dissociated by the light pulse and the D^+ (H^+) ions from the dissociation of D_2^+ (H_2^+) are detected using both a velocity-map-imaging system (VMI) [1] and/or a stereo-phasemeter [2]. A sample of the VMI results is shown in Fig. 1, where the asymmetry of deuteron emission from D_2^+ is shown as a function of the ion energy and the relative phase of the two colors. The yield of the fragments, measured as a function of the ion kinetic energy, shows a clear left-right asymmetry oscillation in the bond-softening, above-threshold-dissociation and rescattering channels. In the energy region of the CREI the asymmetry vanishes, as it should since this channel corresponds to double ionization. We have measured the asymmetry dynamics in the different fragmentation channels as a function of the two-color field intensity.

We compare our results with the results of a theoretical model. For the bond-sofetning and above-threshold-ionization channels the initial ionization event is assumed to launch a wave packet onto the gerade potential curve of the molecular ion, and the subsequent coupling of gerade and ungerade states by the asymmetric laser field is followed. For the rescattering channel, the ungerade channel is directly populated. Many features of the experimental data can be reproduced by the model.

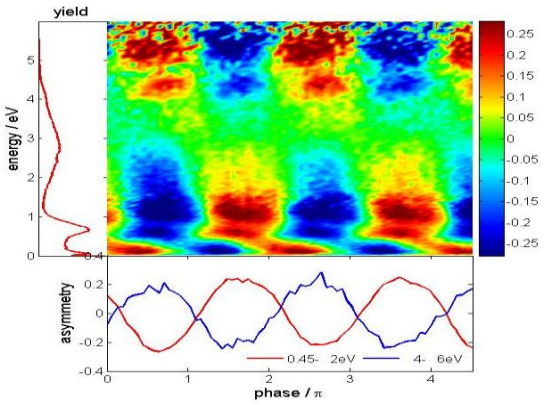

Fig. 1. Asymmetry [(yield $_{left}$-yield $_{right}$)/total yield] plotted as a function of the phase angle of the 400 nm radiation, relative to that of the 800 nm radiation, and the d^+ ion energy. The panel on the left shows the total yield of ions versus energy, while the lower panel shows the yields from the 0.45-2 eV (mainly above-threshold dissociation) and 4-6 eV (mainly rescattering) channels.

This work was supported by Chemical Sciences, Geosciences and Biosciences Division, Office of Basic Energy Sciences, Office of Science, U. S. Department of Energy.

[References

[1] Kling M et al. 2006 *Science* 14 246.
[2] Paulus G G et al. 2003 *Phys.Rev.Lett.* 91 253004.

[1] E-mail: dray@phys.ksu.edu

Intensity dependence of strong field double ionization mechanisms of diatomic molecules: from field-assisted electron recollision to recollision-assisted field ionization

Agapi Emmanouilidou[1]

[1] *Chemistry Department, University of Massachusetts at Amherst, Amherst, Massachusetts, 01003*

Given the state of the art in computational capabilities addressing the double ionization of strongly driven diatomic molecules with three-dimensional (3-d) first-principle techniques, namely quantum mechanical ones, is an immense task. We study the correlated electron dynamics in the double ionization of diatomic molecules with "frozen" nuclei in the non-sequential regime as a function of the intensity of the laser pulse [1]. We do so, using a 3-d quasiclassical technique that we have first developed for conservative systems, namely, the multiple ionization of atomic systems such as Li, Be, by single photon absorption [2]. We have very recently extended this technique to non-conservative systems treating the correlated electron dynamics of the He atom when driven by strong laser fields [3]. Here we further build on this technique by tackling more than one atomic centers. The advantage of this technique is that it is numerically very efficient. In addition, the method treats the Coulomb singularity with no approximation in contrast to techniques that use "soft-core" potentials. Accounting for the Coulomb singularity will be in addition very important in pump-probe set-ups where VUV or XUV pulses are used to pump the process.

For intensities corresponding to the tunneling regime, we find that the recollision time is close to a zero of the field—as expected from the recollision model. We identify the main ionization mechanisms in this regime and show that they have distinct traces when considering the sum of the momenta parallel to the laser field as a function of the inter-electronic angle of escape, see Fig. 2. However, when the laser intensity is increased above the barrier we find an unexpected concentration of the correlated momenta in the second and fourth quadrant in contrast to the concentration in the first and third quadrant for the tunneling regime. We discuss the mechanism responsible for this shift of the correlated momenta, see Fig. 1, [1]. This surprising shift of the correlated momenta is a very nice demonstration of both the strong IR field and the Coulomb potential contributing to double ionization with the IR field playing an important role even before the recollision time—thus the name recollision-assisted field ionization.

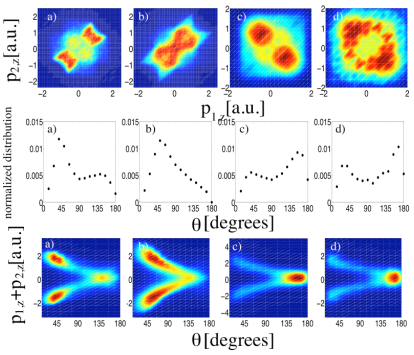

FIG. 1: Form left to right the laser intensity is 10^{14}W/cm^2, 1.5×10^{14}W/cm^2, 3×10^{14}W/cm^2 and 4×10^{14}W/cm^2 for a 3-cycle laser pulse. Top panel: correlated momenta parallel to the polarization axis; Medium panel: the distribution of the inter-electronic angles of escape binned in 14 intervals, $180^\circ(l-1)/14 < \theta < 180^\circ/14 \times l$ with $l = 1, ..., 14$; Bottom panel: sum of the parallel momenta as a function of the inter-electronic angle of escape.

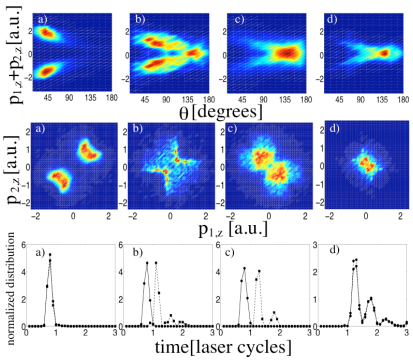

FIG. 2: For 10^{14}W/cm^2 we identify four different double ionization mechanisms depending on each electron's time of ionization: the different columns refer to: a) the SE, b) the RESI , c) the NSE2 and d) the DE mechanisms. First row: the sum of the momenta of the two electrons as a function of the inter-electronic angle of escape; second row: the correlated momenta of the two electrons; and third row: the ionization time of each electron in units of laser cycles.

[1] A. Emmanouilidou and A. Staudte (submitted 2009).
[2] A. Emmanouilidou and J. M. Rost, J. Phys. B **39**, 4037, (2006).
[3] A. Emmanouilidou, Phys. Rev. A **78**, 023411 (2008).

Attosecond Photoelectron Spectroscopy of Metal Surfaces

C.-H. Zhang* [1], **U. Thumm*** [2]

*JRM Laboratory, Kansas State University, Manhattan, KS, 66506-2604, USA

Synopsis We calculate the time delay between photoemitted conduction-band and core-level electrons of a tungsten surface [1].

Attosecond photoelectron (PE) spectroscopy can be used to study the electronic dynamics of different groups of electrons in solids. In this setup, electrons are photoemitted by an attosecond XUV pulse and streaked by a delayed femtosecond IR laser pulse. Such an experiment was carried out by Cavalieri *et al.* [2] on a W(110) surface and shows a relative delay of 110 ± 70 as between the detection of PEs that are emitted by absorption of a single XUV photon from $4f$-core and conduction band levels.

We investigated the mechanism behind this observed relative delay in the PE spectra, describing the XUV photo-release as a one-step single-electron transition from an initial Bloch wave $\Psi_{\mathbf{k}_i}(\mathbf{r},t)$ to an IR-field-dressed damped final Volkov wave $\Psi^V_{\mathbf{k}_f,\kappa}(\mathbf{r},t) = \Psi^V_{\mathbf{k}_f}(\mathbf{r},t)\chi(\kappa,z)$ with the damping factor $\chi(\kappa,z) = e^{\kappa z}$ for $z<0$ and 1 for $z>0$. Here $\mathbf{k}_i$ is the crystal momentum, $\mathbf{k}_f$ designates the (unstreaked) final momentum of the PE, $\kappa = 1/\lambda$ the damping parameter, and $\Psi^V_{\mathbf{k}_f}$ the usual Volkov wave. The PE emission probability in the dipole-length gauge for the interaction with the XUV electric field $E_X(t)$ is

$$P(E,\tau) = \sum_{\mathbf{k}_i} \left| \int dt \langle \Psi^V_{\mathbf{k}_f,\kappa} | z E_X(t) | \Psi_{\mathbf{k}_i} \rangle \right|^2 \quad (1)$$

where E is the final PE kinetic energy and τ the delay between the XUV and IR pulse. We use a jellium wavefunction for the conduction band and a tight-binding wavefunction with zero bandwidth for the core-level electrons. The relative delay $\Delta\tau$ is visible in the center-of-energy $\bar{E}(\tau) = \int P(E,\tau) E dE / \int P(E,\tau) dE - E_c$ of the two spectra (Fig. 1), where E_c is the spectral peak position without the IR field.

Our calculated time-resolved PE spectra depend on the transport of photo-released electrons inside the solid, agree with the experiments of Cavalieri *et al.* [2], and demonstrate that the observed temporal shift is caused by the interference of core-level PEs that originate in different layers of the solid and experience a temporal modulation by the streaking field. We further show how this temporal shift is controlled by the mean free path of the core-level PEs and that the observed 110 as shift is obtained in by choosing $\lambda = 5$ Å.

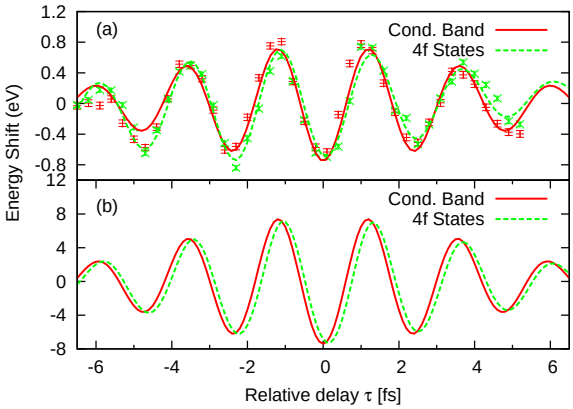

Fig. 1. Streaked electron spectra for photoemission from CB and $4f$-core levels of a W(110) surface: $\bar{E}$ as a function of the delay between the XUV and IR pulse. (a): Experimental results of Fig. 3b in Ref. [2]. The damped sinusoidal curves are fits to the raw experimental data (points with error bars). (b): Calculated results showing a relative shift of $\Delta\tau = 110$ as between the two groups of electrons.

References

[1] C.-H. Zhang, and U. Thumm, *Phys. Rev. Lett.* **102**, 123601 (2009).

[2] A. L. Cavalieri *et al.*, *Nature* **449**,1029 (2007).

[1] E-mail: chhzhang@ksu.edu
[2] E-mail: thumm@phys.ksu.edu

Time-resolved Coulomb explosion imaging of CO ultrafast dynamics using few-cycle IR and EUV laser pulses

A. S. Alnaser*[1], I. Bocharova[2], K. Singh[2], C. Wei[2], M. Kling[3], C. L. Cocke[2], I. V. Litvinyuk[2]

[1] Department of Physics, American University in Sharjah, Sharjah, United Arab Emirates
[2] J. R. Macdonald Laboratory, Physics Department, Kansas State University, USA
[3]Max-Planck Institute for Quantum Optics, Garching, Germany

Synopsis: We have used few-cycle IR and EUV laser pulses in pump-probe arrangement to trace out the dissociation pathways in CO when exploded by strong laser fields. We present two preliminary sets of data of different pump pulses. In these sets, different excited state of CO cations are populated using (< 10 fs) IR, and EUV pulses respectively. We followed the time evolution of these states using the time-resolved Coulomb explosion imaging technique. We compare the time evolution of IR- and EUV-induced excited states by measuring the KER of the fragment ions as a function of the time delay between the pump and the IR probe pulse.

The availability of extremely short intense laser pulses makes it now possible to follow in real time the heavy particle dynamics of light molecules and to determine their different dissociation pathways [1]. A non-stationary wave packet can be launched onto a potential curve of the molecule through ionization of the neutral, and the subsequent motion of this time-dependent wave packet can be followed as it coherently couples to other potential curves in the ionized system.

In this work, we have used intense laser pulses in a pump-probe arrangement to trace out the rapid evolution of wave packets launched onto different states of CO cations. We utilized 8 fs IR and 10 fs EUV laser pulses as ionizing pulses that set CO in different excited ionic states. After a time delay ranging from 0 to 200 fs, a second IR pulse, of controllable intensity removes one or more electrons, causing the system to "Coulomb explode" into different pairs of charged fragments. These fragments were detected in coincidence, and their full momenta were measured, using the well established COLTRIMS techniques. We measured the KER as well as the angular distribution of the resulting fragments as a function of the delay between the pump (whether it is an IR or EUV) and the IR probe pulses.

Figure 1 shows the momentum image generated when CO is dissociated to C^+ and O^+ fragments by Ar EUV attosecond train. As shown in the figure the two fragments exhibit different angular dependence with respect to the radiation polarization; a signature of the excited state that is populated. In addition, we will present time-dependent KER spectrum obtained with EUV (or IR) as a pump and IR as a probe.

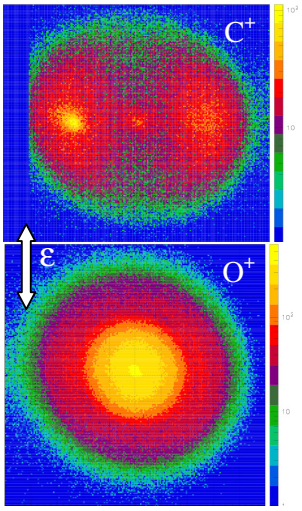

Fig. 1. Momentum image of the C^+ (up) and O^+ ions generated from the dissociation of CO by few-cycle EUV laser pulses. The polarization is vertical.

This work was supported by Chemical Sciences, Geosciences and Biosciences Division, Office of Basic Energy Sciences, Office of Science, U.S. Department of Energy. ASA acknowledges FRG support from American University of Sharjah.

References

1. Alnaser A S *et al*., Phys. Rev. A 72, 030702, (2005).

* aalnaser@aus.edu

Ultrashort IR-visible- and VUV-pulse generation for attosecond pump-probe experiments using a reaction microscope

K. Simeonidis[1], **R. Gopal, H. Rietz, A. Sperl and J. Ullrich**

Max-Planck-Institut fuer Kernphysik, Saupfercheckweg 1, D - 69117 Heidelberg, Germany

Synopsis The status of the new attosecond beamline at Max-Planck-Institut fuer Kernphysik (MPIK), Heidelberg, and ongoing experiments is reported. The beamline is designed for detailed investigation of the electronic response in atoms and molecules by combining a versatile HHG-source with a compact reaction microscope. Ultrashort laser pulses down to 4 fs generatetd by a novel pulse compression setup utilizing filamentation are applied to produce isolated attosecond pulses.

The attosecond beamline at MPIK is designed for the investigation of the electronic response in atoms and molecules in unprecedented detail. A versatile HHG-source producing either attosecond pulse trains or isolated attosecond pulses is combined with a reaction microscope dedicated for attosecond pump-probe experiments. The optical setup is based on a commercially available femtosecond laser system delivering carrier envelope phase (CEP) stabilized mJ pulses with a pulse duration around 25 fs at a center wavelength of approx. 785 nm. The repetition frequency of the cryogenically cooled Ti:Sapphire amplifier is adjustable to values betweeen 3 kHz and 10 kHz. For experiments using attosecond pulse trains the bare amplifier output is applied to pump the HHG, while for obtaining isolated attosecond pulses further compression is necessary since HHG has to be restricted to only one cycle of the driving CEP-stabilized IR-field. IR-pulse compression is achieved through spectral broadening via self-phase-modulation (SPM) and subsequent dispersion management using a

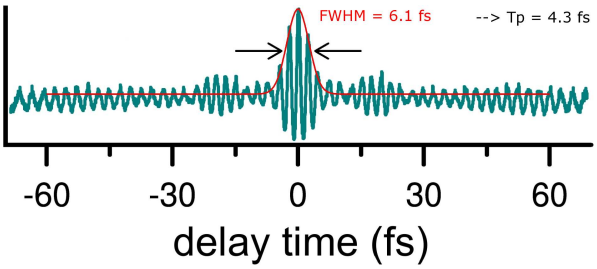

Fig. 1. Autocorrelation measurement after filamentation. From the envelope fit (red line) a pulse duration of the central part of 4.3 fs is derived.

standard chirped mirror pair. A novel double-pass setup loosely focussing the laser twice into a long Argon filled gas cell is used to produce 2 filaments leading to SPM. Pulse durations down to 4 fs while maintaining more than 60 % of the initial pulse energy have been measured (see Fig. 1). Subsequently, the infrared / visible laser pulses are focussed into a gas target, where nonlinear interaction of the intense electromagnetic field with the target atoms leads to the emission of high harmonic radiation. In order to achieve high target pressures up to 400 mbar, the target gas is confined in a cell of some millimeters length. The HHG-setup is housed in a vacuum chamber along with the optics necessary for focussing and delay lines as well as telescopes that adjust the beam diameter. The source is fully optimized for the operation with Argon, where photon fluxes of typically 10^9 photons per second and harmonic order in the plateau region of the UV-spectrum are reached.

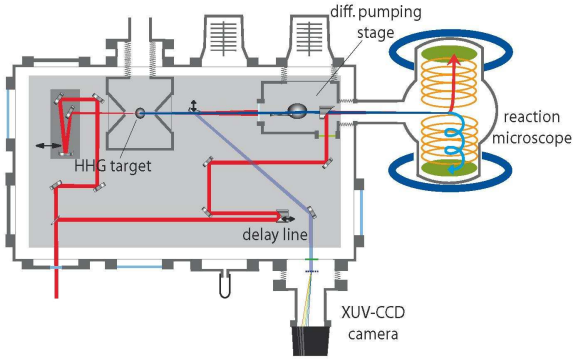

Fig. 2. Schematic of the pump-probe experimental setup. All interferometer components including final focussing optics are mounted on the same breadboard in vacuum.

[1]E-mail: k.simeonidis@mpi-hd.mpg.de

Magnetic-bottle electron energy spectrometer for measuring 25 as pulses

Kun Zhao, Chao Wang, Ximao Feng, Steve Gilbertson, Sabih D. Khan, and Zenghu Chang[1]

JRM Laboratory, Kansas State University, Manhattan, KS, 66506-2604, USA

Synopsis: Non-uniform field in a magnetic-bottle electron energy spectrometer (MBEES) was simulated with finite-element software. The result showed that a field close to 1T may be obtained at the interaction region with a carefully designed NdFeB permanent magnet and soft iron pole piece. This field meets the requirement for 25as pulse duration measurement.

The duration of attosecond pulses is usually retrieved from streaked photoelectron energy spectra produced by XUV attosecond pulses [1]. A time-of-flight (TOF) spectrometer is the most widely used device for electron energy spectrum measurement. Among a variety of different TOF designs, a magnetic-bottle electron energy spectrometer (MBEES) with a non-uniform magnetic field is more preferable due to its large acceptance angle - at least 2π steradian [2]. It is critical to detect as many electrons as possible in attosecond photo-electron measurements because of the low XUV photon flux and low XUV to electron conversion efficiency.

A 25 as pulse corresponds to a spectrum of 75 eV FWHM, which requires the spectrometer to cover a 0~150 eV range. To resolve pre- or post-pulses one laser cycle away from the main attosecond pulse, the resolution of the spectrometer should be better than 0.4 eV [3].

Typically, the field in MBEES consists of a strong field at the interaction region (B_i), produced by a permanent magnet and a pole piece, and a weak field in the drifting tube (B_f) created by a solenoid. The non-uniformity of the field parallelizes the electron trajectories from the interaction region without changing the energy or flying time significantly.

There are three key requirements that affect the energy resolution [2]. First, the ratio of the weak and strong fields should be $B_f/B_i \approx \Delta E/E \approx 0.1\%$. Second, the adiabaticity parameter $\chi_1 = \frac{2\pi m_e v}{eB_z}\left|\frac{dB_z}{dz}\right|$ is smaller than unity. Third, the transition region (the region where the field drops from about 1 T to 100 G) should be small. However, this requirement contradicts the adiabatic requirement. Therefore, a carefully formulated simulation of the magnetic field is required for the design of MBEES.

The field of an NdFeB magnet with a soft iron pole piece was simulated. A cylindrical magnet and a properly shaped pole piece give one of the best results. This field, combined with the solenoid field, is shown in Fig. 1. At the interaction region (0.5 mm from the pole face), B_i is more than 0.8 T while B_f = 10 G in the drifting tube. For 1 eV electrons, χ_1<0.15. Simulations also showed that the field at the interaction region may be further increased if the soft iron pole piece is replaced by a cone-shaped permanent magnet while χ_1 is kept the same.

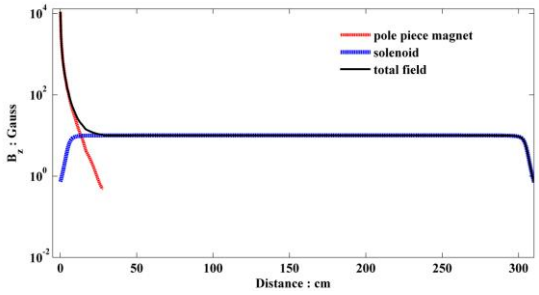

Fig. 1. Calculated magnetic field along z-axis (B_z).

In conclusion, we have designed a magnet and a pole piece to produce a non-uniform magnetic field with $B_f/B_i \approx 0.1\%$ and χ_1<0.15. The MBEES based on this field will be able to measure 0~150 eV electrons with 0.1% energy resolution and 2π-steradian acceptance angle, which guarantees a successful measurement for 25 as pulses. This material is supported by the U. S. Army Research Office under Grant No. W911NF-07-1-0475, and by the Chemical Sciences, Geosciences, and Biosciences Division, U.S. Department of Energy.

References

[1] M. Hentschel, *et al.*, Nature **414**, 509 (2001).
[2] P. Kruit and F. H. Read, J. Phys. E **16**, 313 (1983).
[3] M. Chini *et al.*, Appl. Phys. Lett. **94**, 161112 (2009).

[1] E-mail: chang@phys.ksu.edu

Combining Interferometer Locking with Delay Control in Attosecond Streaking Experiments

Michael Chini, He Wang, Hiroki Mashiko, Shouyuan Chen, Chenxia Yun, Steve Gilbertson, and Zenghu Chang[1]

J. R. Macdonald Laboratory, Kansas State University, Manhattan, KS, 66506-2604, USA

Synopsis: Attosecond streaking experiments suffer from the instability of the time delay between the attosecond pulse and streaking laser field due to fluctuating environmental conditions as well as mechanical vibration of the optical elements. The time delay is commonly introduced by splitting and recombining the XUV and NIR beams with interferometers. Here, we present a novel technique that is able to suppress the fast timing jitter while controlling the delay. Using this scheme, the streaked spectrogram of a single attosecond pulse was measured.

Single isolated few-cycle attosecond pulses have been characterized by the attosecond streaking technique using Mach-Zehnder [1, 2] and collinear [3] interferometer set-ups. Such systems rely on the ability to scan the delay between the extreme ultraviolet (XUV) attosecond pulse and the near infrared (NIR) streaking laser pulse in steps comparable to the duration of the attosecond pulse to be measured [4]. This is especially difficult in the Mach-Zehnder interferometer configuration, for which fluctuations in the environmental conditions as well as mechanical vibrations are likely to affect the optical path length difference between the two interferometer arms. In the past, we demonstrated that an interferometer can be locked with one piezoelectric delay stage (PZT) while the delay is changed by another PZT [2]. Here we show that the interferometer locking and delay change can be done using one PZT.

The experiment used a Mach-Zehnder interferometer attosecond streak camera [2]. A weak 532 nm CW laser beam was copropagated through both the attosecond generation arm and the streaking arm of the interferometer, and the two arms were recombined at a drilled mirror. The interference pattern of the green laser was detected by a CCD camera, and the relative phase and time delay were extracted by a computer. Figure 1(a) shows the time delay drift of the unlocked interferometer due to environmental conditions and mechanical vibrations.

The phase error signal was used for feedback control of a piezoelectric delay stage to suppress the fast jitter at a preset position for the targeted delay value. When the delay was set to a new value, the feedback loop stabilized the interferometer around that value. This technique also allows for fine control of the delay between the XUV and NIR pulses. As is shown in Figure 1(b), the time delay was scanned in steps of 280 as over a range of nearly 20 fs, less than 1/5 of the full range of the PZT stage, while the relative delay was locked to within 80 as RMS. This method was used for the measurement of a streaking trace from isolated attosecond pulses.

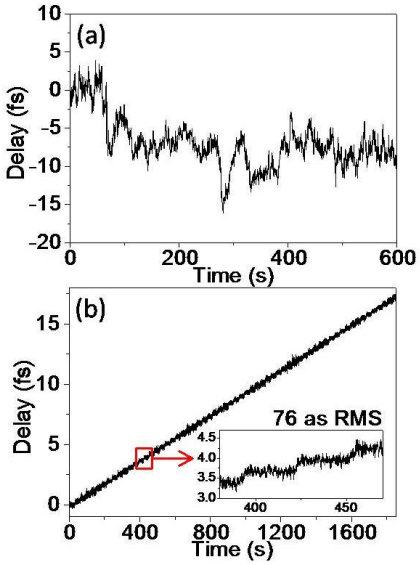

Fig. 1. (a) Time delay drift of free-running interferometer. (b) Time delay when locked and scanned.

In conclusion, by copropagating a CW laser beam through an attosecond streaking camera, the delay between the XUV and NIR pulses was controlled while maintaining interferometric stability of the system. Such a technique allows for complete control of the delay in attosecond pump-probe experiments.

This material is supported by the U.S. Army Research Office under grant number W911NF-07-1-0475 and by the Chemical Sciences, Geosciences, and Biosciences Division, U.S. Department of Energy.

References

[1] G. Sansone *et al.*, Science **314**, 443 (2006).
[2] Z. Chang, International Symposium on Ultrafast Laser Science 7, Kyoto, 24-28 November 2008.
[3] E. Goulielmakis *et al.*, Science **320**, 1614 (2008).
[4] M. Chini *et al.*, Appl. Phys. Lett. **94**, 161112 (2009).

[1] E-mail: chang@phys.ksu.edu

Ab-Initio Modeling of Attosecond Streaking Measurements

M. Korbman[a] [1], Y. Komninos[c], T. Mercouris[c], C.A. Nicolaides[c], F. Krausz[b] and V.S. Yakovlev[b]

[a]Max-Planck-Institute für Quantenoptik, Hans-Kopfermann-Str. 1, D-85748 Garching, Germany
[b]Department für Physik, Ludwig-Maximilians-Universität, Am Coulombwall 1, D-85748 Garching, Germany
[c]Theoretical and Physical Chemistry Institute, National Hellenic Research Foundation, Athens, Greece

Synopsis We model attosecond streaking measurement beyond the single-active-electron approximation. Our model takes advantage of the "state-specific-expansion approach", where a many-electron wave function is described within a basis of relevant atomic and ionic states.

The attosecond streak camera is currently one of the main tools of attosecond metrology. Its theoretical foundations were laid in [1], where a simple quantum-mechanical model was proposed. Within the single-active-electron approximation, this approach has successfully been used for the interpretation of attosecond streaking measurements. Recently, the accuracy and reproducibility of such measurements have dramatically improved [2]; also, angle-resolved streaking measurements are becoming accessible [3]. This demands more accurate and detailed modeling. To provide a realistic theoretical description of attosecond streaking measurements, and to clarify the limits of single-electron simulations, we have developed a model based on accurate atomic structure calculations. The electron correlation and the interaction of the photoelectron with the ion enter this model via matrix elements $D_{\mathrm{i,f}}(\mathbf{p}) = \langle\psi_{\mathrm{f}}(\mathbf{p})|\hat{D}|\psi_{\mathrm{i}}\rangle$ for dipole transitions from an initial atomic state $|\psi_{\mathrm{i}}\rangle$ to a final state $|\psi_{\mathrm{f}}(\mathbf{p})\rangle$. In this final state, the photoelectron is described by a scattering wave, while the state of the remaining ion is described by a set of quantum number (such as L_{ion} and M_{ion}), which we collectively denote by the index f. These matrix elements, evaluated with the aid the multi-configurational Hartree-Fock method [4], enter the conventional formalism describing laser-assisted photoionization by a short pulse of extreme ultraviolet (XUV) radiation. The probability density for observing a photoelectron with a momentum $\mathbf{p}$ is represented as an incoherent sum $S(\mathbf{p}) = \sum_{\mathrm{i,f}} S_{\mathrm{i,f}}(\mathbf{p})$ of contributions from individual channels, which we evaluate within the Coulomb-Volkov approximation:

$$S_{\mathrm{i,f}}(\mathbf{p}) = \left| \int_{-\infty}^{\infty} dt\, \mathcal{E}_{\mathrm{X}}(t) D_{\mathrm{i,f}}(\mathbf{p} + \mathbf{A}(t)) e^{i\Phi_{\mathrm{i,f}}(\mathbf{p},t)} \right|^2 . \quad (1)$$

Here, $\mathcal{E}_{\mathrm{X}}(t)$ is the envelope of the XUV pulse, $\mathbf{A}(t)$ is the vector potential of the streaking field, and the phase $\Phi_{\mathrm{i,f}}$ is defined as $\Phi_{\mathrm{i,f}}(\mathbf{p},t) = \left(\frac{p^2}{2} - W_{\mathrm{i,f}}\right) t - \int_t^{\infty} \left(\mathbf{p}\mathbf{A}(t') + \frac{1}{2}A^2(t')\right) dt'$ with $W_{\mathrm{i,f}}$ specifying the centers of photoemission lines for each of the channels.

While simpler models correctly describe the shift and broadening of photoelectron spectra induced by the streaking field, the knowledge of accurate angle-dependent transition matrix elements $D_{\mathrm{i,f}}(\mathbf{p})$ is required for a more detailed analysis. In particular, we study the role of the momentum-dependent phase of these matrix elements. Also, we investigate how the probability of observing a photoelectron is modulated by the streaking field and show that this modulation has a non-trivial angular dependence.

References

[1] M. Kitzler *et al.* Phys. Rev. Lett. **88**, 173904 (2002).

[2] E. Goulielmakis *et al.* Science **320**, 1614 (2008).

[3] J. Mauritsson *et al.* Phys. Rev. Lett. **100**, 073003 (2008).

[4] Th. Mercouris *et al.* Phys. Rev. A **50**, 4109 (1994).

[1]E-mail: michael.korbman@mpq.mpg.de

Attosecond Hard X-Ray Scattering Spectroscopy

G. L. Yudin[*,†], D. I. Bondar[†,§], S. Patchkovskii[†], P. B. Corkum[†,‡], A. D. Bandrauk[*]

[*]Université de Sherbrooke, Sherbrooke, Québec J1K 2R1, Canada
[†]National Research Council of Canada, Ottawa, Ontario K1A 0R6, Canada
[§]University of Waterloo, Waterloo, Ontario N2L 3G1, Canada
‡University of Ottawa, Ottawa, Ontario K1N 6N5, Canada

Synopsis We formulate an analytic, semi-relativistic theory of laser-assisted attosecond Compton scattering by a weakly bound electron. We (i) present the evidence of the feasibility of measuring the ground-state electron momentum density in the attosecond regime and (ii) investigate the attosecond Compton streak camera and spectral phase interferometry - proposing two new methods of measuring the duration of a hard x-ray pulse without fundamental restrictions on the measurement accuracy.

Very precise synchronization between the soft x-ray attosecond pulse and an intense laser field is prominent in attosecond science because the infrared field provides the nonlinearity needed for attosecond measurement of attosecond pulses [1].

Recent developments in ultrafast x-ray sources demonstrate that it is technically feasible to generate hard x-ray attosecond pulses in Ångström wavelength range [2] with free-electron lasers. At the very heart of these proposals is the temporal synchronization scheme between the free-electron and an external lasers, the so-called seeded attosecond x-ray radiation.

With the practical attosecond hard x-ray sources becoming available, it is essential to generalize the Compton profile theory to attosecond regime. It is also necessary to extend the ideas of attosecond streak camera (ASC) and spectral phase interferometry (ASPI) to the hard x-ray range. Transferring these techniques to laser-assisted Compton ionization is far from trivial. The photon is scattered, not absorbed, by the weakly bound electron, leading to a quite distinct theoretical description. In spite of the differences we will show that the Compton electron contains complete phase information on the incident pulse provided that we select the momentum of the scattered photon.

Starting with an *ab initio* method, we develop a theoretical approach to describe laser-assisted attosecond Compton ionization. To obtain the appropriate semi-relativistic scattering matrix, we generalize the theory [3] of monochromatic photon scattering by a bound electron and incorporate the separable Coulomb-Volkov continuum [4] into the Furry representation. We analyze the Compton ASC and ASPI and demonstrate the feasibility of measuring Compton profiles in attosecond laser-assisted regime. Compton electron spectra depend on the phase of the laser field relative to the x-ray attosecond pulse. Thus, the relative phase of all frequency components of the attosecond pulse can be determined from the spectrum of Compton electrons.

Once the x-ray pulse is characterized using a well understood atom such as hydrogen, a new frontier of attosecond science will be to utilize the Compton streak camera to measure unknown dynamics in target systems – nuclei, atoms, molecules or solids.

Once attosecond hard x-ray pulses are produced and synchronized to other optical sources, they will become powerful tools for following structure dynamics; each delay produces a single frame in an attosecond movie.

References

[1] J. Itatani *et al.*, Phys. Rev. Lett. **88**, 173903 (2002); M. Kitzler *et al.*, *ibid.* **88**, 173904 (2002); F. Quéré, *et al.*, *ibid.* **90**, 073902 (2003).

[2] See A. A. Zholents and M. S. Zolotorev, New J. Phys. **10**, 025005 (2008) and references therein.

[3] A. I. Akhiezer and V. B. Berestetskii, *Quantum Electrodynamics,* 3rd ed. (Nauka, Moscow, 1969).

[4] G. L. Yudin *et al.*, J. Phys. B **40**, F93, 2223 (2007); **41**, 045602 (2008).

Phase-matching of high-order harmonic generation in a semi-infinite gas cell geometry

Daniel S. Steingrube[*,†] [1], **Tobias Vockerodt**[*,†] [2], **Emilia Schulz**[*,†], **Uwe Morgner**[*,†,‡], and **Milutin Kovačev**[*,†]

[*]Institut für Quantenoptik, Leibniz Universität Hannover, Welfengarten 1, D-30167 Hannover, Germany
[†]QUEST, Centre for Quantum Engineering and Space-Time Research, Hannover, Germany
[‡]Laser Zentrum Hannover e.V., Hollerithallee 8, D-30419 Hannover, Germany

Synopsis Phase-matching of high-order harmonic generation in a semi-infinite gas cell geometry is investigated. A systematic study of experimental phase-matching conditions with variation of pressure and focus positions is performed for different focal lengths and in different rare gases. These results are compared to phase-matching simulations.

We study the high-order harmonic generation (HHG) by rare gases in semi-infinite gas cell (SIGC) geometry. This geometry features a straight-forward handling without the need for alignment procedures. Due to the large interaction region and the possibility of high densities, this scheme promises a high photon flux without limit to the pulse repetition rate in contrast to other geometries, i.e. pulsed gas jets.

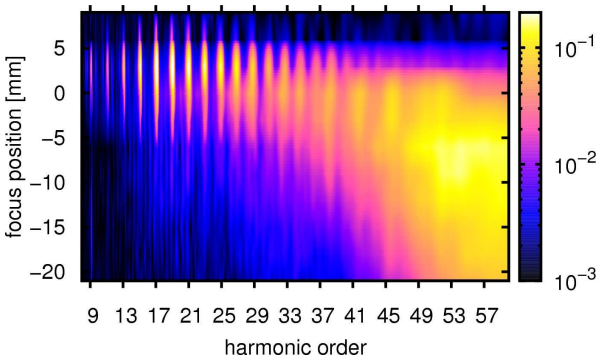

Fig. 1. Experimental map of harmonic yield versus harmonic order and focus position in a SIGC filled with helium.

A systematic study on experimental phase-matching conditions is performed which includes dependency on pressure and the focus position (see Fig. 1). The differences between the phase-matching conditions for a gas with high ionization potential, namely helium, and a gas with low ionization potential, namely xenon, is investigated. Since the gas pressure within the SIGC can be determined accurately, the experimental results can be directly compared to our results of phase-matching simulations (see Fig. 2). In simulations, the harmonic yield in the far field for a SIGC geometry is computed accounting for phase-matching using dipole data from the Lewenstein-model.

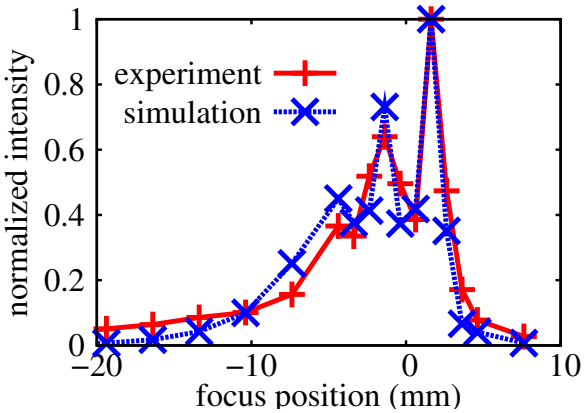

Fig. 2. Comparison of experimental and simulation results for HHG in helium in a SIGC. The harmonic intensity is recorded for various focus positions. For comparison, results from phase-matching simulations at comparable conditions are shown.

The phase-matching is investigated regarding the mentioned dependencies for different focusing. The emphasis of these studies places on short focal lengths to extend towards experimental conditions suited for low-energy pump pulses at high repetition rates. Due to the accurate knowledge and reproducibility of experimental condition in a SIGC, this scheme is a promising tool for the generation of isolated attosecond pulses.

[1]E-mail: steingrube@iqo.uni-hannover.de
[2]E-mail: vockerodt@iqo.uni-hannover.de

Wavelength Scaling of High Harmonic Generation Efficiency

A. D. Shiner*[,1], C. Trallero-Herrero*[,2], N. Kajumba*, H.-C Bandulet[†], D. Comtois[† 2], F. Légaré[†], M. Gigèure[†], J-C. Kieffer[†], P. B. Corkum*, and D. M. Villeneuve*

[*] National Research Council of Canada, 100 Sussex Drive, Ottawa, Ontario, K1A 0R6, Canada
[†] INRS- Énergie, Matériaux, 1650 boul. Lionel-Boulet, C.P. 1020, Varennes (Québec), J3X 1S2, Canada

Synopsis: We present a measurement of the dependence of xuv yield, from high harmonic generation, on laser wavelength. Parameters important to phase matching such as focusing geometry and mode quality were controlled and the measured HHG yield was normalized to the number of emitters in the interaction volume. We find that XUV yield scales as $\lambda^{-6.3\pm1.1}$ in Xe and $\lambda^{-6.5\pm1.3}$ in Kr at a constant laser intensity.

Using longer wavelength laser drivers for high harmonic generation is desirable because the highest XUV frequency scales as the square of the wavelength. Recent numerical studies predict that high harmonic effciency falls dramatically with increasing wavelength, with a very unfavorable $\lambda^{-(5-6)}$ scaling [1].

We performed an experimental study of the high harmonic yield over a wavelength range of 800-1850nm. A thin gas jet was employed to minimize phase matching effects, and the laser intensity and focal spot size were kept constant as the wavelength was changed.

Ion yield was simultaneously measured so that the total number of emitting atoms was known. By simultaneously measuring HHG and ionization we normalize to the number of emitters and isolate the single atom response.

We found that the scaling at constant laser intensity is $\lambda^{-6.3\pm1.1}$ in Xe and $\lambda^{-6.5\pm1.3}$ in Kr over the wavelength range of 800-1850nm, somewhat worse than the theoretical predictions. Our poster describes the experimental details, data analysis and results.

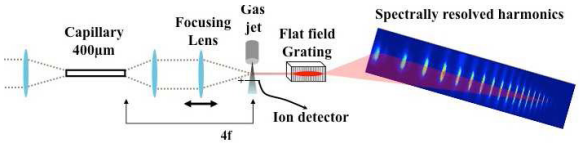

Fig. 1. Experimental layout.

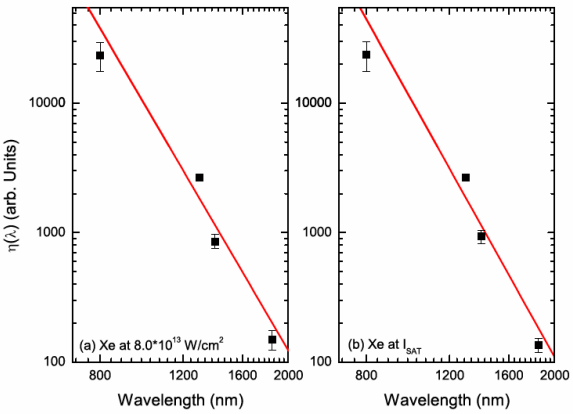

Fig. 2. Wavelength scaling of Xe.

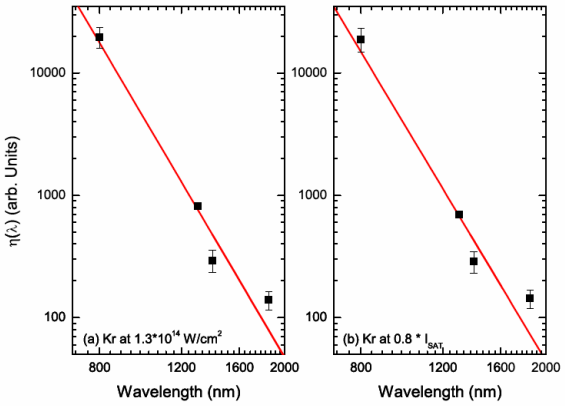

Fig. 3. Wavelength scaling of Kr.

References

[1] J. Tate, T. Auguste, H. G. Muller, P. Saliéres, P. Agostini, and L. F. DiMauro, *Phys. Rev. Lett.* **98** 013901 (2007).

[1] E-mail: andrew.shiner@nrc.ca
[2] E-mail: carlos.trallero@nrc.ca

Femtosecond enhancement cavities for high repetition rate HHG

D. C. Yost[1] **and Jun Ye**

JILA, National Institute of Standards and Technology and University of Colorado
Department of Physics, University of Colorado, Boulder, Colorado 80309-0440, USA

Synopsis High repetition rate high harmonic generation (HHG) has great potential as a source of XUV radiation with exceptional frequency resolution . We present progress in our ability to efficiently create this radiation within a passive optical cavity. This has enabled new tests of the temporal coherence of the harmonic radiation as well as fundamental studies of quantum paths in below-threshold harmonic generation.

Traditional methods for high harmonic generation (HHG) employ low repetition rate optical amplifiers. This low repetition rate produces a source with poor spectral resolution. To overcome this, we have pursued experiments in which broadband, femtosecond pulses are coupled into passive external cavities. This method enhances the pulse energy sufficiently to enable the HHG process without a decrease in the pulse repetition rate. The ability to conduct high repetition rate HHG ($\sim$ 100 MHz) has the potential to create a frequency comb in the XUV which possesses exceptional frequency resolution [1, 2].

To produce high harmonic radiation, we utilize a cavity enhanced 1070 nm ultrafast fiber laser. The laser supplies a train of $\sim$100 fs pulses at 136 MHz with up to 10 W of average power. Within the cavity, the average power is enhanced by a factor of 260. Curved mirrors produce a tight intracavity focal spot with a peak intensity of 4×10^{13} W/cm^2. We inject xenon gas at the intracavity focus to act as a nonlinear medium. An XUV diffraction grating written on a 1070 nm high reflector is utilized as one element of the enhancement cavity so that a portion of the generated harmonic radiation will diffract out of the cavity (efficiency$\sim$ 10%). This method allows the generation of harmonics up to the 21^{st} with individual outcoupled harmonic power of $\sim$50-1000 nW [3] (see Fig. 1).

The ability to conduct high-field studies at a high repetition rate has allowed several new studies of harmonic generation. By investigating below-threshold harmonics, we were able to discover multiple generation pathways with distinct intensity dependent optical phases. These intensity dependent phases were distinct in magnitude from those of above threshold harmonic generation and manifested themselves as oscillations in the harmonic yield as the driving intensity was varied. The high repetition rate has additionally allowed us to conduct tests of pulse-to-pulse coherence through which we were able to demonstrate that the coherence of the 7^{th} harmonic is maintained over at least 10 ns. The manipulation and control of these harmonics and their coherence properties is crucial for the future development of XUV frequency combs.

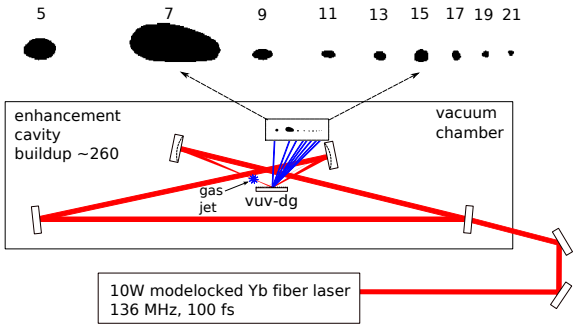

Fig. 1. Experimental setup. A cavity enhanced Yb fiber frequency comb is used to generate harmonics in Xe gas. A VUV diffraction grating (vuv-dg) is used to outcouple harmonic light. The inset shows beam profile of the diffracted harmonic orders.

We gratefully thank M. Gaarde, K. Schafer, J. Tate and J. Hostetter for theoretical support. Funding is provided by DARPA, NIST and NSF.

References

[1] R. J. Jones, K. D. Moll, M. J. Thorpe, and J. Ye, Phys. Rev. Lett. **94,** 193201 (2005).

[2] C. Gohle *et. al.*, Nature **436,** 235 (2005).

[3] D. C. Yost, T. R. Schibli and Jun Ye, Opt. Lett. **33**, 1099 (2008).

[1]E-mail: dylan.yost@colorado.edu

Highly stable, few-cycle, 2.2-μm optical parametric chirped pulse amplifier

Shu-Wei Huang*,[1], Jeffrey Moses*, Kyung-Han Hong*, Edilson L. Falcão-Filho*, Andrew Benedick*, Jeremy Bolger†, Benjamin Eggleton†, and Franz X. Kärtner*

* Department of Electrical Engineering and Computer Science and Research Laboratory of Electronics, Massachusetts Institute of Technology, Cambridge, MA 02139, USA
† CUDOS ARC Centre of Excellence School of Physics, University of Sydney, Sydney, Australia

Synopsis: We demonstrate a 10-GW peak power, 3-optical-cycle, CEP-stabilized, 2.2-μm OPCPA with 1-kHz repetition rate. Implementation of superfluorescence suppression techniques enables rms energy and intensity fluctuations of only 1.5% and 0.8%, respectively.

Since the prediction of high-yield soft X-ray photon generation through high harmonic generation (HHG) with long-wavelength drive pulses [1, 2], the development of high-power, few-cycle, carrier-envelope phase- (CEP-) stabilized sources in the mid-IR has attracted great attention. Ultra-broadband optical parametric chirped pulse amplification (OPCPA) is one of the promising techniques to meet the requirement for the driving source.

In this paper, we report on the development of a 2.2-μm OPCPA which generates 10-GW, 3-optical-cycle pulses (230 μJ, 23 fs) at 1 kHz. Several design features are implemented in our setup to suppress superfluorescence (SF), which is a critical issue for high-power mid-IR OPCPA systems [3, 4]. Especially, we carefully avoided loss in the stretching and introduced additional chirp between pre-amplification stages and power amplification stage to achieve high conversion efficiency, broad signal spectrum, and low SF simultaneously. SF suppression is evidenced by an unprecedented clean spectrum and low energy fluctuation. The current results suggest that this OPCPA design can be scaled to the multi-mJ energy level without SF taking over the signal, which will allow absorption-limited HHG in the water window.

Fig. 1 shows the amplified spectrum (a) and the corresponding interferometric autocorrelation trace (b) of the OPCPA system. The pulse is compressed nearly to its transform limit, i.e., 23 fs, or 3 cycles in FWHM. The CEP stability is characterized using an *f*-to-3*f* spectral interferometer and Fig. 1(c) shows that the rms phase fluctuation is ~150 mrad over 10 s, where the residual phase excursion at time = ~2 s is attributed to the amplitude–phase noise coupling in the *f*-to-3*f* interferometer while any significant drift is not observed during 10 s.

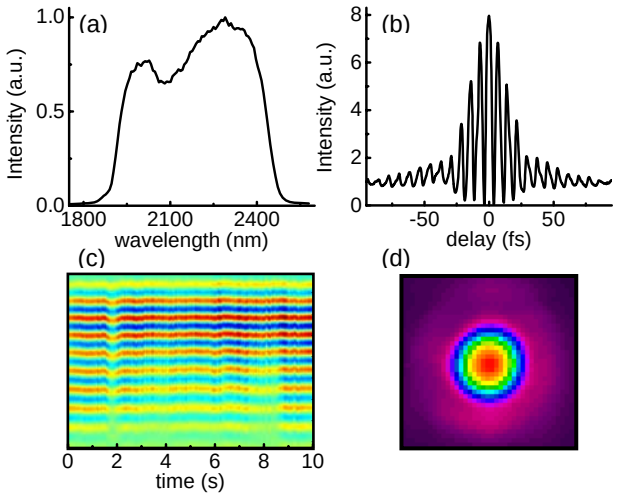

Fig. 1. (a) Amplified spectrum, measuring 500-nm FWHM in bandwidth. (b) IAC of the compressed pulse, measuring 23 fs (3 cycles). (c) *f-3f* spectral interferogram, measuring 150 mrad rms in CEP fluctuation. (d) Pyrolelectric CCD image of the output beam.

The SF level is estimated by measuring the energy fluctuation and the intensity fluctuation, followed by statistical analysis and is about 8%. With slightly less saturation in the power amplification stage, 170 μJ signal energy with SF reduced to 2%is obtained.

References

[1]B. Shan and Z. H. Chang, *Phys. Rev. A*, **65**, 011804 (2002).
[2]A. Gordon and F. X. Kärtner, *Opt. Express,* **13**, 2941 (2005).
[3]X. Gu, G. Marcus, Y. Deng, T. Metzger, C. Teisset, N. Ishii, T. Fuji, A. Baltuska, R. Butkus, V. Pervak, H. Ishizuki, T. Taira, T. Kobayashi, R. Kienberger, and F.Krausz, *Opt. Express,* **17**, 62 (2009).
[4]J. Moses, S.-W. Huang, K.-H. Hong, O. D. Mücke, E. L. Falcão-Filho, A. Benedick, F. Ö. Ilday, A. Dergachev, J. A. Bolger, B. J. Eggleton, and F. X. Kärtner, *Opt. Lett,* **34**, 1639 (2009).

[1] E-mail: klkla@mit.edu

Temperature feedback control for long-term carrier-envelope phase locking

Shouyuan Chen, Chenxia Yun, He Wang, Michael Chini, and Zenghu Chang [1]

JRM Laboratory, Kansas State University, Manhattan, KS, 66506-2604, USA

Synopsis: We report a double feedback loop to improve the long-term carrier-envelope phase stabilization of a chirped mirror based oscillator. By combining the temperature control of the Ti: Sapphire crystal and conventional pump power modulation, the carrier-envelope offset frequency f_{ceo} can be locked for 34 hours, which is many times longer than the stabilization time using pump power modulation only.

The long term carrier-envelop phase (CEP) lock is required in the single attosecond experiments since such experiments usually take many hours to collect sufficient counts to suppress the statistical noise [1]. It is a common practice to obtain CEP stable pulses from the oscillator by modulating the pump power with an acousto-optic modulator (AOM). Due to the change of environmental conditions in laboratories, f_{CEO} may drift out of the AOM locking range, which limits the f_{CEO} stabilization time. We proposed and demonstrated a temperature feedback scheme to compensate the slow f_{CEO} drift and extend the CEP stabilization duration.

The long-term CEP locking setup is shown in Fig. 1. The temperature of the Ti:Sapphire crystal was modulated to compensate the slow f_{CEO} drift. The control range of the AOM signal was set to be ± 0.1 V. When the feedback signal is beyond the limits of this control range, the chiller temperature was changed 0.1° C every 400 s to compensate the slow drift of the f_{CEO} until the AOM driving voltage was returned to the control range. We calculated a f_{CEO} change rate of $df_{CEO}/dK=0.86$ *MHz* for the 2 mm Ti: Sapphire crystal used in the oscillator from a temperature dependent Sellmeier equation [2]. It is close to the measured value of 0.77 *MHz/K*. Given the temperature control range of 8 °C, the temperature feedback can compensate a f_{CEO} drift of 6 MHz, which is comparable to the AOM control range.

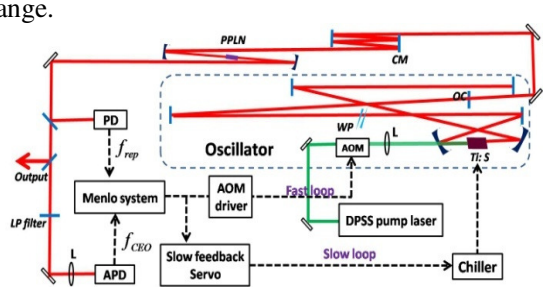

Fig. 1. Schematic of double feedback control for f_{CEO} locking.

As shown in Fig. 2, the CEP stabilization can reach 34 hours with the assistance of temperature control. On a daily basis, the CEP can be locked more than 12 hours using this scheme, about 3-4 times longer than the f_{CEO} locking time with AOM only in the same environment.

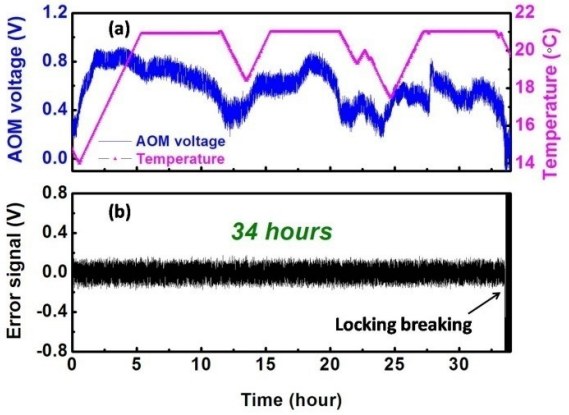

Fig. 2. (a) 34 hours CEP stabilization achieved by employing the double feedback loop; the blue curve shows the AOM driving voltage output; the pink curve shows the temperature of the crystal; (b) Error signal from locking electronics.

In conclusion, we improved the long-term CEP stability of a chirped mirror based oscillator by modulate the temperature of Ti:Sapphire crystal to assist the conventional AOM control. Without adding new optical elements or disturbing the operation of the oscillator, this scheme is compact, easy to operate, and economical.

This material is supported by the U. S. Army Research Office under Grant No. W911NF-07-1-0475, and by the Chemical Sciences, Geosciences, and Biosciences Division, U.S. Department of Energy.

References

[1] H. Wang, *J. Phys. B* **42**, (In Press).
[2] M. E. Thomas, *Infrared Phys. Tech.* **39** 235 (1998)

[1] E-mail: chang@phys.ksu.edu

Fractional Instability of a Phase Stabilized Carbon Nanotube Fiber Laser Frequency Comb

Jinkang Lim[1], Kevin Knabe[1], Yishan Wang[1,2], Rodrigo Amezcua-Correa[3], François Couny[3], Philip S. Light[3], Fetah Benabid[3], Jonathan C. Knight[3], Kristan L. Corwin[1], Jeffrey W. Nicholson[4], and Brian R. Washburn[1]

[1]116 Cardwell Hall, Department of Physics, Kansas State University, Manhattan, KS 66506, USA
[2]State Key Laboratory of Transient Optics and Photonics, Xi'an Institute of Optics and Precision Mechanics, PRC
[3]Centre for Photonics and Photonics Materials, Dept. of Physics, University of Bath, BA2, 7AY, UK
[4]OFS Labs, Somerset, NJ 08873 USA

Synopsis: A 167 MHz repetition frequency fiber ring laser employing single walled carbon nanotubes mode-locker is phase-stabilized for the first time. The stability of the frequency comb generated by this laser has been measured by comparing it with a figure eight laser (F8L) and by beating it against a 1532 nm CW laser stabilized to a $\nu_1+\nu_3$ overtone transition of an acetylene-filled kagome photonic crystal fiber reference. The result shows the stability of comb to be ~10^{-11} in 1 s averaging time.

Phase-stabilized fiber-laser based frequency combs are indispensable tools for optical frequency metrology. The erbium doped fiber ring laser is passively mode-locked using single walled carbon nanotubes (SWCN) as a saturable absorber. The SWCN are optically attached to a fiber connector [1]. In this way the laser shows a substantial simplicity in its design and relatively high repetition frequency (f_{rep}). Our carbon nanotube fiber laser (CNFL) has a 167 MHz repetition frequency and produces 1 mW of average power at 40 mW of pump power. The pulse trains are injected into a parabolic pulse amplifier which allows high power pulse amplification, and then a supercontinuum (SC) spectrum is generated with a highly nonlinear fiber [2-4]. The offset frequency (f_0) is detected using the f-2f self referencing method. The control of both f_0 and f_{rep} is accomplished in a similar manner as reported in prior work [5]. The f_{rep} was phase-locked using feedback control with piezo-electric transducer (PZT) fiber stretcher in the laser cavity. The f_0 was simultaneously phase-locked using feedback control of 980 nm pump power. The 10 MHz reference signal from a GPS disciplined Rb clock (Rb/GPS) referenced all synthesizers and frequency counters (Agilent 53132A). The CNFL comb was phase-locked over 4 hours while f_{rep} and f_0 were simultaneously counted and then their fractional instabilities were calculated. The f_{rep} dominates the stability of the optical frequency comb with ~0.4 mHz deviation at 1 s averaging time in the RF domain, corresponding to ~400 Hz in the optical frequency domain, similar to that of a F8L comb. The f_0 instability is negligible although the f_0 shows a wider linewidth and side peaks probably due to the lower operating pump power and phase noise. We beat the CNFL comb against a 1532 nm CW laser stabilized to a $\nu_1+\nu_3$ overtone transition of an acetylene-filled kagome photonic crystal fiber reference [6]. This measurement shows the instability of comb to be ~10^{-11} in 1 s averaging time limited by Rb/GPS (Fig. 1). At the longer averaging time, the stability is dominated by the acetylene reference.

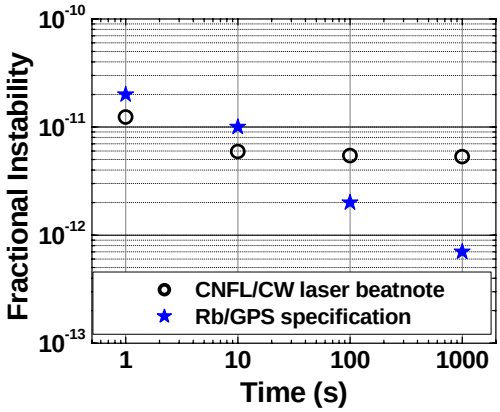

Fig. 1. The fractional instability of the beatnote between an acetylene stabilized CW laser and the CNFL frequency comb.

This research was supported by the AFOSR under contract No. FA9950-08-1-0020.

References

[1] J. W. Nicholson et al, Opt. Express **15, 9176-9183** (2007).
[2] J. W. Nicholson and D. J. DiGiovanni, IEEE Photon. Technol. Lett. **20**, 2123-2125 (2008).
[3] J. W. Nicholson et al, Opt. Lett. **28**, 643-645 (2003).
[4] Y. Wang et al, in *Proceedings of Frontiers in Optics*, *FWF5* (2008)
[5] D. J. Jones et al, Science **288**, 635-9 (2000).
[6] K. Knabe et al, in *Proceedings of Conference on Lasers and Electro-optics (CLEO), JFA5* (2008).

E-mail: washburn@phys.ksu.edu

Coupling between Energy and Carrier-Envelope Phase in Hollow-Core Fiber based *f*-to-2*f* Interferometers

He Wang, Michael Chini, Eric Moon, Hiroki Mashiko, and Zenghu Chang[1]

JRM Laboratory, Kansas State University, Manhattan, KS, 66506-2604, USA

Synopsis: The coupling coefficient between carrier-envelope phase and laser pulse energy is measured for white-light generation from a hollow-core fiber. It is determined that 1% fluctuation in laser energy gives a phase shift of 128 mrad.

For high power few-cycle laser pulse applications, the carrier-envelope (CE) phase plays a critical role. To produce such few-cycle pulses, spectral broadening in hollow-core fiber is typically followed by pulse compression. Previous work has suggested that the hollow-core fiber may introduce significant CE phase noise [1, 2]. However, it was unclear whether the measured CE phase instability was caused by the fiber itself or by measurement error caused by power instability. Here, we demonstrate a measurement of the coupling coefficient between laser pulse energy and CE phase drift for a hollow-core fiber without the ambiguity introduced by measurement based on white-light generation in sapphire.

The experiment was performed using the Kansas Light Source laser system. The 2 mJ, 35 fs pulses centered at 790 nm from the chirped pulse amplifier (CPA) were coupled to a 0.9 m long hollow-core fiber filled with neon gas. The output power and the CE phase of the CPA were locked [3, 4].

The effect of input laser energy fluctuations on the CE phase of the output pulses from a hollow-core fiber was studied using two *f*-to-2*f* interferometers. A variable neutral density (ND) filter was placed in front of the fiber entrance to modulate the input power. By rotating the ND filter periodically within a range of 5 degrees, the power was modulated within 10%. The in-loop hollow-core fiber based *f*-to-2*f* interferometer was used to stabilize the CE phase after the fiber, whereas the out-of-loop sapphire-based *f*-to-2*f* interferometer was used to simultaneously measure the CE phase of the unmodulated beam.

The in-loop CE phase shows a fluctuation of 107 mrad in Fig. 1(a), which is similar to the case without power modulation. Fig. 1(b) shows the anti-correlation between the in-loop power modulations and out-of-loop CE phase measurement. We assume that the out-of-loop CE phase drift is caused only by the modulation of the in-loop pulse energy in order to simplify the analysis. A linear least-squares fit of the data shows that a 1% change in input pulse energy introduced a CE phase drift of 128 mrad in Fig. 1(c).

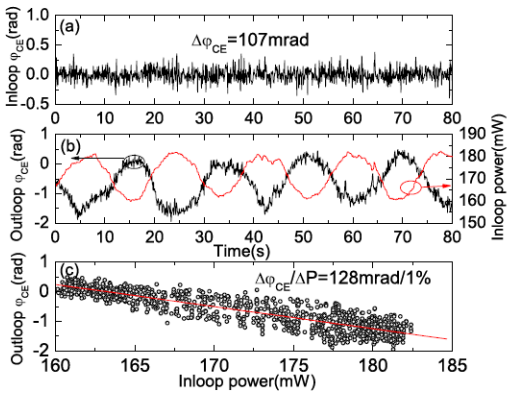

Fig. 1. (a) In-loop CE phase locked by a hollow-core fiber based *f*-to-2*f* interferometer; (b) Out-of-loop CE phase measured by a sapphire plate based *f*-to-2*f* interferometer and the in-loop power modulation; (c) CE phase change to laser power coupling coefficient by a least-square fitting.

In conclusion, we found that the hollow-core fiber based *f*-to-2*f* interferometer provided a higher accuracy of CE phase measurement. Understanding the CE phase properties of such fibers is crucial for attosecond pulse generation, ATI and other experiments at the frontiers of ultrafast science. This material is supported by the U. S. Army Research Office under Grant No. W911NF-07-1-0475, and by the Chemical Sciences, Geosciences, and Biosciences Division, U.S. Department of Energy.

References

[1] H. Mashiko *et al., Appl. Phys. Lett.* **90**, 161114 (2007).
[2] C. Li *et al., Opt. Lett.* **32**, 796 (2007).
[3] H. Wang *et al., Appl. Phys. B* **89**, 275 (2007)
[4] C. Li *et al., Opt. Lett.* 31, 3113 (2006)

E-mail: chang@phys.ksu.edu

An isolated short attosecond pulse produced by using intense few-cycle chirped laser and an ultraviolet attosecond pulse

Xiao-Xin Zhou[*] [1], **Song-Feng Zhao** [*†], **Peng-Cheng Li** [*], **Zhangjin Chen** [†]

[*]College of Physics and Electronic Engineering, Northwest Normal University, Lanzhou, Gansu 730070, China
[†]Department of Physics, Kansas State University, Manhattan, Kansas 66506, USA

Synopsis An efficient method to generate a short attosecond(as) pulse is presented by using an intense few-cycle chirped infrared(IR) laser in combination with an ultraviolet (UV) attosecond pulse. We show that high-order harmonic generation (HHG) plateau near the cutoff is enhanced by one order of magnitude compared with the chirped laser case and the HHG supercontinuum spectrum is generated by adding a UV attosecond pulse to the few-cycle chirped IR laser at a proper time. By enhancing the long quantum path and suppressing the short one corresponding to one major return, an isolated 57-as pulse with a bandwidth of 62 eV is obtained directly.

Attosecond extreme ultraviolet(xuv) pulse allows one to trace and probe ultrafast processes in atoms and molecules in real time. Thus much attempt has been made to obtain attosecond pulses in recent years [1, 2, 3, 4]. So far the HHG is the most promising way to generate attosecond pulses. Because it is very difficult to extract an isolated pulse from an attosecond pulse train, a great deal of effort has been devoted to produce an isolated attosecond pulse. One can obtain an isolated attosecond pulse by using a few-cycle laser [1], polarization gating technique [4], double optical gating [5]. Control of quantum paths is another fascinating way to produce an isolated broadband ultrashort attosecond pulse.

Based on the work of Carrera *et al.* [6], we propose a method to produce a short isolated broadband attosecond pulse by using an intense few-cycle chirped IR laser in combination with a UV attosecond controlling pulse. By enhancing the long quantum path and suppressing the short one correspond to one major return, an isolated 57-as pulse with a bandwidth of 62eV is obtained directly.

Fig.1. shows an isolated 57-as pulse with a bandwidth of 62 eV generated in a chirped IR laser in combination with a UV controlling pulse by superposing the harmonics from 60 ω_{IR} to 100 ω_{IR}. One can clearly see that the isolated attosecond pulse is very regular and the satellite peaks can be neglected.

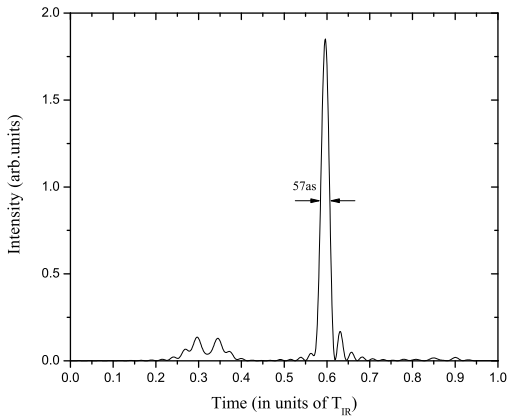

Fig. 1. The attosecond pulse of hydrogen atom in the chirped IR laser in combination with a UV pulse

References

[1] M. Hentschel et al., Nature (London) **414**, 509 (2001).

[2] M. Drescher et al., Science **291**, 1923 (2001).

[3] P. M. Paul et al., Science **292**, 1689 (2001).

[4] G. Sansone et al., Science **314**, 443 (2006).

[5] H. Mashiko, S. Gilbertson, C. Li et al., Phys. Rev. Lett. **100**, 103906 (2008).

[6] J. J. Carrera, and Shih-I Chu, Phys. Rev. A **75**, 033807 (2007).

[1]E-mail: xxzhou@nwnu.edu.cn

Multiple Ionic Channel Formulation for Strong Field Single Ionization of Multielectron Targets

Michael Spanner[1], **Serguei Patchkovskii, Julien Bertrand, and Hans Jakob Wörner**

Steacie Institute for Molecular Sciences, National Research Council of Canada, Ottawa, ON, Canada K1A 0R6

Synopsis We present a novel approach to calculating strong field ionization dynamics of multielectron molecular targets. Adopting a multielectron wavefunction ansatz based on field-free *ab initio* neutral and ionic multielectron states, a set of coupled time-dependent single-particle Schrödinger equations describing the neutral amplitude and continuum electron are constructed. These equations, amenable to direct numerical solution or further analytical treatment, allow one to study multielectron effects during strong field ionization, recollision, and high harmonic generation.

Present theoretical tools for calculating strong field ionization fall into two categories, 1) semianalytical theories based the Strong Field Approximation, often with improvements over the traditional formulation, and 2) direct time-dependent numerical solution of the Schrödinger equation. The first category suffers from approximations necessary to allow a semianalytical treatment, most notably the neglect of the binding potential of the molecular core on the ionization, continuum, and recollision dynamics. The second category has the shortcoming that full numerical treatment becomes impossible as the number of degrees of freedom increases. Time-dependent numerical solutions of the Schrödinger equation including a strong laser field is only feasible for one or two particle systems.

In this work we address both the problems of including the binding potential consistently throughout the strong field dynamics as well as the problem of accounting for multielectron effects. Our approach to strong field ionization of multielectron targets combines *ab initio* quantum chemistry multielectron wavefunctions with single particle time-dependent numerical solutions. Our derived equations coupling the neutral to the continuum electron follow directly from the multielectron Schrödinger equations and contain no adjustable parameters.

Figure 1 shows preliminary calculation and experimental results for the angle-dependent ionization yields from CO_2, where the angle is the angle between the molecular axis and polarization vector of the linearly polarized strong laser field. The theoretical plots show the ionization yield for different final states of the CO_2^+ cation (colored curves) as well as the total yield summed over all these channels (black curve). The experimental curves show analogous angle-dependent ionization yields. In the experimental plots, the red line is the measured yield for a distribution of aligned CO_2 molecules and the green curve shows the molecular frame angle-dependent yields obtained by deconvolving the measure yields from the distribution of molecular alignment. Comparison should be made between the black theoretical curves and the green experimental curves. The theoretical calculations capture the symmetries and trends seen in experimental yields as the intensity is varied. In our formulation it is necessary to include multiple final ion states (i.e. the multielectron nature of the problem) in order to approach the experimental results.

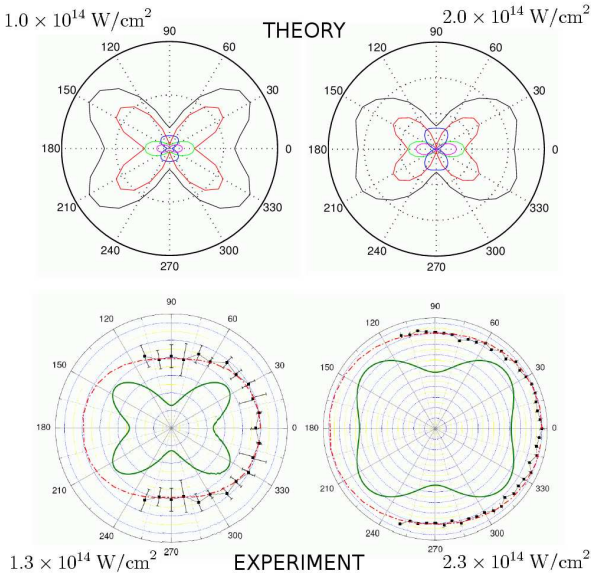

Fig. 1. Theoretical and experimental angle-dependent ionization yields for CO_2.

[1]E-mail: michael.spanner@nrc.ca

Ultrafast Molecular Dynamics Probed Using Strong Field Ionization

Wen Li, Vandana Sharma, Craig Hogle, Agnieszka Jaron-Becker, Andreas Becker, Henry Kapteyn and Margaret Murnane

JILA and Department of Physics, University of Colorado, Boulder, CO, 80309, USA

Synopsis: We report preliminary measurements using strong field ionization to monitor the photodissociation of bromine molecules. The time dependent kinetic energy release (KER) of bromine cations (Br^+) was used to identify the molecular cation states (Br_2^+),which contribute to the production of Br^+. We observe a strong angular dependence of the Br^+ yield, representing the shape of the ionizing molecular orbital. The time evolution of the angular distribution of Br^+ was also obtained. This is the first experimental demonstration of using strong field ionization to monitor orbital rearrangement during a chemical reaction.

Electronic dynamics play a central role in chemical reactions. It is very desirable for a detection technique to have the capability of probing ultrafast electronic motion. Time resolved photoelectron spectroscopy (TRPES) [1] can provide some insights. However, the most direct information - such as mapping electron configurational changes in real time - remains elusive. Recently, strong field ionization has been demonstrated as a probe of the static electron density distribution of the HOMO orbital[2][3]. Here we report preliminary results that use strong field ionization as a probe to study electron rearrangement during the photodissociation of bromine.

The experiment was carried out using a cold target recoil ion momentum spectroscopy (COLTRIMS) apparatus. A neat bromine molecular beam enters the vacuum chamber through supersonic expansion. The photodissociation is initiated by 400 nm ultrafast laser pulses produced by second harmonic generation of the fundamental laser output. Absorption of one 400 nm photon excites the bromine from the ground state to the C ($^1\Pi_u$) dissociative state. An intense, time-delayed, 800 nm laser beam is used to ionize the dissociating bromine molecules to produce Br^+. The momentum distributions of Br^+ at different pump-probe delays are then recorded. Figure 1 shows the kinetic energy release of Br^+. By comparing these data with theoretical calculations, we conclude that the slow Br^+ at early time delay is generated from states arising from removing an electron from a π_u orbital, while the fast Br^+ at later time delays are from ionization of an σ_g orbital.

The yield of fast Br^+ reaches a maximum when the angle between the Br-Br internuclear axis and the probe laser polarization is zero, and monotonically decreases when the angle increases. This is in good agreement with theoretical predictions if a σ_g orbital is ionized. The time evolution shows a narrowing angular dependence of Br^+ yield, which also matches preliminary theoretical calculations.

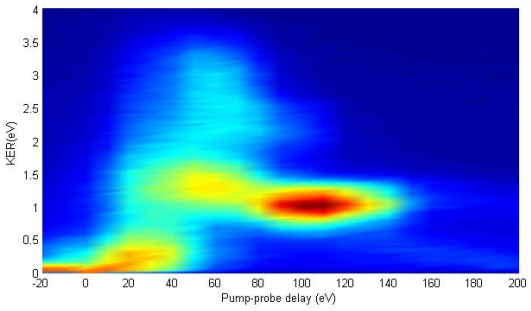

Fig. 1. Time dependent KER of Br^+.

It is also interesting to note that the Br^+ yield peaks around 100 fs (Fig. 1). At this time delay, the Br-Br internuclear distance reaches about 4.2 Angstroms. The origin of this enhancement of the ionization is unclear. Charge resonance enhanced ionization (CREI) is one possible explanation.

In summary, we demonstrate that strong field ionization can be used as a probe of molecular dynamics, in particular of electron rearrangement during a chemical reaction.

References

[1] A. Stolow, *Adv. Chem. Phys.*, 139, 497 (2008).
[2] M. Meckel, *Science*, 320, 1478 (2008)
[3] C.D. Lin, *J. Photochem. Photobiol., A*, 182,213 (2006)

E-mail: wli@jilau1.colorado.edu

SINGLE MOLECULE LASER INDUCED NUCLEAR FUSION,LINF,IN SUPERINTENSE LASER FIELDS

Andre D Bandrauk, Canada Research Chair
Universite de Sherbrooke,Que,J1K 2R1,Canada
and
Gennady K Paramonov
Institut fur Chemie und Biochemie
FU Berlin, 14195,Berlin,Germany

Previous work on single molecule quantum dynamics in superintense static electric [1] and laser fields [2-3] has suggested that one can achieve particle (electron,proton,etc) collision energies and currents comparable with large scale accelerators.We show in the present study the importance of Carrier Envelope Phase (CEP) of current and future ultrashort superintense laser pulses in controlling recollisison processes in the muonic molecular systems du-d,du-t,pu-t, and even in proton-antiproton systems,p+p-p+, at intensities up to I=10**23 W/cm2,ie, below the above barrier breakup intensities.Complete quantum dynamic simulations, beyond Born-Oppenheimer,are used to show the importance of the dipole moments of the nonsymmetric systems such as du-t,pu-t,in enhancing particle recollisions with energies sufficient for LINF.This suggests new methods of carrying out LINF by interaction of ultrashort(few cycles) superintense laser pulses with single molecules of elementary particles.

[1]. J R Hiskes, Phys Rev 122,1207 (1961).
[2].S Chelkowski,A D Bandrauk,P B Corkum,Phys Rev Lett. 93,083602(2004).
[3]. N Milosevic,P B Corkum,T Brabec, Phys Rev lett 92,013002(2004).

Counterintuitive angular shifts in the photoelectron momentum distribution for atoms in strong few-cycle circularly laser pulses

C. P. J. Martiny[1], **M. Abu-samha**[2], **L. B. Madsen**[3]

LTC, Department of Physics and Astronomy, Aarhus University, Aarhus, 8200, Denmark

Synopsis We have recently developed a method for solving the time-dependent Schrödinger equation for a diatomic molecule (atom) interacting with a strong few-cycle elliptically polarized laser pulse. Here we present the first fully ab initio calculations of the photoelectron momentum distributions for a circularly polarized laser pulse interacting with an atom. Furthermore, we provide a precise quantum mechanical explanation of counterintuitive shifts in the dominant direction of electron ejection, observed in a recent experiment [P. Eckle et.al. Science **322**, 1525 (2008)]. Our results underline the importance of including both the laser field and the Coulomb interaction in the description.

There has recently been a growing interest in the ionization of atom and molcules by intense few-cycle elliptically polarized laser pulse. This motivates the development of applicable theory in this regime.

We have recently developed a method for solving the TDSE for a diatomic molecule (or atom) interacting with a strong few-cycle elliptically polarized laser pulse. The method is an extension of the method presented in [1] to the case of a general elliptically polarized pulse. It is based on the fact that the Hamiltonian is sum of operators cylindrically symmetric around different axis.

Here we present the first fully *ab-initio* calculations of the photoelectron momentum distributions for a few-cycle circularly polarized pulse interacting with an atom. Based on these calculations, we are able to provide a precise quantum mechanical explanation of the conterintuitive angular shifts in the dominant direction of electron ejection, observed in a recent experiment [2]. The dominant direction of ejection does not coincide with the axis defined by the vector potential at field maxima, as predicted by standard theories like the strong-field approximation (SFA) or the ADK tunneling theory.

A comparison with the commonly used SFA reveals an important short-coming of the SFA (ADK tunnelling theory) for a few-cycle circularly polarized laser pulse interacting with an atom. Our results clearly reveal the importance of including the combined effects of the Coulomb and laser fields in the desription.

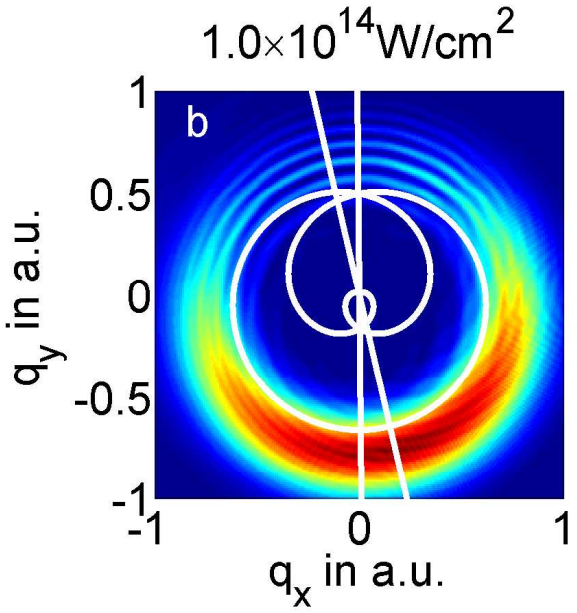

Fig. 1. Momentum distributions in the plane of polarization $dP/dq_x dq_y dq_z|_{q_z=0}$ for strong-field ionization of H(1s). The curves shows the vectorpotential with opposite sign, while the straight lines in highlight the angular shift (see text). The 800 nm, $I = 10^{14}\mathrm{W/cm}^2$ laser field is circularly polarized, and contains 3 optical cycles

References

[1] T. K. Kjeldsen et.al., Phys. Rev. A. **75**, 063427 (2007).

[2] P. Eckle et.al., Science. **322**, 1525 (2008).

[1]E-mail: chrfys@phys.au.dk
[2]E-mail: mahmoud@phys.au.dk
[3]E-mail: bojer@phys.au.dk

Manipulating the torsion of molecules by strong laser pulses

C. B. Madsen[*,1], **L. B. Madsen**[*], **S. S. Viftrup**[†], **M. P. Johansson**[†], **T. B. Poulsen**[†], **L. Holmegaard**[†], **V. Kumarappan**[†], **K. A. Jørgensen**[†], **H. Stapelfeldt**[†]

[*]Lundbeck Foundation Theoretical Center for Quantum System Research, Department of Physics and Astronomy, Aarhus University, 8000 Aarhus C, Denmark

[†]Department of Chemistry, Aarhus University, 8000 Aarhus C, Denmark

Synopsis In recent years the manipulation of molecules by strong laser pulses has attracted much attention. Non-resonant laser fields apply torques on molecules, due to the interaction between the induced dipole moment and the laser field itself. This has proven very useful for controlling both external and internal degrees of freedom of molecules. We extend the use of strong non-resonant laser fields to manipulation of the torsion in a molecule. Specifically, we consider the laser induced dynamics of the two phenyl rings of a biphenyl molecule.

Many studies during the last decade have shown that strong non-resonant laser fields can effectively manipulate the external degrees of freedom of isolated gas phase molecules. The manipulation results from laser-induced forces and torques due to the interaction between the induced dipole moment and the laser field itself. Examples of manipulation include deflection, focusing and slowing of molecules through the dependence of the non-resonant polarizability interaction on the intensity distribution in a laser focus. Likewise, the dependence of the induced dipole interaction on molecular orientation has proven highly useful for controlling the rotation of a variety of molecules. In particular, the spatial orientation of molecules can be sharply confined with respect to axes that are fixed in the laboratory. Molecular manipulation by induced dipole forces extends beyond the external degrees of freedom and has also been demonstrated for the internal degrees of freedom such as vibrational motion in molecular hydrogen.

In the case of larger molecules control of the lowest frequency vibrational modes attracts special interest since some of these modes correspond to motion along well-defined reaction coordinates separating two conformational minima (conformers). Although many molecules contain large number of conformers it is often just two conformers that dominate important chemical properties, for instance chirality. A particularly important example is found in axially chiral molecules such as biaryl systems. In these molecules rotation about a single stereogenic carbon-carbon (C-C) bond axis changes the molecule from one enantiomer into the opposite enantiomer (mirror image).

We demonstrate that the laser-induced non-resonant polarizability interaction can also be used to influence the internal rotation of an axially chiral molecule around the stereogenic C-C bond axis (cf. Fig. 1). In particular, we show that by fixing the C-C bond axis of a substituted biphenyl molecule in space, using laser induced alignment by a long laser pulse, it is possible to initiate torsional motion of the two phenyl rings by a short laser pulse polarized perpendicular to the fixed axis.

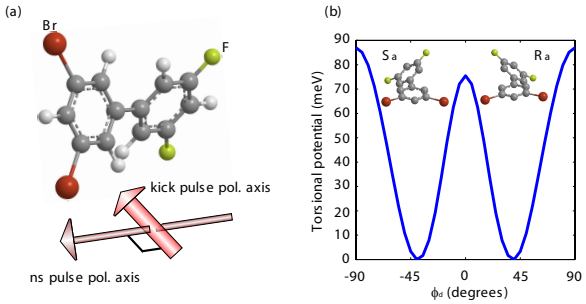

Fig. 1. (a) Model of the substituted biphenyl and the laser geometry of the experiment. (b) The torsional potential as a function of the dihedral angle, ϕ_d, between the two phenyl rings. The minima at $\phi_d = \pm 39°$ result in the R_a and S_a enantimomers.

On the basis of these results we discuss future applications of laser induced torsion, viz., time-resolved studies of de-racemization and laser controlled molecular junctions based on molecules with torsion.

References

[1] Madsen et al. PRL **102**, 073007 (2009).

[1]E-mail: cbm@phys.au.dk

The onset of asymmetry in electron angular distributions for dissociative photoionization of H_2 by ultrashort xuv laser pulses

J. F. Pérez-Torres[*,], F. Morales[*], J. L. Sanz-Vicario[† 1] and F. Martín[* 2]

[*]Departamento de Química, Universidad Autónoma de Madrid, 28049 Madrid, Spain
[†]Grupo de Física Atómica y Molecular, Instituto de Física, Universidad de Antioquia, Medellín, Colombia

Synopsis A method to compute angular distributions for electrons ejected from fixed-in-space molecular hydrogen when exposed to ultrashort xuv laser pulses is proposed based on the ab initio solution of the time-dependent Schrödinger equation. This method allows for a temporal picture of the origin of the asymmetry in the electron angular ejection that arise due to the interference of the two symmetric dissociative ionization channels ($1s\sigma_g$ and $2p\sigma_u$) in which molecular autoionization states decay after photon absorption.

The recent arrival of COLTRIMS reaction microscopes [1] allows for kinematically complete experiments in which the momentum of all ejected photofragments is measured in coincidence after the breakup caused by a laser pulse. For the dissociative photoionization of molecular hydrogen ($H_2+\hbar\omega \rightarrow H^+ + H + e^-$), COLTRIMS gives access to measure proton kinetic energy distributions (KEDs) and photoelectron angular distributions (PADs) associated to a given molecular orientation with respect to the laser polarization direction. This technique is abel to detect the direction along the molecular axis in which the proton H^+ is emitted. This means that by detecting the localization of the ejected H^+, COLTRIMS does not respect the inversion symmetry of the molecule. To satisfy the conditions imposed by the experiment, the aymptotic behaviour of the molecular wavefunction must be modified, in particular when two ionization channels (for instance H_2^+ $1s\sigma_g$ and $2p\sigma_u$) are degenerated at $R\rightarrow\infty$. In our time-dependent method [2], the H_2 wavefunction is expanded in terms of vibronic eigenstates including the continuum for the two H_2^+ ionization channels $1s\sigma_g$ and $2p\sigma_u$. To satisfy the localization condition for the proton emission, the final wavepacket at $t\rightarrow\infty$ (long after the laser pulse of duration T is ended) must be projected onto the correct asymptotic function which results into a entanglement of the amplitudes coming from $1s\sigma_g$ and $2p\sigma_u$ ionization channels and ultimately producing asymmetries in the PADs with respect to nuclei inversion.

Figure 1 shows proton KEDs and PADs for protons emitted at 90^0 with respect to the laser polarization vector for some proton KEDs. The symmetry breaking of PADs emerges along the pulse duration for proton KEDs at ~ 4 eV where the $1s\sigma_g$ and $2p\sigma_u$ contributions interfere, in agreement with stationary results [3].

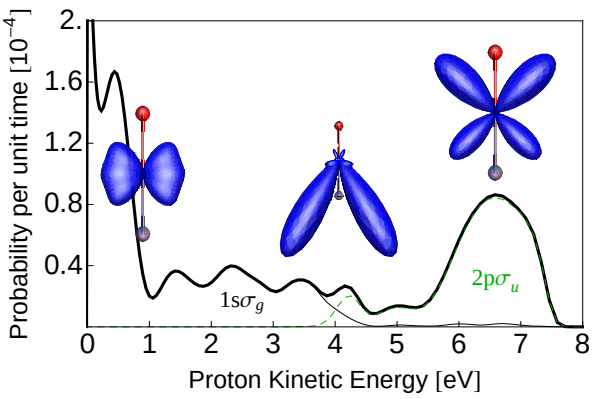

Fig. 1. H_2 exposed to a xuv laser pulse with photon energy E=33eV, intensity I=10^{12} W/cm^2 and duration T=10 fs. Thick solid line: Total ionization probability, thin solid line: contribution from $1s\sigma_g$ ionization channel, thin dashed line: from $2p\sigma_u$ ionization channel. Insets: PADs (in blue) for protons (upper red spheres) measured at 90^0 with respect to polarization axis corresponding to proton kinetic energies 0.9, 4.1 and 6.6 eV.

References

[1] Ulrich J *et al* 2003 *Rep. Prog. Phys.* **66** 1463

[2] Sanz-Vicario J L, Bachau H and Martín F 2006 *Phys. Rev. A* **73** 033410

[3] Martín F *et al* 2007 *Science* **315** 629

[1]**E-mail:** sanjose@fisica.udea.edu.co
[2]**E-mail:** fernando.martin@uam.es

Electron localization following attosecond molecular photionization

F. Kelkensberg[*], G. Sansone[†], M.F. Kling[‡], W. Siu[*], O. Ghafur[*], P. Johnsson[*], M. Swoboda[◇], E. Benedetti[†], F. Ferrari[†], F. Lépine[○], S. Zherebtsov[‡], I. Znakovskaya[‡], M. Yu. Ivanov[•] J.F. Pérez[⋆], F. Morales[⋆], J.L. Sanz-Vicario[⋆], F. Martin[⋆], M. Nisoli[†], M.J.J. Vrakking[1*]

[*]FOM-Institute AMOLF, Science Park 113, 1098 XG Amsterdam, The Netherlands
[†]CNR-INFM, National Laboratory for Ultrafast and Ultraintense Optical Science, Department of Physics, Politecnico of Milan, Piazza Leonardo da Vinci 32, 20133 Milano, Italy
‡Max-Planck Institut für Quantenoptik, Hans-Kopfermann-Strasse 1, D-85748 Garching, Germany
◇Department of Physics, Lund University, P.O. Box 118, SE-221 00 Lund, Sweden
○Université Lyon 1;CNRS;LASIM, UMR 5579, 43 bvd. du 11 novembre 1918, F-69622 Villeurbane, France
•National Research Council of Canada, 100 Sussex Drive, Ontario K1A 0R6 Ottawa, Canada
⋆Departamento de Química, Universidad Autónoma de Madrid, 28049 Madrid, Spain

Synopsis Observation and control of electron dynamics on attosecond timescales are the main driving forces behind the recent emergence of attosecond science. In this experiment an isolated attosecond laser pulse ionizes D_2. and part of the ionized molecules dissociate. Interaction of these dissociating wave packets with a moderately strong IR field localizes the electron on one of the D^+ ions. By varying the delay between the XUV pulse and the few-cycle IR pulse, the localization is controlled with attosecond resolution. A detailed comparison between the experiment and a full-dimensional model is presented.

Using attosecond laser pulses, experiments can be conceived where electron dynamics is initiated on attosecond timescales. Subsequently, the electrons are allowed to evolve and are probed (again, on an attosecond timescale), providing new insights into the fundamentals of photoexcitation, as well as the role of electron-electron correlations and electron-nuclear energy transfer on these ultrafast timescales. A technical breakthrough that has been very influential and that has greatly improved the ability to generate attosecond laser pulses in a controlled manner, was the development of amplified femtosecond laser systems with a controlled carrier-envelope-phase (CEP) in 2003 [1]. This enabled the controlled generation of isolated attosecond laser pulses with a pulse duration down to the present record of 80 attoseconds [2]. In addition, CEP-stable pulses have been used to control atomic ionization and the localization of electrons in D_2^+ molecules [3]. In this experiment an isolated attosecond laser pulse ionizes D_2, and part of the ionized molecules dissociate. Isolated attosecond pulses are produced by means of high-harmonic generation in Krypton using the polarization gating technique [4]. Due to the wide photon energy spectrum (20-40 eV) associated to the attosecond pulse, a large manifold of continuum as well as autoionizing states are populated. Several interfering pathways are then possible, direct dissociative and non dissociative ionization as well as autoionization from the Q_n doubly excited states.Interaction of these dissociating wave packets with a moderately strong IR field localizes the electron on the upper or lower D^+ ion. By varying the delay between the XUV pulse and the few-cycle IR pulse the localization is controlled with attosecond resolution. To include all possible ionization pathways a full dimensional model is developed for the interaction of the molecule with the XUV-IR pulse sequence. We will present a detailed comparison between this theory and the experimental results. It will be also shown that the essence of the electron localization can be understood in terms of a few discrete transitions between the quasi-static states of the dissociating molecule.

References

[1] A. Baltuska et. al., Nature **421**, 611 (2003).
[2] E. Goulielmakis et. al., Science **320**, 1614 (2008).
[3] M.F. Kling et. al., Science **312**, 246 (2006).
[4] I.J. Sola et. al., Nature Physics **2**, 319 (2006).

[1]E-mail: vrakking@amolf.nl

Time-Resolved Molecular Fragmentation at FLASH

Y.H. Jiang[1,*], A. Rudenko[2], M. Kurka[1], K.U. Kühnel[1], M. Toppin[1], O. Herrwerth[3], M. Lezius[3], M. Kling[3], L. Foucar[4], M. Schöffler[4], K. Cole[4], B. Ullrich[4], N. Neumann[4], R. Dörner[4], J. Pérez-Torres[5], E. Plésiat[5], F. Martín[5], A. Cassimi[6], S. Düsterer[7], R. Treusch[7], M. Gensch[7], C. D. Schröter[1], R. Moshammer[1], J. Ullrich[1,2]

[1] Max-Planck-Institut für Kernphysik, 69117 Heidelberg, Germany; [2] Max-Planck Advanced Study Group at CFEL, 22607 Hamburg, Germany; [3] Max-Planck-Institut für Quantenoptik, 85748 Garching, Germany; [4] Institut für Kernphysik, Universität Frankfurt, 60486 Frankfurt, Germany; [5]Departamento de Química C-9, Universidad Autónoma de Madrid, 28049, Spain; [6] CIRIL at Ganil, Caen, France; [7] DESY, 22607 Hamburg, Germany

Synopsis: Multiple ionization and fragmentation of D_2 and N_2 induced by absorption of few photons have been explored in pump-probe measurements at the free electron laser at Hamburg. Photoionization of aligned N_2^+ ions, produced in sequential step, is explored by inspecting the kinetic energy releases and the fragment-ion angular distributions as function of the pump-probe delay time.

Multiple ionization of molecules induced by absorption of few extreme ultra-violet (EUV) photons represents one of the most fundamental non-linear molecular processes. Free electron lasers, delivering coherent pulses of EUV-photons with femtosecond durations at unprecedented intensities, in combination with advanced multi-particle detection systems − the Heidelberg reaction microscope [1] – open a new era in molecular physics. Here we present first results of few photon induced fragmentation of D_2 and N_2, and EUV-pump/EUV-probe experiment.

The measurements were performed at photon energies of 38, 44 and 46 eV, with pulse durations of ≅30 fs, and intensities of $I \cong 10^{13}$ W/cm^2 at FLASH (the free-electron laser at Hamburg).

Sequential and direct two-photon double ionization (DI) of D_2 molecule is studied experimentally and theoretically at 38 eV [2]. Experimental and theoretical kinetic energy releases (KER) of D^++D^+ fragments, consisting of the contributions of sequential DI via the $D_2^+(1s\sigma_g)$ state and direct DI via a virtual state, agree well with each other. The modulation of KER spectra presents first experimental evidence on nuclear interference between direct and sequential DIs, where two photons are absorbed simultaneously and sequentially (with certain time-delay) within one pulse, respectively.

At 44 eV we studied multiple ionization of N_2 induced by absorption of up to 5 photons leading to dominant sequential ionization mechanisms [3]. For various intermediate charge states N_2^{n+} we find a considerable excess of photons absorbed compared to the minimum number that would energetically be required. Rich-structured patterns in the KER-dependent fragment ion angular distributions highlighting alignment-dependent multi-photon absorption and ionization dynamics allowing us to trace SI pathways in details for some of the channels.

Very recently, we succeeded in performing a pump-probe experiment on multiple ionization of N_2 using a multilayer spilt-mirror setup. In Fig. 1 the kinetic energies of N^{2+} ions, resulting from two dissociation channels, namely $N_2^{2+} \rightarrow N^{2+}+N$ (E_{KER}<6 eV) and $N_2^{3+} \rightarrow N^{2+}+N^+$ (E_{KER}>6 eV), are plotted vs. the pump-probe delay time (identical pulses, 46 eV). A very sharp structure (~10 fs FWHM) in the time trace for E_{KER}>10 eV at zero delay (Fig. 1b) might be due to highly nonlinear ionization. Further results and interpretations will be presented.

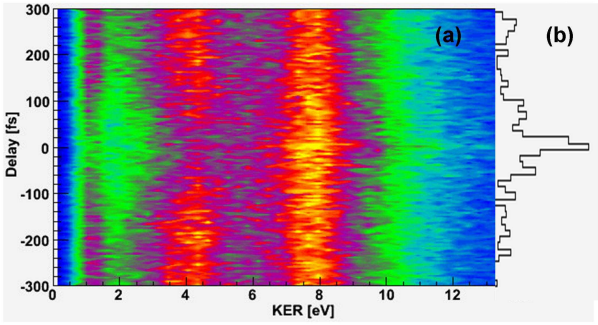

Fig. 1: (a) Kinetic Energies of N^{2+} fragments as function of the time delay between pump and probe pulse. (b) Time trace for events with E_{KER}>10 eV.

YHJ thanks for support from DFG project no JI 110/2-1. Production of multi-layer mirrors by the group of M. Vrakking is acknowledged.

References

[1] J. Ullrich *et al*, Rep. Prog. Phys. **66** 1463 (2003)
[2] Y.H. Jiang *et al*. (in preparation)
[3] Y. H. Jiang *et al*, Phys. Rev. Lett.**102** 123002 (2009)

* E-mail: yuhai.jiang@mpi-hd.mpg.de

Intense-Field Ionization of Cyclic Hydrocarbon Molecules Measured with Spatial Resolution of Focal Ion Distributions

Timothy Scarborough*[,1], James Strohaber[†], David Foote*, and Cornelis Uiterwaal*[,2]

[*] University of Nebraska - Lincoln, Department of Physics and Astronomy, Lincoln, NE 68588-0111, USA
[†] Texas A&M University, Physics Department, College Station, TX 77843-4242, USA

Synopsis: We present experimental results of fully three-dimensionally resolved ion yields for benzene and benzene-like molecules, including some heterocyclic compounds. Full spatial resolution of the ion yields allows circumvention of the "volume effect", in which ions are collected from the entire laser focus at a variety of intensities. As a result of avoiding this effect, our ion yields very closely resemble the true ionization probability, and have allowed us to clearly measure resonance-enhanced multiphoton ionization processes (REMPI).

We present experimental results of spatially-resolved ion densities of benzene and other benzene-like molecules through the use of a "photodynamical test tube" which circumvents volumetric weighting of the laser focus (the volume effect) [1]. Within the volume of the test tube the laser intensity is essentially constant, resulting in ion yield measurements very near to the true ionization probability of the target molecule.

Using laser radiation with a central wavelength of 800 nm and pulse duration of 50 fs focused to intensities of 10^{13} to 10^{15} W/cm^2, we recorded experimental evidence of resonance-enhanced multiphoton ionization (REMPI) processes in benzene, fluorobenzene, chlorobenzene, bromobenzene, and iodobenzene. For all these molecules we observe a six-photon process and a three-photon resonance, which we believe to be the result of the saturation of an intermediate resonant state ($S_0 \rightarrow S_1$).

In addition, we present results of the ionization and fragmentation of the six-member-ring aromatic hydrocarbons toluene (C_6H_5-CH_3), aniline (C_6H_5-NH_2), nitrobenzene (C_6H_5-NO_2), and phenol (C_6H_5-OH), as well as three five-member-ring aromatic heterocycles: thiophene (C_4H_4S), furan (C_4H_4O), and pyrrole (C_4H_4NH). These molecules display a richer behavior than the halogenated benzenes mentioned above; we believe we have observed effects such as a lowered continuum in aniline, a possible shifted resonant intermediate state in phenol, and multiple saturated resonant states in furan. Recent experimental progress and theoretical interpretations will be presented.

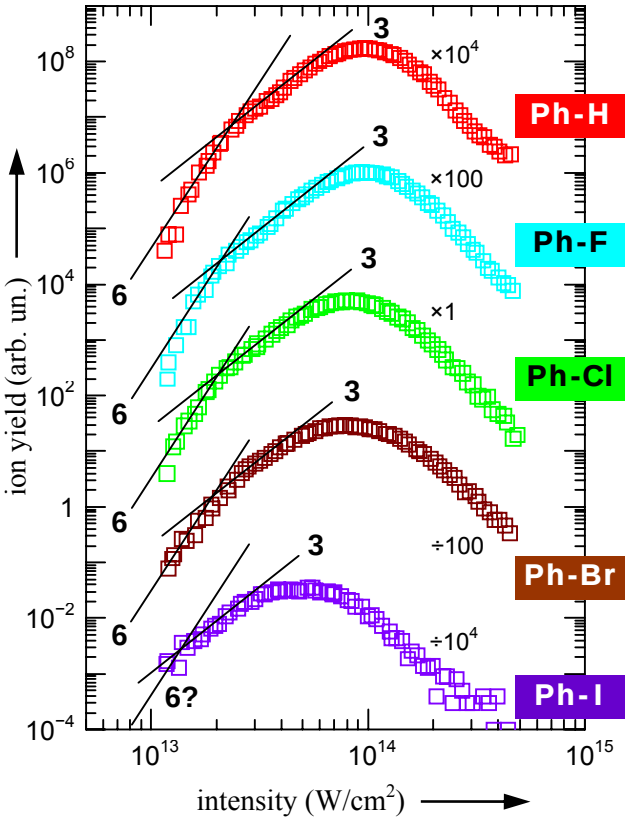

Fig. 1. Measured ion yields of the halogenated benzene series showing (3+3) REMPI processes. The ion yields have been recorded without integrating over the focus.

Reference

[1] J. Strohaber and C.J.G.J. Uiterwaal, "*In situ* measurement of three-dimensional ion densities in focused femtosecond pulses," *Phys. Rev. Lett.* **100,** 023002 (2008). — Highlighted in *Science* **319,** 699 (Editor's Choice, 8 Feb. 2008).

[1] E-mail: tim.scarborough@huskers.unl.edu
[2] E-mail: cuiterwaal2@unl.edu

Electron localization in molecular fragmentation with CEP stabilized laser pulses

Bettina Fischer*[,1], Manuel Kremer*[,2], Bernold Feuerstein*, Vitor L.B. de Jesus[‡], Artem Rudenko[†], Claus Dieter Schröter*, Robert Moshammer* and Joachim Ullrich*

* Max-Planck-Institut für Kernphysik, 69117 Heidelberg, Germany
[†] Max-Planck Advanced Study Group at CFEL, 22607 Hamburg, Germany
[‡] Instituto Federal do Rio de Janeiro – IFRJ, 26530-060 Nilópolis-RJ, Brazil

Fully differential data on dissociating H2 molecules in ultrashort (~6 fs), linearly polarized, intense (~0,4 PWcm-2) laser pulses with stabilized carrier-envelope-phase (CEP) have been measured using a reaction microscope. Depending on the CEP of the laser pulses we see a clear asymmetry in the emission direction of the created protons. Contrary to earlier measurements by Kling et al. [1] we observe the largest asymmetry in a kinetic energy release (KER) range between 0-3 eV. This excludes the recollision mechanism suggested in [1] and requires another explanation.

Recent experiments [1] showed the possibility to measure and even control electron localization in the dissociating D_2^+ molecular ion by intense, ultrashort, CEP controlled laser pulses.

In contrast to these earlier asymmetry measurements that have been performed by using velocity map imaging, we used a reaction microscope [3] that allows us to reconstruct the full three dimensional momentum vectors of all outgoing (charged) particles. Furthermore, measuring electrons and ions in coincidence facilitates a channel separation that is not accessible by other techniques.

For measuring the asymmetry in the proton (deuteron) emission direction, it is useful to define the so called asymmetry parameter $A=(N_{up}-N_{down})/(N_{up}+N_{down})$, where N_{up} (N_{down}) is the number of protons emitted to the upper (lower) hemisphere, respectively.

The result of our experiment is shown in Fig. 1. Here, the asymmetry parameter is plotted as a function of the KER of the dissociating H_2^+ and the CEP of the ultrashort laser pulse. Contrary to [1] we see clear changes in the asymmetry for different CEP in a KER range between 0-3 eV similar to predictions in [3]. Furthermore we see a tilt in the asymmetry stripes that was not observed for the fragments at higher energy measured in [1], where the stripes were vertical. By looking at different emission angles α of the H_2 molecule relative to the laser polarization axis the tilted stripes shift with respect to the CEP.

This behavior can not be explained by the model introduced by Kling et al. who observed KERs between 6-16 eV resulting from the rescattering of the first electron with the H_2^+.

The low energy fragments observed here however can be attributed to bond softening. The CEP-dependent asymmetry is introduced by the coupling of the $1s\sigma_g$ and $2p\sigma_{u\ s}$ states of the H_2^+.

We performed one dimensional TDSE calculations, which qualitatively reproduce our experimental results.

An asymmetry in the electron emission was also observed but did not show any relation to the asymmetry observed in the proton emission.

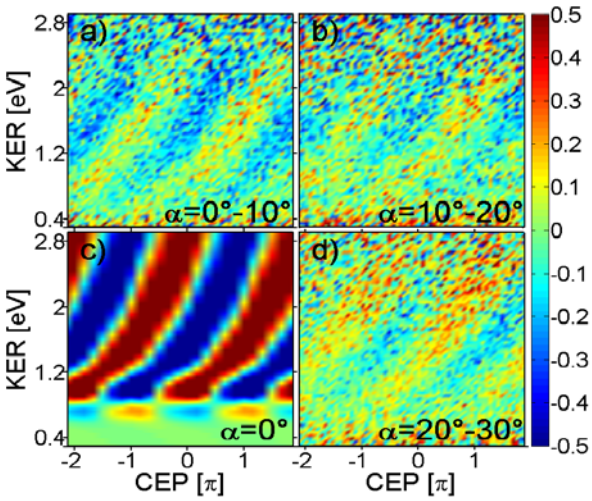

Fig. 1. Asymmetry parameter A in dependence of the proton energy and the CEP for (a) emission angles between 0°-10° and (b) between 10°-20° (d) between 20°-30° with respect to the laser polarization axis. (c) Result of the TDSE calculation for an emission angle of 0° .

References

[1] Kling M F et al., Science **312** 246 (2006)
[2] de Jesus V L B et al., J. Electron Spectrosc. Relat. Phenom. **141** 127 (2004)
[3] Roudnev V and Esry B D, PRA 76, 023403 (2007)
[4] Hua J J and Esry B D, J. Phys. B 42 085601 (2009)

[1] E-mail: Bettina.Fischer@mpi-hd.mpg.de
[2] E-mail: Manuel.Kremer@mpi-hd.mpg.de

Vibrationally cold CO^{2+} probed by intense femtosecond laser pulses

J. McKenna*, A. M. Sayler*, B. Gaire*, Nora G. Johnson*, M. Zohrabi*, F. Anis*, U. Lev†, K. D. Carnes*, B. D. Esry*, and I. Ben-Itzhak*, [1]

*J. R. Macdonald Laboratory, Physics Department, Kansas State University, Manhattan, Kansas 66506, USA
†Department of Particle Physics, Weizmann Institute of Science, Rehovot, 76100, Israel

Synopsis Using a novel approach, we produce a vibrationally cold CO^{2+} beam for study in an intense ultrashort laser field. We observe perpendicular dissociation of the simple two-level CO^{2+} v=0 ion and above-threshold dissociation peaks spaced by the photon energy.

H_2^+ seems the ideal candidate to study ultrashort intense laser-molecule interactions since its simple one-electron structure allows it to be treated accurately by theory. This is aided by the fact that at low intensity ($<5\times10^{13}$ W/cm^2) it may be approximated as a two electronic state system. However, as recently pointed out by Posthumus *et al.* [1], vibrational excitation of H_2^+, with the population often unknown, can severely complicate its dynamics in an intense laser field. This makes experimental observation, and study, of important laser-induced phenomena such as bond-softening and above-threshold dissociation (ATD) more difficult and confusing.

Ion traps are currently used to vibrationally cool H_2^+ [2]. Alternatively, we present novel measurements of intense field dissociation of vibrationally cold CO^{2+}, which is in many respects a similar target to cold H_2^+. Our method involves production of CO^{2+} ions, by electron-impact in an ion source, that predissociate during their travel ($\sim$20 μs transport time) to the laser interaction region — leaving a pure target of v=0 ground state CO^{2+} molecules. Laser-induced fragmentation of CO^{2+} is measured by 3D momentum imaging of the C^+ and O^+ fragments detected in coincidence [3].

Specifically, we demonstrate that cold CO^{2+}, like H_2^+, can be considered as a two-state system at low intensity (involving only its lowest triplet states). This allows some of the important theoretical foundations developed for H_2^+ to be applied and tested on this more complex multielectron system. Work along these lines will be presented in this poster. Moreover, as the CO^{2+} initial state is well-defined, we observe sharp peaks in the kinetic energy release from dissociation [Fig. 1(a)], attributable to one- and two-photon processes, measured for both 790 nm and 395 nm wavelengths. Interestingly, unlike H_2^+ where dissociation occurs for molecules predominantly aligned to the laser polarization [Fig. 1(c)], CO^{2+} displays the opposite behavior, showing a preference to be aligned perpendicular to the laser polarization [Fig. 1(b)] due to the nature of the dominant dissociative transition.

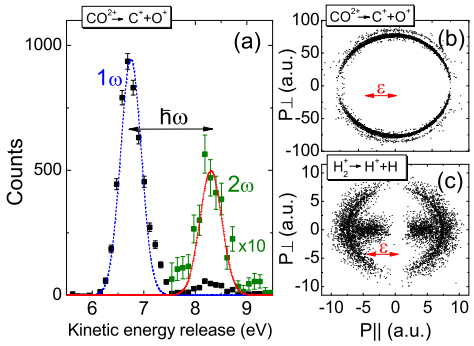

Fig. 1. (a) Kinetic energy release and (b,c) angular distributions for dissociation of CO^{2+} and H_2^+ at 2×10^{15} W/cm^2. The angle θ is between the molecular dissociation axis and the laser polarization. $P_{||}$ and $P_\perp$ denote momentum parallel and perpendicular to the laser polarization, respectively.

This work is supported by the Chemical Sciences, Geosciences, and Biosciences Division, Office of Basic Energy Sciences, Office of Science, U.S. Department of Energy.

References

[1] J.H. Posthumus *et al.*, Phys. Rev. Lett. **101**, 233004 (2008).

[2] P.A. Orr *et al.* Phys. Rev. Lett. **98**, 163001 (2007).

[3] I. Ben-Itzhak *et al.* Phys. Rev. Lett. **95**, 073002 (2005).

[1] E-mail: ibi@phys.ksu.edu

Electron release dynamics in double ionization of Ar and Ne by elliptically polarized laser pulses

A. N. Pfeiffer*[,1], C. Cirelli*, M. Smolarski*, R. Dörner[†], U. Keller*

[*] Physics Department, ETH Zurich, 8093 Zürich, Switzerland
[†] Institut für Kernphysik, Johann Wolfgang Goethe Universität, 60438 Frankfurt am Main, Germany

Synopsis: Elliptically polarized laser pulses are suitable to investigate double ionization isolated from electron recollision effects. For Ar and Ne we observe a characteristic transition in the momentum spectra of the doubly charged ions when the laser peak intensity is varied across the over-barrier intensity of the second ionization level. We find a qualitative agreement of our data with a simulation based on sequential double ionization and interpret our observation as a sensitive fingerprint of depletion.

Double ionization of atoms exposed to strong laser fields can occur via sequential mechanisms, where the electrons interact independently with the laser field, and non-sequential mechanisms, where the electrons cannot be treated separately. For linear polarization, the dominating non-sequential mechanisms involve recollision of the first ionized electron with the remaining ion. Elliptical polarization excludes rescollision, and therefore allows focusing on non-recollision mechanisms.

Laser pulses with a duration of 5.5 fs and a center wavelength of 720 nm were focused onto cold Ar and Ne atoms inside a COLTRIMS setup. The ellipticity was adjusted to about 0.8 with an achromatic quarter-waveplate and the peak intensity was varied from about 5 to 60 x 10^{14} W/cm^2. Whereas the momentum distribution of the doubly charged ions parallel to the major axis of the polarization ellipse (x-axis) is always close to gaussian, the projection onto the y-axis shows a characteristic dependence on intensity (Fig 1): For low intensities the distribution exhibits 3 peaks, whereas high intensities result in a 4-peak structure. An explanation for the 4-peak distribution was given by [1].

We found our observation to be consistent with a simulation based on ADK rates and sequential electron release. Due to depletion the release time of the electrons is shifted from the pulse center towards the beginning of the pulse with increasing peak intensity. Because the depletion is different for the two ionization levels, the average time between the successive ionization steps grows, which causes the center peak in the momentum distribution to split. The characteristic intensity for this transition is the over-barrier intensity for the second ionization level, which is 11.7 x 10^{14} W/cm^2 for Ar.

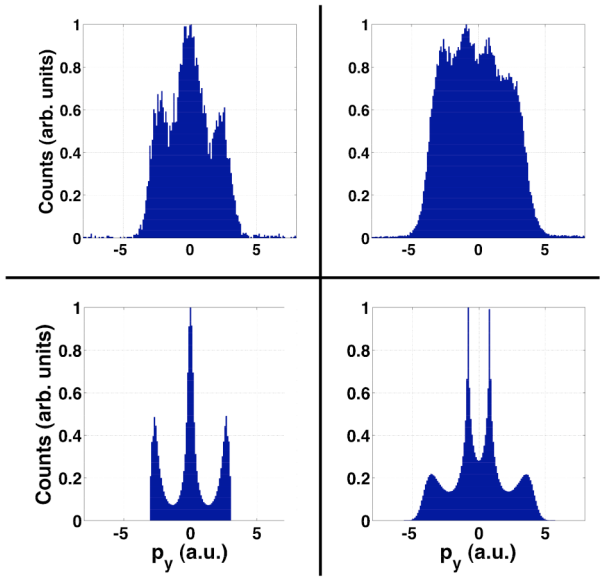

Fig. 1. Momentum spectra of doubly charged Ar ions. Upper panel: Data for low (left) and high (right) intensity. Lower panel: Simulation for 8 x 10^{14} W/cm^2 (left) and 40 x 10^{14} W/cm^2 (right).

The positions of the peaks are reasonably well reproduced by the simulation, and the discrepancies might stem from simplifications in the simulation. Further investigation of potential electron correlation will clarify the validity of the sequential electron release in different intensity regimes.

References

[1] C.M. Maharjan *et al.*, Phys. Rev. A **72**, 041403 (2005).

[1] E-mail: apfeiff@phys.ethz.ch

Auger decay in krypton induced by attosecond pulse trains and twin pulses

Christian Buth[1], **Kenneth J. Schafer**[2]

Department of Physics and Astronomy, Louisiana State University, Baton Rouge, Louisiana 70803, USA

Synopsis: Using attoscience, we study the electron correlations responsible for Auger decay in krypton atoms. The Auger decay is induced by a pulse train or a twin pulse composed of subpulses of attosecond duration. During the Auger decay an optical dressing laser may be present. Interference effects between the ejected Auger electron wave packets are predicted.

Attosecond science aims at studying and controlling the motion of electrons on their natural time scale. The investigation of electronic motion has so far been restricted mostly to one-electron processes. One of the first applications of attoscience was the measurement of the Auger decay time of 3d vacancies in krypton atoms—a well-known datum from frequency-domain spectroscopy—with a single attosecond pulse in the presence of an optical streaking laser.

In the present work, we examine the Auger electron spectrum of krypton induced by an arbitrarily shaped XUV light pulse with and without an optical dressing laser. Specifically, we consider Auger decay after

1. a train of attosecond pulses with a set duration between the pulses and
2. an attosecond twin pulse with varying time delay between the subpulses: an archetypical interference experiment.

The first point refers to a proposed experiment, which will repeat the measurement of the Auger decay lifetime of krypton 3d vacancies with pulse trains [1]. A train produces a stronger signal than a single pulse and enhances the signal to noise ratio in an experiment. Further a train of pulses leads to electron wave packet interference of the wave packets launched by different pulses. An additional optical streaking laser facilitates the control and measurement of the resulting signal. The second point proposes an experiment with a simpler setting compared with a pulse train. Additional flexibility is added by varying the time delay between the two attosecond pulses. Predictions of the second setting are displayed in Fig. 1. The upper panel shows the attosecond twin pulse and the exponential decay of the Auger population from a rate equation model in the time domain. After a pulse, the population of inner-shell ionized atoms decays exponentially. The lower panel shows the Auger electron spectrum from our quantum dynamical model [2,3], if the photoelectron energy is observed in coincidence with the Auger electrons with the stated energy resolution. We predict interference between the two ejected Auger electron wave packets.

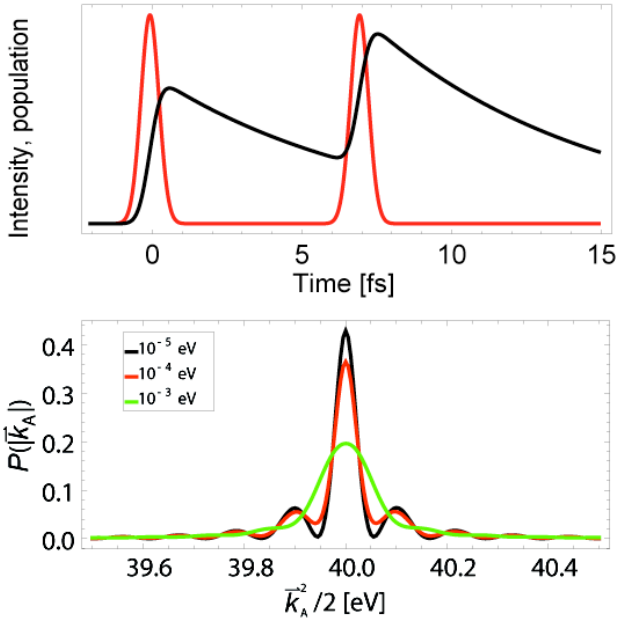

Fig. 1. (Color) Upper panel: intensity of an XUV twin pulse (red) and the krypton 3*d* hole population (black). Lower panel: probability density of Auger electrons with momentum $\vec{k}_A$ in the opposite direction of the linear XUV polarization vector for three energy resolutions of the photoelectron measurement.

In conclusion, our proposed experiments are very fundamental; they represent a crucial test for attoscience: to what degree can we measure and control an electronic process in the time domain?

References

[1] J. Mauritsson, private communication (2009).
[2] C. Buth and K. J. Schafer, in preparation (2009).
[3] O. Smirnova, V. S. Yakovlev and A. Scrinzi, *Phys. Rev. Lett.* **91**, 253001 (2003).

[1] E-mail: christian.buth@web.de
[2] E-mail: schafer@phys.lsu.edu

Photoelectron emission from atoms by ultra-short pulses: Impulse Coulomb-Volkov description.

M.S. Gravielle[*,†,1], D.G. Arbó[*], and J.E. Miraglia[*,†]

[*] Instituto de Astronomía y Física del Espacio, CONICET, C.C. 67, Suc. 28, 1428 Buenos Aires, Argentina.
[†] Dpto. de Física, FCEN, Universidad de Buenos Aires, Argentina

Synopsis: Ionization of atomic targets produced by ultra-short laser pulses is studied within a distorted-wave formalism. We introduce the Impulse Coulomb-Volkov (ICV) approximation, which makes use of the Volkov phase to describe the action of the electromagnetic field on both the initial and final channels. Here photoelectron emission from hydrogen is used as a benchmark for the theory, comparing the results to values derived from the numerical solution of the time-dependent Schrödinger equation (TDSE). We found the ICV method represents an improvement over the CV approach for laser frequencies lower than the initial electronic energy.

As a consequence of recent developments of laser facilities, photoelectron emission from atomic targets induced by strong and ultra-short laser pulses has been the subject of intense theoretical and experimental research in the last few years [1].

To describe this process, in addition to the numerical solution of the time-dependent Schrödinger equation, a considerable number of distorted-wave approaches have been proposed. Most of them are based on the use of the Coulomb-Volkov wave function to represent the final channel, while the initial channel is considered as unperturbed.

In this work we calculate the Impulse Coulomb-Volkov (ICV) approximation, which introduces the electron-laser interaction in the initial and final channels, both on equal footing. Within the ICV approach the final distorted state is represented with the Coulomb-Volkov wave function, while the initial state is described by means of ICV wave function given by Eq. (7) of Ref. [2]. This function takes into account the complete Volkov distortion of the initial bound state, satisfying the proper asymptotic conditions.

The method is applied to evaluate the ionization probability of hydrogen targets, considering different frequencies and durations of the laser pulse. In Fig. 1 and 2 we show ICV results for electromagnetic fields in the multi-photon and collisional regimes respectively, comparing them to values obtained from the numerical solution of the TDSE and the CV approximation.

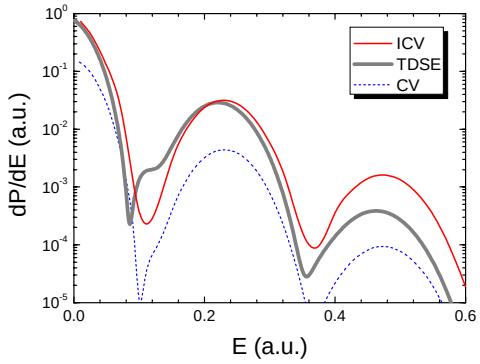

Fig. 1. Electron energy spectra of hydrogen for a six-cycle laser pulse with a field strength $E_0 = 0.05$ a.u. and a carrier frequency ω=0.25 a.u.

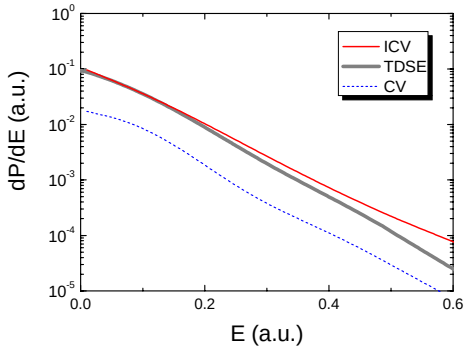

Fig. 2. Similar to Fig. 1 for a pulse with $E_0 = 0.05$ a.u., ω=0.25 a.u., and a duration τ=40 a.u.

References

[1] D.B. Milošević *et al.*, *J. Phys. B* **39** R203 (2006).
[2] P. A. Macri *et al.*, *J. Opt. Soc. Am. B.* **20** 1801 (2003).

[*,†,1] E-mail: msilvia@iafe.uba.ar

Electron emission from metal surfaces by ultra-short pulses

M. N. Faraggi[1], I. Aldazabal[1,2], M. S. Gravielle[3], A. Arnau[1,4] and V. M. Silkin[1,2]

[1]Donostia International Physics Center, (DIPC), Manuel de Lardizabal 4, San Sebastián, Spain.
[2]Centro de Física de Materiales CSIC-UPV/EHU, San Sebastián, Spain.
[3]Instituto de Astronomía y Física del Espacio and Fac. Cs. Exactas y Naturales, Univ. of Buenos Aires, Argentina.
[4]Departamento de Física de Materiales, Facultad de Química UPV/EHU, San Sebastián, Spain.

Synopsis: We study electron emission spectra produced by the grazing incidence of ultra-short laser pulses on metal surfaces. To describe this process we introduce a distorted-wave approach, based on a simple description of the solid, which includes the main features of the process, taking into account the contribution of the induced potential. The method is applied to evaluate photoemission from the valence band of Al(111), considering different frequencies and durations of the pulse. The results so obtained are contrasted with the numerical solution to the time-dependent Schrödinger equation (TDSE), finding a very good agreement through the whole energetic range.

In the last few years developments in the time domain of laser pulses have made it possible to reduce the durations of them up to sub-femtosecond scale. This fact opens up the study of electron dynamics at surfaces to a new dimension [1,2]. Here, we investigate photoelectron emission produced when an ultra-short laser pulse impinges grazingly on a metal surface.

The problem is described by means of a one active electron model developed in the framework of the time-dependent distorted wave formalism [3]. The proposed theory, called *Surface Jellium Volkov* (SJV) approximation makes use of the Volkov phase to represent the interaction of the active electron with the external and induced fields, while the surface potential is described within the jellium model. The induced surface potential is produced by the rearrangement of the valence-band electrons due to the presence of the external electromagnetic field and it is evaluated with a linear response theory.

To verify our approximation we test the SJV results with the numerical solution to the time-dependent Schrödinger equation (TDSE). In Fig. 1 we show, for both method, photoelectron emission spectra originated from the valence band of a typical metal surface, as Al(111). To complete the study, in Fig. 2 we plot the SJV momentum distribution for the same laser parameters of Fig. 1.

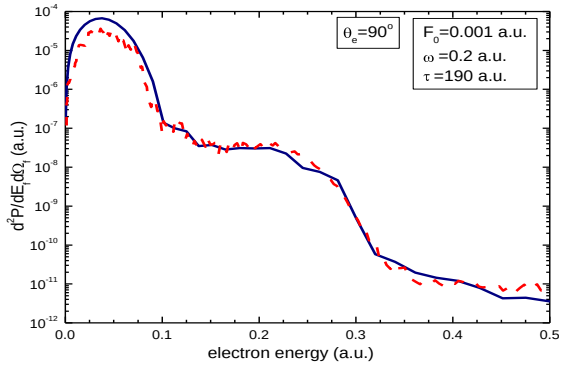

Fig. 1: Electron emission probability, as a function of the electron energy, for the ejection angle θ_e=90°. Solid (blue) line: SJV model; dash (red) line: TDSE results. Laser parameters: F_0=0.001 a.u., ω=0.2 a.u. and duration τ=190 a.u.

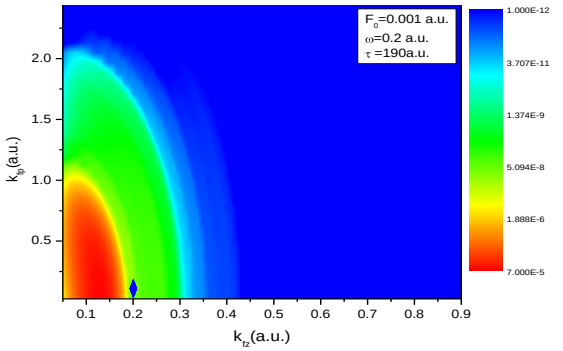

Fig. 2: Electron momentum distribution derived from SJV model.

References

[1] A. L. Cavalieri, *et al*. Nature, 449, 1029 (2007).
[2] L. Miaja-Avila *et al*. Phys. Rev. Lett. 97, 113604 (2006).
[3] M. N. Faraggi, M. S. Gravielle and D. Mitnik *Phys. Rev.* A **79,** 012903 (2007).

[1] E-mail: faraggi@iafe.uba.ar

Interference effects in laser assisted photo-ionization of atoms

Pablo A. Macri[*,1], **Denise Bendersky**[*]

[*]Departamento de Física, FCEyN, Universidad Nacional de Mar del Plata, 7600 Mar del Plata, Argentina

Synopsis Interference effects in laser assisted photoionization of atoms by an XUV pulse is considered by means of the Coulomb Volkov approximation. We find that the interference pattern can be related with the time delay between the laser and the XUV pulse.

In this work, we study the angular and energy distribution of photoelectrons generated by an attosecond-pulse in the presence of a strong laser field. This kind of process is particularly relevant to understand attosecond streak camera experiments [1] where an intense pulse exchange many photons with the electron after it has been ionized by a weaker and shorter pulse. The duration of the attosecond pulse, the shape of the IR streaking field and the time delay between them are the three main parameters that rule the measurements. Henceforth, finding a reliable theory allows to reconstruct some of this features from the available data.

The usual theory for streaking experiments is the strong field approximation (SFA) where the photoelectron is assumed to be influenced only by the strong laser field neglecting the interaction with the the atomic core. However, differences between the predictions of the SFA and more accurate calculations involving Coulomb atomic potential were found in the double differential distributions [2]. The present work is based on the Coulomb Volkov Approximation (CVA) [3]. In this approximation the evolution of the electron after ionization is influenced by both the Coulomb potential and the laser field. In the Figure 1, we present double differential probability for laser assisted XUV photoionization of H in the forward (Figs. 1a and 1c) and backward (Figs. 1b and 1d) direction. The IR laser parameters are wavelength $\lambda = 800$ nm, 8-cycle envelope and laser intensity $I_L = 2 \times 10^{13}$ W cm^{-2}. The XUV pulse has a 8-cycle envelope, with a mean energy of $\omega_X = 90$ eV, and pulse intensity $I_X = 1 \times 10^{11}$ W cm^{-2}. The laser and XUV pulses have a sin^2 profile. In Figs. 1a and 1b the XVU pulse center is delayed half laser cycle respect to the center of the laser pulse while in Figs. 1c and 1d there is no delay between the XVU an the IR pulse. We find that time delay between the pulses produces an interference pattern which is smoothed when the time delay is reduced. This interference can be rooted from ionization pathways of electrons emerged at different instants of the XUV pulse. In this way is possible to estimate the time delay between the pulses characterizing the interference pattern. Preliminary time-dependent Schödinger equation calculations show that this characterization is very sensitive to the fine details introduced by the Coulomb interaction when the electron is in the continuum state.

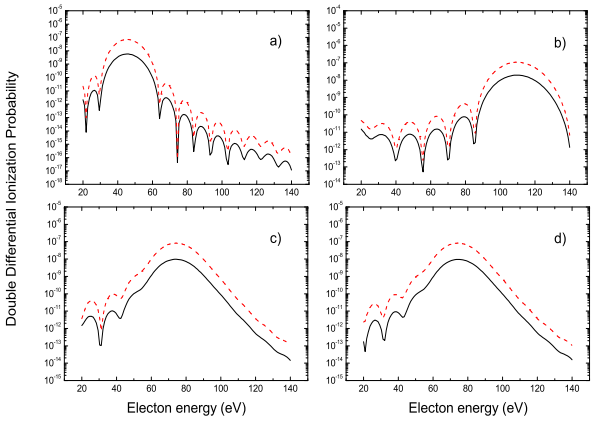

Fig. 1. Double differential ionization probability. Full lines: CVA. Dashed lines: SFA. a) Forward ionization with time delay. b) Backward ionization with time delay. c) Forward ionization without time delay. d) Backward ionization without time delay.

References

[1] Kitzler M, et al., 2002 *Phys. Rev. Lett.* **88** 173904.

[2] Smirnova O, et al., 2006 *J. Phys. B* **39** S323.

[3] Macri P A, et al., 2003 *J. Opt. Soc. Am. B* **20**, 1801 ; Rodríguez V D, et al., 2004 *Phys. Rev. A* **69**, 053402.

[1]E-mail: macri@mdp.edu.ar

Acceleration of neutral atoms in intense short laser pulses

U. Eichmann [1], T. Nubbemeyer, H. Rottke, and W. Sandner

Max Born Institut Berlin, Max Born Str. 2a, 12489 Berlin, Germany

Synopsis We report experimental results on a new acceleration mechanisms for neutral atoms in a strong laser field (I = 10^{16}W cm^{-2}). A simple model can explain the observed accelerations with magnitudes as high as 10^{14} times Earth's gravitational acceleration.

We report on experiments where we have investigated kinematic effects of strong short-pulsed laser fields on neutral atoms. We measure deflections of neutral atoms in laser fields with intensities up to 10^{16}W cm^{-2}, which correspond to an ultra-strong acceleration as high as 10^{14} times Earth's gravitational acceleration. This is - to the best of our knowledge - by far the strongest acceleration of neutral species in external fields. For instance, the new force exceeds those which are used in atomic laser cooling experiments by typically eight orders of magnitude. The experiments have become possible through a recent observation that atoms can survive strong laser pulses in an excited state, where they can be detected directly [1]. Thus, with a position sensitive detector we can measure atomic beam deflection if, during the laser pulse, sufficient momentum is transferred to the atoms. In Fig.1 we show a result for a beam of He atoms intersected by a high intensity pulsed laser beam, where we have measured the distribution of laser excited He atoms with a position sensitive detector located $\sim$ 0.38 m downstream from the interaction region. The distribution of excited atoms along the laser beam direction (z_D axis) is as expected whereas the distribution in radial r_D direction is surprising. We find that it originates from the accelerating forces of the laser field on the neutral atom.

The observed action on neutral atoms during the short interaction time can be quantitatively explained by a simple model based on the three step model of atomic strong field dynamics. The survival mechanism has been dubbed "frustrated tunnel ionization" [1] and has also been found in molecular dissociation in strong laser fields [2]. In essence, it is the recapture of the tunneled electron after the laser pulse is over which is responsible for the excitation. During the laser pulse, the ponderomotive force is acting on the quasi free electron converting quiver energy of the electron partially into centre-of-mass motion of the whole atom. Observed atomic deflections can be fitted within this model with excellent agreement. Besides the fundamental observation of unprecedented acceleration of neutral atoms in external fields we envisage a mapping of the laser intensity distribution in an intense focussed beam, an important information, which is otherwise hardly to obtain.

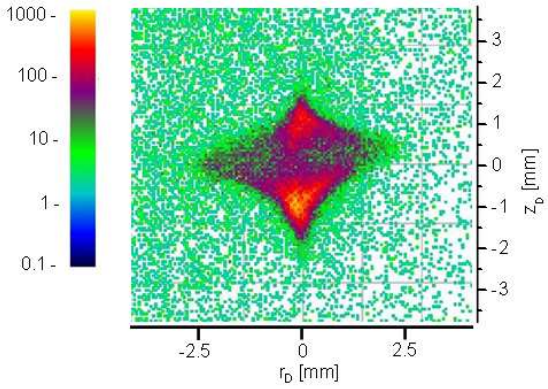

Fig. 1. Shown is the distribution of excited He atoms for a laser pulse with I = 4.2x10^{15} W cm^{-2} on a logarithmic scale.

References

[1] T. Nubbemeyer *et al.*, Phys. Rev. Lett. **101**, 233001 (2008).

[2] B. Manschwetus *et al.*,Phys. Rev. Lett. **102**, 113002 (2009).

[1]E-mail: eichmann@mbi-berlin.de

Extending the upper limit of laser pulse duration for generating single attosecond pulses

Ximao Feng, Steve Gilbertson, Hiroki Mashiko, He Wang, Sabih D. Khan, Michael Chini, and Zenghu Chang[1]

JRM Laboratory, Kansas State University, Manhattan, KS, 66506-2604, USA

Synopsis: We propose and demonstrate a technique called generalized double optical gating for generating isolated attosecond pulses with 20 fs lasers. These pulses are measured to be 260 attoseconds by reconstructing the streaked photoelectron spectrogram.

Since isolated attosecond pulses were first generated in 2001 [1], only a few laboratories can produce and use such pulses. The stringent requirement of few-cycle driving lasers is one of the main obstacles. We report a technique call generalized double optical gating (GDOG), with which multi-cycle laser pulses as long as 20 fs can be used to generated single attosecond pulses. The technique is significant in spreading attosecond optical technologies.

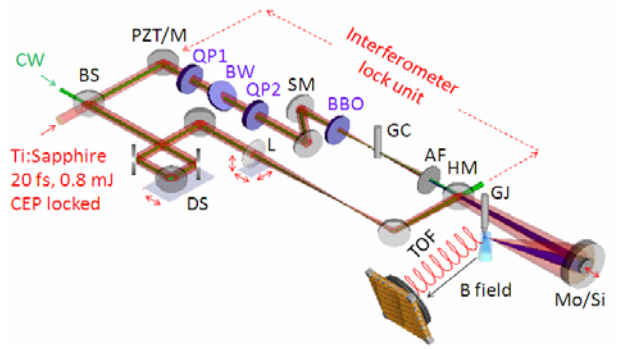

Fig. 1. Experimental setup of double optical gating and for measuring the single attosecond pulses.

GDOG is a generalized version of double optical gating (DOG) that we reported previously [2, 3]. The main idea in GDOG is to create a polarization gating field with two counter-rotating elliptically polarized pulses. The ground state population of the atoms is less reduced in such a field as compared with other gating methods allowing high intensity to be used with long laser pulses.

Figure 1 shows the experimental setup for generating and measuring single attosecond pulses. The GDOG optical components include two quartz plates (QP1 and QP2), a Brewster window (BW), and a BBO crystal. A Mach-Zehnder interferometer configuration was used to control the temporal and the spatial overlap of the attosecond XUV beam and the NIR streaking field. The photoelectron spectrum was collected with a time-of-flight spectrometer.

The isolated XUV pulses from argon gas were measured using the FROG-CRAB method based on attosecond streaking [4, 5]. Figure 2(A) and (B) show the experimental and retrieved CRAB traces. Fig. 2(C) shows the temporal shape and phase of the 260 as XUV pulse. The frequency marginal check shown in Fig. 2(D) indicates good agreement.

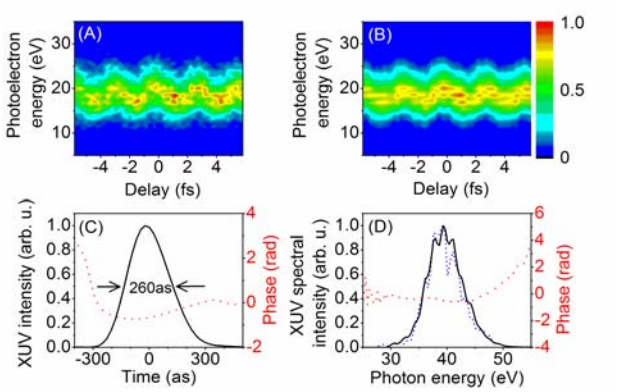

Fig. 2. Attosecond XUV pulse generated using 20 fs laser pulses and the retrieved results.

In conclusion, we have generated 260 as single attosecond pulses from 20 fs multi-cycle laser pulses and measured the pulses with the CRAB method. With the generalized double optical gating demonstrated here, it is conceivable that high energy single isolated attosecond pulses will be generated using high energy chirped pulse lasers directly in the future. This material is supported by the U. S. Army Research Office under Grant No. W911NF-07-1-0475, and by the Chemical Sciences, Geosciences, and Biosciences Division, U.S. Department of Energy.

References

[1] M. Drescher *et al.*, Nature **419**, 803(2002).
[2] H. Mashiko *et al.*, Phys. Rev. Lett. **100**, 103906(2008).
[3] S. Gilbertson *et al.*, Appl. Phys. Lett.**92**, 071109(2008).
[4] Y. Mairesse and F. Quéré, Phys. Rev. A **71**, 011401(2005).
[5] M. Chini *et al.*, Appl. Phys. Lett. **94**, 161112 (2009).

Error! Reference source not found. E-mail: chang@phys.ksu.edu

Electron Localization and Multiple Ionization Bursts in H_2^+ within a Half Cycle of Near-Infrared Laser Light

Norio Takemoto[1] **and Andreas Becker**[2]

JILA and Department of Physics, University of Colorado, 440 UCB, Boulder, CO 80309-0440, USA

Synopsis We found by numerical simulations that H_2^+ irradiated by intense near-infrared laser light shows multiple bursts of ionization current within a half cycle of the electric field oscillation, in contrast to the intuition given by the quasi-static tunneling ionization picture. We attribute the origin of the multiple bursts to the dynamical localization of the electron at one of the nuclei on the sub-laser-cycle time-scale. A relation between the timing of the bursts and the vector potential of the laser light is derived analytically based on a perturbative solution of a two-state model.

In the traditional picture of quasi-static tunneling ionization of atoms and molecules by intense laser light, ionization events are expected to take place predominantly once per half laser-cycle at the peaks of the electric field. In contrast, our numerical simulations for H_2^+ indicate that there can be multiple bursts of ionization current in a half laser-cycle. Fig. 1 exemplifies the results of our numerical simulations and a two-state analysis for H_2^+ exposed to a laser pulse ($\sin^2$-envelope, 5-cycle FWHM, wavelength 1064 nm, peak intensity 6×10^{13} W/cm^2). Fig. 1(a) shows the laser electric field and vector potential as a function of time over one cycle at the peak intensity, and Fig. 1(d) shows, in the same time window, the time-evolution of the electron density obtained by numerically solving the time-dependent Schrödinger equation for a 1D model of H_2^+ (internuclear distance fixed at 7 a.u.). In Fig. 1(d), one can clearly see multiple ionization packets per half cycle. In Fig. 1(c), we absorbed the outgoing wavepackets to separate the bound electron dynamics from rescattering. From this result, we can deduce that there are two major ionization bursts per half cycle in the present case, and that they are induced by localization of the bound wavepacket at one of the two nuclei.

We have further analyzed the bound electron dynamics using a two-state model with the ground ($|g\rangle$) and first-excited ($|u\rangle$) electronic states of H_2^+. Floquet solutions of this system can be obtained using a perturbation method at the limit of strong interaction between the two states [1], and the general solution $|\Psi(t)\rangle$ can be expressed as a superposition of these Floquet states. We derived analytical expressions for the local populations, $(1/2)|(\langle g| \pm \langle u|)|\Psi(t)\rangle|^2$, which are plotted in Fig. 1(b) as a function of time, and identified that their extrema are at the time instants $\{t_n\}$ defined by $A(t_n) = \tilde{A} - (n\pi - \chi)/(2d_{gu})$, where n is an integer, $A(t)$ and $\tilde{A}$ are the vector potential and its time-average, respectively, d_{gu} is the dipole matrix element between $|g\rangle$ and $|u\rangle$, and χ is an angle determined by the superposition coefficients of the Floquet states. Grid lines in Fig. 1(a,b) indicate $\{t_n\}$ and $\{A(t_n)\}$. The electron localization observed in Fig. 1(c) is well reproduced by the two-state model in Fig. 1(b), and, therefore, the timing of the ionization bursts can be predicted as the localization maxima of the simple analytical model.

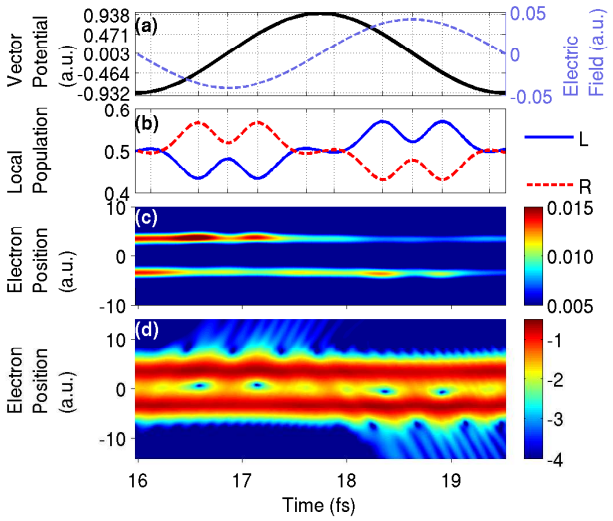

Fig. 1. Results of numerical simulations and a two-state analysis for H_2^+ are shown for one laser-cycle at the peak of a 5-cycle-FWHM pulse.

References

[1] M.Yu. Ivanov, P.B. Corkum, Phys. Rev. A **48**, 580 (1993); A. Santana, J.M. Gomez Llorente, V. Delgado, J. Phys. B **34**, 2371 (2001).

[1]E-mail: norio@jilau1.colorado.edu
[2]E-mail: andreas.becker@colorado.edu

Wavelength Scaling in High Harmonic Tomographic Imaging

Jonathan A. Wheeler[1], **Gilles Doumy**[2], **Terry Miller, Pierre Agostini, Louis F. DiMauro**

Department of Physics, The Ohio State University, Columbus, OH, 43210-1117, USA

Synopsis Increasing the wavelength of the fundamental driving laser at constant intensity in high harmonic generation allows one to significantly increase the upper bound of the harmonic energies produced [1, 2]. This feature of harmonic generation is employed in an effort to improve the spatial resolution achieved in the method of tomographic reconstruction of molecular orbitals from high harmonics [3]. Current experimental measurements and comparison with theoretical work [4] will be presented.

In the harmonic generation process, an electron wavepacket is promoted from a molecule and propagates under the influence of the driving laser, eventually returning to its origin with a maximum cutoff energy, E_{cutoff}, proportional to the field's ponderomotive potential, U_p. The interaction of the returning electron wavepacket with the molecular bound state wavefunction produces harmonics and gives one access to information about the molecular wavefunction. By varying the alignment of the molecular axis of the target gas at known angles to the driving laser's polarization, the returning electron wavepacket interacts with the molecule's wavefunction from differing vantage points. This angular-dependent spectral data can then be used to tomographically reconstruct the molecule's structure. One key point in performing an accurate reconstruction is in producing rescattering electrons with a small deBroglie wavelength capable of resolving molecular features. By extending the harmonic cutoff, the range of the electron deBroglie wavelengths sampling the molecule is also increased, suggesting the abililty to reconstruct a molecular image with finer detail. Because $E_{cutoff} \propto U_p \propto I\lambda_L^2$, the electron deBroglie wavelength for the cutoff scales as $\lambda_e \propto U_p^{-\frac{1}{2}} \propto I^{-\frac{1}{2}}\lambda_L^{-1}$ where I is the laser intensity, λ_L is the fundamental driving laser wavelength and λ_e is the cutoff electron deBroglie wavelength. This suggests increasing the driving laser wavelength as an effective tool for improving the resolution of a molecular tomographic reconstruction, and would be a benefit for imaging experiments with molecules such as N_2 with bond lengths close to 1 $\mathring{A}$. As an example, the shortest deBroglie wavelength for electrons produced at intensities typical for N_2 by a 0.8 μm fundamental laser is $\sim$1.5 $\mathring{A}$ while a 1.3 μm driving laser at the same intensity produces returning electrons with a wavelength $\sim$0.9 $\mathring{A}$.

In our work we compare the resolution from experimental results in N_2 using 0.8 micron light to similar conditions with 1.3 micron light. The spectral data is shown in figure 1. We plan to examine the effects of extending the harmonic cutoff on the tomographic recontruction both in N_2 and other simple molecules.

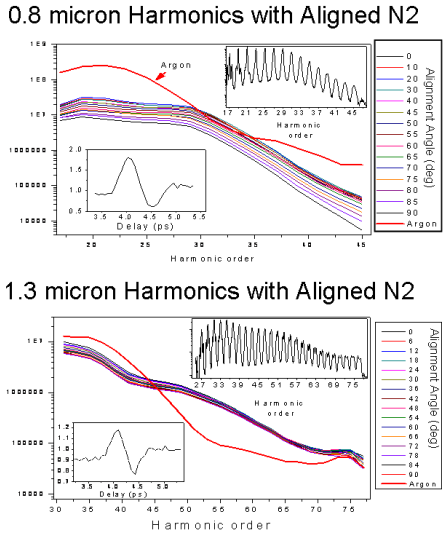

Fig. 1. Harmonic angular dependence in N_2. The insets show typical spectra and harmonic yield around first half revival of alignment for N_2.

References

[1] P. Colosimo *et al*, Nat. Phys. **4**, 386-389 (2008).

[2] G. Doumy *et al*, Phys. Rev. Lett. **102**, 093002 (2009).

[3] J. Itatani *et al*, Nature **432**, 867 (2004).

[4] V.-H. Le *et al*, Phys. Rev. A **76**, 013414 (2007).

[1]E-mail: wheeler@mps.ohio-state.edu
[2]E-mail: Doumy.1@osu.edu

Femtosecond Dynamics and Multiphoton Ionization driven with an Intense High Order Harmonic Source

J. van Tilborg[*,1], **T. K. Allison**[*,†,2], **T. W. Wright**[*], **M. P. Hertlein**[*], **Y. Liu**[*], **H. Merdji**[‡], **R. W. Falcone**[*,†], **A. Belkacem**[*]

[*]Lawrence Berkeley National Laboratory, Berkeley, California 94720, USA
[†]University of California at Berkeley, Berkeley, California 94720, USA
[‡]Service des Photons, Atomes et Molécules, CEA-Saclay, 91191 Gif-sur-Yvette, France

Synopsis We have constructed a high intensity high order harmonic source delivering $\sim 10^9$ extreme ultraviolet photons/shot on a gas target and used it to observe multiphoton ionization and conduct femtosecond EUV-pump IR-probe experiments. Following excitation by 20-25 eV photons, we observed that the excited ethylene cation $(H_2C\text{-}CH_2)^+$ experienced isomerization to the ethylidene configuration $(HC\text{-}CH_3)^+$ in 50±25 fs, followed by an H_2 stretch motion. Experimental data and analysis from several other performed and planned experiments will be presented as well.

At the Lawrence Berkeley National Lab, we have developed an intense high harmonic generation (HHG) system, delivering around 10^9 photons per harmonic per shot into an experimental chamber. The drive laser (λ_0 = 800 nm) has a pulse duration of 35 fs, a pulse energy of around 30 mJ, and operates at 10 Hz. In a 5-cm-long gas cell (filled with krypton, xenon, or argon) the laser produces radiation at odd harmonic frequencies of the fundamental, after which phase matching conditions and optical reflective properties limit the range of photon energies available in the chamber to around 5-50 eV (EUV regime). Insertion of additional foils as well as a multi-layer coating on the final focusing mirror allow for further control of the delivered photon energy.

In a first series of experiments we used 20-25 eV photons to pump ethylene ($H_2C\text{-}CH_2$) to excited cationic states. We probed the subsequent isomerization channels with a NIR probe laser by looking at ion fragments, see Fig. 1. We observed directly the formation of the hydrogen-migrated isomer ethylidene $(HC\text{-}CH_3)^+$ by measuring CH^+ and CH_3^+ fragments. The ethylidene geometry is known to play a role in the internal conversion of electronic to nuclear energy, making ethylene a model molecule to study such processes. Optimum CH^+ and CH_3^+ yields occurred 80 fs after pumping. We explored several other ionic species (for example H_2^+ from a subsequent H_2 stretch), and have applied a model to match the isomerization data.

We will also discuss results on EUV-driven non-linear optics. At our high EUV intensity we find measurable quantities of multiphoton-driven products. For example, we have observed Ar^{2+}, Ne^{2+}, Xe^{3+}, $C_2H_2^{2+}$ and $C_2H_4^{2+}$ from multiphoton excitations. Recently we have finished the construction and implementation of a split-mirror stage, allowing for multi-color EUV-pump EUV-probe experiments with sub-fs temporal control. The latest results from this setup will be addressed.

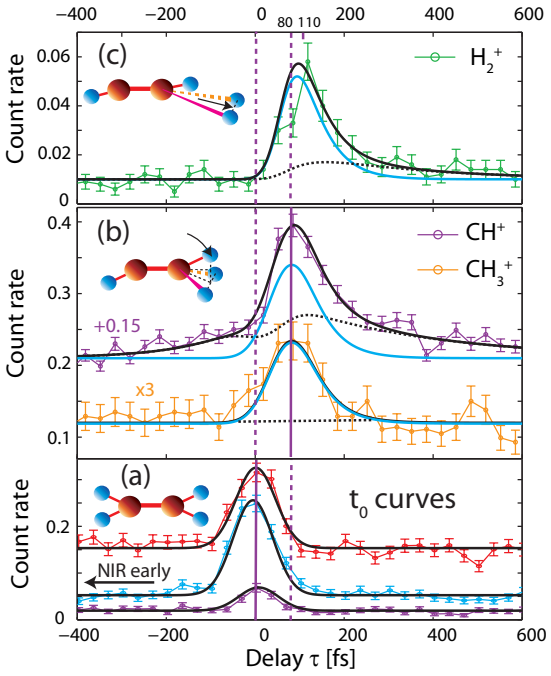

Fig. 1. (a) Ion yields to determine t_0, namely H_2O^+, $C_2H_3^{2+}$ and the isotope $^{29}C_2H_4^{2+}$. (b) Ion yields for the ethylidene fragments CH_3^+ and CH^+. Optimum yield occurs at τ = 80 fs. (c) Ion yield for the fragment H_2^+ (optimum at τ = 110 fs), believed to represent fragmentation from a transient configuration succeeding ethylidene. The solid black curves in (b) and (c) represent modeled curves, consisting of a background (black dotted curves) and a transient signal $S(\tau)$ (solid blue curves).

[1]E-mail: JvanTilborg@lbl.gov
[2]E-mail: TKAllison@lbl.gov

High Harmonic Generation from Multiple Orbitals in N_2

Brian K. McFarland, Joseph P. Farrell, Philip H. Bucksbaum, and Markus Gühr[1]

Stanford PULSE Institute, SLAC National Accelerator Lab, Menlo Park CA 94025 and Physics Department, Stanford University, Stanford, CA 94305

Synopsis: Contribution from the HOMO and HOMO-1 orbitals are observed in high harmonics from N_2. We discuss the harmonic modulations in the rotational revival structure due to the HOMO and HOMO-1.

For molecules, the highest occupied molecular orbital (HOMO) is generally thought to be responsible for ionization and recombination during HHG [1]. We report experimental evidence that the more deeply bound HOMO-1 with its π_u symmetry also contributes to HHG [2]. This opens the route to imaging coherent superpositions of electronic orbitals.

In the experiment, an ultrashort laser pulse (alignment pulse) creates a rotational wave packet resulting in molecular alignment of N_2. A second delayed laser pulse with higher intensity generates high harmonics in the aligned molecules. The harmonic spectrum is detected as a function of delay between alignment and harmonic generating pulses (Fig. 1A).

The molecular axes are preferentially perpendicular with respect to the harmonic generating polarization at 4.1 ps. This appears as a reduction in the signal at harmonic 15 compared to the unaligned case prior to 3.6 ps. At 4.4 ps the molecular axes are partially parallel to the harmonic generating polarization and an increase of the signal at low harmonics is observed compared to the unaligned case. However, as the harmonic number increases above 25, the temporal modulation compared to harmonic 15 becomes inverted.

The first step of HHG, tunnel ionization, is sensitive to the molecular wave function far away from the nuclei in direction of the generation polarization. Thus, the σ_g HOMO orbital ionizes more easily if the generation polarization is parallel to the internuclear axis. Also, the recombination dipole is larger if the molecular axis is aligned with the generation polarization, since the recombination dipole has larger amplitude in the long direction of the orbital. For the HOMO, the HHG signal is maximized for molecules standing parallel to the HHG polarization compared to the perpendicular polarization, consistent with the observed experimental trend in harmonics 15-25 in Fig. 1A.

The peak at 4.1 ps at harmonics 25-39 can be explained by the HOMO-1. Tunnel ionization perpendicular to the molecular axis is higher for the HOMO-1 compared to the HOMO because it has a larger spatial extent in this direction (Fig. 1C). Ionization and recombination parallel to the internuclear axis give rise to a vanishing dipole for the HOMO-1, because of the dipole cancellation due to the opposite sign of the wave function on either side of the axis. In contrast, the recombination dipole perpendicular to the axis is strong.

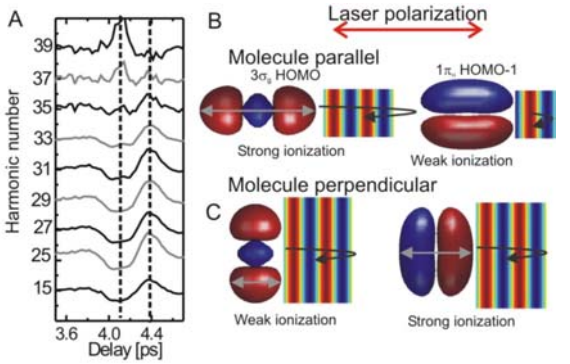

Fig. 1. A) Harmonic signal as a function of alignment-generation pulse delay. Scheme for HHG from HOMO and HOMO-1 for parallel (B) and perpendicular (C) polarization of molecules and harmonic generating laser.

We support our interpretation of the spectral modulations by simple model calculations of the recombination dipole. We thank the Deparment of Energy, BES for funding.

References

[1] J. Itatani et al., Nature 432, 687 (2004)
[2] B. K. McFarland et al., Science 322, 1232 (2008)

[1]E-mail: mguehr@stanford.edu

High accuracy, real time, single-shot measurement of absolute carrier-envelope phase and pulse duration for few-cycle laser pulses

A. Max Sayler*[,1], T. Rathje*, J.V. Hernandez[†], W. Müller*, B.D. Esry[†], and G.G. Paulus*[,2]

[*] Friedrich-Schiller-Universitaet, Institut für Optik und Quantenelektronik, Max-Wien-Platz 1, 07743 Jena, Germany
[†] J.R. Macdonald Laboratory, Kansas State University, Manhattan, KS, 66506-2604, USA

Synopsis: We develop a novel approach which allows for the simultaneous *a priori* single-shot measurement of carrier-envelope phase (CEP) and pulse duration for each and every few-cycle laser pulse in a kHz pulse train, virtually instantaneously. This technique builds upon the previous work of Wittmann *et al.* [1], which outlines a technique for determining CEP using a stereographic ionization measurement [2]. However, our approach allows for real-time assessment of these parameters, thereby permitting the signal to be used as a laser-feedback control mechanism or as an auxiliary measurement providing shot-by-shot pulse characterization for other measurements.

A pulse's electric field asymmetry depends upon its absolute carrier-envelope phase – CEP (φ) and is exaggerated as the pulse length (τ) decreases, where the pulse's electric field is defined as $E(t)=\exp(-(t/\tau)^2)\cos(\omega t+\varphi)$. This asymmetry is reflected in above-threshold laser-induced ionization (ATI) distributions produced from atomic target, e.g. see references [1–3]. Furthermore, as the ATI distribution is dependent upon the absolute CEP and pulse duration, one can work backwards using the measured distribution to determine these quantities, thereby providing an improved alternative to the customary optical methods available that measure only the relative CEP.

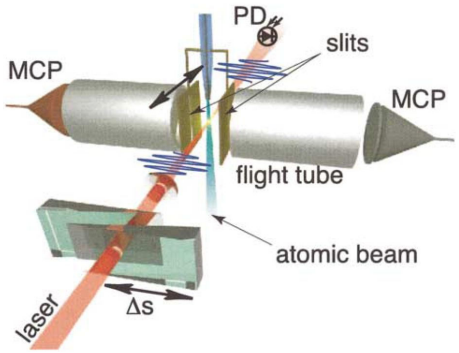

Fig. 1. Stereographic CEP meter [2].

This type of inversion technique was recently employed by Micheau *et al.* [3] to determine the aforementioned parameters using 3D momentum images of high-energy photoelectrons. However, this method requires multiple laser pulses with a constant CEP to generate a clear momentum image, which is then analyzed using rescattering theory.

In contrast, our method utilizes a stereographic ATI measurement, see Fig. 1, and the left / right asymmetry of the two energy regions in the ATI energy spectra to allow for a single-shot real-time determination of the absolute CEP at kHz rates even without CEP stabilization. Fig. 2 shows a parametric plot of the asymmetry coefficient for the two aforementioned energy regions where the polar angle, θ, is roughly equivalent to the absolute CEP. Additionally, this technique allows for the measurement of the pulse duration and intensity along with other laser properties via a comparison to calculated distributions.

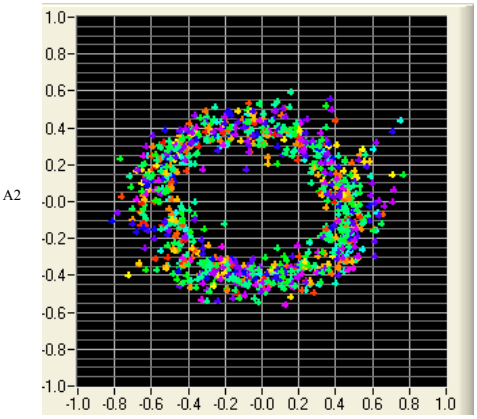

Fig. 2. A typical plot of asymmetry parameters for a non-CEP stabilized ultrashort pulse.

B.D. Esry acknowledges support from the Chemical Sciences, Geosciences, and Biosciences Division, Office of Basic Energy Sciences, Office of Science, U.S. Department of Energy for support.

References

[1] T. Wittmann *et al.*, Nature Phys. **5,** 357 (2009).
[2] G.G. Paulus *et al.*, Phys. Rev. Lett. **91**, 253004 (2003).
[3] S. Micheau *et al.*, Phys. Rev. Lett. **102**, 073001 (2009).

[1] E-mail: sayler@uni-jena.de
[2] E-mail: gerhard.paulus@uni-jena.de

Analytic Formulas for High-Order Harmonic Generation

M.V. Frolov*, N.L. Manakov*, T.S. Sarantseva*, Anthony F. Starace†, [1]

*Department of Physics, Voronezh State University, Voronezh 394006, Russia

†Dept. of Physics and Astronomy, The University of Nebraska, Lincoln, NE 68588-0111, USA

Synopsis We present closed-form analytic formulas for high-order harmonic generation (HHG) rates for both negative ions and neutral atoms. These formulas provide a fully quantum justification for the famous classical three-step scenario (TSS) of HHG as well as a correction to the well-known classical law for the HHG plateau cutoff energy.

For the case of an electron bound in a short-range potential, we present a closed-form analytic formula for high-order harmonic generation (HHG) rates (obtained in the quasiclassical limit [1]) that shows excellent agreement with exact time-dependent effective range results over the high energy part of the HHG plateau (and beyond). It justifies the empirical parametrization of HHG rates suggested in Refs. [2]. Our analytic results allow one to describe the dependence of the oscillatory patterns of HHG rates on both the harmonic number N and on the laser parameters (for a given N), as well as the dependence of the HHG rates on the orbital angular momentum, l, of the bound electron. Our analytic formula for HHG rates can be presented as the product of three factors, which have clear physical meanings within the TSS:

$$R_N = I(F_0)W(E)\sigma(E), \quad E = N\hbar\omega - |E_0|. \quad (1)$$

$I(F_0)$ describes the first (*ionization*) step in the TSS: it is proportional to the detachment rate in a static electric field, whose strength F_0 is that of the laser electric field at the moment of tunneling. $W(E)$ describes the second step, the *propagation* of the detached electron in the laser field from the moment of tunneling up to the recombination event. This factor is essentially independent of the shape of the atomic potential. It involves a single Airy function that describes interference of two ("short" and "long") classical electron trajectories and depends on the difference $E - E_{max}$, where E_{max} is the maximum kinetic energy gained by the active electron from the laser field. The photorecombination cross section $\sigma(E)$ describes the final step in the TSS: the *recombination* of the active electron with energy E to the initial bound state of energy E_0 with emission of the harmonic photon. Note that an HHG rate involving a combination of the Airy function and its first derivative was obtained previously in Ref. [3] for a zero-range potential model within the uniform approximation; however, the arguments of these functions were not expressed in closed analytic form.

Our analytic result (1) was obtained in Ref. [1] for the case of an electron in a short-range potential (negative ion). However, as each of the three factors in (1) has a transparent physical meaning within the TSS (which, as is commonly accepted, does not depend on the atomic species), one can expect that Eq. (1) can be generalized appropriately to describe HHG for atoms. This generalization consists in the replacement of the ionization and recombination factors, $I(F_0)$ and $\sigma(E)$, by their atomic counterparts. We show that the resulting Coulomb-modified expression (1) gives results for the high energy part of the HHG spectrum for the H atom that are in perfect agreement with those obtained by numerical solution of the time-dependent Schrdinger equation.

This work was supported in part by RFBR Grants No. 07-02-00574 and No. 09-02-12034, by NSF Grant PHY-0601196, and by the Dynasty Foundation (T.S.S.).

References

[1] M.V. Frolov, N.L. Manakov, T.S. Sarantseva and A.F. Starace, J. Phys. B **42**, 035601 (2009).

[2] J. Itatani et al., Nature (London) **432**, 867 (2004); T. Morishita, A.T. Le, Z. Chen and C.D. Lin, Phys. Rev. Lett. **100**, 013903 (2008).

[3] D. B. Milošević and W. Becker, Phys. Rev. A **66**, 063417 (2002).

[1] E-mail: astarace1@unl.edu

Zero Photon Dissociation of H_2^+ in Few Cycle Pulses

B. Gaire, J. McKenna, A. M. Sayler, M. Zohrabi, Nora G. Johnson, F. Anis, J.J. Hua, K.D. Carnes, B.D. Esry, and I. Ben-Itzhak [1]

J.R. Macdonald Laboratory, Physics Department, Kansas State University, Manhattan, KS, 66506, USA

Synopsis Evidence for dissociation caused by an intense laser field with the net absorption of zero photons is conflicting. We have measured very low kinetic energy release upon H_2^+ dissociation in few cycle pulses – a signature of zero photon dissociation. Comparison with solutions of the time dependent Schrödinger equation supports this assertion.

At this conference we will focus on the zero photon dissociation (ZPD) of H_2^+ in few cycle laser pulses. This mechanism is illustrated in Fig. 1. At the beginning of the pulse the field is weak and the potential energy curves $|1s\sigma_g\text{-}0\omega>$ and $|2p\sigma_u\text{-}1\omega>$ are diabatic. In the leading edge of the pulse, as intensity increases, the coupling becomes stronger and the curves can be considered as adiabatic. In this case there is a potential well just above the crossing, which "traps" part of the wavepacket corresponding to the vibrational levels in this region of the well and is called vibrational trapping (VT). Later in the pulse, some of the trapped wavepacket will spill over the well and onto the $|1s\sigma_g\text{-}0\omega>$ curve. The net number of photons absorbed in this process is zero and hence the name zero photon dissociation. The kinetic energy release (KER) in this process is very low and also depends on how fast the field of the pulse is changing.

This ZPD effect has been observed in the dissociation of the H_2^+ with 266 nm pulses of width about 250 fs [1]. However, recently the same authors [2] have given an alternative explanation for the low KER observed in Ref. [1]. Our calculations also suggest that for the pulse length used in Ref.[1], the ZPD mechanism might be too weak to be observed.

We will discuss our results of H_2^+ dissociation in intense (up to 10^{15} W/cm^2), few cycle (about 10 fs) 800 nm laser pulses. The experimental set up is a modified version of our coincidence 3D imaging apparatus used in our other studies [3]. This modified system allows us to separate the fragments that have very low KER down to zero eV, in time and position. We compare these results with theoretical calculations obtained by solving the time dependent Schrödinger equation in the Born-Oppenheimer representation and find favorable agreement.

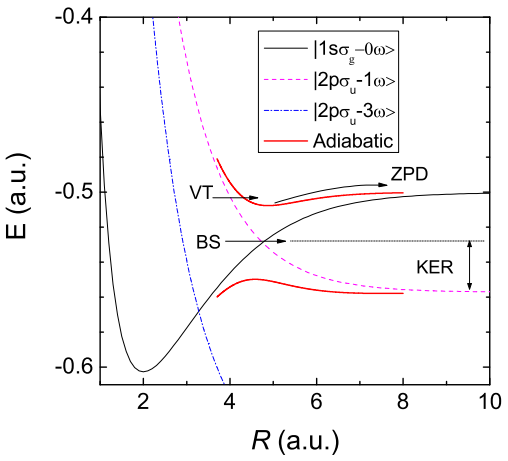

Fig. 1. H_2^+ potentials dressed by net absorbed number of photons, $n\omega$. Also indicated are the zero photon dissociation (ZPD), vibrational trapping (VT), and bond softening (BS) mechanisms.

This work is supported by the Chemical Sciences, Geosciences, and Biosciences Division, Office of Basic Energy Sciences, Office of Science, U.S. Department of Energy.

References

[1] J.H. Posthumus *et al.*, J. Phys. B **33**, L563 (2000).

[2] J.H. Posthumus *et al.*, Phys. Rev. Lett. **101**, 233004 (2008).

[3] I. Ben-Itzhak *et al.*, Phys. Rev. Lett. **95**, 073002 (2005).

[1] E-mail: ibi@phys.ksu.edu

Theoretical study of carrier-envelope phase effects on the 3D momentum distribution of H_2^+ dissociation fragments

Fatima Anis[1] **and B. D. Esry**[2]

J. R. Macdonald Laboratory, Kansas State University, Manhattan, KS, 66506-2604, USA

Synopsis The carrier-envelope phase (CEP) of few-cycle laser pulses can be used to control the strong-field dynamics of atoms and molecules. To study CEP effects in H_2^+, we have solved the time-dependent Schödinger equation including nuclear vibration and rotation as well as electronic excitation, only ionization is excluded. Including nuclear rotation is essential to obtaining results directly comparable with experiment such as the momentum distribution. We show that the momentum distribution is quite sensitive to the CEP.

Being the simplest molecule, H_2^+ has been an attractive candidate for studying molecular dynamics in intense laser pulses by both theorists and experimentalists for almost two decades. Since the time-dependent Schrödinger equation (TDSE) for H_2^+ can be solved accurately with some restrictions, the results should be directly comparable to experimental observations. This comparison, however, depends crucially on being able to analyze the time-dependent wave function. We present here a careful analysis of the momentum distribution of p and H following H_2^+ dissociation appropriate to most experiments.

To be measurable, carrier-envelope phase (CEP) effects require few-cycle pulses. The fact that such pulses for the common 785 nm Ti:S laser are much shorter than the free rotational period of H_2^+ has led many groups to neglect nuclear rotation in the theoretical analysis of CEP effects [1, 2]. Our results indicate that even a 5 fs pulse can populate a large number of rotational states which, in turn, continue to evolve freely as the fragments head to the detector. Including rotation is thus essential for predicting the momentum distribution of the fragments. The complex interference between the different angular momentum states also vary with other laser parameters such as intensity, wavelength, and CEP.

Figure 1(a) shows the distribution of the relative p+H momentum parallel to the linearly polarized laser field $P_\parallel$ and perpendicular to the field $P_\perp$. It shows a clear up and down asymmetry for a pulse length of 5 fs, wavelength of 785 nm, and intensity of 10^{14} W/cm^2. The angular distribution for a few CEP is shown in Fig. 1(b) and reveals only relatively weak CEP dependence. Figure 1(c), on the other hand, shows strong CEP effects in the up-down asymmetry, A=2($P_{\rm up}$–$P_{\rm down}$)/($P_{\rm up}$+$P_{\rm down}$) where $P_{\rm up}$ ($P_{\rm down}$) is the probability for being in the upper (lower) half plane. From these three panels, we see that there is strong CEP-dependent asymmetry and that it is most clearly revealed as a function of the relative p+H kinetic energy.

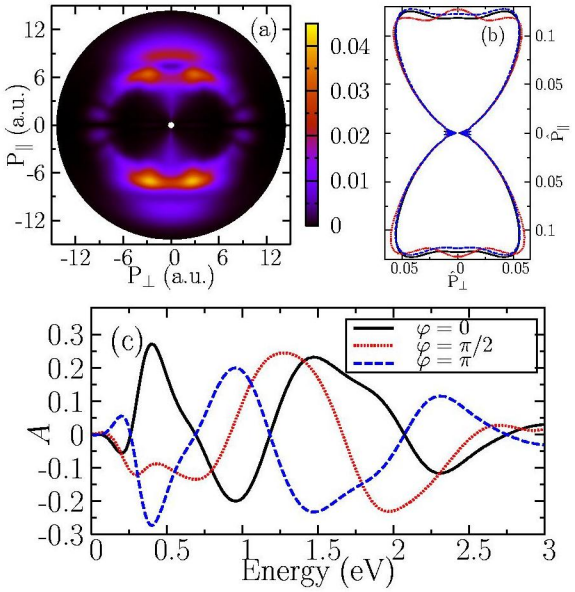

Fig. 1. (a) p+H relative momentum distribution for zero CEP (φ=0). (b) Angular distribution for the three CEP in (c). (c) Up-down asymmetry A as a function of p+H relative kinetic energy.

This work is supported by the Chemical Sciences, Geosciences, and Biosciences Division, Office of Basic Energy Sciences, Office of Science, U.S. Department of Energy.

References

[1] V. Roudnev, B. D. Esry, and I. Ben-Itzhak, Phys. Rev. Lett. **93**, 163601 (2004).

[2] M. F. Kling et al., Science **312**, 246 (2006); X. M. Tong and C. D. Lin, Phys. Rev. Lett. **98**, 123002 (2007).

[1]E-mail: fatima@phys.ksu.edu
[2]E-mail: esry@phys.ksu.edu

Two-source double-slit interference in angle-resolved high-energy above-threshold ionization spectra of diatoms

M. Okunishi*, R. Itaya*, K. Shimada*, G. Prümper*, K. Ueda*, M. Busuladžić†, A. Gazibegović-Busuladžić‡, D. B. Milošević‡,§ [1], and W. Becker§

*Institute of Multidisciplinary Research for Advanced Materials, Tohoku University, Sendai 980-8577, Japan
†Medical Faculty, Čekaluša 90, University of Sarajevo, 71000 Sarajevo, Bosnia and Herzegovina
‡Faculty of Science, Zmaja od Bosne 35, University of Sarajevo, 71000 Sarajevo, Bosnia and Herzegovina
§Max-Born-Institut, Max-Born-Strasse 2a, 12489 Berlin, Germany

Synopsis Experimental data are reported and compared with molecular strong-field-approximation calculations that display an interference where four electronic quantum orbits conspire. For random orientation of the molecule, footprints of the destructive interference survive for O_2, but not for N_2.

Owing to the two centers of a diatom, the typical high-order above-threshold ionization quantum orbit of a freed electron is replaced by four such orbits, depending upon at which center the electron is ionized and rescatters. The coherent superposition of the contributions of these four orbits in the ionization amplitude gives rise to a particular destructive interference, which defines a curve in the angle-energy plane of the ionized electron along which the electron yield is almost zero. These curves, which depend on the orientation of the molecule, are almost identical for the two molecules N_2 and O_2, in contrast to the usual two-center destructive interference, which depends on the symmetry of the molecular ground state (σ or π).

For randomly oriented molecules, this interference pattern is washed out. However, for orientation of the molecule with respect to the field intermediate between parallel and perpendicular, the yield is suppressed for emission in the field-polarization direction. For O_2, due to its π symmetry there is little emission for parallel and perpendicular orientation, and the suppression survives in the averaged yield (see Fig. 1). For N_2 emission from perpendicular alignment is dominant, and the suppression cannot be seen (not shown).

We present calculations based on the molecular strong-field approximation (MSFA) extended to include rescattering [1, 2] and compare them with experimental data obtained with a setup used previously [3]. The agreement is good with respect to the essential features of the phenomenon, including the intensity dependence.

[1] E-mail: milo@bih.net.ba

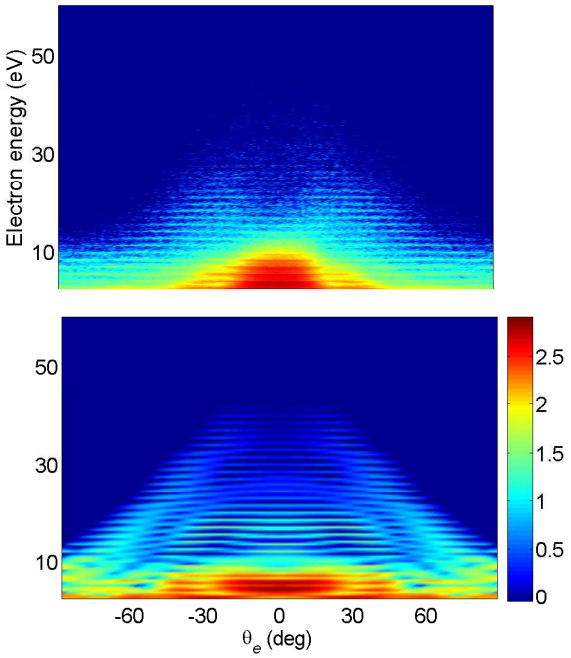

Fig. 1. Angle-resolved electron energy spectra of randomly oriented O_2 as a function of the angle θ_e between electron emission and field polarization. Upper panel: experimental data for a 100-fs 800-nm laser pulse with estimated peak intensity of 7×10^{13} Wcm^{-2}. Lower panel: calculation via the MSFA, averaged over the molecular orientation.

References

[1] D. B. Milošević, Phys. Rev. A **74**, 063404 (2006).

[2] M. Busuladžić, A. Gazibegović-Busuladžić, D. B. Milošević, and W. Becker, Phys. Rev. Lett. **100**, 203003 (2008).

[3] M. Okunishi, K. Shimada, G. Prümper, D. Mathur, and K. Ueda, J. Chem. Phys. **127**, 064310 (2007).

Ultrafast Science and Development at the Astra-Artemis Facility

Edmond Turcu[1], Emma Springate[1], Chris Froud[1], John Collier[1,5], Jon Marangos[2], John Tisch[2], Ricardo Torres La Porte[2], Thomas Siegel[2], Yasin C. El-Taha[2], Nathaniel Kajumba[2], Leonardo Brugnera[2], Immacolata Procino[2], Roy Newell[3], Ian Williams[4], Jason Greenwood[4], Chris Calvert[4], William Bryan[5,1], Andrea Cavalleri[6,8], Sarnjeet Dhesi[7], Jonathan G. Underwood[3,1], Ian Mercer[9], Mads Gabrielsen[10], Richard J. Cogdell[10], Luca Poletto[11], Paolo Villoresi[12,11], Fabio Frassetto[11], Stefano Bonora[11], Mark Roper[13].

[1]Central Laser Facility, STFC Rutherford Appleton Laboratory, UK. [2]Blackett Laboratory, Imperial College London, UK. [3]Department of Physics and Astronomy, University College London, UK. [4]School of Mathematics and Physics, Queen's University Belfast, UK. [5]Department of Physics, Swansea University, UK. [6]Department of Physics, Clarendon Laboratory, University of Oxford, UK. [7] Physical Science Division, Diamond Light Source Ltd, UK. [8]Max Planck Research Group for Structural Dynamics, Centre for Free Electron Laser Science and University of Hamburg. [9]School of Physics, University College Dublin, Ireland. [10]Faculty of Biomedical and Life Sciences, University of Glasgow, Glasgow, UK. [11]LUXOR, CNR-INFM, Padova, Italy. [12]DEI-University of Padova, Italy. [13]STFC Darsebury Laboratory, UK

Astra-Artemis is a unique, new, ultrafast science facility under development in the UK. The paper will report on the: (a) ultrafast science experimental results obtained with Artemis on: HHG mapping of electronic structure; ultrafast molecular process; HHG with 2-colour laser fields, energy transfer in photosynthesis and (b) Artemis facility development of new ultrafast XUV and laser beamlines and time-resolved science end-stations.

Astra-Artemis is a unique, new, ultrafast science facility open to UK and EU university groups as well as to world-wide collaborations. The paper will report on the:

- New ultrafast science experimental results and
- Artemis facility capabilities and development. The facility development proceeds in parallel with the ultrafast-science experimental schedule.

The ultrafast science programme bringing together the expertise of a large number of university groups produced new results in the:

Investigation of HHG mapping of electronic structure of polyatomic molecules (ICL, UCL, CSIC, Napoli, CLF);

- Investigation of HHG with 2-colour laser fields (ICL, UCL, CLF);
- Measurement and control of ultrafast molecular process: vibrational and rotational states in simple molecules (UCL, QUB, SU, CLF); dissociation of vibrationally cold simple molecules held in an ion trap (QUB, DCU, SU, Denison, CLF);
- Energy transfers and coherences in a photosynthetic protein (UCD, ICL, Glasgow, CLF).

The Astra-Artemis facility provides three ultrafast laser beams, two ultrafast XUV beamlines, and two end-stations for ultrafast science. All the femtosecond laser and XUV beams are synchronized to sub-femtosecond resolution. Either beam combination can be temporally and spatially overlapped (delayed and focused) on targets into either of the two end stations.

The two end-stations are dedicated to ultrafast time-resolved:

- materials science (solid target)
- atomic and molecular physics (gas-phase target)

The laser and XUV beamlines consist of the:

- Red Dragon (KML) Ti: sapphire laser driver generating 14Watt with 1kHz repetition, sub-30fs pulse duration and carrier-envelope-phase (CEP) lock.
- Hollow fibre sub-10fs laser compressor (ICL, CLF)
- TOPAS (Light Conversion) opto-parametric-amplifier (OPA) laser tuneable from UV into the mid-IR.
- The XUV beams are produced by focusing either of the laser beams in the high-harmonic-generator (HHG) chamber. The XUV photon energy range is 10eV – 100eV. The two beamlines provide:
  - Monochromatic and tuneable XUV photon pulses spectrally selected from the HHG beam with a novel time-preserving XUV monochromator (CNR, DEI, CLF, DL). This beamline is optimized for the materials science end-station
  - Broad-band XUV beamline optimized for the atomic and molecular physics end station.

E-mail: Edmond.Turcu@stfc.ac.uk

Inner and Outer Ionization of Atomic Clusters by an Intense Attosecond Laser Pulse

A.V. Gets[1] **and V.P. Krainov**

Moscow Institute of Physics and Technology (State University), Dolgoprudny, Moscow Region, Russia

Synopsis: The dynamics of inner and outer ionization of atomic clusters irradiated by intense attosecond laser pulses has been considered. A comparison with the case of femtosecond pulses has been made.

The theory of inner and outer ionization of large atomic clusters by an intense attosecond laser pulse has been developed. Simple new expressions have been suggested for the rate of inner field ionization within the approximation of a strong sudden perturbation. It was shown that a simultaneous detachment of several electrons from atomic core inside the cluster occurs during the intense attosecond laser pulse. The charge multiplicity of atomic ions produced at the inner ionization of noble gas atomic clusters was determined. The conclusion has been made about significant difference between the action of attosecond and femtosecond laser pulses upon the atomic clusters.

Outer filed ionization by an attosecond pulse was investigated also within the frames of strong sudden perturbations. The charge of remaining ionized cluster depends significantly on the cluster size. All electrons produced during inner ionization are ejected from small atomic clusters. There is no cluster expansion during the whole attosecond laser pulse.

It was found that a significant decrease of the ionization potentials of atomic ions inside the cluster takes place due to plasma screening, analogously to the case of femtosecond pulses. The latter case was investigated by us previously [1].

References

[1] A.V. Gets and V.P. Krainov, *J. Phys. B: At. Mol. Opt. Phys.* **39** 1787-1795 (2006).

[1] E-mail: AGets@inbox.ru

Long-term CEP stabilization of a high-power femtosecond laser by the direct locking method

Jae-hwan Lee[*1], Yong Soo Lee[*], Juyun Park[*], Tae Jun Yu[†], and Chang Hee Nam[*]

[*] Dept. Of Physics and Coherent X-ray Research Center, KAIST, Daejeon, 305-701, Korea
[†] Advanced Photonics Research Institute, GIST, Gwangju 500-712, Korea

Synopsis: The carrier-envelope phase (CEP) of a grating-based high-power femtosecond laser was stabilized using the direct locking method. The CEP stabilization of a femtosecond oscillator was successfully maintained for a whole day. Also CEP of amplified pulses was stabilized for several hours with phase jitter of 180 mrad by adjusting the grating separation of a pulse compressor.

Carrier-envelope phase (CEP) stabilization of a femtosecond laser has been intensively investigated for attosecond physics (time-domain application) and frequency metrology. The stabilization scheme called the direct locking (DL) method has been developed especially for time-domain application. Contrast to the conventional PLL method, the direct locking method directly makes the CEP slip between successive pulses to zero. In this case, the stabilized oscillator generates identical pulses so that combining the direct locking method with a CPA laser is easier than the PLL method. Due to the direct use of the beat signal, the setup is very simple and complex equipments used in the case of the frequency domain method are not needed. For precise measurement of CEP slip and long-term operation, homodyne balanced detection and double feedback techniques have been proposed and implemented [1, 2].

Even if the CEP of an oscillator is stabilized, the CEP drift of amplified pulses, due to pumping fluctuation, beam pointing fluctuation, air turbulence, and mechanical vibration, has to be compensated. The CEP drift can be measured using a spectral interferometry (SI). We have stabilized the CEP of amplified laser pulses using a slow feedback loop from SI measurements.

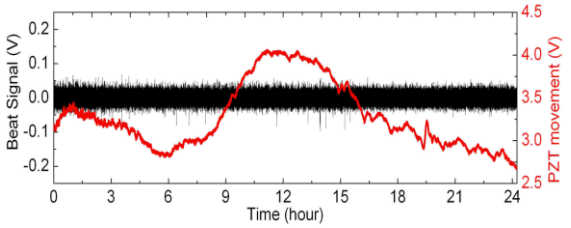

Fig. 1. CEP stabilization of an oscillator for a day

Practical experiment such as isolated attosecond pulse generation requires long-term CEP stabilization. To achieve the operation, the CEP of an oscillator should be stabilized for long time period first. We have achieved CEP stabilization for a day employed by the direct locking method containing double feedback loop. Figure 1 shows the result for the CEP stabilization for a whole day [2].

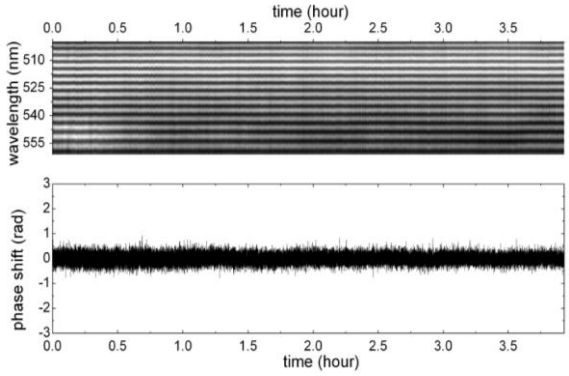

Fig. 2. CEP stabilization of amplified pulses

Based on the long-term CEP stabilization of the oscillator, we have stabilized CEP of amplified pulses. To compensate for the large CEP drift, separation of the grating pair in the pulse compressor was adjusted. Figure 2 shows the result of CEP stabilization of amplified pulses. It was maintained for almost four hours, limited by the movement range of PZT attached to the oscillator prism, and the estimated phase jitter was 180 mrad [3]. Large amplitude noise was not observed and breaking down of CEP stabilization did not occur during the operation. This result shows the good performance of the direct locking method for the CEP stabilization of both oscillator and amplified pulses. The duration of CEP stabilization of amplified pulses will be further extended by replacing the PZT with a longer movement range.

References

[1] T. J. Yu *et al.*, *Opt. Express* 15, 8203 (2007).
[2] J. –h. Lee *et al.*, *Opt. Express* 16, 12624 (2008).
[3] J. –h. Lee *et al.*, *Appl. Phys. B* (Accepted).

[1]E-mail: glisten8@kaist.ac.kr

Attosecond control of electron dynamics in enhanced nanolocalized fields

S. Zherebtsov, I. Znakovskaya, I. Ahmad, A. Wirth, O. Herrwerth, S. Trushin, V. Pervak, S. Karsch, M. Stockman, F. Krausz, M.F. Kling*

Max-Planck Institut für Quantenoptik (MPQ), Hans-Kopfermann-Str. 1, 85748 Garching, Germany

J. Plenge, E. Antonsson, B. Langer, C. Graf, E. Rühl

Physikalische Chemie, Institut für Chemie und Biochemie, Freie Universität Berlin, Takustr. 3, 14195 Berlin, Germany

M.J.J. Vrakking

FOM Institute for Atomic and Molecular Physics (AMOLF), Science Park 113, 1098 XG Amsterdam, The Netherlands

Th. Fennel

Universität Rostock, Institut für Physik, Universitätsplatz 3, 18051 Rostock, Germany

Synopsis: We investigated the waveform control of the electron emission from isolated SiO_2 nanoparticles in intense few-cycle laser fields and compare the results to experiments in Xe for the same laser parameters. The cut-off for the emission of electrons from the nanoparticles is found to be significantly higher as compared to Xe. Model calculations indicate that the high-energy electrons arise from electron recollision in a locally enhanced field near the particle surface.

We report on first experiments on the interaction of isolated SiO_2 nanoparticles with strong few-cycle waveform-controlled light fields. Few-cycle laser light with a controlled evolution of the electric field $E(t) = a(t)\cdot\cos(\omega t + \varphi)$ with amplitude $a(t)$, frequency ω and carrier-envelope phase (CEP) φ has recently allowed steering the motion of electrons in and around atoms, the emission of electrons from surfaces and has been applied to steer electron localization in molecules on a sub-femtosecond timescale [1]. Here, we report on first experiments on isolated SiO_2 nanoparticles (100 nm diameter) in strong ($4\cdot10^{13}$ W/cm^2), linearly polarized few-cycle (<5 fs) laser fields using velocity-map-imaging which allows the reconstruction of their full 3d momentum distributions. SiO_2 nanoparticles have been prepared by wet chemical techniques yielding a narrow particle size and shape distribution. The nanoparticles are inserted into the gas phase by state-of-the-art aerosol preparation and aerodynamic lens focusing. Our approach delivers a beam of isolated nanoparticles and was successfully used to study the VUV-light scattering from ultrafine SiO_2 particles [2].

In the current experiments a significant increase in the cut-off in the electron energy spectra of SiO_2 particles as compared to Xe for the same laser conditions is observed (Fig. 1a). The asymmetry of the electron emission towards the directions along the laser polarization axis (Fig. 1b) shows a pronounced CEP dependence, which oscillates in-phase for the high energy electrons (a behavior different to Xe).

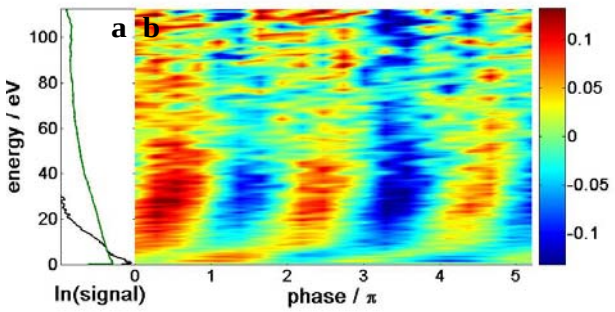

Fig. 1. a) Electron kinetic energy spectrum obtained from SiO_2 nanoparticles (green) and Xe (black); b) Asymmetry in the emission direction of electrons from SiO_2 vs. electron kinetic energy and CEP.

Model calculations are presented that indicate an important role of field enhancement near the nanoparticle surface for the creation of the extended cut-off and the observed CEP dependence.

References

[1] M.F. Kling and M.J.J. Vrakking, *Annu. Rev. Phys. Chem.* **59**, 463 (2008).
[2] J. Shu *et al.*, *J. Chem. Phys.* **124**, 034707 (2006).

* E-mail: matthias.kling@mpq.mpg.de

10 kHz Accuracy Spectroscopy in Acetylene-filled Hollow-core Kagome Fiber as Measured with Optical Frequency Combs

Kevin Knabe*,[1], Andrew Jones*, Jinkang Lim*, Rajesh Thapa*, Karl A. Tillman*, Shun Wu*, François Couny[†], Phillip S. Light[†], Natalie Wheeler[†], Fetah Benabid[†], Jeffrey W. Nicholson[‡], Brian R. Washburn*, and Kristan L. Corwin*,[2]

*116 Cardwell Hall, Department of Physics, Kansas State University, Manhattan, KS, 66506-2604, USA
[†] Centre for Photonics and Photonics Materials, Dept. of Physics, University of Bath, BA2 7AY, UK
[‡] OFS Labs, Somerset, NJ 08873 USA

Synopsis Two frequency combs are used to characterize the accuracy and stability of an optical reference based on a $^{12}C_2H_2$–filled, kagome-structured hollow-core photonic crystal fiber. The accuracy of this reference is ±9 kHz, and the fractional instability is 1.2×10^{-11} or less in 1 s.

High-accuracy, fiber-based spectroscopy is desirable for many portable applications, including frequency references and trace gas analysis. The narrowest sub-Doppler linewidths attained in hollow core photonic crystal fiber (HC-PCF) use large-core kagome structured fiber [1], but their large core size supports multiple spatial modes [2] which could potentially degrade the accurate determination of a sub-Doppler line center. Here we demonstrate that such fibers can yield highly accurate frequency measurements despite these modal properties. The accuracy and stability of such a system approaches that of high-finesse free-space setups [3, 4], making this frequency reference attractive for portable optical telecommunication systems.

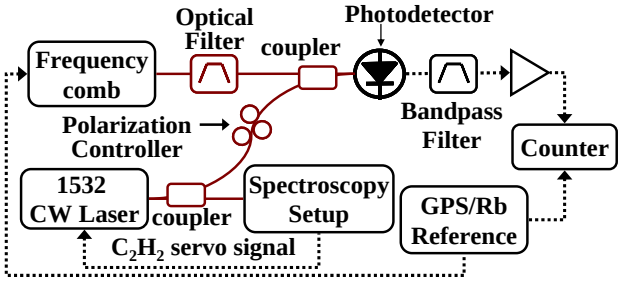

Figure 1. Schematic of the heterodyne beat.

The optical reference under investigation is a continuous-wave (CW) fiber laser frequency-stabilized to the $^{12}C_2H_2$ P(13) $\nu_1+\nu_3$ overtone transition inside kagome HC-PCF using a frequency modulation (FM) saturated absorption spectroscopy (SAS) setup, where the ends of the kagome fiber reside in separate vacuum chambers. The frequency of the CW laser locked to the optical reference is determined by heterodyning it with a self-referenced carbon nanotube fiber laser frequency comb [5] or Cr:forsterite laser frequency comb. Both combs are referenced to a GPS disciplined Rb clock, and a schematic of this setup is shown in Fig. 1. The beat between a comb and the reference has a fractional frequency instability of 1.2×10^{-11} in 1 s, as calculated with a triangle deviation.

The comb's repetition frequency and carrier-envelope offset frequency are counted and averaged to calculate the absolute frequency of the reference. Alignment into the multimode kagome fiber was found to have ~100 kHz shifts on the frequency of the optical reference, so ~20 measurements were conducted where the spectroscopy setup was realigned between refilling of the kagome fiber with various pressures of acetylene. The absolute frequency of the $^{12}C_2H_2$ P(13) $\nu_1+\nu_3$ overtone at zero pressure is found to be 195,580,979,377 kHz ±9 kHz, in agreement with previous measurements [3, 6] and is therefore the highest accuracy measurement in fiber to date [7]. The standard deviation of the data at a given pressure is ±15 kHz, but could be lower in a completely sealed cell (solid core fibers spliced to the ends of HC-PCF) where the input alignment would be fixed, and the presence of a frequency offset is likely. Investigation into linewidth reduction techniques [8] is underway to try to further reduce alignment sensitivity. This work establishes that large-core hollow photonic crystal fibers are suitable for optical frequency references and precise molecular spectroscopy. This research was supported by the AFOSR under contract No. FA9950-08-1-0020, the NSF under Grant No. ECS-0449295.

References

[1] K. Knabe *et al.*, in *Proceedings of CLEO* CWB5 (2009).
[2] F. Benabid, Philos. Trans. R. Soc. London, Ser. A **364**, 3439 (2006).
[3] A. A. Madej *et al.*, J. Opt. Soc. Am. B: Opt. Phys. **23**, 2200 (2006).
[4] H. S. Moon, W. K. Lee, and H. S. Suh, IEEE Trans. Instrum. Meas. **56**, 509 (2007).
[5] J. Lim *et al.*, in *Proceedings of CLEO* CTuK2 (2009).
[6] C. S. Edwards *et al.*, J. Mol. Spectrosc. **234**, 143 (2005).
[7] A. M. Cubillas, J. Hald, and J. C. Petersen, Optics Express **16**, 3976 (2008).
[8] J. Hald, J. C. Petersen, and J. Henningsen, Phys. Rev. Lett. **98**, 213902 (2007).

[1]Email: kok6785@ksu.edu
[2]Email: corwin@phys.ksu.edu

Controlling the Carrier-Envelope Phase of Single-Cycle Waveforms Synthesized from Raman Generated Frequency Combs

Zhi-Ming Hsieh[1,2], Chien-Jen Lai[2], Han-Sung Chan[3], Sih-Ying Wu[2], Chao-Kuei Lee[4]. Wei-Jan Chen[2], Ci-Ling Pan[3,5], Fu-Goul Yee[1], and A. H. Kung[2,3]

[1]Physics Department, National Taiwan University, Taipei, Taiwan
[2]Institute of Atomic and Molecular Sciences, Academia Sinica, Taipei, Taiwan
[3]Department of Photonics & Institute of Electro-Optical Engineering, National Chiao Tung University, Hsinchu, Taiwan
[4]Department of Photonics, National Sun-Yat-Sen University, Kaohsiung, Taiwan
[5]Physics Department & Institute of Photonics Technologies, National Tsing Hua University, Hsinchu, Taiwan

Synopsis: We proposed and experimentally verified that the carrier-envelope phase of single-cycle waveforms synthesized from Raman generated frequency combs can be precisely set and controlled by generating the comb using an infrared laser tuned near a Raman resonance and the second harmonic of the laser to drive the Raman coherence.

In the interaction of single- to few-cycle pulses with matter it is essential that the carrier-envelope phase (CEP) of these pulses is stable since the electric field waveform of the pulses can vary substantially depending on the value of the CEP. The CEP of the pulses synthesized from frequency combs generated by CW mode-locked Ti:saphire lasers can be routinely controlled either actively [1] or passively [2] with high precision. However, while the Raman technique is very promising in the production of multi-octave spanning frequency combs [3] the CEP of waveforms constructed with these combs has varied randomly from one pulse to the next. In this report we demonstrate that by using the fundamental frequency and its second harmonic to drive a Raman coherence the carrier-envelope phase of the resulting waveform becomes fixed at all time.

The source of the problem of a random CEP in the Raman technique is that two driving pulses of vastly different frequencies are required to drive the Raman coherence. These two pulses normally come from different lasers that have a random phase difference between them, thus causing the CEP to vary greatly from one laser pulse to another. Our solution to this problem is to derive the two driving pulses from the same laser source. This way the two pulses will be phase-locked. It can then be shown that a comb generated from these two pulses will have a constant static phase that transforms into a constant CEP for the waveform at all time.

We experimentally verified the long-term inter-pulse phase locking and control of the static phase in a Raman comb whose components are generated by using an infrared laser tuned near a vibrational Raman resonance of the hydrogen molecule and the second harmonic of the laser to drive a H_2 vibrational Raman coherence. We allowed each Raman frequency component to beat with a beam formed from the summing of two lower order components to the same frequency. The resulting heterodyne signal is shown to be stable and the signal modulates as expected as a function of the relative phase between the two input driving beams. Consequently by setting the value of this relative phase we can control the CEP of waveforms synthesized from this Raman comb.

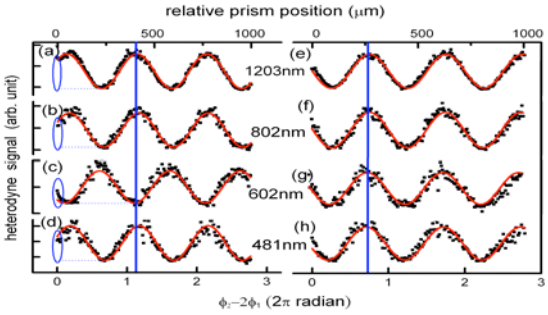

Figure 1. Heterodyne signals from several Raman components and the corresponding sum mixed frequncy in a BBO crystal as a function of the phase difference $\phi_2 - 2\phi_1$.

References:

[1] D. J. Jones et al., Science **288**, 635 (2000) and A. Apolonski et al., Phys. Rev. Lett. **85**, 740 (2000).
[2] A. Baltuška, T. Fuji, and T. Kobayashi, Phys. Rev. Lett. **88**, 133901 (2002).
[3] S. E. Harris and A. V. Sokolov, "Subfemtosecond Pulse Generation by Molecular Modulation", Phys. Rev. Lett. **81**, 2894 (1998).

akung@pub.iams.sinica.edu.tw

Generation of 3.7-fs, 1.2-mJ pulses using a hollow-fiber pulse compressor

Juyun Park[1], **Jae-hwan Lee, Luu Tran Trung, and Chang Hee Nam**

Dep. of Physics and Coherent X-ray Research Center, KAIST, Daejeon 305-701, Korea

Synopsis: A differentially pumped neon-filled hollow-fiber pulse compressor was investigated to generate high-power few-cycle laser pulses. The pulse compression was optimized by adjusting neon pressure and laser chirp to produce the shortest laser pulses. Precise dispersion control enabled the generation of laser pulses with duration of 3.7 fs and energy of 1.2 mJ. This corresponds to an output of 1.5-cycle, 0.3-TW pulses at a 1-kHz repetition rate.

High-power few-cycle lasers have been developed for the investigation of ultrafast phenomena. The hollow-fiber pulse compression method has been utilized in compressing high power femtosecond laser pulses to few-cycle pulses [1]. While laser pulses are propagating through a hollow fiber filled with a noble gas, spectral broadening is induced by self-phase modulation due to Kerr and ionization effects. The spectrally broadened pulses can form few-cycle pulses after compensating for the chirp remained in output pulses.

For the generation of high-power few-cycle laser pulses, a differentially pumped hollow-fiber pulse compressor was utilized in a femtosecond Ti:Sapphire laser at 1 kHz. Laser pulses with 29-fs pulse duration and 5.0-mJ energy were launched into a neon-flowing hollow-fiber pulse compressor [2]. The residual laser chirp of the output beam was compensated by two sets of chirped mirrors. Temporal characterization of the compressed pulses was carried out using the second-harmonic generation (SHG) frequency-resolved optical-gating (FROG) method.

Spectral broadening of intense femtosecond laser pulses in ionizing gas is sensitive to the gas pressure and input laser chirp. The neon gas pressure in the hollow-fiber pulse compressor was adjusted to achieve wide spectral broadening while preventing self-focusing. Higher pressure leads to a broader output spectrum but too high gas pressure can result in propagation instabilities due to self-focusing effects. The output spectra changed very delicately to laser chirp. With negatively chirped pulses, spectral broadening was reduced, while the broadening was effective with positively chirped pulses. The broadest spectrum capable of generating 3.2-fs pulses was produced with positively chirped 33-fs pulses. Thus, appropriate gas pressure and positive chirp of initial pulses were needed for maximum spectral broadening.

The remaining laser chirp of spectrally broadened laser pulses was compensated to achieve near transform-limited pulses. The output laser chirp was precisely controlled by adjusting neon pressure and input laser chirp, together with 2-sets of chirped mirrors having total GDD of -170 fs^2. As shown in Fig. 1, the spectral phase of the output pulse indicates that the laser chirp was almost compensated. The shortest pulse of 3.7 fs with energy of 1.2 mJ, corresponding to 1.5-cycle, 0.3-TW output was generated in the conditions of positively chirped 33-fs pulse and 1.6-bar neon. CEP stabilized few-cycle high-power laser pulses will be applied to attosecond physics investigations.

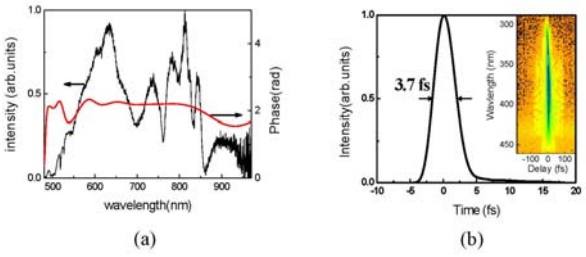

Fig. 1. (a) Spectral profile and phase of the laser output taken with 1.6-bar neon and positively chirped 33-fs laser pulse, and (b) temporal profile of the laser pulse measured using the SHG FROG method. The inset shows the FROG trace.

References

[1] M. Nisoli, S. De Silvestri, O. Svelto, Appl. Phys. Lett. 68, 2793 (1996).

[2] J. H. Sung, J. Y. Park, T. Imran, Y. S. Lee, C. H. Nam, Appl. Phys. B 82, 5 (2006).

[1] E-mail: juyuni@kaist.ac.kr

Generation of high-order harmonics with ultra-short pulses from filamentation

E. Schulz[*,†1], **D. S. Steingrube**[*,†2], **T. Vockerodt**[*,†], **U.Morgner**[*,†,‡], **and M. Kovačev**[*,†]

[*]Institut für Quantenoptik, Leibniz Universität Hannover, Welfengarten 1, D-30167 Hannover, Germany
[†]QUEST, Centre for Quantum Egineering and Space-Time Research, Hannover, Germany
[‡]Laser Zentrum Hannover e.V., Hollerithallee 8, D-30419 Hannover, Germany

Synopsis We obtain 7-fs-pulses with 0.3 mJ after filamentation and pulse compression by double-chirped-mirrors (DCM). We use these pulses to generate high-order harmonics in a semi-infinite gas cell setup. Spectral broadening of the harmonics in different gases is observed. Especially in neon an extended continuous cut-off region down to 10 nm (124 eV) can be realized. This opens up the way to attosecond-pulse generation from filamented pulses.

We present high-order harmonic generation (HHG) in a semi-infinite gas cell from filamented pulses. The 30-fs-pulses from a CPA-laser-system with pulse energy of 1.2 mJ, a repetition rate of 3 kHz and a central wavelength of 776 nm are spectrally broadened in a filament and compressed down to 7 fs.

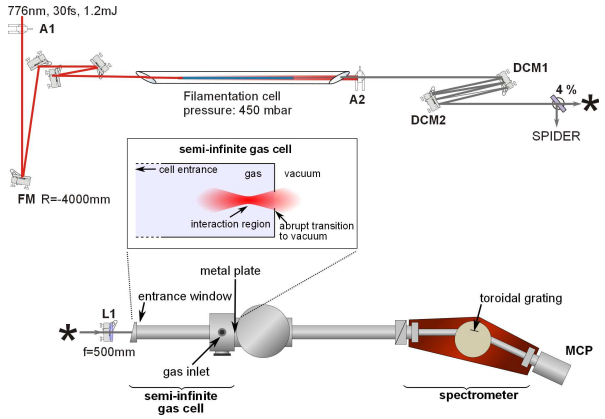

Fig. 1. Sketch of filamentation and HHG setup. The CPA-pulses are compressed in a filament setup and the harmonics are generated in a semi-infinite gas cell. The entrance window of the cell is far from the interaction region. A pinhole ensures an abrupt transition to vacuum for absorption-less propagation.

For filamentation we focus the beam into a gas cell filled with argon and select only the center of the beam profile that contains the octave spanning spectrum from 400 nm to 900 nm. A pulse energy of 0.3 mJ can be used to generate the high-order harmonics in a semi-infinite gas cell setup [1] [2] as shown in figure 1.

We generate high-order harmonics in different noble gases. The broadening of the harmonic spectra is measured for argon, xenon, and neon. The broadest continuum and the highest cut-off energy is observed in neon, see figure 2, which is the gas with the highest ionization energy of the investigated rare gases.

Singe attosecond pulses via few-cycle pulses from filamentation are now in reach. Due to the energy scaling properties of the filamentation process higher photon and pulse energies in isolated attosecond pulses become feasible.

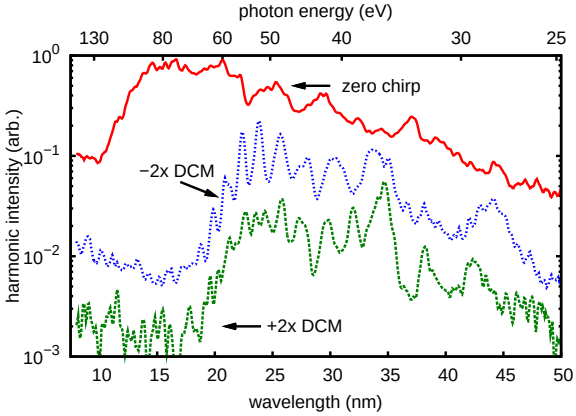

Fig. 2. Harmonic spectra in 40 mbar neon and the effect of dispersion on the cut-off energy. The spectra for positively (+2x DCM), negatively (-2x DCM) chirped and compressed pulses (zero chirp) are shown.

References

[1] N. Papadogiannis et al., Appl. Phys. B **73**, 687-692 (2001).

[2] J. Peatross et al., J. Mod. Opt. **51**, 2675-2683 (2004).

[1]E-mail: schulz@iqo.uni-hannover.de
[2]E-mail: steingrube@iqo.uni-hannover.de

Reflective and Diffractive Optics for Coherent Ultrafast Radiation at Extreme Ultraviolet and Soft X-Ray Wavelengths

Yanwei Liu*†[,1], Andrew L. Aquila*†, Farhad Salmassi*, Anne Sakdinawat*†, and Eric Gullikson*

[*] Center for X-Ray Optics, Lawrence Berkeley National Laboratory, Berkeley, CA 94720, USA
[†] NSF EUV Engineering Research Center, University of California at Berkeley, CA 94720, USA

Synopsis: We present recent developments of novel reflective and diffractive optics at the Center for X-Ray Optics (CXRO), Lawrence Berkeley National Lab, for use with coherent ultrafast x-ray sources such as high order harmonic generation and free electron lasers. At extreme ultraviolet (EUV) wavelengths, we demonstrated high efficiency multilayer-based reflective optics and the capability to fabricate aperiodic structure with optimized thickness variations for desired bandwidth and phase response, enabling pulse shaping at sub-femtosecond scale. Also described is an attosecond beam splitter, which converts a single attosecond incoming pulse into two replicas with precisely controlled time delay. This can be used in SPIDER experiments for full characterization of attosecond pulses. For coherent soft x-rays, novel diffractive optics designs implementing Fourier optics technique enables phase manipulation and provides phase contrast enhancement and extended depth-of-focus.

At EUV wavelengths, the efficiency of reflective optics can be greatly enhanced by multilayer coatings. CXRO has developed coatings using various material combinations to achieve reflectivity higher than 45% across the whole EUV spectrum from 30 to 120 eV, and as high as 70% at ~ 90 eV.

Aperodic multilayer, consisting of layers with varied thickness, offers greater flexibility on tweaking the bandwidth and phase response. By incorporating practical coating parameters, we have successfully fabricated aperodic multilayers whose characterization matched the prediction of simulation model [1] (fig. 1a).

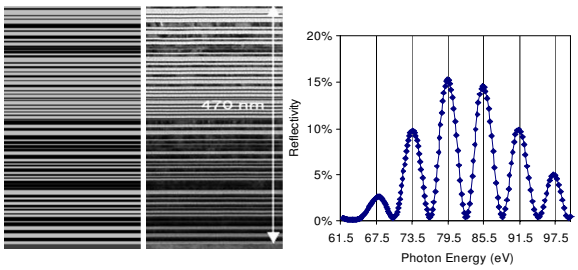

Fig. 1. (a)An aperiodic multilayer coating. (b) Spectral response of an attosecond beam splitter.

Attosecond SPIDER experiment has been proposed [2] to fully characterize an attosecond pulse. A key component for such experiment is a beam splitter that can produce two replicas of the incoming pulse, with their time delay precisely controlled. We developed a Fabre-Perot-like structure with two multilayer stacks separated by a silicon layer. The spectral response of this structure (fig. 1b) confirms the existence of two duplicated pulses separated by 67 as (¼ period of the 800 nm pump field).

At soft x-ray wavelengths, Frsenel zone plates fabricated by electron beam lithography are used in x-ray microscopes, achieving better than 15 nm spatial resolution[3]. Novel diffractive optics being developed at CXRO, for example spiral [4], Zernike [5], and cubic zone plates, utilize coherence properties of radiation to achieve phase contrast enhancement or extended depth-of-focus.

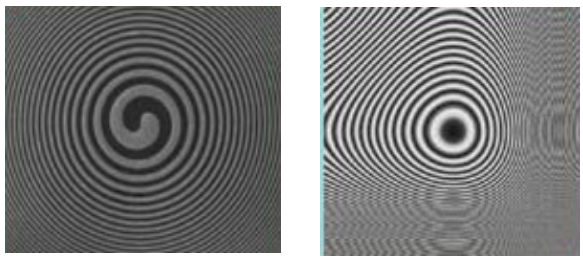

Fig. 2. A spiral (left) and cubic (right) zone plate.

The novel optics mentioned here will find new applications with the newly available coherent ultrafast sources, and together they can open new opportunities in attosecond sciences.

References

[1] A. Aquila *et al.*, Opt. Express 14, 10073 (2006).
[2] F. Quéré *et al.,* Phys. Rev. Lett. 90, 073902 (2003)
[3] W. Chao et al., Nature, 435, 1210 (2005).
[4] A. Sakdinawat and Y. Liu, Opt. Lett. 32, 2635 (2007).
[5] A. Sakdinawat and Y. Liu, Opt. Express 16, 1559 (2008).

[1] E-mail: ywliu@lbl.gov

The Robustness of Attosecond Streaking Measurements

Justin Gagnon[*,1] **and Vladislav S. Yakovlev**[†,2]

[*]Max-Planck-Institut für Quantenoptik, Hans-Kopfermann-Str. 1, D-85748 Garching
[†]Ludwig-Maximilians-Universität, D-85748 Garching, Germany

Synopsis We investigate the robustness of one of the key tools of attosecond metrology: the attosecond streak camera. We consider the case of single and double attosecond pulses. For several key parameters of the electron wave packet, we systematically investigate how each one's uncertainty affects the spectrogram and the accuracy of the attosecond FROG retrieval.

Current models used to describe attosecond streaking measurements [1, 2], and the analysis techniques that are thence derived [3, 4], ignore the experimental fact that the recorded spectrogram actually results from a statistical ensemble of electron wave packets. This statistical ensemble might result from changes in the waveform of the laser field which is used both for generating and streaking, and can occur either from shot to shot or over the spatial profile. Certain streaking measurements may contain uncertainties that cannot be decoupled from the experiment. For example, when streaking is performed on electrons ejected from a conduction band, an inherent uncertainty in the electrons' central energy is present in the recorded spectra.

In this work, we address the issue of uncertainties in streaking measurements by identifying several key properties of an electron wave packet, and looking at how an uncertainty in each of them affects the streaking spectrogram and the resulting attosecond FROG reconstruction. We consider spectrograms for two types of electron wave packets: a single isolated pulse, and a sequence of two pulses separated by a laser half-cycle. The former is an ideal case of attosecond metrology, where a perfect gating mechanism has denied the contribution of all but one laser half-cycle. The latter is a more realistic case: due to the periodicity of the generating laser field, attosecond pulses are typically produced from two or more laser half-cycle. Even cutting edge gating techniques such as DOG [5], dynamic phase-matching [6] or the use of very short generating fields of $\approx 3.3\,\mathrm{fs}$ [7] still allow at least two half-cycles to contribute to the harmonic generation.

For an isolated pulse, we study uncertainties in the central energy, group-delay dispersion (GDD) and bandwidth of the electron wave packet. We find that the central energy uncertainty plays the largest role in smearing the spectrogram, resulting in an underestimated pulse duration, whereas uncertainties in the GDD and bandwidth have a minor effect.

For a sequence of two pulses, the spectrogram displays a fringe pattern resulting from the interference between the two pulses. For this case, we consider uncertainties in the relative phase, relative timing and relative intensity between the two pulses. These quantities each have their own foot print on the fringe pattern in the spectrogram. We show that the main effect of these uncertainties is a smearing of the fringe pattern, which curtails the accurate characterization of the satellite pulse (the smaller of the two pulses). However, we find that the main pulse is nevertheless correctly retrieved.

[1]E-mail: Justin.Gagnon@mpq.mpg.de
[2]E-mail: Vladislav.Yakovlev@physik.uni-muenchen.de

References

[1] J. Itatani *et al.*, Phys. Rev. Lett. **88**, 173903 (2002).

[2] M. Kitzler *et al.*, Phys. Rev. Lett. **88**, 173904 (2002).

[3] Y. Mairesse and F. Quéré, Phys. Rev. A **71**, 011401 (2005).

[4] J. Gagnon, E. Goulielmakis and V. S. Yakovlev, Appl. Phys. B **92**, 25 (2008).

[5] H. Mashiko *et al.*, Opt. Expr. **100**, 103906 (2008).

[6] I. Thomann *et al.*, Phys. Rev. Lett. **17**, 4611 (2009).

[7] E. Goulielmakis *et al.*, Science **320**, 1614 (2008).

Strong-Field Modulated Diffraction Effects in the Correlated Electron-Nuclear Motion in Dissociating H_2^+

Feng He*, Andreas Becker†, and Uwe Thumm* [1]

*James R. Macdonald Laboratory, Kansas State University, Manhattan, Kansas 66506-2604, USA
†Department of Physics and JILA, University of Colorado, Boulder 80309-0440, USA

Synopsis : By solving the time dependent Schrödinger equation for H_2^+ in a pump-probe numerical experiment, we found that the electronic motion can follow or oppose the laser electric force. Our results show that the internal electron dynamics in H_2^+ is determined by both, the external laser field and intra-molecular electron diffraction.

Current sub-fs laser technology allows for the control of the final localization of the electron in a dissociating hydrogen molecular ion [1, 2]. However, the complex dynamics of the active electron in the time-dependent fields of both nuclei and external laser pulse(s) *before* the electron is localized on one of the nuclei by the rising interatomic barrier is not understood in detail. One may expect that the electron dynamics in the dissociating molecule is an interplay of, at least, field-induced and structural (i.e., interference) effects. We solved the time-dependent Schrödinger equation in three dimensions, and found that the direction of the electronic motion inside the dissociating H_2^+ can follow or oppose the external laser electric field, depending on the laser intensity [3].

Our model describes a 2-cycle (FWHM), 106 nm, 10^{13} W/cm^2, Gaussian attosecond pump pulse that excites a dissociating nuclear wave packet on the $2p\sigma_u$ electronic potential curve of H_2^+. A time-delayed infrared laser pulse (2 cycles, 800 nm) is introduced to manipulate the wave function. Fig. 1 shows the evolution of the electronic probability density towards one of the nuclei. For all laser intensities the electron at first oscillates between the two nuclei, as one would expect classically. During the second half of the laser field, the increasing interatomic barrier starts to hinder electron transfer between the nuclei [2], and the electron eventually localizes near one of the protons. Details of the electronic motion are strongly intensity dependent and yield electron localization on opposite centers at different laser peak intensities. For example, the comparison of Figs.1 (b) and (c) near 5.5 fs shows that the electron is moving along either the negative (b) or the positive z-axis (c), even though the laser profiles are the same. This surprising result shows that the expected electronic motion does not necessarily follow the direction of the laser field. By increasing the intensity further, to 10^{14} W/cm^2, the electron-transfer dynamics again changes dramatically (d).

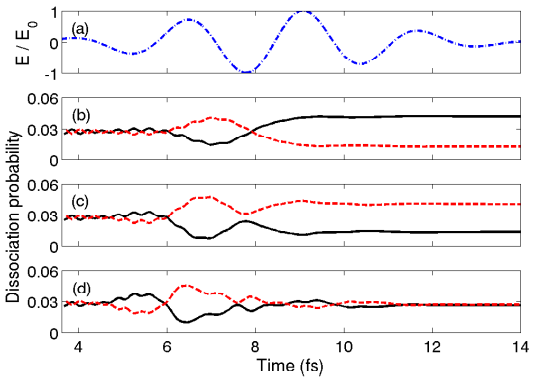

Fig. 1. (color online) IR laser electric field for a time delay of 5.8 fs (a). Dissociation probability $P_-(t)$ (solid line) and $P_+(t)$ (dashed line) for the electron to remain in the $z < 0$ and $z > 0$ half space, respectively, for IR laser intensities of 3×10^{12} (b), 2×10^{13} (c), and 10^{14} W/cm^2 (d).

By analyzing the evolution of the molecular wave function in phase space, the corresponding Wigner distribution indicates the path towards electronic localization in terms of the passage of electronic flux through diffraction-induced "momentum gates" that may or may not allow the electron to transfer to the other nucleus [3]. It reveals that the IR laser field dynamically shifts the gates, causing the electron to explore different gates at different laser intensities.

References

[1] M.F.Kling *et al.*, *Science* **312**,246 (2006).

[2] F.He, C.Ruiz, and A.Becker, *Phys. Rev. Lett.* **99**, 083002 (2007)

[3] F.He, A.Becker, and U.Thumm, *Phys. Rev. Lett.* **101**, 213002 (2008)

[1] E-mail: thumm@phys.ksu.edu

Retrieval of target photorecombination cross sections from high-order harmonics generated in a macroscopic medium

Cheng Jin[1], **Anh-Thu Le**[2], **and C. D. Lin**[3]

J. R. Macdonald Laboratory, Physics Department, Kansas State University, Manhattan, Kansas 66506, USA

Synopsis We investigate high-order harmonic generation (HHG) in a thin macroscopic medium by solving Maxwell's equation using microscopic single-atom induced dipole moment calculated from the recently developed quantitative rescattering (QRS) theory. We show that macroscopic HHG yields calculated from QRS compared well with those obtained from solving the single-atom time-dependent Schrödinger equation but with great saving of computer time. We also show that macroscopic HHG can be expressed as a product of a macroscopic wave packet and the photorecombination cross section of the target gas. The latter enables us to extract target structure from the experimentally measured HHG spectra, thus paves the way to use few-cycle infrared lasers for time-resolved chemical imaging of transient molecules with few-femtosecond temporal resolution.

In recent years high-order harmonic generation (HHG) by a strong infrared laser field interacting with a gas of atoms has been widely used for the production of subfemtosecond pulses in the extreme ultraviolet (XUV) radiation. The physical origin of the harmonics emission in a single atom can be easily described by a three-step model [1, 2]. Since HHG is generated by a focused laser beam over all the atoms in a macroscopic medium, the induced dipole moment on each atom should be inserted as a source term in the propagation equations of the harmonic field to obtain the macroscopic response of the excited nonlinear medium. Thus a typical HHG calculation consists of two parts: first, the calculation of single-atom response; second, the propagation of Maxwell's wave equation. Due to the limitation of strong field approximation (SFA) for the description of single-atom response, we have proposed a quantitative rescattering (QRS) theory recently [5]. The QRS is about as fast as the SFA, and the accuracy of it has been carefully tested against single-atom HHG spectra obtained by solving the time-dependent Schrödinger equation (TDSE). With QRS-based single-atom induced dipole moments, the macroscopic HHG spectra are nearly as accurate as those from TDSE based and are much better than SFA based. The macroscopic HHG yield can be expressed as the product of a "macroscopic wave packet" (MWP) and the single-atom recombination dipole moment [6].

In our simulation we assume that there is no ionization effect of the medium on the fundamental laser field. This condition can be satisfied when we consider low intensity laser, low density and short gas medium. The propagation equation of harmonic field in the moving coordinate frame is [3, 4]

$$\nabla_\perp^2 \widetilde{E}_h(r,z',\omega) - \frac{2i\omega}{c}\frac{\partial \widetilde{E}_h(r,z',\omega)}{\partial z'} = -\mu_0\omega^2 \widetilde{P}_{nl}(r,z',\omega). \quad (1)$$

The macroscopic HHG spectra are obtained by

$$S_h(\omega) \propto \int_0^\infty |\widetilde{E}_h(r,z',\omega)|^2 2\pi r dr. \quad (2)$$

Electric field of laser pulse in t'' frame is

$$E_1(r,z',t'') = |\varepsilon(r,z')|\cos^2(\frac{\pi t''}{\tau_p})\cos(\omega_0 t'' + \varphi_{CE}). \quad (3)$$

Nonlinear polarization term in moving coordinate frame can be obtained by

$$\widetilde{P}_{nl}(r,z',\omega) = \widehat{F}[P_{nl}(r,z',t'')]e^{-i\frac{\omega}{\omega_0}\varphi_{laser}(r,z')}. \quad (4)$$

References

[1] P. B. Corkum, Phys. Rev. Lett. **71**, 1994 (1993).

[2] M. Lewenstein *et al.*, Phys. Rev. A **49**, 2117 (1994).

[3] E. Priori *et al.*, Phys. Rev. A **61**, 063801 (2000).

[4] M. B. Gaarde *et al.*, Phys. Rev. A **74**, 053401 (2006).

[5] A. T. Le *et al.*, Phys. Rev. A **78**, 023814 (2008).

[6] C. Jin *et al.*, Phys. Rev. A **79**, 053413 (2009).

[1] E-mail: cjin@phys.ksu.edu
[2] E-mail: atle@phys.ksu.edu
[3] E-mail: cdlin@phys.ksu.edu

Accurate Retrieval of Structural Information of Atoms and Molecules from Laser-Induced Photoelectron and High-Order Harmonic Spectra by Intense Laser Pulses

Toru Morishita*[†,1], Toshihito Umegaki*, Shinichi Watanabe*, Oleg.I. Tolstikhin[#], Anh-Thu Le[§], Zhangjin Chen[§], and C.-D. Lin[§]

[*] Department of Applied Physics and Chemistry, University of Electro-Communications, 1-5-1 Chofu-ga-oka, Chofu-shi, Tokyo, 182-8585, Japan
[†]PRESTO, Japan Science and Technology Agency, Kawaguchi, Saitama 332-0012, Japan
[#]Russion Research Center "Kuruchatov Institute," Kurchatov Square 1, Moscow 123182, Russia
[§]Department of Physics, Cardwell Hall, Kansas State University, Manhattan, Kansas 66506, USA

Synopsis: By analyzing accurate theoretical results as well as experimental results, we established the general conclusion that laser-generated high-energy electron momentum spectra and high-order harmonic spectra can be used to extract accurate differential elastic scattering and photo-recombination cross sections of the target ion with *free* electrons, respectively. Since both electron scattering and photoionization are the conventional means for interrogating the structure of atoms and molecules, this result implies that existing few-cycle infrared lasers can be implemented for ultrafast imaging of transient molecules with temporal resolution of a few femtoseconds.

When an atom or a molecule is exposed to an intense infrared laser, the atom is first tunnel ionized with the release of an electron. This electron is placed in the oscillating electric field of the laser and may be driven back to revisit its parent ion. This reencounter incurs various elastic and inelastic electron-ion collision phenomena where the structural information of the target is embedded. The possibility of using such laser-induced returning electrons for self-imaging molecules has been discussed frequently in the past. By analyzing accurate theoretical results from the solution of the time-dependent Schrödinger equation for rare gas atoms in few-cycle intense laser pulses, we established the general conclusion that the high-energy photoelectron momentum spectra and the high-order harmonics spectra can be simply expressed as the following factorization formula[1],

$$S = \sigma\, W,$$

where S is the photoelectron spectrum or the high-order harmonic spectrum, and σ is the elastic or photo-recombination cross section of the target ion by ***free*** electrons. Here, W is interpreted as the momentum distribution of the returning electron wave packet which depends only on the laser parameters.

That conventional electron scattering as well as photorecombination cross sections yield structural information of the atoms and molecules implies that returning electrons induced by existing few-cycle infrared laser pulses can be indeed used for implementation of temporal resolution from a few femtoseconds down to sub-femtoseconds[2].

We will present recent experimental results for extracting a wide range of angular and momentum distributions of the photoelectron cross sections [3] and photo-recombination cross sections [4] of rare gas atoms. We will also discuss several developments, including theoretical and experimental results for molecular targets as well as a detailed structure of the factorization formula based on an adiabatic theory for rescattering processes [5].

E-mail: toru@pc.uec.ac.jp

References

[1] T. Morishita, A.-T. Le, Z. Chen, and C. D. Lin, Phys. Rev.Lett. **100**, 013902 (2008).
[2] T. Morishita A.-T. Le, Z. Chen, and C. D. Lin, New J.Phys. 10, 025011 (2008).
[3] T. Morishita, *et al*., J. Phys. B. **42**, 105205 (2009).
[4] S. Minemot, *et al*., Phys. Rev. A **78**, 061402 (2008) .
[5] O. I. Tolstikhin and T. Morishita, *et al*., in preparation.

High order harmonic generation in fullerenes

A. Jaroń-Becker*[1], M.F. Ciappina, and A. Becker***

* JILA and Department of Physics, University of Colorado, 440 UCB, Boulder, CO 80309-0440, USA
** Institute of High Performance Computing, 1 Fusionopolis Way, 16-16 Connexis, Singapore 138632

Synopsis Within the Strong Field Approximation we have found that the high harmonic spectra for icosahedral fullerenes at midinfrared wavelengths show modulations in the plateau region. These modulations are due to the coherent superposition of the contributions to the dipole moment from different atomic centers of the molecule and are present in spectra for ensembles of aligned fullerenes as well as randomly oriented ones. In the case of the larger fullerenes the radius of the fullerene can be determined from the positions of the interference minima in the high harmonic spectra using a spherical model.

One of the exciting goals in intense laser science is that of imaging dynamical changes in molecular structure and molecular reactions on an ultrafast time scale. A promising tool for such investigations is high-order harmonic generation (for a review, see [1]), since an initially ionized electron is driven back by the field to the parent ion and recombines under the emission of a high-energy photon. The harmonic spectrum is, in general, sensitive to the orientation and structure of the molecule and the symmetry of the molecular orbital involved.

In order to evaluate the potential of molecular imaging using harmonic generation it is important to study the process in large polyatomic molecules. We have therefore analyzed high harmonic generation in fullerenes of icosahedral fullerenes [2, 3] using the strong-field approximation. Our results for the high harmonic spectra generated in C_{20},C_{60},C_{80}, and C_{180} show modulations in the plateau at midinfrared but not at the near-infrared wavelengths. We have shown that these modulations are due to a multislit interference effect arising from the coherent superposition of the contributions to the dipole moment, from different atomic centers of the molecule (see Figure). Due to the highly symmetric geometric structure of the fullerenes the modulations are present in spectra for ensembles of aligned fullerenes as well as randomly oriented ones. The Figure shows that the positions of these minima agree with minima of the recombination matrix element. We further used a simple spherical-shell model of a fullerene to reproduce the minima of the recombination matrix element and determine the radius of the fullerene from the positions of the interference minima. The observation of high harmonic spectra may be therefore useful to identify structural changes in such complex molecules induced by an intense laser pulse.

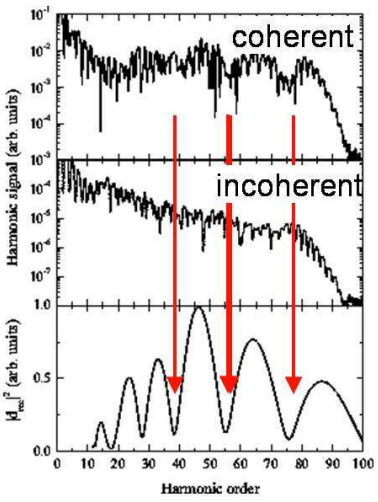

Fig. 1. Theoretical predictions for high-order harmonic spectra generated in C_{180} at $\lambda = 1800$ nm (upper panel) and an intensity of $I = 5 \times 10^{13}$ W/cm^2 [3]. The characteristic minima in the high harmonic spectra are induced by destructive interference effects between the partial electron waves emanating from the different atomic centers of the molecule (middle panel) and correspond to zeros in the recombination matrix element (lower panel).

References

[1] M. Lein, J. Phys. B **40**, R135 (2007).

[2] M.F. Ciappina, A. Becker and A. Jaroń-Becker, Phys. Rev. A **76**, 063406 (2007)

[3] M.F. Ciappina, A. Jaroń-Becker and A. Becker, Phys. Rev. A **78**, 063405 (2008)

[1] E-mail: jaron@jila.colorado.edu

Extreme ultraviolet (XUV) pulse shaping with aligned molecules

Zhinan Zeng[1], **Ruxin Li, Zhizhan Xu**

State Key Laboratory of High Field Laser Physics, Shanghai Institute of Optics and Fine Mechanics, Chinese Academy of Sciences, Shanghai, People's Republic of China 201800

Synopsis: We theoretically propose a simple scheme to shape the xuv pulse on attosecond timescale with the aligned molecule. This may offer a new way to manipulate and control the photon emission on attosecond timescale.

Many experiments, e.g. the tomographic imaging of molecular orbitals, the quantum interference during HHG and the proton dynamics in molecules, have been carried out with the HHG generated by the molecules, e.g. O_2, N_2, CO_2 [1, 2]. With the orientation dependence of the molecular HHG and the field-free alignment of the molecule, we can produce the xuv pulse of different shape just by adjusting the time delay between the laser pulse to induce the nonadiabatic molecular alignment and the laser pulse to generate the HHG.

We use the CO_2 molecule to demonstrate this process numerically. For CO_2 molecule whose valence orbital has even parity symmetry, the valence orbital can be expressed by

$$\Psi_g(\vec{x}) = N\left[\Phi\left(\vec{x}+\vec{R}/2\right)+\Phi\left(-\vec{x}+\vec{R}/2\right)\right] \quad (1)$$

Where N is normalization factors, $\Phi(\vec{x})$ is the atomic orbital, $\vec{R}/2$ and $-\vec{R}/2$ the positions of the nuclei (for CO_2 molecules, the positions of the two O atoms). With the molecular orbital expression and the Lewenstein model [3], we can calculate the molecular dipole moment $d(\theta,t)$ of any orientation in the time domain in which θ is the angle between the polarization of the laser pulse and the axis of the CO_2 molecule.

The laser-induced orientation dynamics of CO_2 can be calculated by solving the time-dependent Schrodinger equation (TDSE) [4], in which the rigid-rotor approximation is used. After solving the TDSE, we can obtain the angular distribution $\rho(\theta,\tau)$ of the molecules, where τ is the delay time after the intensity peak of the laser pulse which induced the orientation dynamics. In the simulation, the pulse intensity is 0.03a.u. ($3.16\text{X}10^{13}\text{W/cm}^2$) and the pulse duration is 60fs. The rotational temperature of CO_2 molecules is taken to be 40K.

With $d(\theta,t)$ and $\rho(\theta,\tau)$, we can calculate the delay time dependent dipole moment with expression below,

$$S(\tau,t) = 2\pi\int_0^\pi \rho(\theta,\tau)d(\theta,t)d\theta \quad (2),$$

where τ is the delay time between two laser pulses. Then we can easily calculate the delay time dependent HHG by performing the Fourier-Transform (FT) on the $S(\tau,t)$.

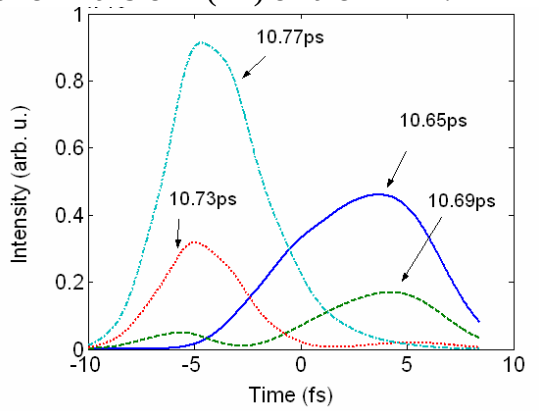

Fig. 1. the temporal profiles of the xuv pulses with different delay time.

In Fig. 1, when the delay time changes from 10.65ps to 10.77ps, the xuv pulse changes from a single-peak pulse to a double-peak pulse. Then right peak of the double-peak pulse becomes weaker and weaker gradually. When the delay time becomes to be 10.77ps, the xuv pulse becomes to be a single-peak pulse again.

In conclusion, we have proposed a simple scheme to shape the temporal profile of the xuv pulse. This result may offer a new way to manipulate and control the photon emission in the xuv domain.

References

[1] J. Itatani et al, *Nature* **432**, 867 (2004)
[2] T. Kanai et al, *Nature* **435**, 470 (2005)
[3] M. Lewenstein et al, *Phys. Rev. A* **49**, 2117(1994)
[4] A. B. Haj-Yedder et al, *Phys. Rev. A* **66**, 063401 (2002)

[1]Email: zhinan_zeng@mail.siom.ac.cn

Strong field dynamics with ultrashort electron wave packet replicas

P. Rivière[1], **O. Uhden, U. Saalmann and J. M. Rost**

Max Planck Institute for the Physics of Complex Systems, Nöthnitzer Straße 38, D-01187 Dresden, Germany

Synopsis We investigate theoretically electron dynamics under a VUV attosecond pulse train which has a controlled phase delay with respect to an additional strong infrared laser field. We analyze the dynamics in terms of electron wave packet replicas created by the attosecond pulses. The absorption probability shows strong modulations as a function of the phase delay for VUV photons of energy comparable to the binding energy of the electron, while for higher photon energies the absorption probability does not depend on the delay, in line with the experimental observations for helium and argon, respectively.

Technological advance has made it possible to expose atoms and molecules to a combination of attosecond pulse trains (APT) and infrared (IR) laser pulses with an accurate control of their phase delay [1]. The photo electron spectrum of atoms, as well as above threshold ionization or photoassociation have been studied in this combined light field [2].

A dynamically very interesting regime emerges when the energy of the VUV photon from the APT is comparable to the ionization potential but the IR pulse alone (typically 780 nm wavelength) is not intense enough to ionize the atom. The combined action of both fields leads to a time-dependent wave packet dynamics which is very sensitive to the phase delay, equivalent to the carrier-envelope phase (CEP) of the IR field. It has been recently shown that the phase delay modulates the total ionization and absorption probability [3]. A solution of the one-electron time-dependent Schrödinger equation (TDSE) yields excellent agreement with this experiment [3], but the exact reason and systematics of these oscillations are difficult to identify in a fully numerical solution.

Here, we formulate a minimal analytical approach [4]. It elucidates the mechanism behind the pronounced structures in the electron observables as a function of phase delay in the spirit of the "simple man's approach" [5].

Using the strong field approximation, we arrive at a minimal analytical model for the kinetic energy distribution of the electron and photoabsorption probability, as a function of the phase delay between the fields. We analyze the dynamics in terms of EWP replicas created by the attosecond pulses.

[1]E-mail: riviere@pks.mpg.de

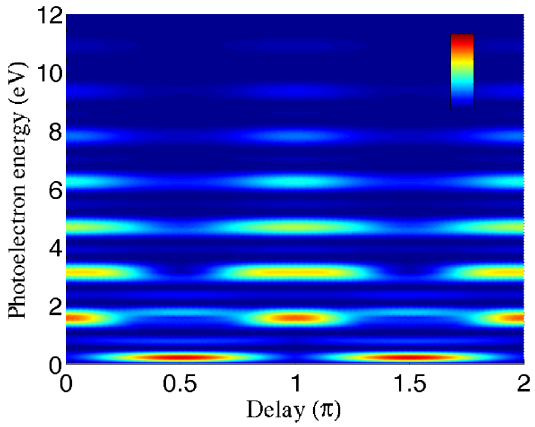

Fig. 1. Photoelectron energy spectrum for $I = 1.3 \times 10^{13}$ W/cm^2, 6 IR cycles and 2 atto pulses per cycle [4].

The absorption probability is the product of two terms: a *comb* function which filters particular values of the momentum and depends on the number of pulses in the APT, and a wave packet that suffers streaking in the IR field. It shows strong modulations as a function of the phase delay for VUV photons of energy comparable to the binding energy of the electron, while for higher photon energies it does not depend on the delay, in line with the experimental observations for helium and argon, respectively [3].

References

[1] Paul P. M. *et al.* 2001 *Science* **292** 1689

[2] Johnsson P. *et al.* 2005 *Phys. Rev. Lett.* **95** 013001, Rivière P., Ruiz C. and Rost J. M. 2008 *Phys. Rev. A* **77** 033421

[3] Johnsson P. *et al.* 2007 *Phys. Rev. Lett.* **99** 233001

[4] Rivière P., Uhden O., Saalmann U. and Rost, J. M. 2009 *New J. Phys*, in press.

[5] Lewenstein M. *et al.* 1994 *Phys. Rev. A* **49** 2117

Secondary electron cascade in attosecond photoelectron spectroscopy from metals

Jan Conrad Baggesen[1] **and Lars Bojer Madsen**[2]

Lundbeck Foundation Theoretical Center for Quantum System Research
Department of Physics and Astronomy, Aarhus University, 8000 Aarhus C, Denmark

Synopsis In a recent attosecond photoelectron spectroscopy experiment from a metal surface [A. L. Cavalieri *et al.* Nature (London) **449**, 1029 (2007)] a tail of unexplained low-energy electrons was measured. These electrons are shown to be due to electron-electron scatterings as the photoelectrons leave the metal. We develop a model for single scattering and a model based on cascade theory to describe these electrons. Our model explains the observed background, and the amplitude of the measured streaking spectrum.

In spectroscopy from metals, as compared to atoms or molecules, there is a lot of secondary processes that may blur the picture. When an electron is leaving a metal, there is a host of other, lightly bound electrons that the primary electron may scatter from, leading to two electrons with energy below the primary peak. Furthermore, each of these electrons may scatter of other electrons releasing a cascade of lower energy electrons. Here, we present theory for both primary electrons, electrons leaving after exactly one scattering and electrons that come out of the metal as part of a cascade.

Starting from a three step model, we are able to find a simple, closed expression for the amount of electrons that come out as a result of one scattering and for the energy distribution. This is done under the assumption that only the density of states is important in the probability of scattering from one energy, E' and to another E within the metal.

Another model is presented, in which Boltzmann's transport equation is used to describe the propagation of the primary electron to the surface, while scattering with any number of electrons, releasing any number of electrons with lower energy than the primary. This is an extention of earlier work on secondary electrons from electron bombardement of surfaces [1], to the current scenario of very short xuv pulses as the source of the primary electrons. Our theory gives reasonable agreement with the tail of electrons seen in the experiment [2].

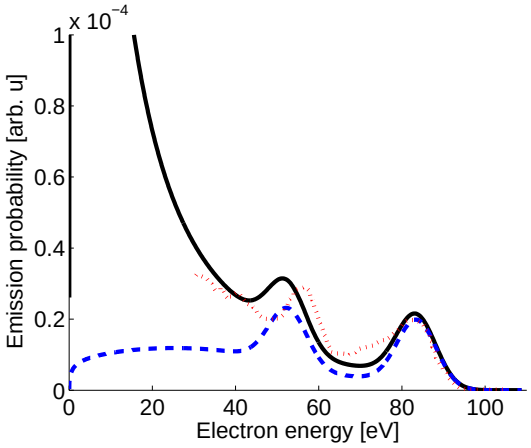

Fig. 1. Photoelectron distribution following a 300 asec pulse with up to one scattering (blue, dashed) and with the cascade theory (Black, full). The experimental results from [2] is shown too (red, dotted)

References

[1] P.A. Wolff, Phys. Rev. **95**, 56 (1954)

[2] A.L. Cavalieri et al., Nature (London) **449**, 1029 (2007).

[1] E-mail: jcb@phys.au.dk
[2] E-mail: bojer@phys.au.dk

Monte Carlo wave packet theory of dissociative double ionization

Henriette Astrup Leth[1], **Lars Bojer Madsen and Klaus Mølmer**

Lundbeck Foundation Theoretical Center for Quantum System Research, Department of Physics and Astronomy, Aarhus University, 8000 Århus C, Denmark

Synopsis Nuclear dynamics in strong-field double ionization processes are predicted using a stochastic Monte Carlo wave packet technique. The model takes input from electronic structure calculations and strong-field electron dynamics, and allows for field-dressed dynamics within a given molecule as well as several jumps between different charge states. The method is computationally efficient, applicable to a wide range of systems and relies on no empirical parameters. Nuclear kinetic energy release spectra for H_2 (D_2) in strong near-infrared laser pulses of 40 fs duration are compared to experiments and excellent agreement is obtained, showing the importance of accounting consistently for both neutrals and ions during the pulse.

When a molecule is exposed to a strong laser pulse the system is excited and ionizes and the nuclei start to dissociate. For pulses of current interest, e.g., 800 nm, 10^{14} W/cm^2 and durations in the femtosecond regime, all these processes are in principle accurately described by the time-dependent Schrödinger equation. The nonlinearity introduced by the external field is, however, so strong that the solution of this equation is impossible even for H_2, and modeling has focused separately either on ionization or dissociation dynamics. The purpose of the present poster is to provide a consistent theoretical framework that treats ionization and dissociation on an equal footing, and is applicable to any molecular system where electronic structure, dipole moment functions, and ionization dynamics can be determined. We illustrate the methodology using H_2 (D_2) since this is the simplest system, and experiment and theory exist. Our work shows, that the feeding of the molecular ion from the neutrals throughout the pulse, not accounted for in previous theory, is essential to explain details in the experiments.

Starting from $H_2((1s\sigma_g)^2)$, we study the nuclear dynamics as the population is transferred to the $1s\sigma_g$ and $2p\sigma_u$ states of H_2^+ and subsequently ionized leading to Coulomb explosion. This is done by treating ionization as a decay process, incorporated in a master equation for the molecular density matrix. The so-called Monte Carlo wave packet technique involves wave functions instead of density matrices and is computationally easier for this problem.

An outline of the physical processes accounted for by our treatment are given in Fig. 1. We assume the Born-Oppenheimer approximation and an initial nuclear wave function consistent with the electronic ground state [Fig. 1(a)]. The laser field excites the electronic state and with a given probability, the molecule is ionized and jumps to the lowest state in H_2^+[Fig. 1(b) → Fig. 1(c)]. The dynamics proceeds in the coupled $1s\sigma_g$-$2p\sigma_u$ system [Fig. 1(c)] until further ionization (a second jump) leaves the bare nuclei in the $1/R$ Coulomb potential [Fig. 1(d)]. To obtain the kinetic energy release (KER), a projection onto Coulomb scattering state is made after the second ionization.

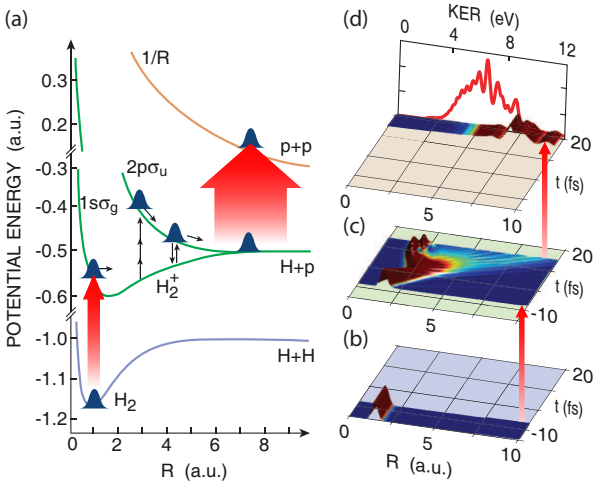

Fig. 1. Left panel: Sketch of the double ionization process for H_2 using field free BO curves. Right panel: One realization of the wave function dynamics in neutral, singly ionized and doubly ionized H_2.

[1]E-mail: hleth@phys.au.dk

Analytic Theory of Few-Cycle XUV Attosecond Pulse Photoionization of Atoms

E.A. Pronin[*, 1], **M.V. Frolov**[†], **N.L. Manakov**[†], **Anthony F. Starace**[*, 2]

[*]Dept. of Physics & Astronomy, The University of Nebraska, Lincoln, NE 68588-0111, USA
[†]Department of Physics, Voronezh State University, Voronezh 394006, Russia

Synopsis The doubly differential probability (DDP) for ionization of an atom by a few-cycle attosecond XUV pulse is analyzed using first and second orders of time-dependent perturbation theory (PT). We factorize the carrier-envelope phase (CEP) and angular dependence of the DDP for an initial bound S-state and analyze the general properties of CEP-induced asymmetries in photoelectron angular distributions (PADs) for an XUV pulse with *arbitrary* polarization and shape.

The importance of carrier-envelope phase (CEP) effects for few-cycle pulses has been demonstrated for IR pulses both experimentally and theoretically [1], and several theoretical works on CEP effects for XUV attopulses have appeared, e.g. [2, 3]. For few-cycle IR pulses, typical intensities lie in the non-perturbative regime, thus requiring appropriate analytical methods (e.g., SFA) or direct numerical solution of the TDSE. These methods have also been applied to the case of few-cycle XUV pulses. However, the clearest physical insight is provided by perturbation theory (PT), which is highly accurate for describing the interaction of atomic systems with XUV pulses up to $I_0 \sim 10^{15} - 10^{16}$ W/cm^2 [4].

In this work the doubly differential probability for ionization of an atom by a few-cycle attosecond XUV pulse is analyzed using first and second orders of time-dependent PT:

$$d^2W/(dEd\Omega) = p\big[|A_1|^2 + 2\mathrm{Re}(A_1^* A_2)\big]. \quad (1)$$

Here A_1 and A_2 are the first and second order amplitudes for ionization from a bound state of energy E_0 to a final state with energy $E = p^2/2$. The term $2\mathrm{Re}(A_1^* A_2)$ is non-zero only in the case of ionization by a short pulse, as it describes interference of the first and second orders of PT leading to the same final state. We factorize the CEP and angular dependence of $d^2W/(dEd\Omega)$ for an initial bound S-state and analyze the general properties of CEP-induced asymmetries in photoelectron angular distributions (PADs) for an XUV pulse with *arbitrary* polarization and shape. For the case of a linear polarization, our general parametrization gives:

$$d^2W/(dEd\Omega) = \alpha_0 I_0 \cos^2\theta + I_0^{3/2}\mathrm{Re}\{[\alpha_1 \cos\theta + \alpha_2 \cos^3\theta]\exp(i\phi)\}, \quad (2)$$

where θ is the angle between the polarization axis and electron momentum $\mathbf{p}$, and α_0, α_1, α_2 are atom-specific dynamical parameters dependent on both pulse shape and energy. The interference term changes sign when $\theta \to \pi - \theta$, leading to an asymmetry in the PAD and providing a means to determine the CEP of the pulse by measuring the PAD. Comparisons of PT results with numerical solutions of the TDSE [3] for the hydrogen atom show excellent agreement, including the $I_0^{3/2}$ dependence of CEP effects in (2) found numerically in Ref. [3]. Note also that the CEP dependence in (2) is in agreement with the general parametrization of CEP effects presented in Ref. [5]. The interference term in (1) also leads to dichroism in the PAD, i.e. dependence on the sign of the degree of circular polarization ξ of an attopulse.

This work was supported in part by DOE Grant No. DE-FG02-96ER14646 and RFBR Grants No. 07-02-00574 and No. 09-02-12034.

References

[1] D.B. Milošević, G.G. Paulus, D. Bauer and W. Becker, J. Phys. B **39**, R203 (2006).

[2] L.Y. Peng and A.F. Starace, Phys. Rev. A **76**, 043401 (2007).

[3] L.Y. Peng, E.A. Pronin and A.F. Starace, New J. Phys. **10**, 025030 (2008).

[4] L.A.A. Nikolopoulos and P. Lambropoulos, Phys. Rev. A **74**, 063410 (2006).

[5] V. Roudnev and B.D. Esry, Phys. Rev. Lett. **99**, 220406 (2007).

[1]E-mail: pronin@unlserve.unl.edu
[2]E-mail: astarace1@unl.edu

Angle-resolved high-order above-threshold ionization spectra of inert gases in the low-frequency approximation

D. B. Milošević[*,1], **A. Čerkić**[*], **B. Fetić**[†], **E. Hasović**[*], **and W. Becker**[‡]

[*]Faculty of Science, University of Sarajevo, Department of Physics,
Zmaja od Bosne 35, 71000 Sarajevo, Bosnia and Herzegovina
[†]First High School, Gimnazijska 3, 71000 Sarajevo, Bosnia and Herzegovina
[‡]Max-Born-Institut, Max-Born-Strasse 2a, 12489 Berlin, Germany

Synopsis We compare angle-resolved high-order above-threshold ionization spectra of inert gases obtained using the improved strong-field approximation with the spectra obtained using the low-frequency approximation.

In the improved strong-field approximation (ISFA), which describes high-order above-threshold ionization (HATI), rescattering of the ionized electron off its parent ion is usually described within the first-order Born approximation (1BA). Coulomb effects in the rescattering process can be taken into account by replacing the final Volkov wave by the Coulomb-Volkov wave [1]. One can go beyond the 1BA by replacing in the rescattering amplitude the atomic scattering potential according to $V \to T(E) = V + VG_V(E)V$, where $G_V(E)$ is the stationary Green's operator at the energy $E(\tau)$ of the recolliding electron at the recollision time τ. This is similar to the low-frequency approximation for laser-assisted scattering ([2] and references therein). We have recently derived the low-frequency approximation (LFA) for HATI [3].

In the present contribution we will show our numerical results for the angle-resolved HATI energy spectra of inert gases; see Fig. 1. We show that the difference between the ISFA and the LFA is significant for scattering away from the laser polarization axis. In the context of quantum-orbit theory and the uniform approximation, we also show that on the back-rescattering ridge, the rescattering T-matrix element can be factorized into the product of the incoming flux and the elastic scattering cross section. Hence, the differential cross section of laser-free elastic electron-ion scattering can be extracted from the angle and energy resolved HATI spectra as proposed recently [4].

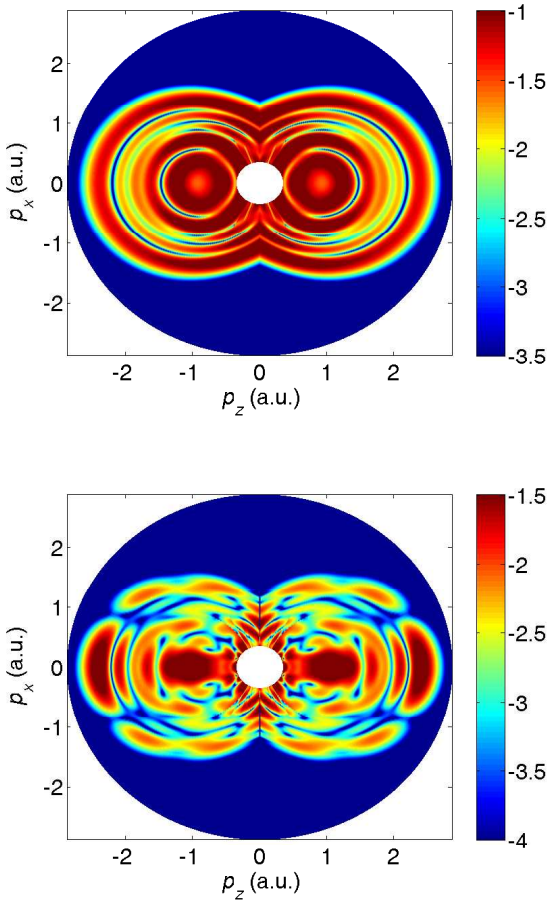

Fig. 1. 2D momentum distributions for Xe at 1.5×10^{14} W/cm^2 and 760 nm. The upper (lower) panel: the results obtained using the ISFA (LFA).

References

[1] D. B. Milošević and F. Ehlotzky, Phys. Rev. A **58**, 3124 (1998).

[2] D. B. Milošević, J. Phys. B **28**, 1869 (1995).

[3] A. Čerkić, E. Hasović, D. B. Milošević, and W. Becker, Phys. Rev. A **79**, 033413 (2009).

[4] X. X. Zhou, Z. J. Chen, T. Morishita, A. T. Le, and C. D. Lin, Phys. Rev. A **77**, 053410 (2008).

[1]E-mail: milo@bih.net.ba

Amplitude and phase spectroscopy of attosecond electron wave packets

Kyung Taec Kim[*,†,1], Dong Hyuk Ko[†], Juyun Park[†], Chang Hee Nam[†] and Jongmin Lee[*]

[*]Advanced Photonics Research Institute and Center for Femto-Atto Science and Technology, GIST, Gwangju, Korea
[†]Department of Physics and Coherent X-ray Research Center, KAIST, Daejeon, Korea

Synopsis: The interference of attosecond electron wavepackets, created by high harmonic and femtosecond laser pulses, is measured. The first electron wavepacket is generated by direct ionization of He, and the second one by the two step process of resonant excitation by the attosecond high harmonic pulse and subsequent ionization by the laser pulse. The amplitude and phase retrieved from the interferogram show the ionization dynamics of He.

An interferogram generated by the superposition of two coherent waves is quite functional in analyzing an unknown system. Since the coherence of a light source is transferred to an ionized electron, The interferogram of electron wavepackets may provide the information on the electron dynamics in atoms and molecules [1]. In this work, we present the interferogram of the electron wave packets created from He ionized by attosecond high harmonic and laser pulses, which shows the ionization dynamics of the atom.

The interference of electron wave packets can be generated by creating two coherent waves in the continuum with attosecond high-harmonic and femtosecond laser pulses. The attosecond harmonic pulses are generated from Ar gas by focusing intense femtosecond laser pulse, and the probe pulse is obtained by splitting a part of the femtosecond laser pulse. The first electron wave packet, directly ionized by the attosecond harmonic pulse from the ground-state helium atom to the continuum, plays a role of the reference pulse. The attosecond harmonic pulse also initiates the resonant excitation to the 1s3p state of He. The excited electron is, then, ionized by the probe laser pulse, creating the second electron wave packet in the continuum. Since two coherent electron wavepackets are superposed with a time delay τ, the interferogram is generated in the frequency domain.

Figure 1 shows the photoelectron spectra obtained by the attosecond pulses generated from an Ar cell with an intensity of $2.0\text{x}10^{14}$ W/cm^2. The amplitude and phase of the probed electron wave packets can be obtained by extracting the oscillating signal contained in the photoelectron spectra. The result shows the different behavior depending on the ionization process of the electron. When the the probe laser pulse is overlapped with the attosecond harmonic pulse, the interferogram is quite similar to that appearing in continuum-continuum transitions

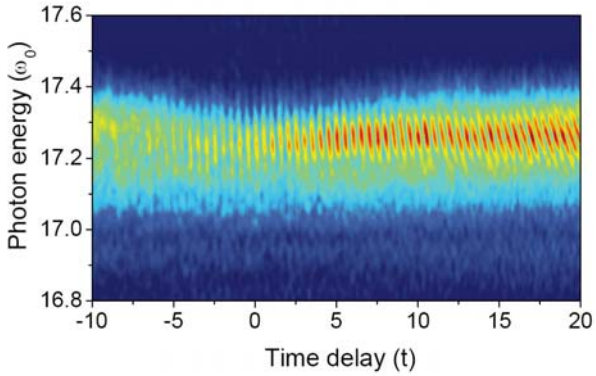

Fig. 1. Photoelectron spectra obtained by the attosecond pulses generated from an Ar cell at an intensity of $2\text{x}10^{14}$W/cm^2 in the presence of a probe laser pulse.

[2]. However, the signal is very similar to that of spectral interferometry when the probe laser pulse is temporally separated from the attosecond pulse [3]. This allows monitoring the time-dependent amplitude and phase of the second electron wavepacket.

In summary, the interference of electron wavepackets, separated in time, is measured. The phase of the electron wavepacket shows the electron dynamics in the ionization process. At a long time delay, the signal is similar to that of the spectral interferometry, which can be used for the characterization of the time-dependent amplitude and phase of the ionized electron after resonant excitation.

References

[1] T. Remetter *et al.*, Nature phys. **2**, 323 (2006).
[2] P. M. Paul *et al.*, Science **292**, 1689 (2001).
[3] M. Wollenhaupt *et al.*, Phys. Rev. Lett. **89**, 173001 (2002).

[1]E-mail: kyungtaec@gist.ac.kr

Polarization Characterization of High Harmonic Generation from Transiently Aligned Molecules

Xibin Zhou*[1], Robynne Lock*, Henry Kapteyn*, and Margaret Murnane*

[*] JILA, University of Colorado and National Institute of Standard and Technology, Boulder, CO, 80309-0440, USA

Synopsis: We perform an accurate polarimetry measurement of high harmonic emission from aligned molecules. We find that harmonic emission from nitrogen molecules can be strongly elliptically polarized; even when driven by linearly polarized laser fields. We also vary the ellipticity of the driving laser used to generate the high harmonic emission. We find that the HHG intensity from aligned molecules does not optimize with linear polarization of the driving laser (as in the atomic case), but rather peaks at a small positive or negative ellipticity. The sign and degree of this ellipticity depend on the molecular orientation.

High-order harmonic generation (HHG) results from the extreme distortion of an electron wave function in an atom or molecule in the presence of a strong laser field. In the case of HHG from molecules, the intensity and phase of the EUV light can encode structural information - particularly if the molecular sample is aligned and thus this information is not averaged-out.

In principle, the amplitude, phase and polarization of HHG emission from molecules can be measured and used to extract the electronic orbital structure from the transition dipole matrix element of the recombination step of the HHG process. However, until very recently, only the intensity of HHG from molecules could be measured. Fortunately, new approaches have made it possible to determine the phase of HHG. In this abstract, we present two experiments where the polarization state of high harmonics from an ensemble of aligned molecules is characterized.

In the first experiment, we perform the first accurate polarization measurement of the ellipticity of HHG emission from molecules [1]. We extract the phase difference between the HHG components parallel and perpendicular to the driving laser field, which depends only weakly on molecular alignment but strongly on the harmonic order. Our findings differ from previously published results [2], where only linearly-polarized harmonic emission was observed, because we obtain a stronger molecular alignment and better signal-to-noise ratio (1~2% uncertainty). This allows us to detect ellipticity in the HHG emission even when molecules are driven by linearly-polarized laser fields. These findings cannot be explained by a plane-wave SFA, and will be very useful to benchmark new and more complete theories of molecules in strong fields.

From the measured ellipticity and orientation angle of the HHG polarization ellipse, we can extract the phase difference and amplitude ratio of the orthogonal HHG polarization components. The observed nontrivial variation in relative phase indicates a breakdown of the plane wave approximation. In the second experiment, we varied the ellipticity of the driving laser used to generate the high harmonic emission. We find that the HHG intensity generated from an ensemble of aligned molecules does not peak for linear polarization of the driving laser (as in the atomic case), but at a small positive or negative ellipticity. The sign and degree of this ellipticity depends on the molecular orientation. The most probable explanation for this behavior is the manipulation of the returning electron wave packet by the elliptical polarization of the laser.

In summary, we have uncovered unexpected polarization properties of high harmonic emission from N_2 and CO_2 molecules that have broad implications for the theory of molecules in strong fields. Furthermore, we show that HHG from aligned molecules driven by an elliptically-polarized laser pulse can also yield new information information. More-sophisticated models of the laser molecule interaction will be required to fully understand these experimental data.

References

[1] X.-B. Zhou et. al., *Phys. Rev. Lett* **102** 073902 (2009).

[2] J. Levesque *et al.*, *Phys. Rev. Lett.* **99**, 243001 (2007).

[1] E-mail: Xibin.Zhou@Colorado.edu

Angular distribution of high-order harmonic generation from aligned molecules

Peng Liu [1], Zhinan Zeng, Pengfei Yu, Ruxin Li [2], Zhizhan Xu

State Key Laboratory of High Field Laser Physics, Shanghai Institute of Optics and Fine Mechanics, Chinese Academy of Sciences, Shanghai 201800, China

Synopsis: We experimentally investigate the high-order harmonic generation (HHG) from aligned CO_2 molecules and demonstrate that the modulation inversion of harmonic yield with respect to molecular alignment can be altered dramatically by the intensity of the driving laser pulse. The laser field dependent inversion can be explained by the shift angular distribution of harmonic emission calculated with the strong field approximation (SFA) model including a ground state depletion factor. The observed angular distributions of harmonics are discussed according to the available theoretical models.

The HHG from aligned molecules attract intensive studies due to its potential applications in the imaging of molecular orbital and controlling of the harmonic generation. The HHG from CO_2 represents an interesting feature of molecular alignment dependence - quantum interference effect. The two-center interference model has the limit in explaining the variation of inverted harmonic orders in different reports [1,2]. By taking into account the ground state depletion effect on HHG, A.-T. Le et al. [3,4] proposed theoretically that the harmonic yield inversion can be varied by changing driving laser intensity. The experimental verification of this model is strongly desired.

Our result [5,6] indicates that as the driving laser field increases from 1.6×10^{14} W/cm^2 to 2.4×10^{14} W/cm^2, the 25th order harmonic intensity evolution becomes inverted with the molecular alignment modulation (See Fig. 1, in which the dashed line is the alignment degree as a function of delay time, and the dot + solid line is the harmonic intensities of aligned molecules at the delay times). This is the direct confirmation of the laser field dependence of the HHG angular distribution.

Using the extended Lewenstein's strong field approximation (SFA) model, the harmonic emissions are calculated for the angles θ between the molecular axis and the laser polarization direction. By taking into account the alignment distribution of molecules, the harmonic intensities of the aligned and anti-aligned molecules are calculated, showing that the inversion of harmonic emission happens at the laser field of 1.4×10^{14} W/cm^2, which is close to the observed 1.6×10^{14} W/cm^2. The calculation by neglecting the ground ionization factor indicates no harmonic intensity inversion in the laser field range discussed, showing that the ground state depletion influences the harmonic emissions.

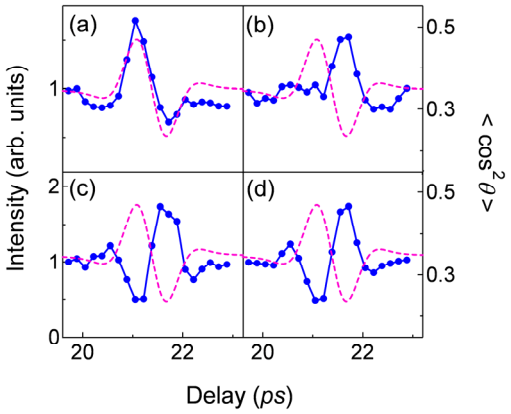

Fig. 1. Time evolution of the 25th order harmonic intensity from aligned CO_2 at around half revival for the laser intensities of (a) 1.6×10^{14} W/cm^2, (b) 1.9×10^{14} W/cm^2, (c) 2.1×10^{14} W/cm^2, and (d) 2.4×10^{14} W/cm^2.

Angular dependence of the harmonics is also investigated experimentally by adjusting the angle of aligning laser polarization and HHG driving laser polarization. The results are compared with the available theoretical models, and the applicability of SFA model on larger molecules is discussed.

References

[1] T. Kanai, et al., Nature 435, 470 (2005).
[2] C. Vozzi, et al., PRL 95, 153902 (2005).
[3] A.-T. Le, et al., PRA 73, 041402 (2006).
[4] A.-T. Le, et al., Journal of Modern Optics 54, 967 (2007).
[5] P. Liu, et al., PRA 78, 015802 (2008).
[6] P. Yu, et al., PRA 79, 053814 (2009).

[1] E-mail: peng@siom.ac.cn

[2] E-mail: ruxinli@mail.shcnc.ac.cn

A new test of optical tunnel ionization

L Arissian[*,†], C Smeenk[*,1], C Trallero[*] and P B Corkum[*]

[*] Joint Laboratory for Attosecond Science, University of Ottawa and National Research Council, 100 Sussex Drive, Ottawa, Canada

[†] Department of Physics, Texas A & M University, College Station, USA

Synopsis Optical tunnel ionization is a powerful phenomenon at the core of attosecond science. Experiments in circularly polarized light at 800 and 1400 nm avoid electron recollision and provide a means to directly observe the tunneled electrons. We compare the measured electron wavepacket in argon to the predictions of tunneling theory.

Optical tunnel ionization is important for attosecond science. In a strong laser field, tunnel ionization and subsequent recollision leads to numerous attosecond processes. Applications of recollision include imaging of electron orbitals in atoms [1] and molecules [2, 3].

Structural imaging of atoms and molecules requires a precise understanding of the tunneled electron features. Although tunneling has been investigated experimentally and theoretically for many years, the structure of the tunneled electron itself has received less attention. Previous experiments in linearly polarized light [4] uncovered considerable distortion due to the ion Coulomb potential.

We use circularly polarized light to test tunneling without the complexity of recollision. Concentrating on argon, we measure the lateral momentum of the tunneled electron. The lateral momentum is least affected by the laser field and should give the most direct test of tunneling. Using 800 and 1400 nm light and a range of intensities we present experiments spanning the Keldysh parameter values $0.38 \leq \gamma \leq 1.08$. The experimental measurements are compared with theoretical calculations including integration in time and space of the Gaussian laser beam.

References

[1] D Shafir, Y Mairesse, D M Villeneuve, P B Corkum and N Dudovich. Nature Physics, doi:10.1038/nphys1251, 2009

[2] J Itatani, *et al.* Nature. **432**, 7019, 867-871 (2004)

[3] M Meckel *et al.* Science, **320**, 5882, 1478-1482 (2008)

[4] D Comtois, D Zeidler, H Pépin, J C Kieffer, D M Villeneuve, and P B Corkum. J Phys. B, **38**, 12, 1923-1933 (2005)

[1] E-mail: christopher.smeenk "at" nrc.ca

Angular dependence of the strong-field ionization in randomly oriented hydrogen molecules

Maia Magrakvelidze, Feng He, Sankar De, Irina Bocharova, Dipanwita Ray,
Uwe Thumm and I.V. Litvinyuk[1]

JRM Laboratory, Kansas State University, Manhattan, KS, 66506-2604, USA

Synopsis: Use coincident detection of ionized electrons and deuteron fragments to investigate angular anisotropy of tunneling ionization and correlate electron energy spectra with molecular structure.

We report two experiments on D_2 using electron-ion coincidence momentum spectroscopy using COLTRIMS. In both experiments we measure electron momentum in coincidence with momentum of one D^+ ion.

In the first experiment we used 50 fs circularly polarized pulses of 1850 nm wavelength to measure angular anisotropy of tunneling ionization for D_2. By measuring the relative angle between an ionized electron and deuteron resulting from field dissociation of the molecular ion produced by a circularly polarized pulse we deduce the angular dependence of the molecular ionization probability without having to align the molecules first. We determined that with 50fs pulses of 1850nm wavelength and 2×10^{14} W/cm^2 intensity neutral D_2 molecules are 1.15 times more likely to be ionized when the laser electric field is parallel to the molecular axis than for the perpendicular orientation. This is in excellent agreement with our theoretical model which is based on solving the time dependent Schrödinger equation in the velocity gauge using single active electron approximation and two dimensional Cartesian coordinates.

In the second experiment, we used pump-probe technique with two few-cycle (7.5 fs) 800 nm pulses separated by variable time delay. Neutral molecule is singly ionized with a weak pump pulse and then the dissociating molecular ion is exploded by a stronger probe pulse. The fragments (electrons and ions) of the reaction are detected in coincidence at various time delays. Gating the electron energy spectra on pump-probe delays and kinetic energies of D^+ (both related to internuclear separation) we observe an interesting evolution of these spectra indicative of changing electronic structure of the dissociating D_2^+ molecular ion.

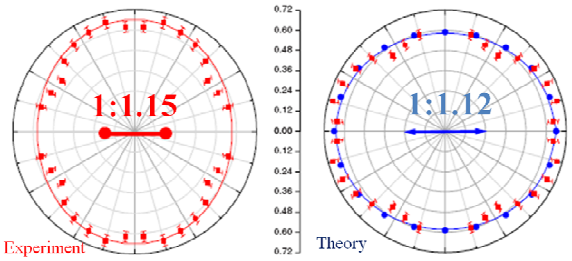

Fig. 1. The experimental and calculated distribution of the relative angles between the ion and electron momenta.

The electron ionization angular dependence exhibits a weak anisotropy with an ionization yield ratio of 1.15 ±0.05 favoring the ionization of molecules that are aligned parallel to the electric field. Our numerical model generated, which accurately predicts the measured anisotropy, as well as its intensity dependence for both, our experiment [3] at 1850nm and Staudte *et al.*'s [1] at 800nm wavelength.

References

[1] A. Staudte, S. Patchkovskii, D. Pavičić, H. Akagi, O. Smirnova, D. Zeidler, M. Meckel, D. M. Villeneuve, R. Dörner, M. Y. Ivanov, and P. B. Corkum, *Phys. Rev. Lett.* **102,** 033004 (2009).

[2] I. A. Bocharova, H. Mashiko, M. Magrakvelidze, D. Ray, P. Ranitovic, C. L. Cocke, and I. V. Litvinyuk, *Phys. Rev. A* **77,** 053407 (2008).

[3] M.Magrakvelidze, F.He, S.De, I.Bocharova, D.Ray, U.Thumm and I.Litvinyuk, *Phys. Rev. A*, **79,**033408 (2009).

E-mail: ivl@phys.ksu.edu

Towards Disentangling High Harmonic Generation: Multiple Active Electrons in Strong Field Ionization of Polyatomic Molecules

Arjan Gijsbertsen[*,†], Andrey E. Boguslavskiy[*], Jochen Mikosch[*] [1], Michael Spanner[*], Niklas Gador[◇], Marc J. J. Vrakking[†], Olga Smirnova[•], Serguei Patchkovskii[*], Misha Y. Ivanov[‡], Albert Stolow[*] [2]

[*]National Research Council of Canada, 100 Sussex Drive, Ottawa, Ontario K1A 0R6, Canada
[†]FOM Instituut voor Atoom en Molecuulfysica (AMOLF), Amsterdam, The Netherlands
[◇]Lund University, Lund, Sweden
[•]Max-Born-Institut, Berlin, Germany
[‡]Imperial College, London, United Kingdom

Synopsis We investigate Strong Field Ionization - the first step in High Harmonic Generation - of polyatomic hydrocarbon molecules. By utilizing a novel covariance technique we show that multiple bound electrons respond simultaneously to the strong laser field. The driven sub-cycle ionization process cannot be described within a single continuum approximation.

The process underlying the generation of attosecond light pulses, High Harmonic Generation (HHG) by a strong laser field, is itself one of the most powerful dynamical probes of attosecond timescale dynamics. It is successfully applied to atoms and small molecules based upon a three-step model comprised of adiabatic ionization of a single electron, its acceleration in the laser field and its subsequent radiative recombination. Here we investigate Strong Field Ionization (SFI) - the first step in HHG - of polyatomic molecules and explore how the response of multiple bound electrons to the laser field may affect attosecond timescale measurements.

Strong Field Ionization (SFI) of the four similar hydrocarbon molecules butane, 1-butene, trans-2-butene and 1,4-butadiene have been studied by a novel covariance technique, correlating the kinetic energy of the photoelectron with the mass of the ion. We observe different ionic fragments indicating that the neutral molecule has a probability to ionize into an electronically excited, dissociative cation state. The correlated photoelectron spectra show peaks spaced by the photon energy, the typical pattern linked to Above Threshold Ionization (ATI). Interestingly, photoelectron spectra correlated to different fragmentation channels are shifted in energy depending on the molecule. This implies that: (i) the cation excited state was not prepared post-ionization, and (ii) at least two electronic continua are directly coupled to the sub-cycle SFI of these molecules.

Our results unambiguously demonstrate driven sub-cycle electron dynamics which cannot be described within a single continuum approximation. In principle, these multiple continua can be prepared by both adiabatic (i.e. tunnel ionization of multiple orbitals) and non-adiabatic mechanisms. As Attosecond Science progresses to the more complex world of polyatomic molecules, such multi-electron dynamics driven in the strong laser field will play an increasingly prominent role.

[1] E-mail: jochen.mikosch@nrc.ca [2] E-mail: albert.stolow@nrc.ca

High-Harmonic Generation in Polyatomic Molecules

M. C. H. Wong[1], J.-P. Brichta, and V. R. Bhardwaj

Department of Physics, University of Ottawa, 150 Louis Pasteur, Ottawa, Ontario K1N 6N5, Canada

Synopsis: We investigate signatures of suppressed ionization by observing high-harmonic generation in polyatomic chlorocarbon molecules CH_2Cl_2, $CHCl_3$ and CCl_4 using 800nm infrared light. An extension of the high-harmonic cut-off in all molecules was observed compared to atomic Xe which has a similar ionization potential. Ellipticity measurements show broader electron wave-packet spreading for highly polarizable molecules, demonstrating the influence of multi-electron dynamics in the high-harmonic generation process.

Strong field laser interactions with atoms and molecules lead to incredible nonlinear processes such as above threshold ionization, laser induced electron diffraction, and high harmonic generation (HHG). HHG has quickly become the quintessential method to push the field of ultrafast science into the attosecond domain[1]. The semi-classical model for HHG accurately describes the underlying physics behind this process for a simple atom but the influence of multi-electron dynamics in a polyatomic molecule can lead to results unexplainable by the atomic model.

In this paper we report on experimental results demonstrating suppressed ionization in polyatomic molecules and the influence of polarizability on the HHG process.

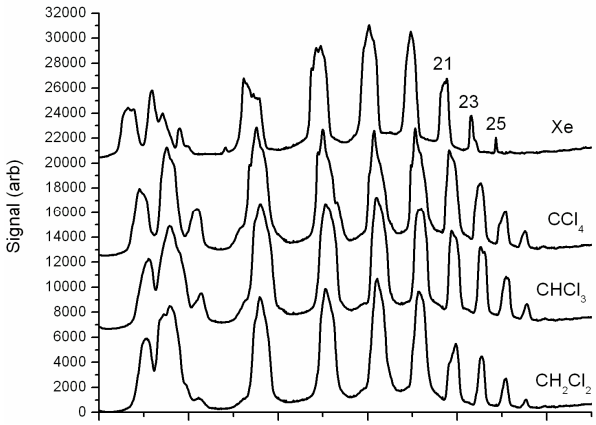

Fig. 1 Harmonic spectra of Xe and chlorocarbons

Signatures of suppressed ionization in HHG in linear di- and tri-atomic molecules have been demonstrated by comparison of extended cut-offs with their partner atoms having the same ionization potentials (IP)[2]. We choose three chlorocarbon molecules, CH_2Cl_2, $CHCl_3$, and CCl_4 because (a) they have similar IP's (11.33, 11.37, and 11.47 eV respectively), (b) they all possess three-dimensional tetrahedral geometry, (c) their highest occupied molecular orbitals (HOMO) exhibit similar symmetries but also contain varying degrees of complexity, and (d) they have different electron polarizabilities (6.5, 8.5 and 10.5 $Å^3$ respectively). **Fig. 1** shows the harmonic spectra for Xe and the chlorocarbons at an intensity of 5×10^{14} W/cm^2. The harmonic cut-off is extended in the chlorocarbons compared to Xe (IP = 12.13 eV) indicating the role of suppressed ionization. Saturation intensity measurements for the chlorocarbons along with their observed HHG spectra and HOMO symmetries indicate that destructive interference is greater in CCl_4 than the others.

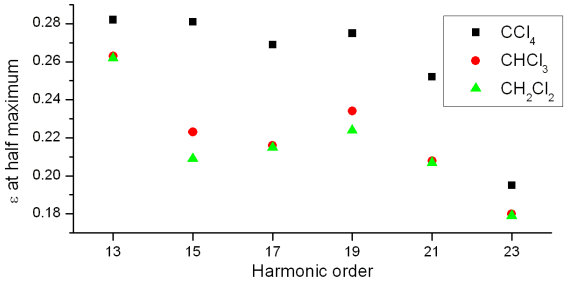

Fig. 2 Ellip. at half-maximum signal for each harmonics

Ellipticity dependence of HHG provides information on the electron wave-packet spreading. Our results show that the half-widths at half-maximum for all harmonics in CCl_4 are consistently larger (see **Fig. 2**). The electron wave-packet spreading depends only on the ionization potential and, in large molecules, on the polarizability [3,4]. Since the IP of the molecules under consideration were similar, this is the clear evidence of the role of multi-electron dynamics in HHG in larger molecules.

We expect that experiments using longer wavelength light will provide new insight into the multi-electron influence on HHG in polyatomic molecules.

References

[1] PB Corkum & Ferenc Krausz, Nature Physics **3**, 381 (2007)
[2] C. Altucci *et al*, PRA **71**, 013409 (2005)
[3] V. R. Bhardwaj *et al*., PRL 93, 043001 (2004)
[4] T. Brabec *et al*, PRL **95**, 073001 (2005)

[1] E-mail: mwong017@gmail.com

Effects of laser pulse duration and intensity on Coulomb explosion of CO_2: signatures of charge-resonance enhanced ionization

Igor V. Litvinyuk[1,*], Irina Bocharova[1], Joseph Sanderson[2], Jean-Paul Brichta[3], Jean-Claude Kieffer[4] and François Légaré[4]

[1] J.R. Macdonald Laboratory, Physics Department, Kansas State University, Manhattan, KS 66506, USA
[2] Department of Physics, University of Waterloo, Waterloo, Ontario N2L 3G1, Canada
[3] Department of Physics, University of Ottawa, Ottawa, Ontario, Canada K1N 6N5
[4] Centre Énergie, Matériaux et Télécommunications, INRS, Varennes, QC, J3X 1S2, Canada

Synopsis We studied laser-induced Coulomb explosion of CO_2 by full triple-coincidence momentum resolved detection of resulting ion fragments. From the coincidence momentum data we can reconstruct molecular geometry immediately before explosion. We observe the dynamics of Coulomb explosion by comparing reconstructed CO_2 geometries for different Ti:Sapphire laser pulse durations (at the same intensity) ranging from few cycles (7 fs) to 200 fs. We conclude that for longer pulse durations (≥100 fs) Coulomb explosion proceeds through the enhanced ionization mechanism taking place at the critical O-O distance of 8 a.u., similarly to well known charge-resonance enhanced ionization (CREI) in H_2.

CREI at the critical internuclear distance is a well established mechanism for strong-field double ionization of hydrogen by sufficiently long (>20 fs) near-IR laser pulses [1, 2]. Whether a similar mechanism also operates during multiple ionization of larger molecules is still a matter of some debate. Here we present experimental evidence that multiple ionization of tri-atomic CO_2 molecules by intense femtosecond laser pulses can also proceed through enhanced ionization at a critical distance.

The experiments were performed on the 5 kHz Ti:Sapphire beamline of the Advanced Laser Light Source (ALLS) at Varennes, Quebec. A hollow-core fiber compressor was used to produce 7 fs pulses. A supersonic jet of CO_2 molecules intersected a tightly focused laser beam inside a uniform-electric-field ion spectrometer equipped with a time- and position-sensitive delay-line anode detector. All resulting ion fragments were detected and their full 3D momentum vectors were determined.

The triple coincidences of the type (O^{k+}, C^{l+}, O^{m+}) characterized by a near-zero total momentum were identified as resulting from Coulomb explosion of a single molecule into a specific (k,l,m) channel: $CO_2 \rightarrow O^{k+}+C^{l+}+O^{m+}$. For the (2,2,2) explosion channel we reconstructed the molecular structure, using an iterative procedure based on integration of the classical equations of motion for the fragments with pure Coulomb interactions.

We compared the results for various pulse durations from 7 fs to 200 fs (Figure 1). The 7 fs pulses generated the most energetic fragments and reconstructed structures were nearly identical to that of a neutral CO_2 molecule. As the laser pulses become longer the kinetic energy decreases and the O-O distance increases due to the dynamics occurring before the explosion. For 100 fs pulses the O-O distance reaches 8 a.u., and it remains the same for longer pulses.

We consider it a manifestation of the enhanced ionization process taking place in CO_2 molecular ions. However, the fragments in the (1,1,1) dissociation channel appear not to result from the enhanced ionization, pointing to the molecular tri-cation CO_2^{3+} as an intermediate state which undergoes this CREI-like process at the critical O-O separation of 8 a.u.

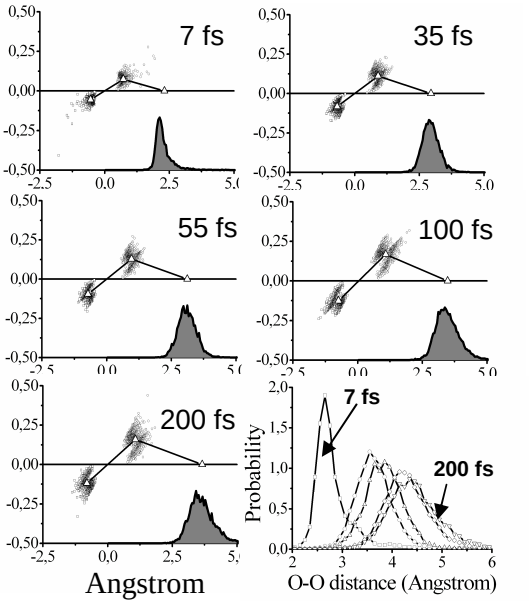

Fig. 1. Structures of CO_2 reconstructed for (2,2,2) explosion channel with different pulse durations. Note the different X- and Y-scales.

References:

1. T. Zuo and A.D. Bandrauk, Phys. Rev. A **52**, R2511 (1995).
2. T. Seideman, M.Y. Ivanov and P.B. Corkum, Phys. Rev. Lett. **75**, 2819 (1995)

* ivl@phys.ksu.edu

Dynamic field-free orientation of polar molecules by intense two-color femtosecond laser pulses

Sankar De[1*], Dipanwita Ray[1], Irina Znakovskaya[2], Fatima Anis[1], Nora G. Johnson[1], Irina Bocharova[1], Maia Magrakvelidze[1], B. D. Esry[1], C. L. Cocke[1], Matthias F. Kling[2] and Igor V. Litvinyuk[1†]

[1] J. R. Macdonald Laboratory, Physics Department, Kansas State University, Manhattan, KS 66506-2604, USA
[2] Max-Planck Institute of Quantum Optics, Hans-Kopfermann Strasse 1, D-85748 Garching, Germany

Synopsis: We present the first experimental observation of dynamic field-free orientation of a heteronuclear molecule (CO) induced by intense two color (800 and 400 nm) femtosecond laser pulses. We have used the two color pulse as pump to orient the molecules and a more intense 800 nm pulse as probe to measure the angular distributions. In addition to dynamic alignment seen in time dependence of $\langle\cos^2\theta\rangle$, we observe clear orientation in $\langle\cos\theta\rangle$ traces, which revives with the rotational period and can be reversed by changing the relative phase of the two colors. We studied the dependence of degree of orientation on the pump pulse intensity, and compared the results with theoretical calculations.

Combining a fundamental frequency of a laser and its second harmonic with a definite relative phase results in an asymmetric electric field and broken inversion symmetry. Such field-asymmetric laser pulses can generate macroscopic orientation in polar molecules. Here we present the first experimental implementation of this technique.

In our experiments we combined 50 fs 800 nm pulses from a Ti:Sapphire laser with their second harmonic field of 400 nm wavelength. The resulting field-asymmetric two-color pulses were focused onto a supersonic jet of CO molecules inside a velocity-map imaging (VMI) spectrometer. Rotationally excited CO molecules were interrogated at a varying time delay by a more intense single-color (800 nm) laser pulse. The probe pulse Coulomb exploded the molecules and the resulting C^{2+} fragments were momentum analyzed using VMI.

Figure 1 shows the experimental time traces of $\langle\cos^2\theta\rangle$ and $\langle\cos\theta\rangle$, where θ is the angle between the CO molecular axis (represented by the momentum direction of C^{2+}) and the laser polarization. $\langle\cos^2\theta\rangle$ represents the alignment of CO and the values of $\langle\cos\theta\rangle$ indicate a net macroscopic orientation of the molecular ensemble. The observed orientation exhibits rotational revivals after each rotational period. The results demonstrate field-free orientation of CO, which might be used to study angle-differential properties of this heteronuclear molecule, such as various ionization and scattering cross-sections.

We studied the dependence of the degree of orientation on the pump pulse peak intensity and identified an optimal pulse intensity for the maximum degree of orientation. We also compare our experimental results to a series of theoretical calculations and confirm that the orientation of CO is dominated by an asymmetry in the molecular hyper-polarizabilities rather than the molecules' permanent dipole moment.

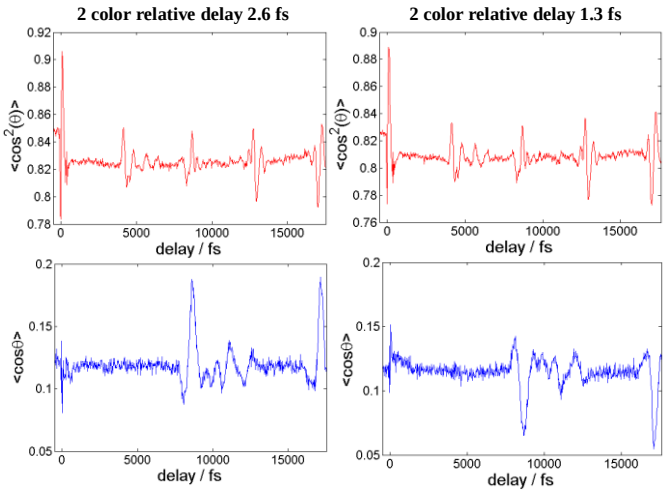

Fig. 1. Time dependence of molecular alignment ($\langle\cos^2\theta\rangle$ - upper row) and orientation ($\langle\cos\theta\rangle$ - lower row) for two different relative phases of 800 nm and 400 nm beams corresponding to opposite asymmetric fields.

This work was supported by Chemical Sciences, Geosciences and Biosciences Division, Office of Basic Energy Sciences, Office of Science, U.S. Department of Energy.

* E-mail: sankar@phys.ksu.edu

† E-mail: ivl@phys.ksu.edu

Controlling Asymmetric Coulomb Explosion Using 2-Color Fields

K. J. Betsch [1], **D. W. Pinkham** [2], **R. R. Jones** [3]

Department of Physics, University of Virginia, Charlottesville, VA, 22904, USA

Synopsis Intense, asymmetric, two-color laser fields have been used to control directional Coulomb explosion in several small molecules. A strong asymmetry in the forward/backward fragment directionality from asymmetric dissociation channels is detected as a function of the relative phase between the 800 nm and 400 nm pulses. Manipulation of the optical phase enables control over native and/or induced electron localization in the strong optical field. The robust effect might be utilized as an effective phase-meter for few-cycle laser pulses.

Recently, the ability to specifically tailor the electric field of an ultrashort laser pulse through carrier-envelope phase (CEP) stabilization has become available. Application of such asymmetric CEP stabilized pulses to D_2 molecules has illustrated control of electron localization between nuclear centers during the dissociation process [1]. Asymmetric electric fields are also readily created by combining a laser field at fundamental frequency ω with its second harmonic at 2ω; variation of the relative phase between the two components tailors the field asymmetry [2].

In our experiments, laser pulses of 35 fsec duration at 800 nm are frequency doubled in a BBO crystal, resulting in a two-color laser field with total intensities of $10^{13} - 10^{14}$ W cm^{-2} and field asymmetries $0.2 \leq (|E_f/E_b| - 1) \leq 0.9$. The relative phase between the red and blue components is continuously varied as the pulses are applied to the dissociation of N_2, O_2, CO, HBr, and CO_2. Coulomb explosion occurs along the laser polarization, which is parallel to the axis of a single-stage time of flight (TOF) mass spectrometer. In the symmetric molecules, a distinct phase-dependent asymmetry in the forward/backward fragment directionality is observed for asymmetric dissociation channels, i.e. $N_2^{+(p+q)} \rightarrow N^{+p} + N^{+q}$, $p \neq q$, for $(p+q) \geq 3$. Charge symmetric channels in hetero-nuclear molecules, e.g. $CO^{+4} \rightarrow C^{+2} + O^{+2}$, also exhibit this asymmetry.

The target molecules were selected to explore the role of orbital structure in the asymmetric dissociation. Oxygen, which has a π-shaped highest occupied molecular orbital (HOMO), was found to exhibit an asymmetry parameter as large as that for N_2, which has a σ-shaped HOMO. Carbon dioxide, also possessing a π-shaped HOMO, exhibits asymmetries in several dissociation channels, indicating that HOMO structure is not a barrier to electron localization.

Repeating the N_2 and CO experiments with an elliptically polarized field also resulted in large phase-dependent fragment directionalities. This suggests that electron recollision is not the dominant mechanism for the observed asymmetric dissociation.

By adding a third, time-delayed probe pulse, the possibility of laser-induced molecular orientation in CO and HBr is explored. No field-free orientation at the characteristic revival times was observed, indicating that transient molecular orientation does not occur. Instead, our results are consistent with the notion of charge localization and enhanced ionization in the asymmetric field.

Analogous fragmentation directionality induced by CEP-stabilized pulses [3] could be used to measure the carrier-envelope phase.

References

[1] M. F. Kling, Ch. Siedschlag, A. J. Verhoef, J. I. Kahn, M. Schultze, Th. Uphues, Y. Ni, M. Uiberacker, M. Drescher, F. Krausz, and M. J. J. Vrakking, Phys. Rev. A **312**, 246 (2006).

[2] H. G. Muller, P. H. Bucksbaum, D. W. Schumacher, and A. Zavriyev, J. Phys. B **23**, 2761 (1990). B. Sheehy, B. Walker, and L. F. DiMauro, Phys. Rev. Lett. **74**, 4799 (1995). H. Ohmura, N. Saito, and M. Tachiya, Phys. Rev. Lett. **96**, 173001 (2006).

[3] G. L. Kamta and A. D. Bandrauk, Phys. Rev. A **76**, 053409 (2007).

[1] E-mail: kjb9x@virginia.edu [2] E-mail: dwp3k@virginia.edu [3] E-mail: bjones@virginia.edu

Time-resolved laser Coulomb explosion imaging of ultrafast molecular dynamics induced in N_2, O_2 and CO by interaction with intense laser field

Irina Bocharova*[,1], Sankar De, Dipanwita Ray, Maia Magrakvelidze, Uwe Thumm, Lew Cocke, Ali Alnaser[†] and Igor V Litvinyuk.

[*] JRM Laboratory, Kansas State University, Manhattan, KS, 66506-2604, USA
[†] Department of Physics, American University in Sharjah, Sharjah, United Arab Emirates

Synopsis: We present a series of pump-probe experiments with 8 fs 800 nm laser pulses to study the evolution of a nuclear wave packet in molecular nitrogen, oxygen and carbon monoxide following an interaction with intense laser field. We also present classical and quantum simulations of a nuclear wave packet motion which account well for our experimental data.

In our work we employed COLTRIMS and VMI technique in combination with pump-probe experiment to continue study nuclear dynamics of diatomic molecules following their interaction with short intense near IR laser pulses [1]. Kinetic energy release spectra for N_2, O_2 and CO reveal the same main features as those for H_2 and D_2: dissociation and bound nuclear wave packet motion. However, these features are much more complex due to many available intermediate charged states Fig.1.

In the experiment we used two pulses of the same duration 8 fs and wavelength 800 nm but different intensity in the range of 5×10^{14}-5×10^{15}Wcm^{-2} produced from a single pulse by Mach-Zender interferometer. Pump pulse initiates dynamics in a molecule. Probe pulse induces multiple ionization which results in Coulomb explosion. The recoil fragments are collected and analyzed to measure KER as a function of delay between the pump and probe.

Experimental KER spectra for nitrogen molecule for breakup channel $N_2^{4+}\rightarrow N^{2+}+N^{2+}$ are presented on Fig.1. Intermediate charged states for dissociation dynamics are indicated: N_2^{+}, N_2^{2+} and N_2^{3+}. Each parent ion is also characterized with a set of contributing electronic states. To recover the detailed information about nuclear motion from experimental plots we performed a series of classical and quantum simulations. Calculated spectra are in a very good agreement with experimental ones.

Similar experiments and calculations were carried out for oxygen O_2 and carbon monoxide CO diatomic molecules.

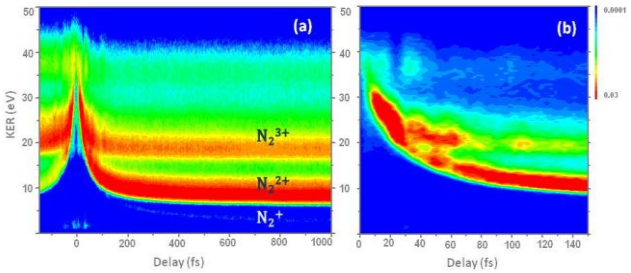

Fig. 1. Time-dependent kinetic energy release (KER) spectra (integrated over 4π angle) for N_2 for $N^{2+}+N^{2+}$ breakup channel. COLTRIMS technique. Pump pulse 8fs, intensity - 8×10^{14} W/cm^2; probe pulse 8fs, intensity - 17×10^{14} W/cm^2. (a) shows full spectrum with intermediate charged states indicated. (b) the same spectrum zoomed on the short delays part.

This work was supported by Chemical Sciences, Geosciences and Biosciences Division, Office of Basic Energy Science, US Department of Energy.

References

[1] I.A. Bocharova et al., *Phys. Rev.* A 77, 053407 (2008).

[1] E-mail: irina2@phys.ksu.edu

Molecular Frame High Harmonic Dipole Amplitude and Phase Measurements

Julien B. Bertrand*[,1], Hans Jakob Wörner, David M. Villeneuve and Paul B. Corkum

[*] Joint Laboratory for Attosecond Science, National Research Council Canada and University of Ottawa, 100 Sussex Drive, Ottawa, K1A 0R6, Canada

Synopsis: We use field-free alignment to generate high-order harmonics in the molecular frame. We perform parallel measurements of the harmonic yield and the ionization probability as a function of molecular alignment. Assuming the degree of alignment achieved in the experiment, we deconvolve both the molecular frame angular ionization and harmonic yield from the alignment distribution. We further discuss the coherent retrieval of the high-order harmonic dipole in the molecule's reference frame using additional two-source [4] phase measurements.

The XUV light emitted in the High Harmonic Generation (HHG) 3-step process contains information about the interference (step 3) between a laser-driven recolliding electron wave packet (step 2) and the bound state from which it was initially tunnel-ionized (step 1)[1]. In molecules, the process can be highly sensitive to the molecular alignment. This is the basis of quantum tomographic imaging where HHG spectra were taken at different alignment with respect to the driving laser field (linearly polarized) and used to reconstruct the σ_g valence orbital of N_2 [2].

We present measurements where the ionization probability and the high harmonic intensity as a function of molecular alignment are measured in parallel, in the same experiment. For N_2 and Br_2 and CO_2 molecules, we observe that the measured angular-dependent ionization probability reflects, respectively the σ_g and π_g character of their highest occupied molecular orbitals (HOMO). The high harmonic signal modulates together with the ionization rate for the case of N_2 but anti-correlates in the case of Br_2 and CO_2.

Assuming the degree of alignment achieved in the experiment, we perform a deconvolution [3] of the ionization and harmonic signals from the distribution of molecular alignment to obtain the true molecular frame profiles. In fig. 1, we show the measured harmonic signal (a) and the ionization rate (b, scatter). After deconvolution, we obtain the molecular frame ionization probability (b, green solid curve) and harmonic yield (c). Since, the harmonic signal contains necessarily the contribution of the ionization (step 1), we perform another deconvolution of the harmonic signal but now incorporating the retrieved molecular frame ionization probability, it now represents the squared recombination dipole (d). The result is similar to the direct lab measurement (a). However, in Br_2 and CO_2, the deconvolution incorporating the ionization profile results in strong angular modulation not apparent in the raw experimental measurement.

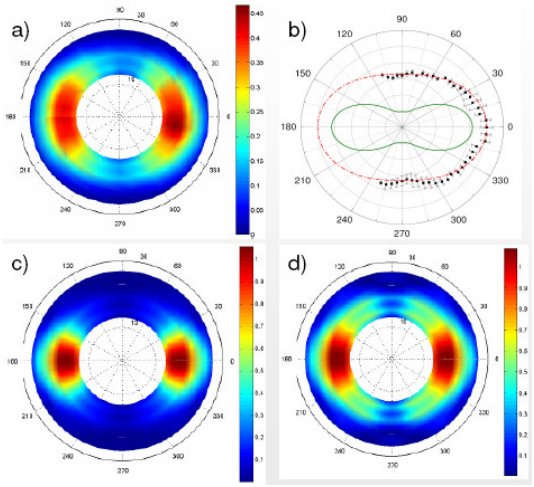

Fig. 1. a) N_2 High harmonic signal (radius: q=13 to 27, angle: Lab. molecular alignment), b) Ionization rate (scatter:exp, solid line: retrieved molecular frame ionization rate), c)Deconvoluted Squared Dipole , d) deconvoluted Squared Dipole including the measured ionization. I_{HHG}~$1.5x10^{14}$W/cm^2 and I_{Align}~$I_{HHG}/3$.

We will finally present two-source angular phase measurements in the above molecules and discuss the coherent deconvolution of the molecular frame complex dipole amplitude and phase.

References

[1] P. B. Corkum, Phys. Rev. Lett. 71, 1994 (1993).
[2] J. Itatani *et al*., Nature **432**, 867 (2004).
[3] D. Pavicic *et al*, Phys. Rev. Lett. 98, 243001 (2007).
[4] C. Corsi *et al*, Phys. Rev. Lett. 97, 023901 (2006).

[1] E-mail: Julien.Bertrand@nrc.ca

Attosecond Transient Absorption of High Order Harmonics in Helium

Mirko Holler[*,1], Florian Schapper[*], Johan Mauritsson[†], Kenneth J. Schafer[o], Lukas Gallmann[*] and Ursula Keller[*]

[*] Physics Department, ETH Zurich, 8093 Zurich, Switzerland
[†] Department of Physics, Lund University, P. O. Box 118, SE-221 00 Lund, Sweden
[o]Department of Physics & Astronomy, Louisiana State University Baton Rouge, LA 70803-4001, USA

Synopsis: We experimentally observe IR-assisted absorption of an attosecond pulse train in a helium gas target. We find that the transmitted photon yield not only modulates on the timescale of the envelope of the IR pulse but also detect oscillations with twice the fundamental laser frequency. We consider our experiment a first step to all-optical experiments in the attosecond domain.

Recently, it was demonstrated that the probability of ionization of He atoms with XUV photons close to the threshold can be controlled by the presence of a delayed IR field [1]. In that experiment, time-resolved photoelectron-spectra were recorded showing modulations with a periodicity of twice the fundamental laser frequency.

We performed a complementary experiment, detecting photons instead of electrons. We generated high harmonics in a xenon gas target with 30 fs laser pulses centered at a wavelength of 800 nm. The IR radiation was removed from the harmonics using a thin aluminum foil. The obtained harmonics (orders 13 to 19) were confirmed by RABITT to form an attosecond pulse train (data not shown). The harmonics are collinearly recombined with a time-delayed replica of the driving laser pulse using an infrared mirror with a center-hole for transmitting the harmonics. The combined beam is then focused into a second gas target by a toroidal mirror. We reach IR intensities on the order of $5 \cdot 10^{12}$ W/cm^2. The harmonic radiation transmitted through the second gas target is detected in a XUV spectrometer.

Helium was chosen as target medium. Its ionization potential is lower than the photon energy of harmonic order 17. Harmonic photons with order $\geq$17 are absorbed by single photon ionization. The density of the jet was adjusted such that about half of these photons were absorbed. Photons of harmonic 15 and below can only be absorbed in a multiphoton process. As the intensity of the harmonics is low, this is in our arrangement only possible in the presence of an additional and suitably strong IR field.

When adding the IR field and changing the delay between IR and the APT, the envelope structure is clearly visible in harmonics 13 and 15 corresponding to an IR induced absorption in helium. A typical delay scan is shown in Fig. 1. In addition to this femtosecond structure, a sub-cycle modulation of the transmission appears at a periodicity of twice the laser frequency. This modulation is visible on all harmonics, even for those with photon energy higher than the ionization potential of helium.

We experimentally show that the relative phase of this modulation does not depend on the chirp of the attosecond pulses in the train. However, the phase relation clearly changes with the intensity of the IR present in the helium target.

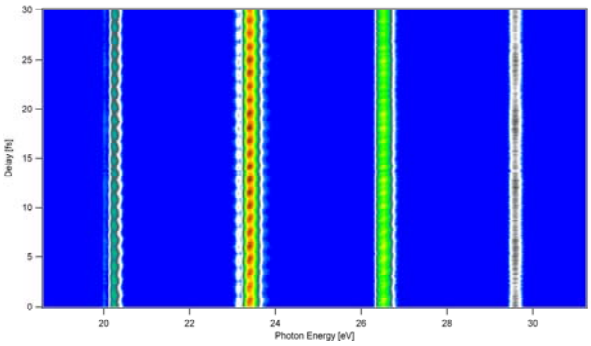

Fig. 1. Harmonics 13 to 19 versus IR/XUV delay.

We think that our measurement will help to gain deeper insight into ionization processes in the vicinity of the threshold. Furthermore, we consider our experiment a first step to all-optical experiments in the attosecond domain with the benefit of easier, faster, and cleaner data acquisition compared to the traditional detection of photoelectrons.

References

[1] P. Johnsson *et al.*, *Phys. Rev. Lett.* **99,** 233001 (2007).

[1] E-mail: mholler@phys.ethz.ch

Ultrafast electronic dynamics in Helium nanodroplets studied by femtosecond time-resolved EUV photoelectron imaging

Oliver Gessner*,[1], Oleg Kornilov*,†, Stephen R. Leone*,†, and Daniel M. Neumark*,†

* Chemical Sciences Division, Lawrence Berkeley National Laboratory, Berkeley, CA, 94720, USA
† University of California Berkeley, Berkeley, CA, 94720, USA

Synopsis: We have performed the first femtosecond EUV-pump, IR-probe experiment to study the photoionization dynamics of pure Helium nanodroplets below the atomic Helium IP in real-time. Using Velocity-Map Imaging (VMI) photoelectron spectroscopy we were able to discern processes with associated timescales ranging from tens of femtoseconds to tens of picoseconds. The results will be discussed in the light of complementary energy-domain studies and theoretical models of the droplet's electronic and nuclear dynamics.

The emerging field of ultrafast x-ray science is at a point at which its true potential for revealing electronic and structural dynamics in the chemical and material sciences has to be demonstrated. In particular the study of complex systems will provide critical benchmarks for the transition from a specialists' discipline to a widely-used tool.

Helium nanodroplets constitute a unique cryogenic matrix for the creation, isolation and spectroscopy of regular and exotic species, such as free radicals and molecules in high-spin states. Comprised of thousands to millions of atoms at cryogenic temperatures of ~0.4 K the droplets readily pick up atoms and molecules but interact only very weakly with the respective dopants due to their superfluid nature. The electronic structure and relaxation dynamics of Helium droplets have been subject of a number of synchrotron-based studies which have revealed rich but so far largely unexplained structures in EUV absorption and photoemission spectra [1].

We have set up a high harmonic generation based femtosecond EUV-pump, IR-probe photoelectron imaging experiment, Fig. 1, to extend EUV photoemission studies into the time-domain. In the first series of experiments we have monitored the electronic relaxation dynamics of large ($N\sim10^6$) pure Helium droplets from the initial EUV excitation at 23.7 eV to the emergence of both neutral and charged products in real-time. Transient photoelectron energy- and angular-distributions recorded by means of VMI photoelectron imaging reveal rich dynamics with associated timescales ranging from the femtosecond to the picosecond regime. Clear correlations between spectral features, angular distributions and dynamics timescales have been established.

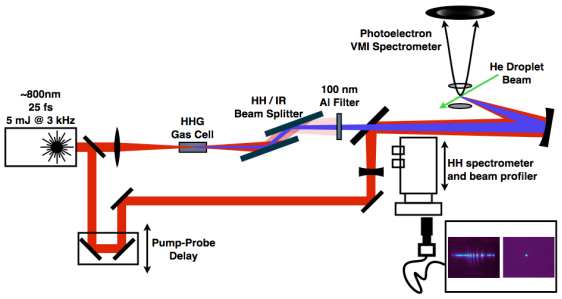

Fig. 1. Schematic of the experimental setup.

We observe transient spectral features similar to atomic Rydberg state photoionization spectra but which display dramatically different dynamics compared to free Rydberg atoms. Despite the complexity of the system, these and other findings can be explained by a relatively simple model that involves contributions from atoms that reside either on the droplet surface or in the bulk. The model will be discussed along with possible alternatives and the results of *ab-initio* calculations on the EUV excited states of Helium clusters.

References

[1] D. S. Peterka *et al.*, *Phys. Rev. Lett.* **91**, 43401 (2003).

[1] E-mail: OGessner@lbl.gov

Direct Determination of Spatial Electric Field Variations Using Isolated Attosecond Pulses

Steve Gilbertson, Ximao Feng, Sabih Khan, Michael Chini, He Wang, Hiroki Mashiko, and Zenghu Chang[1]

J. R. Macdonald Laboratory, Kansas State University, Manhattan, KS, 66506-2604, USA

Synopsis: Using single isolated 276 attosecond pulses of extreme ultraviolet radiation, the transverse electric field of an 8 femtosecond Bessel-Gaussian beam was directly measured for the first time. A photoelectron replica of an attosecond burst was generated to act as a probe for the electric field of the Bessel-Gaussian beam. By monitoring the momentum shift of the photoelectrons, the direction reversing field of the laser was accurately mapped.

By placing an attosecond burst of electrons in the field of an ultrashort laser, the electric force, via a momentum shift, can be directly measured to reconstruct the electric field oscillations of the pulse [1]. Here we extend this technique to measure the electric oscillations of the Bessel beam in space.

A Bessel-Gaussian laser pulse has a non-trivial transverse profile. These pulses can, in principle, be indirectly mapped since the direction reversal of the adjacent rings can be treated as a π phase shift. This is indirect however since even scalar Bessel beams also exhibit this property [2]. A true verification should be demonstrated by the first principle of electrodynamics, namely that the field is defined as the force exerted on a point charge.

To conduct the experiment, an interferometric streak camera was used. An 8 fs, 1mJ laser pulse was split by an 80% transmitting beamsplitter. The transmitted portion passed through double optical gating optics to generate an ellipticity dependent pulse [3]. The pulse was then focused onto an argon filled gas cell to generate the extreme ultraviolet (XUV) single attosecond burst. Meanwhile, the reflected near-infrared (NIR) portion of the initial laser pulse recombined with the XUV at a hole drilled mirror. The mirror allowed the XUV to pass and reflected the NIR. The two beams then were reflected and focused by a double mirror assembly consisting of an Mo/Si mirror and a silver mirror concentric to it. The two beams were temporally locked and spatially overlapped at a second gas target to generate photoelectrons from the XUV burst and to give a momentum shift from the NIR.

In the reflected portion of the interferometer, a thin lens was installed on a movable translation stage for overlap of the two beams at the second target. Since the double mirror assembly truncated the NIR beam, a Bessel-Gaussian beam was produced as shown in figure 1(a). Also shown is a lineout of the intensity profile (b).

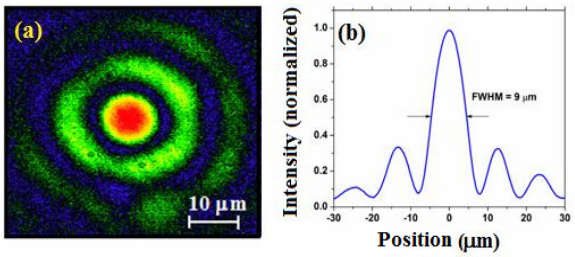

Fig. 1 (a) CCD image of the laser image. (b) Lineout of the center of (a).

The NIR beam was moved over a range transverse to the stationary attosecond burst thereby giving a spatially dependent momentum shift to the photoelectrons as seen in figure 2. This method allows for the spatial varying field strength of the pulse to be calculated directly.

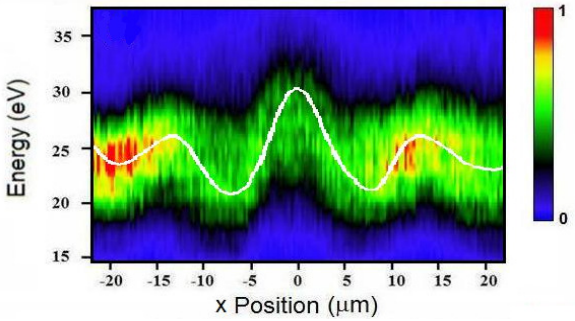

Fig. 2. Photoelectron spectrum as a function of position.

In conclusion, the transverse electric field of a Bessel-Gaussian laser beam was directly measured with single attosecond pulses. Coupling this with an accurate temporal scan of the pulse gives a full classification of femtosecond laser pulses. This material is supported by the U. S. Army Research Office under Grant No. W911NF-07-1-0475, and by the Chemical Sciences, Geosciences, and Biosciences Division, U.S. Department of Energy.

References

[1] E. Goulielmakis *et al*, Science **305**, 1267 (2004)
[2] J. Lu *et al*, IEEE Trans, On UFFC **37**, 438 (1990)
[3] S. Gilbertson *et al*, Appl. Phys. Lett. **92**, 071109 (2008)

[1] E-mail: chang@phys.ksu.edu

Carrier-envelope phase control and stabilization by an acousto-optic programmable dispersive filter

N. Forget
FASTLITE, Ecole Polytechnique bât. 403, 91128 Palaiseau, France
nicolas.forget@fastlite.com

L. Canova, X. Chen ,1 A. Jullien and R. Lopez-Martens
Laboratoire d'Optique Appliquée, Ecole Nationale Supérieure des Techniques Avancées, ParisTech, CNRS, Ecole Polytechnique, 91761 Palaiseau Cedex, France

Abstract: We demonstrate arbitrary control of the carrier-envelope (CE) phase using an acousto-optic programmable dispersive filter (AOPDF) inserted in a chirped-pulse amplification (CPA) Ti:S laser. We also demonstrate, for the first time, closed-loop CEP stabilization using an AOPDF to correct for the CEP slow drifts.

In chirped-pulse amplification (CPA) lasers, the CE phase can be locked for tens of minutes by stabilizing the CE phase offset of the oscillator. However, amplifying stabilized pulses raises some new issues. First, all the optically dispersive components of the amplification chain (crystals, stretcher, compressors…) add some offset on the CE phase. Second, thermal effects and/or acoustic vibrations induce mechanical drifts causing dispersion fluctuations and, eventually, CE phase drifts. Since the CE phase value must be kept constant on target, a slow-loop stabilization of backend CE phase is most often required, to ensure reproducible results but also to give control over the CE phase of the amplified pulses. To date several mechanisms have been proposed and demonstrated to control the CE phase: modulation of the power of the pump laser at the oscillator level, insertion of glass wedges plates, control of the grating separation in grating-based compressors… These devices are all based on dispersion modulation which might change the pulse duration, sometime use moving parts and do not allow shot-to-shot arbitrary control of the CE phase at kHz repetition rates.

In this paper, we demonstrate arbitrary control of the CE phase using an acousto-optic programmable dispersive filter. Opposite to other devices, the CE phase control is completely decoupled from dispersion control (though is allows phase and amplitude control of the spectral phase), does not involve moving parts and allows arbitrary but precise and quantitative shot-to-shot CE phase offsets. In the low-jitter configuration, the electronic generator of the AOPDF is able to control the CE phase of the acoustic wave within <40 mrad (value limited by our measurement device). Since the acoustic CE phase is transferred on the optical CE phase through the acousto-optic interaction, the CE phase of the diffracted pulse can be changed with respect to the CEP of the input pulse by an arbitrary amount within 40 mrad. As a proof of control, Fig. 1 shows the effects of successive CE phase jumps applied by the AOPDF. These phase steps were performed at a low repetition rate, corresponding to the repetition rate of the CE phase measurement device (f-2f interferometer), i.e., not limited by the refresh rate of the AOPDF.

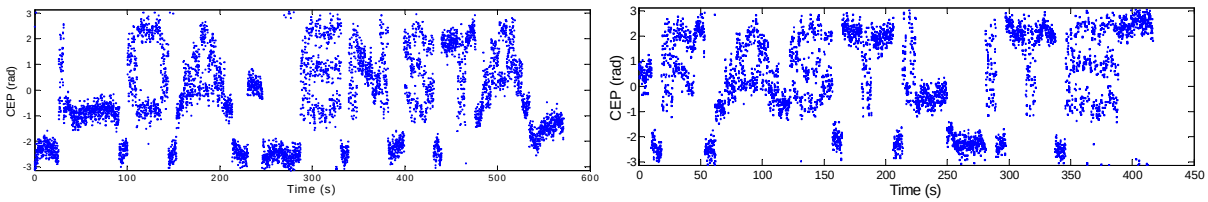

Fig.1 Demonstration of CEP control.

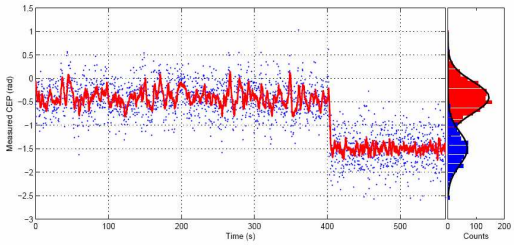

Fig.1: CE phase stabilization. Left part (<400s): open-loop. Right part (>400s): closed-loop.

Closed loop control was implemented using a f-2f interferometer and CE phase stabilization with repetition rate >15Hz were demonstrated.

Carrier-envelope phase stabilization of a high-power regenerative amplifier

Fraser Turner*, Andrei Naumov*[,1], Chengquan Li[†], and Alan Fry[†]

[*] National Research Council of Canada, 100 Sussex Dr., Ottawa, ON, K1A 0R6, Canada
[†] Coherent Inc., 5100 Patrick Henry Dr., Santa Clara, CA, 95054, USA

Synopsis: We present the results of the carrier-envelope phase stabilization of the commercially available high-power regenerative amplifier. We show the comparison between in-loop and out-of-loop phase noise measurements and discuss the effect of the Pockels cells on the carrier-envelope phase stability.

During the last several years significant progress has been made in carrier-envelope phase (CEP) stabilization of laser systems. Most of this work has focused on amplifiers with a multi-pass configuration, however as regenerative amplifiers are widely used as a primary amplification stage, stabilizing such systems is an important step in the realization of high power CEP stabilized lasers. It had previously been demonstrated that it is possible to maintain some degree of phase stability through a regenerative amplifier [1], subject to additional short-term noise sources and long-term drift in the stretcher, amplifier, and compressor. In the present work we show that a commercially available regenerative amplifier can be successfully CEP stabilized in the long term using a fast and slow feedback loop.

In our system, a Coherent Legend-HE regenerative amplifier was seeded by a temperature-stabilized Coherent Micra oscillator with an integrated Verdi V5 pump laser. About half of the oscillator output was re-compressed and sent into a Menlo Systems XPS800 f-to-2f interferometer, which was integrated into a thermalized baseplate together with the Micra oscillator. This produced a beatnote signal with more than 40dB signal-to-noise, and could stabilize the oscillator CEP to within 100mrad for several hours.

The Legend-HE Ti: Sapphire crystal was cooled to -5°C using a thermo-electric cooler, and optically pumped with the Coherent Evolution 30 diode pump laser. The amplification process required about 15 passes through the laser cavity, including the crystal and two Pockels cells. The grating-based stretcher and compressor allowed for sub-40fs, 3mJ pulses at 1kHz.

The CEP stability of the amplified pulses was characterized with two Menlo APS800 f-to-2f self-referencing interferometer systems, one to control the slow feedback loop and the other for an out-of-loop phase noise measurement. The spectrometers were externally triggered to allow for precise and reproducible data acquisition.

In order to identify the sources of CEP noise, the entire system was placed on a floating optical table. While the oscillator was found to be susceptible to acoustic noise, the amplifier was instead sensitive to vibrations, the majority of which were suppressed by floating the table. Phase noise due to the electro-optic action of Pockels cells in the regenerative amplifier cavity was initially a concern. However, our analysis has shown that its' contributions to the phase noise are negligible.

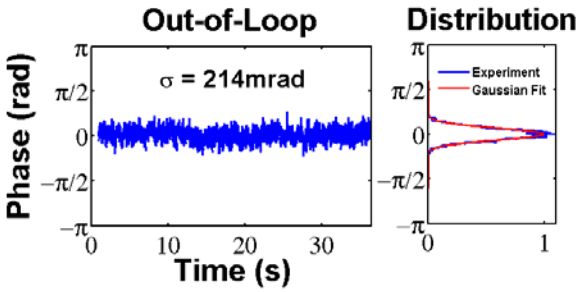

Fig. 1. Out-of-loop phase measurement of amplified laser pulse with a 5ms exposure time.

To date, we have achieved an out-of-loop phase stability of 214mrad for a spectrometer exposure time of 5ms (see Fig. 1). Phase-stable operation of the system could be maintained on the scale of hours.

References

[1] M. Kakehata et al., *Opt. Express* 12, 10 (2004)

1 E-mail: andrei.naumov@nrc.ca

A robust all-non-optical method for the complete characterization of single-shot few-cycle laser pulses

Zhangjin Chen[*,1], **T. Wittmann**[†2], **C. D. Lin**[*3]

[*]JRM Laboratory, Kansas State University, Manhattan, KS, 66506-2604, USA
[†]Max-Planck-Institue für Quantenoptik, Hans-Kopfermann-Str. 1, 85748 Garching, Germany

Synopsis We analyse the "left" and "right" asymmetry of high-energy photoelectrons along the polarization axis generated by few-cycle infrared laser pulses from atomic targets. Based on the recently developed quantitative rescattering theory, we show that the carrier-envelope phase, the pulse duration and the peak intensity of each single-shot laser pulse can be accurately and efficiently retrieved, thus providing a robust all-non-optical method for the complete characterization of single-shot few-cycle laser pulses.

Observation of the interaction of laser pulses with matter requires the knowledge and control of the waveform of the laser field. The waveform is characterized by its pulse envelope, including the peak intensity and pulse duration, as well as the carrier-envelope phase (CEP) which measures the offset between the peak of the electric field and the peak of the envelope. Specifically, such a CEP-fixed waveform can be written as $E(t) = E_0(t)\cos(\omega t + \phi)$, where ω is the frequency of the carrier wave, ϕ is the CEP .

Recently, Wittmann *et al.* [1] reported that the left/right photoelectrons from individual laser shots can be measured. We propose a robust theoretical method to determine the CEP from each single shot data, the peak laser intensity at the laser focus and the pulse duration, thus providing a complete non-optical method for the full characterization of each few-cycle laser shot in the interaction region.

The present method of characterizing single-shot laser pulses is based on the recently developed quantitative rescattering (QRS) theory [2] for describing the momentum distributions of high-energy above-threshold-ionization (HATI) photoelectrons generated by infrared lasers from atoms . According to the QRS, the momentum distributions $D(p,\theta)$ of HATI electrons can be expressed as the product of a returning electron wave packet $W(p_r)$ with the elastic differential cross section (DCS), $\sigma(p_r,\theta_r)$, between the field-free electrons with the target ion, i.e., $D(p,\theta) = W(p_r)\sigma(p_r,\theta_r)$. The wave packets $W(p_r)$ are obtained from SFA2 [2] calculations and the DCS's are evaluated in partial wave expansions.

The peak intensity and the pulse duration can be determined by a single quantity called energy moment; The CEP of each single shot can be retrieved from the asymmetry of the left/right HATI electron yields, which is shown in Fig. 1.

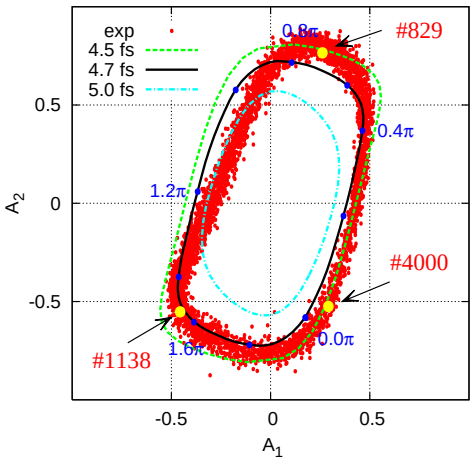

Fig. 1. Retrieval of CEP for each single shot: comparison of ellipse from experiment with theory.

References

[1] T. Wittmann, B. Horvath, W. Helml, M. G. Schätzel, X. Gu, A. L. Cavalieri, G. G. Paulus, and R. Kienberger, Nature Phys. **5**, 357 (2009).

[2] Zhangjin Chen, Anh-Thu Le, Toru Morishita, and C. D. Lin, Phys. Rev. A **79**, 033409 (2009).

[1]E-mail: zjchen@phys.ksu.edu
[2]E-mail: Tibor.Wittmann@mpq.mpg.de
[3]E-mail: cdlin@phys.ksu.edu

Chirp-controlled polarization gating for isolated attosecond pulse generation

Florian Schapper[1], **Mirko Holler, Lukas Gallmann, and Ursula Keller**

Physics Department, ETH Zurich, 8093 Zurich, Switzerland

Synopsis: We generate continuous high harmonic spectra in Argon by a superposition of two time-delayed, cross-polarized 12 fs pulses with a small imbalance of group delay dispersion (GDD) between the pulses. Our technique improves overall harmonic flux compared to traditional polarization gating methods. Recorded spectra indicate that the continuum generation is insensitive to the carrier-envelope offset phase (CEP).

The nonlinear interaction of strong ultrashort laser pulses with a target medium leads to the emission of a train of pulses with attosecond duration. To generate single attosecond pulses, one ideally has to restrict the harmonic emission to one half-cycle of the driving laser pulse. Up to now, two different schemes have been implemented. The first approach recently culminated in the generation of sub-100 as pulses with a nearly single-cycle driving laser pulse (duration 3.3 fs) and suitable spectral filtering [1]. In a different approach, the strong dependence of the efficiency of the harmonic generation process on the ellipticity of the driving laser pulse was exploited [2]. With a combination of two quarter-wave plates, the linearly polarized part of the driving laser field could be restricted to a sub-cycle window, thus forming a suitable temporal gate.

We propose a new scheme to generate a temporal gate within a few-cycle laser pulse, which does not lack from the low overall harmonic flux of the traditional polarization gating method and works with longer input pulses. We demonstrate the generation of harmonic continua with 12-fs pulses centered at 770 nm and show that our technique is insensitive to the carrier-envelope offset phase (CEP).

In our setup, we overlap two time-delayed replica of a 12 fs driving laser pulse with crossed polarization (see Fig. 1). A small amount of chirp is added on one of the replicas through the linear dispersion of a thin glass plate. For properly chosen delays between the two replicas, this leads to an overall electric field which is linearly polarized at only one or few positions within the laser pulse. Our approach is similar to the idea put forward by Altucci *et al.* [3], which uses self-phase modulation to generate the chirp. In contrast to traditional polarization gating, we can freely choose the instant of linear polarization within the pulse envelope, thereby alleviating the intensity limitation imposed by ionization of the medium.

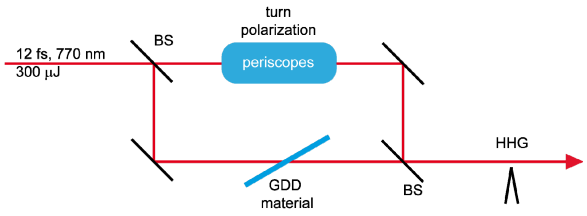

Fig. 1. Schematic of the optical setup.

In Fig. 2, two typical harmonic spectra generated in Argon are shown. When changing the delay between the two cross-polarized pulses, we can generate a continuum (Fig. 2a), discrete harmonics (Fig. 2b) or even suppress the emission by one order of magnitude (not shown). When changing the CEP of the driving laser pulse, the spectra recorded do not change significantly (data not shown), indicating that the continuum generation is insensitive to the CEP. Indeed, the only effect of changing the CEP is expected to be a small change of intensity of the linear polarization component of the waveform.

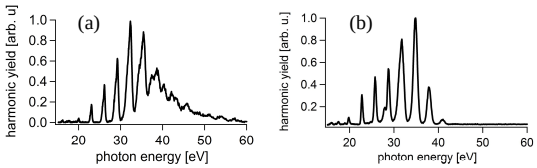

Fig. 2. Harmonic spectra for two different delay times.

In conclusion, we implement a new method that presumably enables isolated attosecond pulse generation in a simple and robust manner with higher harmonic flux, longer pulses, and reduced CEP sensitivity compared the traditional polarization gating technique.

References

[1] E. Goulielmakis *et al.*, *Science* **320** 1614 (2008).
[2] I. J. Sola *et al.*, *Nature Phys.* **2** 319 (2006).
[3] C. Altucci *et al.*, *Opt. Lett.* **33** 2943 (2008).

[1] E-mail: **schapper@phys.ethz.ch**

Generation of continuum harmonic spectrum using multi-cycle two-color infrared laser fields

Eiji J. Takahashi,[1] **Pengfei Lan, and Katsumi Midorikawa**

Extreme Photonics Research Group, RIKEN Advanced Science Institute,
2-1 Hirosawa, Wako, Saitama 351-0198, Japan

Synopsis By mixing two infrared laser pulses of different wavelengths, we generate the continuum harmonic spectrum around a cut-off region. Our obtained harmonic spectra clearly show the possibility of generating isolated attosecond pulses from many-cylse laser pulse of the two color laser fields, 30 fs laser pulses centered at 800 nm and 1300 nm. This scheme makes it possible to easily create a high-energy attosecond pulse with a well-established conventional femtosecond laser system.

We propose and demonstrate a novel two-color scheme for generating intense isolated attosecond pulses. In this scheme, a weak multi-cycle infrared field is added to an intense 30 fs, 800 nm main driving laser field. Optimum conditions of the weak infrared pulse for generating an isolated attosecond pulse are predicted by theoretical calculation and confirmed by experiment. Figure.1 (a) shows the mixed intensity profile when a 800 nm, 30 fs pulse is mixed with a 1300 nm, 40 fs pulse. Here, the intensity ratio ($I_{1300\mathrm{nm}}/I_{800\mathrm{nm}}$) and the relative phase is fixed to be 10 % and 0 rad, respectively. As can be seen around the central peak, the amplitude of the nearest neighbors on both side are well suppressed by mixing a weak longer wavelength field. The intensity ration between the central peak and the side peak attains 0.8, which is almost the same as a ratio of 5-fs cos-wave pulse of 800 nm. Consequently, we can expect generating the continuous harmonic spectrum at the cut-off region, though many-cycle laser fields are used for the pump pulse.

To demonstrate and verify our proposed concept, we have carried out the two-color experiment by using high-energy IR sources[1] based on an OPA scheme. Figure 1 (b) shows a single shot harmonic spectrum by using the two-color laser filed. When the one-color field (800 nm: 1×10^{14} W/cm^2) is focused in Ar gas, the harmonic spectrum has a discrete structure. In the two-color scheme, we can also see a discrete harmonic spectrum at the lower order region (see the inset of Fig.1 (b)). This discrete harmonic spectrum can be treated as generation of high-order sum and difference frequencies. On the other hand, the discrete components disappear at harmonic orders higher than 29th, we can clearly see a continuum harmonic spectrum around the cut-off region. Though the spectrum at cut-off region varies slightly every laser shot because of the relative phase of two-color laser pulse is not stabilized, we were able to obtain the continuum spectrum with high probability. This scheme has an advantage to generate an isolated attosecond pulse over two-color schemes ever reported[2].

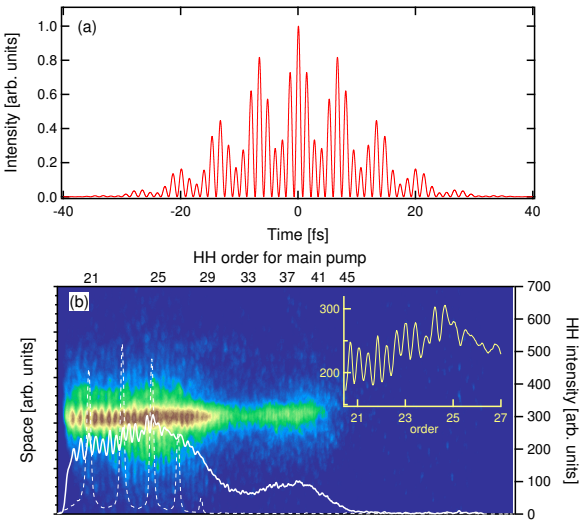

Fig. 1. (a): Temporal intensity distribution of the two-color field. (b): Single shot HH spectrum by using two-color pulse ($I_0 \sim 1.1 \times 10^{14}$ W/cm^2). The solid and dashed lines show the 1D spectrum by using two-color and one-color pulse, respectively.

References

[1] E. J. Takahashi *et al.*, Appl. Phys. Lett. **93**, 041111 (2008)

[2] Y. Oishi *e al.*, Opt. Express **14** 7230 (2006)

[1]E-mail: ejtak@riken.jp

Control of electron localization in a molecule using XUV and IR pulses

Kamal P. Singh[1], **W. Cao , P. Ranitovic, S. De, D. Ray, H. Mashiko, S. Chen, F. He, A. Becker**[†], **U. Thumm, I. Litvinyuk, C. L. Cocke**[2]

JRM Laboratory, Kansas State University, Manhattan, KS, 66506-2604, USA
[†] University of Colorado at Boulder, JILA, 440 UCB Boulder, CO 80309-0440, USA

Synopsis: We demonstrate an experimental control of electron localization in the deuterium molecular ion created and dissociated by the combined action of an attosecond pulse train (APT) and a multicycle IR laser pulse. A left-right asymmetric ejection of the deuterium ions, characterized by an asymmetry parameter *A*, exhibits oscillations with a full IR period when the time-delay between the APT and IR pulses is scanned with 300as resolution.

The control of electron localization in molecules is crucial in order to manipulate and steer many chemical reactions [1]. A key experimental step in this direction has been achieved by a recent experiment whereby a few cycle IR laser pulse was used to control the electron localization in molecular dissociation [2]. This technique requires the generation of strong few fs long phase stabilized pulses.

Here we experimentally demonstrate an alternative but powerful approach to control the electron localization using a combined action of linearly polarized attosecond pulse train (APT) and 50fs long IR pulse. The APT is synthesized using a two color technique by combining 800nm IR pulse with its second harmonic. The resulting APT contains one attosecond pulse per IR laser cycle which is necessary in order to observe the electron localization effect [3]. Moreover, because second harmonic is phase-locked to the fundamental 800nm pulse, any need for carrier phase stabilization is eliminated. Both the APT and the fundamental IR pulse are focused simultaneously on the deuterium target gas inside the COLTRIMS reaction microscope and the time-delay between them is scanned in steps of 300as.

The produced ionic fragments are ejected either parallel (left) or anti-parallel (right) to the laser polarization axis. The asymmetry between left-right ejection of the D^+ ions is quantified by the asymmetry parameter, *A*, defined as

$$A = \frac{C_{left} - C_{right}}{C_{left} + C_{right}},$$

where C_{left}, C_{right} are the corresponding counts.

The Fig. 1 shows the parameter *A* versus the time-delay between the IR and APT pulses (zero delay corresponds to overlapping pulses). The parameter *A* clearly oscillates with full laser cycle period of 2.7fs with about 5% contrast. Furthermore, an analysis of the kinetic energies of the released ionic fragments suggests that the underlying mechanism of the localization control takes place primarily as the IR induces the molecular dissociation for selected internuclear distances.

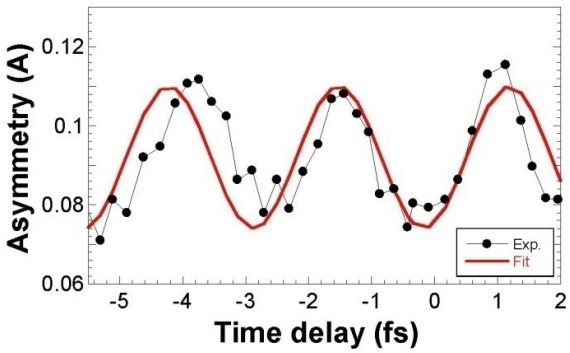

Fig. 1. The asymmetry parameter *A* versus the time delay between APT and IR pulses. Red solid line is a fit to sinusoidal function with the laser period.

Our data are supported by theoretical calculations based on numerically solving time-dependent Schrodinger equation for the system, which reproduces well the observed oscillations of the asymmetry.

References

[1] A. D. Bandrauk, S. Chelkowski, H. S. Nguyen, 2004 *J. Quant. Chem.* **100** 834.
[2] M. F. Kling *et al.* 2006 *Science* **312** 246.
[3] F. He and A. Becker 2008 *J. Phys. B* **41** 074017; F. He, U. Thumm and A. Becker 2008 *Phys. Rev. Lett.* **101** 213002.

[1] E-mail: kpsingh@phys.ksu.edu
[2] E-mail: cocke@phys.ksu.edu

High Harmonic Generation seeded by a XUV pulse train

F. Kelkensberg*, G. Gademann*, W. Siu*, P. Johnsson*, M.J.J. Vrakking[1]*

*FOM-Institute AMOLF, Science Park 113, 1098 XG Amsterdam, The Netherlands

Synopsis In the process of high harmonic generation multiple interfering quantum paths are responsible for the harmonic emission. In a theoretical study from 2004 it was shown that attosecond pulse trains can be used to select a single quantum path. The first experiment to demonstrate this effect showed an enhancement of harmonics emission by seeding it with an attosecond pulse train. Here we present for the first time the delay dependence of this enhancement, demonstrating quantum path control.

The result of a strong-field process can normally be described as the coherent sum of a few quantum orbits. In a theoretical study by Schafer et al. [1] it was shown that attosecond pulse trains (APT) can be used to selectively launch a single quantum path. In the proposed experiment harmonic generation in He is controlled in such a way that only one of the trajectories contributes to the emission of harmonics. This proposal led to the first experiment where it was shown that in HHG in He, when seeded with an APT pulse train, certain harmonics are enhanced. To date however, control of the seeding exploiting the APT-IR time delay remains to be demonstrated.

The control mechanism is based on the fact that the electrons are not launched in the continuum by tunneling ionization but by a single-photon ionization by the APT. Choosing a specific delay with respect to the phase of the IR-field, the moment of ionization can be controlled and a certain quantum path is selected. The continuum electrons are subsequently accelerated by the IR driving field. Here we show the first experimental indication that quantum path control in HHG can be achieved by combining an APT with an IR field.

In the experiment an APT consisting of harmonics 11-19 was produced by HHG in xenon. The APT was recombined with the IR driving field at a chosen delay and collinearly focused into a helium gas cell. Harmonic emission resulting from this was detected by a flat field XUV spectrometer. Additional harmonics are created when APT and the IR fields are overlapped (see figure 1). When we zoom in on the time axis we observe that the intensity of these harmonics oscillate as a function of the APT-IR delay with a period of half the optical cycle of the IR field. This is a strong indication that these harmonics indeed result from ionization by the APT followed by acceleration and recombination in the IR field.

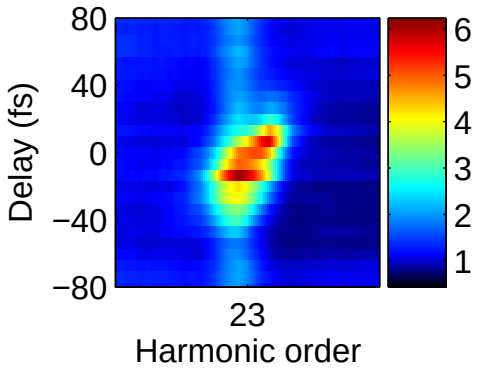

Fig. 1. Appearance of the harmonic 23 from HHG in He seeded by an attosecond pulse train produced in Xe.

In the future we are planning to extend this work in a way such that conditions are created in which a harmonic seeding experiment can be accompanied - in one and the same setup - by an experiment where photoelectrons from two-color APT-IR ionization can be measured, thereby allowing to connect the observations in the harmonic seeding experiment to information on the atomic ionization as revealed in streaking/wavepacket interferometry experiments [3].

References

[1] K.J. Schafer et. al., Phys. Rev. Lett. **92**, 023003 (2004).

[2] J. Biegert et. al., Laser Physics **15**, 899 (2005).

[3] T. Remetter et. al., Nature Physics **2**, 323 (2006).

[1] E-mail: vrakking@amolf.nl

Mapping attosecond electron wavepacket motion in a molecule by using two-color laser pulses

Hiromichi Niikura*,†[1], D. M. Villeneuve*, and P. B. Corkum*‡

* National Research Council of Canada, 100 Sussex Dr., Ottawa, ON, K1A0R6 Canada
†PRESTO, Japan Science and Technology Agency, Sanbancho Building, 5-Sanbancho,Chiyodaku, Tokyo, Japan
‡Department of Physics, University of Ottawa, 150 Luis Pasteur, Ottawa, ON, K1N6N5 Canada

We measure high harmonic generation spectra of D_2, N_2, CO_2, N_2O and hydrocarbons by using simultaneously 800nm and 400 nm laser pulses generated with perpendicular polarization. The intensity of high harmonic spectra is modulated as we change the relative phase of the two pulses. The phase of intensity modulation depends on the symmetry of molecular orbitals from which high harmonics are emitted. We show that this allows us to identity any molecular orbital that can contribute high harmonic generation even randomly aligned molecule. Using this approach, we also show the observation of electron wavepacket motion occurring in a few-hundred attoseconds.

A high harmonic generation spectrum contains information on vibration, electronic structure, and its dynamics of molecules from which high harmonics are generated. Molecular orbital tomography approach allows us to measure the amplitude of an electron wavefunction [1]. However, the experimental example of this approach has been limited to the N_2 molecular orbital.

Recently, another route for orbital tomography was demonstrated by using orthogonally polarized, 800nm and 400 nm laser pulses [2]. We extend this approach to identify molecular orbital symmetry and observe the dynamical motion occurring within a few-hundred attosecond time-scale.

To identify molecular orbital symmetry, we use the following method. High harmonic emission is generally polarized. The polarization angle (ϕ_{HHG}) depends on both angle of electron re-collision (θ_c) and the symmetry of molecular orbital that contributes high harmonic generation. Therefore, by measuring the relationship between the two angles, we identify the molecular orbital symmetry. If molecular orbital changes in the spatial distribution of amplitude and phase until electron re-collision, then the ϕ_{HHG} also must be changed. From this, dynamical changes of molecular orbital can be measurable. For non-aligned molecules, harmonics are preferentially generated from that portion of the ensemble which dominates the ionization probability. It allows us to apply this method without aligning molecule.

We generate 400nm laser pulses from 35fs, 800nm laser pulses (~1.5×10^{14}W/cm^2) by passing a BBO crystal. We measure high harmonic generation spectra as a function of the relative delay. Changing the delay between the two pulses changes the θ_c. We obtain the ϕ_{HHG} by comparing the relative intensity between two adjacent harmonic pairs (*i.e.*, 13th and 14th) as a function of harmonic number and the delay.

We observe that at the θ_c of ~0 degrees, the ϕ_{HHG} is ~0 for D_2 and N_2,while the ϕ_{HHG} is ~90 degrees for CO_2 and N_2. At the θ_c is ~45 degrees, the ϕ_{HHG} is ~45 degrees for D_2 and N_2, while the ϕ_{HHG} is ~0 degrees for CO_2 and N_2O. This observation is consistent with the calculated results when the high harmonics are generated from the σ_g state for D_2 and N_2, while the π_g (or quasi-π_g) state for CO_2 and N_2O. Since CO_2's (or N_2's) highest occupied molecular orbital (HOMO) has π_g (or σ_g) symmetry, the experiments suggest that HOMO is a dominant role for high harmonic generation process in the present laser intensity.

For the hydrocarbon, we observe the double peak structure of the ϕ_{HHG} as a function of the delay. Our analysis indicates that the molecular orbital symmetry changes as the harmonic number increases. The result cannot be accounted for two independent orbital contribution. Instead, the observation agrees with the result of calculation where the molecular orbital changes its spatial distribution in the range1.3 ~1.7fs after the tunnel ionization due to coherent superposition of two states.

References

[1] J.Itatani *et al.*, *Nature* **432**, 867 (2004).
[2] D.Shafir *et al.*, *Nature Phys.* **4**, 1 (2009).

†[1] E-mail: Hiromichi.Niikura@nrc.ca

Attosecond chirp-encoded dynamics of light nuclei

S. Haessler*, [1], W. Boutu*, S. Weber*, J. Caillat†, R. Taïeb†, A. Maquet†, P. Breger*, B. Carré* and P. Salières*

*CEA Saclay, IRAMIS, Service des Photons, Atomes et Molécules, 91191 Gif-sur-Yvette, France
†UMPC Univ. Paris 06, CNRS, UMR 7614, LCPMR, 11 rue Pierre et Marie Curie, 75231 Paris, France

Synopsis We use the attosecond emission from light molecules to probe the ultrafast nuclear dynamics occurring between the ionization and recombination steps. By measuring the phase of the XUV emission, we have direct access to the mapping of harmonic frequency to the excursion time, which represents the delay after which the evolved molecular ion is probed. The small difference in the harmonic phase between H_2 and D_2 calculated theoretically is consistent with our experimental results.

An experimental method for tracking ultrafast nuclear re-arrangements termed PACER (probing attosecond dynamics by chirp encoded recollision) has been proposed [1] and demonstrated experimentally [2] a few years ago. The three steps, ionization, acceleration and recombination, commonly used to describe high harmonic generation (HHG), are considered as a pump, a delay-stage, and a probe process. In the case of H_2 and D_2, the molecular ion has a larger equilibrium internuclear separation than the neutral, so that during the excursion of the continuum electron, the molecular ion expands. The positive chirp of the re-colliding continuum electron wavepacket, assumed to be the same as that measured for rare-gas atoms [3], was exploited to map different pump-probe delays to the different harmonic frequencies.

Using the RABITT (Reconstruction of Attosecond Beating by Interference of Two-photon Transitions) [5] technique, we measure the group delay of the harmonic emission, which, for rare gas atoms, has been shown to be equal to the electron re-collision times, also called emission time [3]. As shown in figure 1, the emission times measured for argon, H_2 and D_2 under the same conditions are very similar. This experimentally confirms for H_2 and D_2 molecules the theoretical time-frequency mapping predicted by a strong field approximation (SFA) theory including nuclear dynamics [1] and verifies one of the basic assumptions made for PACER.

We then study the small difference in the measured group delay for H_2 and D_2. Within the SFA, the phase difference of the high-harmonic emissions from the two isotopes is given by the phases of the nuclear overlap integrals $C(\tau) = \int \chi_0(R)\chi(R,\tau)\mathrm{d}R$, where R is the internuclear distance, τ is the excursion time, mapped to harmonic order, and $\chi_0(R)$ and $\chi(R,\tau)$ are the nuclear wavefunctions of the neutral and the molecular ion, respectively [4]. A fully quantum mechanical calculation of $C(\tau)$ yields a small phase difference between H_2 and D_2, which encodes the nuclear dynamics just as the harmonic intensities considered in [1, 2]. Our experimental results are compatible with this phase difference.

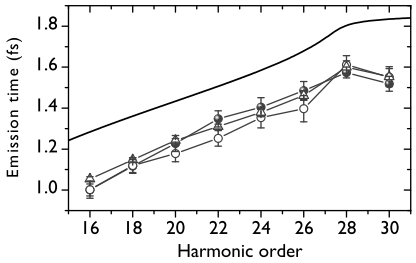

Fig. 1. Measured group delay or emission times for H_2 (◯), D_2 (△) and Ar (•). The line shows recollision times calculated with the SFA for Ar and an intensity of 1.2×10^{14} W cm^{-2}. The ≈ 200 as offset between theory and experiment is attributed to a macroscopic effect.

References

[1] M. Lein , Phys. Rev. Lett. **94**, 053004 (2005).

[2] S. Baker *et al.*, Science **312**, 424 (2006).

[3] Y. Mairesse *et al.*, Science **302**, 1540 (2003).

[4] S. Haessler *et al.*, J. Phys. B, in press (2009).

[5] V. Véniard, R. Taïeb and A. Maquet, Phys. Rev. A **54**, 721 (1996) and P.M. Paul *et al.*, Science **292**, 1689 (2001).

[1] E-mail: stefan.haessler@cea.fr

Atomic wavefunctions probed through strong field light-matter interactions

D. Shafir*, Y. Mairesse†, J. Higuet†, B. Fabre†, E. Mével†, E. Constant†, D. M. Villeneuve, P. B. Corkum** and N. Dudovich***

*Department of Physics of Complex Systems, Weizmann Institute of Science, Rehovot 76100, Israel
† CELIA, Universit'e Bordeaux I, UMR5107, 351 Cours de la Lib'eration, 33405 Talence, France
** National Research Council of Canada, 100 Sussex Drive, Ottawa, Ontario K1A 0R6, Canada

The spatial properties of atomic wavefunctions were probed through the strong field process of high harmonic generation. Using elliptically polarized laser fields and two color fields we were able to manipulate the 2D motion of free electrons and probe the atomic wavefunctions from different angles. The atomic orbitals in turn were used as spatial probes to investigate the dynamics of the ionization process.

Strong field light-matter interactions can encode the spatial properties of the electronic wave functions which contribute to the process. Recently it has been established that the broadband harmonic spectra, measured for a series of molecular alignments, can be used to create a tomographic reconstruction of molecular orbitals [1]. We take tomography one step forward, extending the approach to systems that cannot be naturally aligned. We demonstrate this ability by probing the two dimensional properties of atomic wavefunctions. By manipulating an electron ion recollision process, we are able to resolve the symmetry of the atomic wavefunction with notably high contrast. Finally we demonstrate how such approach can be extended to resolve the ionization mechanism.

Manipulating the 2D dynamics of the free electron can be achieved using either an ellipticaly polarized single color field or an orthogonally polarized two color field. Tunnel ionization which is a selective process that determines the wave function to be probed [2] occurs along the instantaneous electric field direction. The free electron accelerates in the electric field and is then driven to recollide with the parent ion at an angle. By manipulating the parameters of the field such as the two fields delay, in a two color scheme, or the laser ellipticity, in a single color scheme, we can tune the recollision angle and perform a 2D scan of the atomic wavefunction.

We have recently demonstrated this approach experimentally, using a two color scheme, by probing the wavefunction of He (1s state) and Ne (2p state) [3]. The experimental results show a striking difference between the two atomic wavefunctions. We conclude that the symmetry of the ground state is imprinted in the high harmonic spectrum.

Finally, we analyzed the high harmonic spectrum to resolve the orbital. Specifically, by analyzing the measurements using a simple classical model we resolve the degree of selectivity achieved during tunnel ionization. We find that tunnel ionization of Ne atoms generates almost a pure aligned state, with a relative population of 90% in the main quantization axis.

Our measurement provides a direct insight into the outcome of tunnel ionization. Therefore, we can extend our approach and apply the probing mechanism to resolve the ionization process. In this approach the atomic wavefunction serves as a spatial probe utilizing its simple structure and static nature.

Ionization in strong laser fields is commonly described by the ADK theory relying on the fundamental work of Keldysh [4]. The Keldysh theory separates two distinct ionization mechanisms: tunnel ionization and multiphoton absorption, characterized by the Keldysh parameter. We perform a systematic study of the ionization process by manipulating the fundamental parameters of the interaction – the laser intensity and wavelength. By using the atomic wavefunction as a probe while tuning the Keldysh parameter we study the two regimes of the ionization process with extremely high contrast.

References:

[1] J. Itatani *et al.*, Nature **432**, 867 (2004).
[2] L. Young *et al*., Phys. Rev. Lett. **97,** 083601 (2006).
[3] D. Shafir *et al.*, accepted to Nature physics (2009).
[4] L. V. Keldysh, Sov. Phys. JEPT **20** (1964).

E-mail: dror.shafir@weizmann.ac.il

High order harmonic generation with mid-infrared driven pulses

Han Xu[1,*], Hui Xiong[1], Yuxi Fu[1], Jinping Yao[1], Bin Zeng[1], Wei Chu[1], Ya Cheng[1], Zhizhan Xu[1]

[1]Shanghai Institute of Optics and Fine Mechanics, Chinese Academy of Sciences,
No. 390, Qinghe Road, Jiading District, Shanghai 201800, China

Abstract: We report on coherent water-window radiation by high-order harmonic generation in a gas cell with midinfrared femtosecnd pulses . With optimized parmeters, photon energy upto ~420 eV could be observed.

High-order harmonic generation (HHG) has been studied intensively since its discovery nearly two decades ago [1]. One of the attractions of HHG is generation of highly coherent light source in water window region. The main drawbacks of 800 nm pump laser for generating the coherent X-ray in water window lies in the fact that high peak intensity laser pulses must be used in order to provide sufficiently high ponderomotive energies to the ionized electrons, which could lead to highly ionization of the generating medium and destroying the whole process. It has been proposed that employing mid-infrared laser pulses could bypass the problem [2]. Recently, coherent water window X-ray has been demonstrated by HHG with a gas jet using a home-built high-energy midinfrared pump laser operating at 10 Hz repetition rate and 1550 nm wavelength [3-4]. In this report, we demonstrate the generation of the water window X-ray at 1 kHz repetition rate in a 4-mm long gas cell using a commercially available optical parametric amplifier (OPA) which could deliver wavelength tunable mid-infrared femtosecond pulses.

In this experiment, midinfrared pulses of 1500 nm carrier wavelength, maximum pulse energy of ~1.6 mJ, pulse duration of ~50fs, and M^2 of ~1.3 are produced by OPA system (HE-TOPAS, Light Conversion Inc.). With fused silica lens with a focal length of ~15cm, the infrared beams is focused into a 4 mm long gas cell filled with neon gas. A flat-field grating spectrometer equipped with a soft-X-ray CCD (Princeton Instruments, 1340×400 imaging array PI:SX 400) is used for measurement of the HHG spectra. The spectrometer consists of a spherical concave gold mirror and a flat field grating (Hitachi, 001-0266, 1200 grooves/mm). In order to block the low-order harmonics and the residual infrared driving pulses, a 150nm thick aluminium foil was placed at the entrance of the spectrometer.

Fig. 1 shows the HHG spectra obtained at ~800 nm, ~1300 nm and ~1500 nm wavelengths in neon gas at nearly constant focal intensity of ~6.0×10^{14} W/cm^2. With the 800 nm driving pulse, the highest cutoff energy achieved is only ~135eV. And with the 1300 nm driving pulse, the harmonic spectrum in water window can be merely observed. In the case of using the 1500 nm driving pulse, the cutoff is greatly extended to ~420eV. Therefore, the cutoff energy roughly obeys the wavelength scaling law of HHG [5]

$$E_{\text{cutoff}} = \text{h}\omega_{\max} = I_{\text{p}} + 3.17U_{\text{p}} \qquad (1)$$

, where I_P denotes the binding energy of the target atom and ponderomotive energy U_P is proportional to square of the driven wavelength.

The dip around the carbon K-edge (284eV) should be caused by a thin layer of pump oil absorbed on the optical components of the spectrometer or on the soft X-ray CCD, as had been pointed out in Ref. [6].

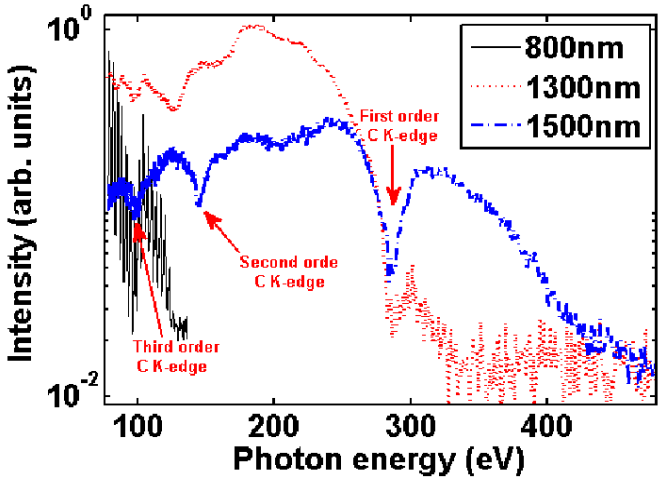

Figure 1. Normalized HHG spectra optimized at different wavelengths of the driving pulses. Black solid curve: 800 nm; red dotted curve: 1300 nm; and blue dashed-dotted curve: 1500 nm. The intensity of the laser beams is fixed at ~6.0×10^{14} *W/cm²* for the three wavelengths.

[1] P. Agostini, and L. F. DiMauro, Rep. Prog. Phys., **67**, 813 (2004).

[2] J. Tate, T. Auguste, H. G. Muller, P. Salieres, P. Agostini, and L. F. DiMauro, Phys. Rev. Lett., **98**, 013901 (2007).

[3] E. J. Takahashi, T. Kanai, K. L. Ishikawa, Y. Nabekawa, and K. Midorikawa, Phys. Rev. Lett., **101**, 253901 (2008).

[4] E. J. Takahashi, T. Kanai, Y. Nabekawa, and K. Midorikawa, Appl. Phys. Lett., **93**, **041111** (2008).

[5] P. B. Corkum, Phys. Rev. Lett., **71,** 1994 (1993).

[6] W. Schwanda, K. Eidmann, and M. C. Richardson, J. X-Ray Sci. Technol., **4**, 8 (1993).

* Hanxu1981@gmail.com

High Harmonic Generation using 1425 nm sub-3 cycles laser pulses

F. Légaré*[,1], B. E. Schmidt[*,§], A. D. Shiner[†], C. Trallero[†], H. Worner[†], M. Giguère[*], P. B. Corkum[†,§], J-C. Kieffer[*], and D. M. Villeneuve[†]

[*] INRS, Énergie Matériaux et Télécommunications, 1650 Boulevard Lionel-Boulet, Varennes, Qc Canada J3X1S2
[†] National Research Council Canada, 100 Sussex Drive, Ottawa, On Canada K1A 0R6
[§]Department of Physics, 150 Louis Pasteur, University of Ottawa, Ottawa, On Canada K1N6N5

Synopsis: 13.1 fs pulses with 400 μJ pulse energy at 1425 nm have been generated using spectral broadening of OPA (Optical Parametric Amplifier) signal beam in an Ar filled hollow core fiber. Chirped mirrors are used for temporal compression and the IR few-optical-cycle pulses are applied to study the extension of the high harmonic cut-off frequency with noble gas.

Generation of intense few-optical-cycle laser pulses at 800 nm (Titanium-Sapphire) has been the key technological breakthrough for attosecond science – high harmonic generation [1]. At the moment, using carrier-envelope phase stabilized 1.5 cycle Ti-Sa laser pulses and an interaction media with a large ionization potential (neon, Ip = 21 eV), pulse duration of 80 attoseconds has been generated. Since the cut-off of the harmonic spectra scales with $I\lambda^2$ (I is the laser intensity and λ the laser wavelength), few-optical-cycle infrared laser pulses are required to further decrease the duration of attosecond laser pulses. Such development will also be highly beneficial for molecular orbital tomography since shorter harmonic wavelength implies better spatial resolution [2], and few-optical-cycle duration will allow using this promising approach in the context of high temporal resolution pump-probe imaging experiments.

We report generation and characterization of sub-3 optical cycle pulses at 1425 nm using the standard approach used at 800 nm, i.e. spectral broadening in a hollow core fiber followed by dispersion compensation using chirped mirrors. The experiment was conducted at the Advanced Laser Light Source (ALLS). Using 7 mJ of Ti-Sa, 1.2 mJ 60 fs 1425 nm laser pulses are produced using Optical Parametric Amplification. The IR laser beam is coupled into the hollow core fiber compressor using an f=1 m plano-convex lens. Using Argon at 1.7 Atm of pressure in the fiber, we have generated broadband spectra supporting 12.2 fs pulse duration (less than 3 optical cycles). After the hollow core fiber setup, newly designed chirped mirrors were introduced to compensate the quadratic spectral phase carried by the pulses due to self phase modulation.

Temporal characterisation of the laser pulses was performed using SHG-FROG. In Fig. 1, we are presenting the retrieved temporal profile of the laser pulses obtained using the SHG-FROG reconstruction. The fact that the obtained FWHM duration of 13.1 fs is only 1.07 times the Fourier limit (12.2 fs assuming flat spectral phase) proves the good compressibility of the SPM broadened spectra at 1425 nm. The intensity profile is asymmetric with a flat temporal phase covering the main pulse, shown as dash-dotted line. At 1425 nm, 13.1 fs is less than 3 optical cycles, equivalent to about 7.5 fs pulse duration at 800 nm.

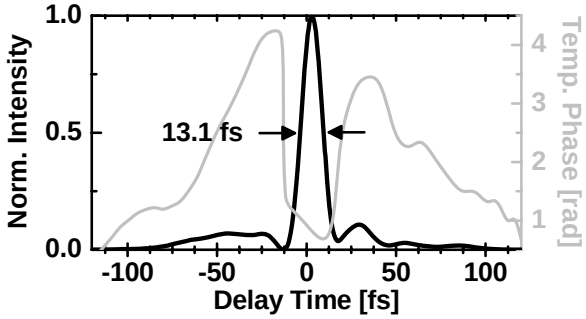

Fig. 1: Reconstructed temporal intensity (black line) and phase (gray line) of the sub-3 optical cycle pulses at 1425 nm.

Using few-optical-cycle pulses at 1425 nm, we measured that the HHG spectrum in Argon extends to 160 eV. Furthermore we are comparing the cut-off region generated by either few-optical-cycle pulses or with 60 fs pulses delivered from the OPA in different noble gas.

References

[1] E. Goulielmakis et *al. Science* **320**, 1614 (2008).
[2] J. Itatani et *al. Nature* **432**, 867 (2004).

[1]E-mail: legare@emt.inrs.ca

Phase and population control of a vibrating wavepacket

W. A. Bryan[*,1] **C. R. Calvert**[†] **R. B. King**[†] **J. Nemeth**[*] **J. B. Greenwood**[†] **J. D. Alexander**[†] **E. L. Springate**[‡] **C. A. Froud**[‡] **I. C. E. Turcu**[‡] **I. D. Williams**[†] **W. R. Newell**[⋆]

[*]Department of Physics, Swansea University, Singleton Park, Swansea SA2 8PP, UK
[†]School of Mathematics and Physics, Queen's University Belfast, Belfast BT7 1NN, UK
[‡]Central Laser Facility, STFC Rutherford Appleton Laboratory, Didcot OX11 0QX. UK
[⋆]Department of Physics and Astronomy, University College London, WC1E 6BT, UK

Synopsis We present experimental evidence of the manipulation of vibrational phase and population by light-induced dynamic potential surface deformation. A vibrational wavepacket is created in D_2^+ in a 10 fs NIR pump pulse; the evolution of the wavepacket is non-destructively modified by a control pulse. Depending on the pump-control delay, population is up- or down-shifted and the relative phase delayed or advanced with respect to the unperturbed motion.

Substantial efforts have been made to control the motion of vibrational wavepackets, with applications in quantum computation, chemical reactivity and actively steering molecular structure. The challenge in engineering the vibrational state of a molecule is two-fold: not to destroy the quantum system during manipulation and to quantify the evolution of the system.

Three NIR few-cycle (10 fs) laser pulses of moderate intensity generate, control and image a vibrational wavepacket in deuterium. First, a 'pump' pulse of intensity $I \simeq 10^{14}$ Wcm^{-2} causes ionization $D_2 \rightarrow D_2^+$, populating a range of vibrational states. The ionization step launches the vibrational wavepacket on the D_2^+ potential energy surface (PES). The propagation of a wavepacket on such a PES has been observed by the authors and other groups [1, 2], and is well understood theoretically [3, 4].

The 'control' pulse ($I \simeq 3 \times 10^{13}$ Wcm^{-2}) then dynamically distorts the PES through the Stark effect and the dipole transition; depending on the intensity and time of application of the control pulse, the varying potential gradient causes vibrational components to phase shift without destroying the coherence of the wavepacket. Population transfer is also possible: the deformation chirps the oscillation frequencies, analogous to a Raman interaction induced by the applied field. Changing the pump-control separation phase shifts different components, and selectively transfers population up or down the available vibrational states.

The final 'probe' pulse has an intensity $I \simeq 3 \times 10^{14}$ Wcm^{-2}; the influence of the control pulse is experimentally observed by recording the dissociation yield as the pump-probe delay is scanned for a range of pump-control delays.

At the conference we will present a quantitative comparison between observations of control-moderated wavepacket motion and a novel quasi-classical model (QCM). The wavepacket is represented by an ensemble of classical trajectories propagating on the PES; the dynamic deformation of the molecular bond by the control pulse is readily incorporated. Comparisons between the QCM and quantum mechanical solutions [3] for identical optical conditions indicate the QCM is a valid description of the system.

The agreement between the experimental observations and the QCM has implications for the dynamic control of molecular structure. The QCM is readily extended to complex chemically and biologically significant systems, intractable to more widely applied theoretical methods. Furthermore, the NIR pump could be replaced by a UV attosecond pulse, and multiple control pulses employed. The QCM could easily be adapted to such conditions, offering a route to exploring non-BOA molecular dynamics.

References

[1] W. A. Bryan et al, Phys. Rev. A 76, 053402 (2007)

[2] A. S. Alnaser et al, Phys. Rev. A 72, 041402 (2005)

[3] T. Niederhausen and U. Thumm, Phys. Rev. A 77, 013407 (2008)

[4] B. Feuerstein et al, Phys. Rev. Lett. 99, 153002 (2007)

[1]E-mail: w.a.bryan@swansea.ac.uk

Generation of continuum XUV radiation by CE-phase stabilized 5-fs laser pulse

H. Teng*, C.X. Yun, H.H. Han, J.F. Zhu, X. Zhong, Z.Y. Wei%

Institute of Physics, Chinese Academy of Sciences,
Beijing National Laboratory for Condensed Matter Physics, Beijing 100190, P.R. China
**Email address: hteng@aphy.iphy.ac.cn*
%Email address: zywei@aphy.iphy.ac.cn

Gaining insight into the nuclear motion or electronic transitions, which falls within the attosecond (10^{-18} second) time scale, is the driving force to pursue new faster laser source. The coherence and short duration of attosecond laser pulses make it an attractive extreme ultraviolet (XUV) source in atomic, molecular, plasma, and solid state physics [1]. Our goal aims to deliver a source of isolated attosecond optical pulses with shorter and more powerful for interrogating a wide range of these fundamental electronic processes in matter evolving on a ultrafast, sub 100-as timescale.

Coherent extreme- ultraviolet (XUV) radiation was studied by interaction of Carrier-Envelope (CE) phase stabilized high energy sub-5-fs infrared (760 nm) laser pulses [2] [3][4] with neon gas at a repetition rate of 1 kHz. The CE phase is very sensitive to generation of XUV continuum spectra for few-cycle laser pulses. To investigate the dependence of the resultant XUV spectrum on CE phase of driving laser pulses, XUV spectra were recorded for different setting of CE phase. As shown in Figure 1, notably, with a change of the CE phase, the cut-off XUV spectrum gradually transform from discrete modulated harmonic peaks to continuum spectral distribution. Figure (b) shows the when the CE phase is defined as zero, a broad structureless continuum spectrum appear in the cut off region. As the CEO phase is slowly varied between zero and π, by inserting a wedge in optical path, the continuum spectrum in the cut-off region become much modulated and discrete harmonic peaks, and this modulation will become maximum when the phase is equal to $\pm\pi/2$. The broadband continuum XUV spectrum at cut-off region was demonstrated when CE phase is shift to about zero, which show generation of isolated sub-femtosecond XUV pulses. The characterization of this XUV pulse will be carried out in future experiment.

In this talk, I will present three parts as following: firstly, introduction; secondly, I will introduce the carrier-envelope (CE) phase controlled intense 5-fs laser system and experiment setup for HHG; thirdly, I will present the recent results of high harmonic generation based on this laser system as shown above.

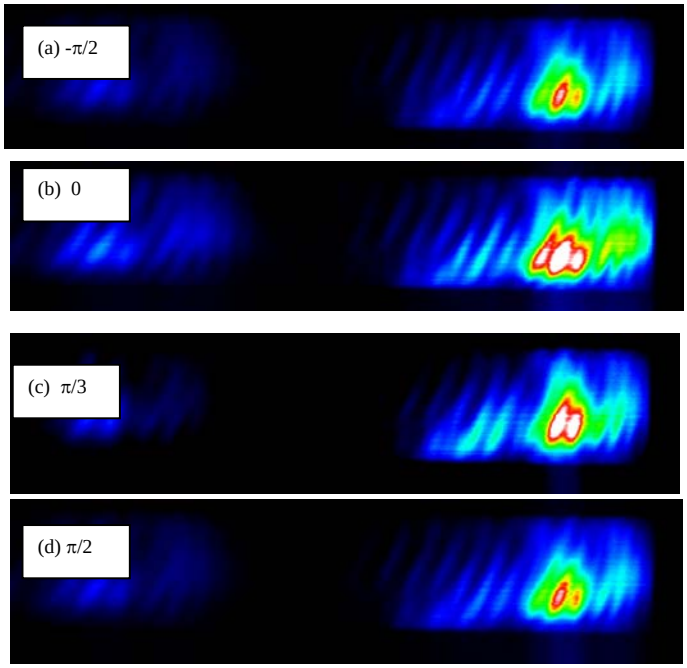

Figure 1. Measured XUV Spectrum from interaction of neon gas with CE-phase stabilized 5-fs laser pulse. (a)-(d) obtained for different CE-phase settings, by changing the insert of fused silica wedge

References

[1] P. H. Bucksbaum, Science. **317,** 766 (2007).
[2] Q Du e*t al*., Chinese Science Bulletin. **53**, 40 (2008)
[3] H. H. Han *et al.*, ACTA PHYSICS SINICA. **56**, No.5, 2756 (2007)
[4] Y. Y. Zhao *et al.,* Science in China, Series G. **37,** 123 (2007)

Statistical Noise in Isolated Attosecond Pulse Retrieval

Sabih D. Khan, Michael Chini, He Wang, Steve Gilbertson, Ximao Feng, and Zenghu Chang[1]

J. R. Macdonald Laboratory, Kansas State University, Manhattan, KS, 66506-2604, USA

Synopsis: Measurement of single isolated attosecond pulses suffers from low photoelectron counts in the streaked spectrogram, and is thus susceptible to shot noise. We show that the reconstructed spectrogram and attosecond pulse depend on the number of photoelectron counts at the peak of the spectrogram, and find that spectrograms with a peak count number of 50 or more can be reconstructed accurately.

Attosecond pulses can be reconstructed from a streaked photoelectron spectrogram using the CRAB (complete reconstruction of attosecond bursts) technique [1]. CRAB traces, unlike their optical FROG counterparts, suffer from low count numbers in the spectrogram. When the photon flux [2], photoabsorption probability, and efficiency of the optics and detector are considered, the number of photoelectrons detected is limited to ~1 per laser shot [3]. Maintaining high power carrier-envelope (CE) phase stabilized laser pulses over a long enough period to obtain enough counts such that shot noise is negligible is currently unachievable, and it is thus necessary to determine how many photoelectron counts are needed for accurate reconstruction of the attosecond pulse.

CRAB traces in the presence of shot noise were simulated [3]. The attosecond pulse was assumed to have a spectrum supporting a 90 as transform-limited pulse, and a linear chirp of 5000 as^2 was added. The streaking laser pulse was assumed to be 5 fs in duration with a peak intensity of 10^{12} W/cm^2. The retrieval was performed using a blind iterative algorithm.

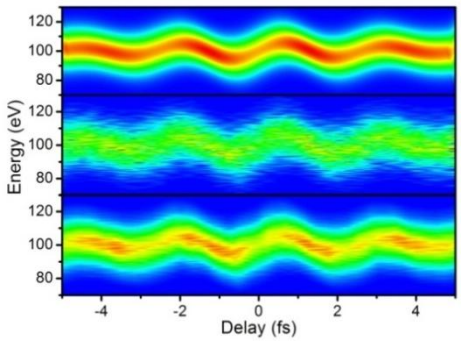

Fig. 1. Simulated CRAB traces with no noise added (top) and with shot noise (middle). Retrieved trace (bottom)

Figure 1 shows the results of the retrieval for the case when the photoelectron count at the peak of the spectrogram was 50. Clearly, the retrieved trace in Figure 1(c) matches the features of the noise-free trace in 1(a) more than the noisy trace shown in 1(b), which was given to the algorithm. In fact, for peak count numbers above 50, we found that the pulse duration and linear chirp could be retrieved within 5% of their actual values when the streaking intensity was greater than 5×10^{11}.

To further test the pulse retrieval with CRAB, experimental streaking data was used [4]. Because our data acquisition system saves the photoelectron energy spectrum recorded for each laser shot, we are easily able to select only a sample of data taken within a given time frame. By analyzing the data only from selected laser shots, we can observe what the resulting CRAB trace would be for accumulation times smaller than those used in the experiments. We found that all retrieved pulse durations for accumulation times of 4 seconds per delay step (corresponding to roughly 80 or more counts) and larger were within 5% of 141 as [3].

We have shown that shot noise has little effect on the retrieval of single attosecond pulses for traces with at least 50 photoelectron counts at the peak of the spectrogram. Such a result is significant as it suggests a lower limit to the number of counts necessary for CRAB retrieval. Due to the difficulty of maintaining CE phase stabilized laser pulses over a long period of time, this makes measurement of single attosecond pulses more accessible to laboratories without state-of-the-art lasers.

This material was supported by the U.S. Army Research Office under grant number W911NF-07-1-0475 and by the Chemical Sciences, Geosciences, and Biosciences Division, U.S. Department of Energy.

References

[1] Y. Mairesse and F. Quéré, Phys. Rev. A **71**, 011401 (2005).
[2] H. Mashiko *et al.*, Phys. Rev. A **77**, 063423 (2008).
[3] H. Wang *et al.*, J. Phys. B **42** (in press).
[4] Z. Chang, International Symposium in Ultrafast Intense Laser Science 7, Kyoto, 24-28 November 2008.

E-mail: chang@phys.ksu.edu

Generation of XUV continuum in the plateau region of high-order harmonics driven with 7fs/800nm laser pulses

Yinghui Zheng*, Zhinan Zeng*, Hui Xiong*, Yan Peng†, Xuan Yang†, Heping Zeng†, Ruxin Li*,[1], and Zhizhan Xu*,[2]

* State Key Laboratory of High Field Laser Physics, Shanghai Institute of Optics and Fine Mechanics, Chinese Academy of Sciences, Shanghai 201800, China

† Key Laboratory of Optical and Magnetic Resonance Spectroscopy of Ministry of Education, Department of Physics, East China Normal University, Shanghai 200062, China

Synopsis: We show that extreme ultraviolet (XUV) continuum in the plateau of high-order harmonics (HH) can be generated in an argon gas cell by 7fs/800nm phase-stabilized laser pulses. It is based on the successful selection of single quantum path of the returning electrons during the propagation process in the gas cell. It is promising to obtain intense isolated sub 100 attosecond pulses with subsequent amplitude and phase control of the supercontinuum ranging from plateau to the cutoff region of the HH spectrum.

Isolated attosecond pulses extracted from plateau harmonics cause matter of great concern due to its relatively high efficiency and the broad bandwidth. So far single attosecond pulse emission in the plateau region has been achieved by single-cycle linear polarized laser pulses, by a polarization gating technique and two-color field schemes. Recently, many authors put forward some robust technologies to generate isolated attosecond pulses even though a train of pulses predicted by single-atom models. In this paper, we demonstrate a new approach to generate HH continuum in the plateau using a 7fs/800nm laser pulses in the experiment, which is supported by the calculation results in our previous work [1].

Figure 1 shows the gas pressure dependence of the harmonic continuum from Ar with CEP stabilized 0.4mJ/7fs laser pulses. At a low gas pressure of 10Torr the continuum in the region from 45eV to 73eV is firstly achieved. As the backing pressure rises, the harmonics become discrete and well-resolved. Up to ~40Torr, the harmonic structures vanish and the spectra become supercontinuous over all of the recorded bandwidths from ~32eV-~73eV, including the plateau with weak modulations. When the pressure continues to increase, the spectra have clear harmonic structures again. The changing trend indicates that there is a certain optimal gas pressure to generate the supercontinuum. When gas pressure exceeds the optimal pressure, the spectra will become discrete again.

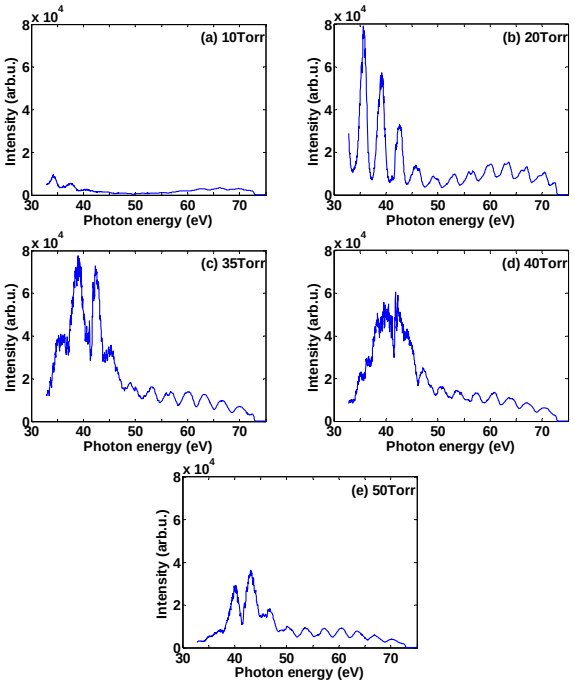

Fig. 1. Pressure dependence of the harmonic continuum from Ar with CEP stabilized 0.4mJ/7fs laser pulses.

In conclusion, a new method to obtain the HH continuum in the plateau is proposed in an argon gas cell driven by 0.4mJ/7fs laser pulses. The plateau continuum is generated by the successful selection of single quantum path of the returning electrons. It is promising to obtain isolated sub 100 attosecond pulses with subsequent amplitude and phase control of the supercontinuum ranging from plateau to the cutoff region of the HH spectrum.

References

[1] C. Liu, Y. Zheng, Z. Zeng, R. Li, and Z. Xu, Phys. Rev. A **79**, 043826 (2009).

[1] E-mail: ruxinli@mail.shcnc.ac.cn

[2] E-mail: zzxu@mail.shcnc.ac.cn

Practical Issues of Retrieving Isolated Attosecond Pulse from CRAB

He Wang, Michael Chini, Sabih D. Khan, and Zenghu Chang[1]

JRM Laboratory, Kansas State University, Manhattan, KS, 66506-2604, USA

Synopsis: The effects of streaking speed, time delay jitter, laser intensity variation and collection angle of streaked electrons on the reconstruction of isolated attosecond extreme ultraviolet (XUV) pulses from the streaked spectrogram are studied.

Single isolated attosecond XUV pulses can be characterized by a technique termed CRAB (Complete Reconstruction of Attosecond Burst) [1]. However, the experimental imperfections of CRAB traces may lead to reconstruction errors. We studied the effects of four major factors on the attosecond retrieval: the streaking speed, the time jitter between the XUV and the streaking field, the streaking laser intensity variation, and the collection angle of streaked electrons [2].

According to the Rayleigh criterion, in order to resolve a sub-100 as XUV pulse, IR laser intensity of at least $5.5\times10^{13}W/cm^2$ is required. Such a high intensity IR field can produce electrons through above-threshold ionization (ATI). When the energy of the ATI electron overlaps with that of the XUV photoelectron, it adds large background noise to the CRAB trace. When the PCGPA algorithm was used on synthetic data, it was found that even with the intensity which is two orders of magnitude smaller than that based on Rayleigh criterion, PCGPA can still retrieve XUV pulse, as shown in Fig.1.

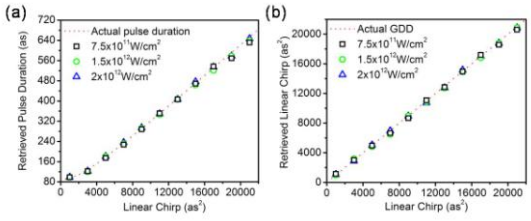

Figure 1 (a) Retrieved XUV pulse duration as a function of input linear chirp for different streaking intensities. (b) Retrieved linear chirp as a function of input linear chirp for different streaking intensities.

The IR streaking beam and XUV beam propagate through different optics. Due to mechanical vibration, the time delay between them changes from one laser shot to the next. This time delay jitter broadens the CRAB trace. In our simulation when the delay jitter goes to one quarter of the IR laser cycle, the XUV pulse duration can still be retrieved within an error of 6% and the linear chirp can be retrieved within an error of 10%. Thus, this property of the CRAB relaxes the need for tight CE phase locking and delay stability in streaking experiments.

The streaked electrons are produced in a finite volume of the gas target. The IR intensity is a function of both transverse and longitudinal positions. In our simulation even when the XUV spot size is comparable to the IR spot size at the focus, the XUV pulse duration and linear chirp can still be retrieved within an accuracy of 5%. This releases the constraint of constant streaking intensity and can easily be realized experimentally.

Due to the low photon flux and small cross section of the XUV interaction with atoms, the streaked electrons are usually collected within a certain range of solid angle. In our simulation, even when the collection angle is increased to 90 degrees, the XUV pulse duration and linear chirp can still be retrieved within an error of 5%. This property of the CRAB opens the door for detection schemes with large collection angles, such as magnetic bottle detectors and velocity map imaging.

In conclusion, four practical issues in attosecond streaking experiments were discussed when PCGPA was applied to retrieve the XUV pulse from the CRAB trace. We found that the streaking can be performed at a laser intensity level much lower than that estimated from the Rayleigh criterion, which is desirable to suppress the ATI background. The reconstruction is robust against time jitter, volume effects and large collection angle, which releases the constraints on the experiments. This material is supported by the U. S. Army Research Office under Grant No. W911NF-07-1-0475, and by the Chemical Sciences, Geosciences, and Biosciences Division, U.S. Department of Energy.

References

[1] Y. Mairesse *et al.*, Phys. Rev. A **71**, 011401(R) (2005).
[2] H. Wang *et. al. J. Phys. B* **42** (in press).

E-mail: chang@phys.ksu.edu

Accurate Retrieval of Satellite Pulses of Single Isolated Attosecond Pulses

Michael Chini, He Wang, Sabih D. Khan, Shouyuan Chen, and Zenghu Chang[1]

J. R. Macdonald Laboratory, Kansas State University, Manhattan, KS, 66506-2604, USA

Synopsis: When isolated attosecond pulses are reconstructed from an ideal streaked spectrogram, the relative intensity of accompanying satellite pulses can be identified from interference. However, the interference pattern can be distorted by variation of the streaking laser intensity in the focal volume or by the use of large delay steps in acquiring the spectrogram. We investigate these effects on the reconstruction of satellite pulses with full- and half-cycle separations and find that satellite pulses with full-cycle separation are largely unaffected by these issues.

Single isolated attosecond pulses with duration less than 300 as have been generated by several gating schemes [1, 2, 3]. However, pre- and post-pulses always accompany the main pulse, separated by a half or full cycle of the driving laser field. Accurate characterization of the relative intensity of satellite pulses is crucial for improving the pulse quality for experimental applications. Typically, attosecond pulses are measured using the near infrared (NIR) assisted streaking method. The resulting spectrogram can be analyzed using frequency-resolved optical gating (FROG) to retrieve the pulse, a technique known as CRAB (complete reconstruction of attosecond bursts) [4].

Ideally, the presence of satellite pulses can be determined from interference in the XUV spectrum. However, the NIR streaking field may influence the interference, and the trace may be distorted by experimental issues such as spatial variation of the streaking intensity within the XUV focus and limited delay resolution in the spectrogram.

In the following simulations, the streaking NIR pulse was assumed to be 9 fs in duration with a peak intensity of 10^{12} W/cm^2. The XUV spectrum was assumed to support a transform-limited pulse 90 as in duration, with satellite pulses separated by a half or full cycle of the streaking field. The pulse contrast I_s/I_m was set to be 10^{-1} or 10^{-2}, as indicated, where I_m and I_s are the peak intensities of the main and satellite pulses, respectively. A linear chirp of 5000 as^2 was added to the XUV spectrum.

To study the effect of intensity variation in the focal volume, averaged CRAB traces were created and used for retrieval. The results are shown in Figure 1(a), where w_{XUV} and w_{IR} are the $1/e^2$ radii of the XUV and NIR focal spots. As the spot size ratio is increased, the satellite pulses with full-cycle separation can be retrieved accurately, whereas those with half-cycle separation are severely underestimated. This can be explained by differences in the streaking in the two cases [5].

Similar retrieval error can be seen when the delay step size is large. The results are shown in Figure 1(b). The contrast is underestimated for satellite pulses with half-cycle separations for delay steps greater than ~100 as, whereas it is retrieved well for full-cycle separation.

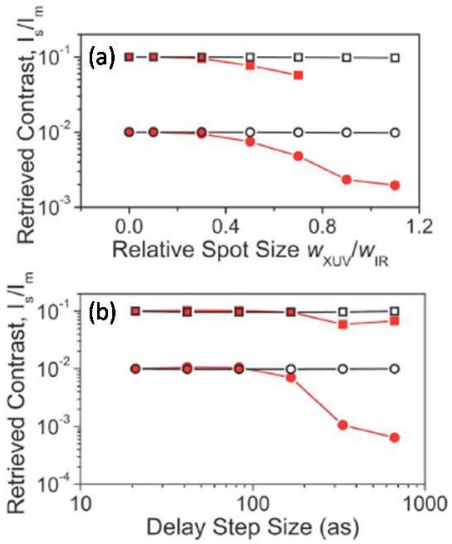

Fig. 1. Retrieved contrast as a function of (a) the spot size ratio and (b) the delay step size for full- (black open shapes) and half-cycle separation (red filled shapes).

In conclusion, we find that the retrieval of satellite pulses with full-cycle separation, as in the case of double optical gating, is largely unaffected by streaking laser intensity variation and large delay step sizes, whereas those with half-cycle separation can be severely underestimated.

This material was supported by the U.S. Army Research Office under grant number W911NF-07-1-0475 and by the Chemical Sciences, Geosciences, and Biosciences Division, U.S. Department of Energy.

References

[1] E. Goulielmakis *et al.*, Science **320**, 1614 (2008).
[2] G. Sansone *et al.*, Science **314**, 443 (2006).
[3] Z. Chang, International Symposium in Ultrafast Laser Science 7, Kyoto, 24-28 November 2008.
[4] Y. Mairesse and F. Quéré, Phys. Rev. A **71**, 011401 (2005).
[5] M. Chini *et al.*, Appl. Phys. Lett. **94**, 161112 (2009).

[1] E-mail: chang@phys.ksu.edu

Strong-field Below Threshold Harmonics

Jennifer Tate*[,1], Kenneth Schafer[†], Mette Gaarde[†]

[*] Center for Computation and Technology, Louisiana State University, Baton Rouge, LA, USA
[†] Department of Physics and Astronomy, Louisiana State University, Baton Rouge, LA, USA

Synopsis: We study the generation of below and near threshold harmonics in atomic gases, via calculations including single atom as well as macroscopic effects. Calculations in xenon indicate that the below threshold harmonics have multiple contributions, including one with a strongly intensity dependent dipole phase analogous to the well known long trajectory in above threshold high harmonic generation. We will also show preliminary results modeling absorption of the low energy harmonics in the presence of the strong IR field.

We study the production of below and near threshold harmonics excited in a gas of atoms by a short-pulse near-IR laser. Although the semi-classical model of high harmonic generation is not directly applicable to below threshold harmonics, results in xenon show that these harmonics still include a contribution with a strongly intensity-dependent dipole phase, analogous to the familiar long trajectory in above threshold harmonics [1]. Preliminary results modeling absorption of the below threshold harmonics in the presence of a strong IR field also allow us to explain the relative strengths of the harmonic orders.

Our method for calculating harmonic spectra by solving the coupled, non-adiabatic solutions of the single-atom time-dependent Schrödinger equation (TDSE) and the Maxwell wave equation for a gas of atoms is described in detail in [2]. However, the previously used approach of calculating the harmonic response via the strong field approximation (SFA) is insufficient for studying low energy harmonics where the atomic potential becomes increasingly important. We have instead developed a code which couples the solution of the wave equation to a direct numerical integration of the TDSE within the single active electron approximation [3]. This approach allows us to treat the laser electric field and the atomic potential on equal footing.

Calculations using this code in xenon with a driving wavelength of 1070 nm indicate that multiple generation processes contribute to the below and near threshold harmonics; one such process appears to be multi-photon in nature while another process is initiated by tunneling. The tunneling contribution, while strongly influenced by the atomic potential, still has an intensity-dependent phase that originates in laser-driven continuum dynamics similar to the above threshold harmonics.

The integration of the TDSE also provides information on single atom time-dependent ionization. This allows us to model the process of IR-assisted ionization due to absorption of below threshold harmonics. Figure 1 illustrates the effect this absorption has on the harmonic spectrum. In addition to studying the ionization process itself, we are able to more accurately model the relative strengths of the individual harmonics.

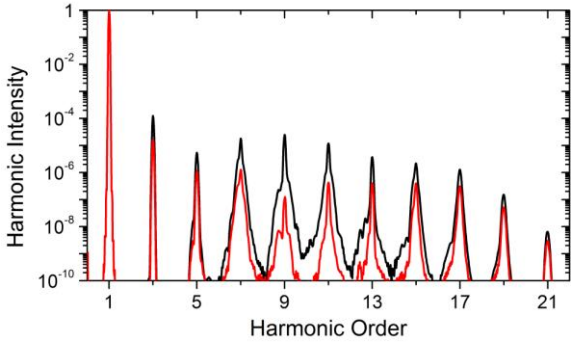

Fig. 1 (Color Figure) Harmonic spectrum in xenon with (red) and without (black) IR-assisted absorption of the harmonics.

References

[1] D. C. Yost, T. R. Schibli, J. Ye, J. L. Tate, J. Hostetter, K. J. Schafer and M. B. Gaarde, Phys. Rev. Lett., submitted (2009).
[2] M. B. Gaarde, J. L. Tate and K. J. Schafer, J. Phys. B **41**, 132001 (2008).
[3] K. J. Schafer and K. C. Kulander, Phys. Rev. Lett. **78**, 638 (1997).

[1] E-mail: jltate@phys.lsu.edu

Carrier-Envelop Offset Frequency Linewidth Narrowing Using an Intracavity Spatial Filter

Karl A. Tillman, [1] Brian R. Washburn, and Kristan L. Corwin

116 Cardwell Hall, Department of Physics, Kansas State University, Manhattan, KS, 66506-2604, USA

Synopsis: Significant carrier envelope offset frequency linewidth narrowing is observed in a self-referenced prism-based Cr:forsterite frequency comb when a knife edge is insert into the intracavity beam. The normally broad free-running linewidths (Δf_{ceo}) of ~1 MHz can be reduced by as much as an order of magnitude, and then further reduced after phase-locking to <100 Hz. A simple model has been used for comparison with the observed linewidths.

The linewidth of the carrier envelope offset frequency (Δf_{ceo}) of a stabilized frequency comb can be an indication of the total frequency noise present within the femtosecond laser. Broad linewidths indicate substantial noise and can limit the use of a frequency comb. Cr: forsterite frequency combs have been shown to possess broad linewidths. [1, 2] However because Cr:forsterite occupies a useful region of the near infrared spectrum (~1.25 μm) we have developed a self-referenced, prism-based Cr:forsterite frequency comb. During the course of its development significant Δf_{ceo} narrowing was observed when a knife edge was inserted into the intracavity beam as shown in Fig. 1. The inset in Fig. 1 shows a plot of the measured Δf_{ceo} with the comb stabilized for the case with (red) and without (black) the knife inserted.

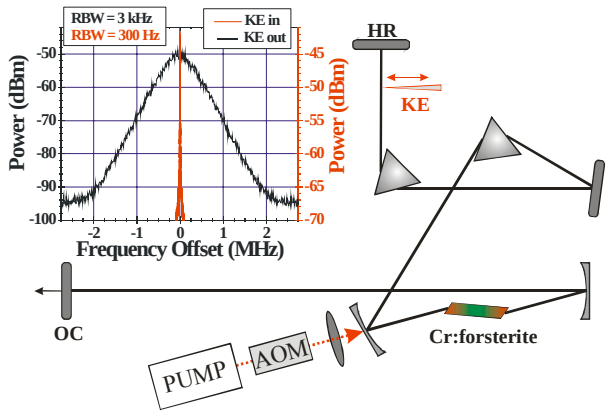

Fig. 1. Cr:forsterite cavity configuration showing the location of the knife edge (KE). HR: high reflector, OC: output coupler, AOM: acousto-optic modulator. The inset shows locked Δf_{ceo} with (red) and without (black) the knife edge inserted.

The introduction of the intracavity knife edge enabled the free-running Δf_{ceo} to be tuned through a minimum. If the comb is stabilized when Δf_{ceo} has been minimized then its locked Δf_{ceo} can be reduced to <100 Hz, implying the knife edge significantly reduces the frequency noise of the entire system.

To better understand the mechanism behind the noise reduction, a simple model for calculating Δf_{ceo} based on frequency noise was adopted [3], which is shown by Eq. 1.

$$\Delta f_{ceo} \sim \pi \left(\left(\mathrm{P} \frac{df_{ceo}}{d\mathrm{P}} \right)^2 \int_0^{f_{-3dB}} \mathrm{RIN}_I(\upsilon)\, d\upsilon \right)^{1/2} \quad (1)$$

P represents the pump laser power, df_{ceo}/dP the f_{ceo} response to pump power changes and $\mathrm{RIN}_I(\nu)$ describes the relative intensity noise on the femtosecond laser.

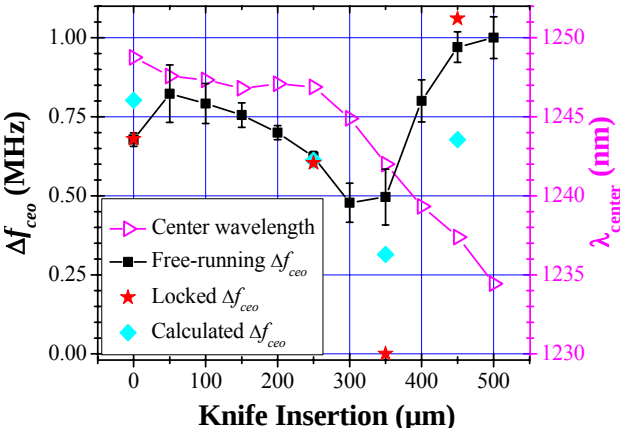

Fig. 2. Comparison between observed and calculated Δf_{ceo} plotted as a function of knife insertion

Figure 2 shows a comparison between the observed and calculated linewidths, where the free-running measurement is an upper limit and the calculated value is based on df_0/dP measured at low frequencies (~2 Hz). The locked width for the knife inserted by 350 μm represents the location of the minimum free-running linewidth and has a value of <100 Hz.

Further details will be presented including a study of the frequency dependence of df_{ceo}/dP. We believe the mechanism behind the noise reduction is related to intracavity dispersion changes caused by the knife acting as a spatial filter.

This research was supported by the AFOSR under contract No. FA9950-08-1-0020 and the NSF under contract No. ECS-0449295.

References

[1] K. Kim, *et al*, Opt. Lett. **30**, 932 (2005).
[2] R. Thapa, *et al*, in *proceedings of CLEO*, CMKK7 (2007).
[3] J. J. McFerran, *et al*, Appl. Phys. B. **86**, 219 (2007).

[1]Email: tillman@phys.ksu.edu

Conversion efficiency and scaling for high harmonic generation: an analytical approach

Edilson L. Falcão-Filho[1], **V. M. Gkortsas, Ariel Gordon and Franz X. Kärtner**

Department of Electrical Engineering and Computer Science and Research Laboratory of Electronics, Massachusetts Institute of Technology, Cambridge, MA 02139

Synopsis: Closed form expressions for the high harmonic generation (HHG) conversion efficiency are given for the plateau and cutoff regions. The results are obtained considering propagation effects, the single atom response and the single active electron (SAE) approximation. Measured absorption cross sections are used, and no parameter fitting is employed. The calculated efficiencies agree well with the experimental values published in the literature.

High harmonic generation is exciting rapidly developing field not only from the basic science enabling it, but also due to the number of promising applications involving HHG in the XUV region. Comparatively to others XUV sources, HHG is unique due to its complete spatio-temporal coherence enabling attosecond pulse generation.

In this work, applying the saddle point treatment to the dipole acceleration of the improved three step model (ITSM) [1], analytic formulas for the HHG conversion efficiencies for the plateau and the cutoff region including both laser and material parameters as well as 1D propagation effects were obtained. For fixed harmonic wavelength, a scaling for the HHG efficiency with the driving frequency of ω_0^5 at the cutoff and ω_0^6 at the plateau region were obtained. This result is in accordance with numerical simulations using the time dependent Schrödinger equation [2] which includes the single-atom response only, and with preliminary experimental results [3]. Besides the single-atom response, our derivation indicates that another major contribution to be considered in the wavelength scaling is the medium characteristics, such as, recombination amplitude, absorption cross section and phase matching. These quantities exhibit a strong wavelength dependence which has an important role if cutoff extension is the goal. As can be observed in Fig. 1(a), considering absorption limited conditions for Ne, the maximum efficiency at the cutoff shifts for different driver wavelength, but the peak does not exhibit any strong dependence with the driver wavelength, as one may expect from the scaling of the single-atom response. This behavior is also reproduced via numerical evaluation of the ITSM at constant field amplitude E_0 while varying ω_0, as shown in Fig. 1 (b). The reason for that is due to the absorption cross section of neon which decreases more than two orders of magnitude for that wavelength range.

In summary, our derived formulas simplify the HHG optimization problem and enable a complete HHG scaling analysis. Thus, we believe that the theory presented in this work can have a significant impact on the development of any HHG based EUV sources, including attosecond pulse generation.

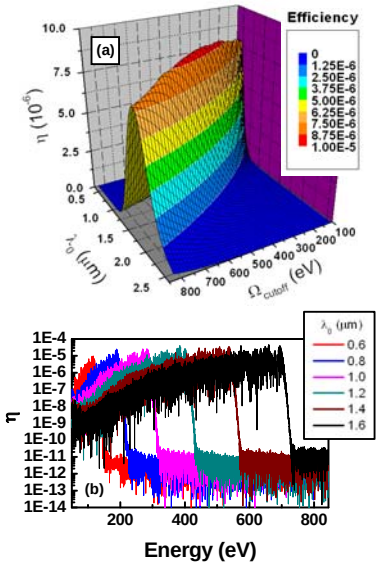

Fig. 1. (a) Neon HHG efficiency at the cutoff region, as a function of the driver wavelength, λ_0, and the cutoff energy, Ω_{cut}. (b) Full spectrum obtained considering a Gaussian pulse with $E_0 = 0.16$ a.u. for different driver wavelengths. For both cases absorption limited conditions and a 5-cycle-driver-pulse were assumed.

References

[1] A. Gordon and F. X. Kärtner, Phys. Rev. Lett. 95, 223901 (2005).
[2] J. Tate *et al.*, PRL 98, 013901 (2007).
[3] P. Colosimo *et al.*, Nature Physics 4, 386 (2008).

[1] E-mail: elff@mit.edu

Generation of CE Phase Stabilized 5 fs, 0.5 mJ, Pulses from Adaptive Phase Modulator

He Wang, Yi Wu, Michael Chini, Hiroki Mashiko and Zenghu Chang[1]

JRM Laboratory, Kansas State University, Manhattan, KS, 66506-2604, USA

Synopsis: By improving the throughput of the 4*f* system and by increasing the input laser pulse energy, milli-joule level two cycle pulses were produced with a liquid crystal spatial light modulator. The carrier-envelope phase of the two-cycle pulses was measured directly by using its over-one-octave output spectrum and stabilized by feedback controlling the grating separation of the stretcher in the chirped pulse amplifier. To the best of our knowledge, this is the first time that carrier-envelope phase locked few-cycle, milli-joule level pulses were generated by using phase modulator compressors. When the pulses were used in high harmonic generation, it was found that the harmonic spectra depended strongly on the high order spectral phases of the driving laser fields.

Few-cycle laser pulses with milli-joule level energy are crucial for attosecond pulse generation and many other strong field physics studies. So far, such pulses have been produced by compressing white light with chirped mirrors. However, the high order dispersions are not compensated resulting in poor pulse contrast. Adaptive pulse compression has been demonstrated before to generate sub-4 fs light pulses. Unfortunately, the compressed pulse energy was only 15 μJ [1], which is too low for high field applications such as high harmonic generation (HHG). We focused on resolving the pulse energy problem associated with the phase modulator pulse compressor.

The experiment was performed using the Kansas Light Source laser system. The 1.1 mJ pulse from the neon fiber covered the spectrum from 400nm to 1000 nm. By the combination of high input white light energy and high throughput, we obtained 0.5 mJ output pulse energy from the phase modulator.

We adopted the Multiphoton Intrapulse Interference Phase Scan (MIIPS) [2] to measure the spectral phase of white-light pulses. The chirp compensation was done by applying a corrective phase to the SLM. The pulse duration was measured by the Frequency Resolved Optical Gating (FROG). The retrieved pulse duration was 5.1 fs as shown in Fig. 1. We performed coherent control of high harmonic generation with such pulses by independently changing the GDD and high order spectral phases [3].

The modulator was designed to perform spectral phase correction in the range of 500nm to 1000nm. However, the light around 460nm could go through the 4*f* system by the second order diffraction of the grating, overlapped with the fundamental component of 920nm. With such an octave spanning spectrum, an *f*-to-2*f* interferometer was used to measure and stabilize the CE phase after the adaptive phase modulator. The RMS of the CE phase was 184 mrad.

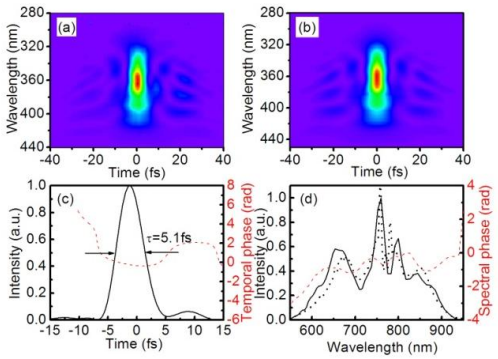

Fig. 1. Characterization of the laser pulse by the FROG. (a) The measured FROG trace. (b) The reconstructed FROG trace. (c) The retrieved pulse shape and phase (dashed curve). (d) The retrieved power spectrum (solid curve), phase (dashed curve) and independently measured spectrum (dotted curve).

In conclusion, CE phase locked, 0.5 mJ, 5fs laser pulses were generated from an adaptive phase modulator for the first time. It was found that the harmonic spectra depended strongly on the high order spectral phase. The ability to generate high energy, CE phase controllable, few-cycle pulses provides a new tool to study attosecond science and perform other coherent control experiments in high field physics. This material is supported by the U.S. Army Research Office under Grant No. W911NF-07-1-0475, and by the Chemical Sciences, Geosciences, and Biosciences Division, U.S. Department of Energy.

References

[1] B. Schenkel, et. al. *Opt. Lett.* **28**, 1987 (2003).
[2] B. Xu, et. al. *Opt. Exp*. **14**, 10939 (2006).
[3] H. Wang et. al. *Opt. Exp*. **16**, 14448 (2008).

E-mail: chang@phys.ksu.edu

Probing Doubly Excited Helium with Isolated Attosecond Pulses

Steve Gilbertson, Ximao Feng, Sabih Khan, Michael Chini, He Wang, and Zenghu Chang[1]

J. R. Macdonald Laboratory, Kansas State University, Manhattan, KS, 66506-2604, USA

Synopsis: Single attosecond pulses generated with a neon gas target were used to probe two electron excitation and autoionization in a helium gas target. By adding an intense near infrared laser beam, the population of the excited atoms in the $2s2p\,^1P^0$ state was modified in a controllable manner for the first time.

Studying the temporal evolution of electron dynamics is a main application goal of generating single isolated attosecond pulses. Helium is an especially attractive target due to interest in time resolved studies of the Fano profile [1]. When the doubly excited states are formed by using single isolated attosecond extreme ultraviolet (XUV) pulses, it was predicted that the autoionization process could be modified by intense few femtosecond near infrared (NIR) laser pulses overlapping with the XUV pulses [2]. Here we report results of the first attosecond streaking experiments on the He $2s2p\ ^1P^o$ resonance.

The experiments were conducted with a streak camera in an interferometric configuration. An 8 fs, 1mJ laser pulse was split by an 80% transmitting beamsplitter. The high power side was used for attosecond pulse generation in a neon gas target with an ellipticity modulated pulse from double optical gating [3]. This resulted in a single attosecond pulse which was then recombined with the remaining NIR laser pulse at a hole drilled mirror. The mirror transmitted the XUV and reflected the NIR to a two component annular focusing mirror. The inner mirror focused the XUV and the outer mirror focused the NIR to a second helium filled gas target. Here photoelectrons were produced by the XUV, given a momentum shift by the NIR and recorded with a time of flight detector.

Figure (a) shows an experimentally obtained streaked spectrogram with a clearly visible autoionization resonance at 34 eV. The resolution of the detector gives this peak nearly a 0.7 eV width. The streaking of the photoelectrons shows the pulse to be a single attosecond pulse and the intensity of the NIR pulse can be extracted from the degree of streaking. In this case, the NIR intensity was estimated at 5 x 10^{11} W/cm^2.

Figure (b) shows the counts of the autoionization resonance as a function of delay between the XUV and the NIR (dashed line). The decay is attributed to single ionization of the doubly excited state. Since the ionization potential from the 2s2p level is 5.2 eV, the NIR laser has sufficient intensity to deplete this level leaving the helium atom in $He^+(2s)$. The ionization probability calculated from the PPT method is indicated by the solid red line.

In conclusion, the doubly excited state of helium was studied with the attosecond streaking method.

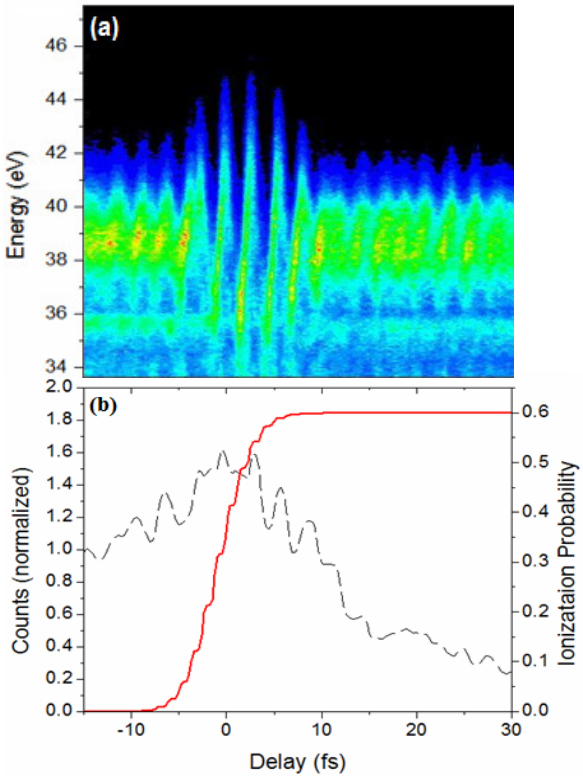

The electron dynamics were also modified by the presence of the NIR laser. The physical process described here is different than what is proposed in other numerical simulations [2, 4]. This material is supported by the U. S. Army Research Office under Grant No. W911NF-07-1-0475, and by the Chemical Sciences, Geosciences, and Biosciences Division, U.S. Department of Energy.

References

[1] M. Wickenhauser *et al*, Phys. Rev. Lett. **94**, 023002 (2005)
[2] X. M. Tong and C. D. Lin, Phys. Rev. A, **71**, 033406 (2005)
[3] S. Gilbertson *et al*, Appl. Phys. Lett. **92**, 071109 (2008)
[4] Z. X. Zhao and C. D. Lin, Phys. Rev. A, **71**, 060702 (2005)

[1] E-mail: chang@phys.ksu.edu

Double Ionization of Helium Atom in Combined Near-infrared and XUV Pulses

Shaohao Chen[1], **Andreas Becker**[2]

JILA and Department of Physics, University of Colorado, Boulder 80309-0440, USA

Synopsis We investigate the double ionization process in He atom by applying an XUV attosecond pulse in the presence of an intense near-infrared femtosecond few-cycle laser pulse. To this end, we solve the time-dependent Schrödinger equation based on a three-dimensional model. We compare the double ionization signals obtained with and without the application of the attosecond pulse.

The advent of sub-femtosecond laser technology with the generation of attosecond pulses in recent years has opened new perspectives towards observation and analysis of multi-electron dynamics in atoms and molecules[1]. For example, the correlated electron dynamics in double ionization (DI) processes of atoms induced by intense infrared femtosecond laser fields has been one of the interesting topics[2, 3].

It is well known that such dynamics can be interpreted by the rescattering mechanism [4]. According to this picture, first one electron is ionized to the continuum at a maximum of the field, then it is accelerated and driven back by the strong oscillating field, and recollides with the parent ion at about 3/4 cycle after the ionization. A few interesting topics have been established according to different pathways, that is, elastic scattering contributing to above-threshold ionization, direct non-sequential double ionization, recollision-induced excitation of the parent ion plus subsequent ionization by the field (RESI)[5], recombination to the parent ion plus high harmonic generation.

We theoretically investigate the RESI process in He atom by applying an XUV attosecond pulse in the presence of an intense near-infrared femtosecond few-cycle laser pulse. The population in excited states of He^+ ion is first pumped by the infrared laser field at the time of rescattering, then it is subsequently ionized most probably at the next maximum of the field. Therefore, there is a population and decay of ionic excited states within about a quarter of a field cycle (i.e. a few hundred attoseconds). We apply an XUV attosecond pulse during this period of time to ionize and probe the excited populations.

To this end, we solve the time-dependent Schrödinger equation by the Crank-Nicholson method, based on a three-dimensional model for He atom in linearly polarized laser fields [2], in which the center-of-mass motion of the two electrons is restricted to the field direction, while the electron correlation is fully retained via the relative coordinate of the electrons. An 800 nm near-infrared femtosecond laser pulse (5×10^{14} W/cm^2) and a 70 nm XUV attosecond pulse (1×10^{14} W/cm^2) both polarized along the same direction with various time delays are used in our calculations. Comparing the DI probabilities induced by the femtosecond pulse only and by the femtosecond pulse plus the attosecond pulse, we observe some new interesting DI signals arising from the excited states of He^+ ion due to the attosecond pulse. We also obtain the correlated momentum and energy spectra of the two ionized electrons at the end of the attosecond pulse, and analyze the relationship between these spectra and the excited structures of He^+ ion.

References

[1] F. Krausz and M. Ivanov, Rev. Mod. Phys. **81(1)**, 163 (2009).

[2] C. Ruiz et al., Phys. Rev. Lett. **96**, 053001 (2006).

[3] A. Staudte et al., Phys. Rev. Lett. **99**, 263002 (2007).

[4] P.B. Corkum, Phys. Rev. Lett. **71**, 1994 (1993).

[5] B. Feuerstein et al., Phys. Rev. Lett. **87**, 043003 (2001).

[1]E-mail: shaohao@jilau1.colorado.edu
[2]E-mail: andreas.becker@colorado.edu

Multi-color attosecond control of single ionization

J. V. Hernández[1], **B. D. Esry**[2]

J. R. Macdonald Laboratory, Kansas State University, Manhattan, KS, 66506-2604, USA

Synopsis We present the results of *ab initio* 6-D calculations of atomic He in intense laser fields. In particular we investigate the effect of a delay between an infrared field and an attosecond pulse train on single ionization. By casting the combined electric field of the infrared and attosecond pulse train in terms of multiple colors, an analytic framework is developed to interpret the numerical results.

At the heart of atomic and molecular physics is the motion of bound electrons. Since the relevant time scale for movement of an electron wavepacket between energy levels in atoms and molecules is on the order of a few atomic units (1 a.u. $\approx$ 24 as), detailed experimental studies on electron motion require forces that act on such time scales. With such ultra-fast forces, the avenue for control of the electron dynamics is opened up. When synchronized to an infrared field, attosecond-scale UV pulses which occur every IR period can provide such quick forces, and therefore the possibility of macroscopic control of electronic dynamics.

Because an attosecond pulse is often produced via high harmonic generation, the resultant attosecond pulse train (APT) will contain a large of harmonics of the fundamental frequency of an intense IR laser. With selective filtering, a specific range of harmonics can be isolated and used to illuminate the target. Control is exercised by varying the delay between the APT and IR field on a tens-of-attoseconds scale. The experimental demonstration of control of ionization probability using this method has been realized [1], as well as control of the angular distribution of the ionized electrons [2, 3].

In this work we account for the observed modulation in the ion yield of helium in an IR+APT field with respect to delay with an analytic framework verified by fully time-dependent 6-D calculations. Toward this end, we recast APT+IR experiments in terms of a many-color control problem. By employing a Floquet-like approach [4, 5], the control parameter (the delay between colors) is analytically separated from the wavefunction. This picture also gives us the ability to remove all of the time-dependence from the Hamiltonian other than the relatively slowly-varying envelopes of the pulses.

Our nonperturbative, *ab initio*, 6-D calculations utilize the adiabatic hyperspherical representation. This approach is appealing because it requires no modeling for helium — it is a full two-electron calculation and can be made exact by increasing the number of included channels. Another benefit of this approach is the natural incorporation of singly-excited states and their effect on ionization.

Ultimately, the solution to the time-dependent Schrödinger equation and the analysis of observed phenomena boils down to using dipole selection rules, energy conservation, and counting photons. Using these natural ideas, the attosecond control of single-ionization can be explained by the interference between various photon pathways. While we examined the APT+IR on helium experiments, our picture is general enough to analyze any system that uses the delay between different harmonics as a control mechanism.

This work is supported by the Chemical Sciences, Geoscience, and Biosciences Division, Office for Basic Energy Sciences,Office of Science, U.S. Department of Energy.

References

[1] P. Johnsson, J. Mauritsson, et al., Phys. Rev. Lett. **99, 233001** (2007).

[2] O. Guyétand, M. Gisselbrecht, et al., J. Phys. B: At. Mol. Opt. Phys **38, L357** (2005).

[3] O. Guyétand, M. Gisselbrecht, et al., J. Phys. B: At. Mol. Opt. Phys **38, L357** (2008).

[4] V. Roudnev and B. D. Esry, Phys. Rev. Lett. **99, 220406** (2007).

[5] J. J. Hua and B. D. Esry, J. Phys. B: At. Mol. Opt. Phys **42, 085601** (2009).

[1] E-mail: chuy@phys.ksu.edu
[2] E-mail: esry@phys.ksu.edu

Attosecond photoionization of a coherent superposition of bound and dissociative molecular states: effect of nuclear motion

Szczepan Chelkowski[*,1], **André D Bandrauk**[*], **Paul B Corkum**[2,3], **Jörn Manz**[4], **and Gennady L Yudin**[*,3]

[*] Laboratoire de Chimie Théorique, Faculté des Sciences, Université de Sherbrooke, Sherbrooke, Québec J1K 2R1, Canada, [2] University of Ottawa, Ottawa, Ontario K1N 6N5, Canada, [3] National Research Council of Canada, Ottawa, Ontario, K1A 0R6, Canada, [4] Institut für Chemie und Biochemie, Freie Universität Berlin, Takustr.3, 14195 Berlin, Germany

Synopsis We study numerically the possibility for monitoring electron motion in a dissociating molecule using an attosecond XUV probe pulse which photoionizes a coherent superposition of two nuclear wave packets prepared using a femtosecond pump pulse. We present the photoelectron spectra and forward-backward asymmetries in these spectra obtained from a numerical solution of the time-dependent Schrödinger equation.

Ultrashort flashes of light allow us to take snapshots of microscopic structures and let us to reconstruct their motion. Recently, pulses as short as 80 attoseconds have been obtained [1]. At such time scale monitoring the electron motion becomes in principle possible. A simplest scheme allowing to watch the electron motion inside the atom using two laser pulses [2, 3] relies on the preparation of the coherent two bound electronic states (e.g. 1s+2s or 1s+$2p_0$ states of the hydrogen atom) followed by an attosecond pulse which photoionizes the atom. Measuring the photoionization signal as function of the time-delay between two pulses allows to "watch" the oscillating electron.

Recently, we have investigated such schemes for monitoring the electron motion in H_2^+ at a fixed internuclear distance R [4, 5]. We found that in the case when both states have the opposite parity (like 1s and $2p_0$ states in the hydrogen atom) a particularly convenient way for watching those structures is via the measurement of the photoelectron asymmetries as function of the pump-probe delay time, which is a normalized difference between the photoelectron signal for the momentum $\mathbf{p}$ and $-\mathbf{p}$.

All previous theoretical studies (except [6]) of attosecond photoionization of a coherent superposition in molecules were restricted to the molecules fixed at a internuclear distance R and the preparation stage using pump pulse was not included in the dynamics at all. We include the nuclear motion in both stages, i.e. in the preparation of the superposition and in photoionization, by solving numerically the time-dependent Schrödinger equation (TDSE) for a molecular ion H_2^+ in 1-D interacting with both the pump and the probe pulse. More specifically, we consider two cases of coherent superpositions, case (I): initial vibrationial bound state superposed on a dissociative upper state prepared with a resonant pump pulse and case (II): a superposition of two dissociating wave packets prepared by two pump pulses. We show that the asymmetries in photoelectron spectra in both cases exhibit oscillations as function of the time delay between XUV probe and the pump pulse, as expected from the model with fixed nuclei. In case (I), the oscillations disappear when the dissociating wave packet looses the overlap with the initial state. In case (II), if one achieves the synchronization of the movement of two dissociating overlapping wave packets (using two laser pump pulse), the oscillations persist for much longer time delays than in case (I) despite the fast nuclear motion in the H_2^+ molecule.

[1] E-mail: S.Chelkowski@usherbrooke.ca

References

[1] E. Goulielmakis, *et al.*, Science **320**, 1614 (2008).

[2] F. Krausz, Phys.World, **14**, 41 (2001)

[3] A. Scrinzi, M. Geissler, and T. Brabec, Las. Phys. **11**, 169 (2001).

[4] A.D. Bandrauk, S. Chelkowski, and H.S. Nguyen, Int. J. Quant. Chem. **100** 834 (2004).

[5] S. Chelkowski , Yudin G L and A.D. Bandrauk, J. Phys. B **39**, S409 (2006).

[6] Gräfe S, Engel V and Ivanov M Yu 2008 Phys. Rev. Lett. **101** 103001 (2008).

Tomographic measurement of 3D ion velocity distributions from rotationally cold molecules using a kHz VMI spectrometer

Xiaoming Ren, Varun Makhija, and Vinod Kumarappan[1]

J. R. Macdonald Laboratory, Kansas State University, Manhattan, KS 66506, USA

Synopsis: We measure a series of 2D velocity map images of I^+ fragments from laser-aligned iodobenzene and use a filtered back-projection algorithm to reconstruct the full non-cylindrical 3D ion velocity distribution. The use of tomography in VMI is not restricted to any particular symmetry of the velocity distribution.

The use of velocity map imaging [1] to measure 2D projections of 3D ion/electron momentum distributions has found increasingly wide application due to the ease of use and rapid data acquisition rates. VMI is most often used in experiments where cylindrical symmetry in the momentum distribution allows the use of Abel inversion to reconstruct the full 3D distribution. We overcome this constraint on the symmetry of the distribution by measuring a series of 2D projections along different directions in the plane of polarization (the laser polarization vector is rotated to do this), and reconstruct the 3D distribution using a filtered back-projection algorithm.

The method will be demonstrated for non-adiabatically aligned iodobenzene. The molecules are aligned with a linearly-polarized pump pulse, and a probe pulse polarized perpendicular to the alignment axis produces I^+ fragments. Tomographic reconstruction the 3D velocity distribution demonstrates the effect of probe selectivity on the measurement of alignment from 2D projections ($\langle\cos^2\theta_{2D}\rangle$), and makes it possible to measure the 3D value of $\langle\cos^2\theta\rangle$ from a slice of the 3D distribution (the probe applies no torque on the molecules and has no angle selectivity in the v_y=0 plane (Figure 1(a)).

The VMI spectrometer uses a fast phosphor, a CMOS camera and a multi-processor workstation to determine the position of each ion hit with sub-pixel resolution on a shot-to-shot basis at 1 kHz. The fast data acquisition rate allows the 3D measurement to be completed in a reasonable amount of time. A kHz supersonic valve provides a rotationally cold molecular target for laser-induced alignment experiments.

Tomographic reconstruction of 3D momentum distributions should be widely applicable because it can be used for a completely general velocity distribution. It also requires no modifications to a standard VMI spectrometer, only the ability to rotate the velocity distribution in space by simultaneously rotating all the laser polarizations in a collinear setup. The requirement that the VMI electric field doesn't influence the distribution is a potential limitation (for instance, the field might be strong enough to orient the molecules [2]).

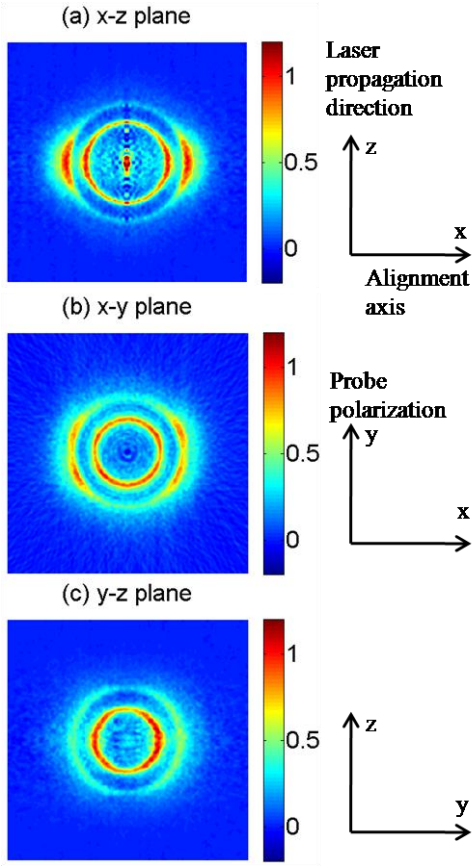

Figure 1: Three representative orthogonal slices of 3D I^+ ion velocity distribution.

References:

1. Andre T. J. B. Eppink and David H. Parker, Review of Scientific Instruments **68**, 3477-3484 (1997).
2. L. Holmegaard *et al.*, PRL **102**, 023001-4 (2009).

[1] E-mail:vinod@phys.ksu.edu

Controlling the Double Photoionization Dynamics of Li Atoms by Optical Pumping

G. Zhu*, J. Steinmann*, M. Schuricke*, J. Albrecht*, A. Dorn*[1] I. Ben-Itzhak⋆, T.J.M. Zouros§, J. Colgan†, M.S. Pindzola‡, and J. Ullrich*

*Max-Planck-Institut für Kernphysik, Heidelberg, D-69029, Germany
⋆J.R. Macdonald Laboratory, Physics Department, Kansas State University, Manhattan, KS 66506, USA
§Dept. of Physics, Univ. of Crete, P.O. Box 2008, 71003 Heraklion, Crete, Greece
†Los Alamos National Laboratory, Los Alamos, NM 87545, USA
‡Department of Physics, Auburn University, Auburn, AL 36849 USA

Synopsis Double photoionization (DPI) of lithium atoms in a magneto-optical trap by 85 eV and 91 eV photons from the Hamburg Free Electron Laser (FLASH) is investigated using cold target recoil ion momentum spectroscopy. For ejection of a $1s$ and the optically excited $2p$ electron we demonstrate that the DPI cross section significantly depends on the alignment of the $2p$ valence orbital. Thus, the dynamical electron-electron correlation can be manipulated giving insight into the DPI mechanisms close to threshold.

With the goal to perform kinematically complete double and triple ionization studies on lithium we have set up a new apparatus implementing a magneto-optical trap for Li atoms into a Reaction Microscope (MOTREMI) capable of multi-particle imaging. Thus, in combination with ultra-intense free electron lasers, fully differential studies of photon-induced triple ionization of Li with tiny cross section of several barns and even below will become possible in future.

This pilot work on DPI of Li was performed at FLASH, which delivered VUV photon pulses with duration about 30 fs and up to 10^{12} photons per pulse. Our setup allowed for the preparation of the target initial electronic state by optical pumping and, for the first time, this was demonstrated to be used to control the DPI dynamics. With a linearly polarized laser beam on the transition $\mathrm{Li}(2s\,^2S_{1/2}) \rightarrow \mathrm{Li}(2p\,^2P_{3/2})$ a fraction of about 45% of the atoms could be excited and aligned along the laser polarization. Besides single ionization, the subsequent FLASH pulse initiated double ionization involving one of the two $1s$ electrons and the valence electron.

Interestingly, the DPI cross section sensitively depends on the spatial alignment of the $2p$ excited initial state. This could be understood intuitively as illustrated in Fig.1: DPI should be more likely if the $2p$ orbital is parallel to the $1s$ dipole emission pattern, since the electron-electron interaction is stronger compared to the perpendicular alignment. Preliminary theoretical calculations confirm this assertion. Thus, just by modifying the geometry of the system without changing its internal energy, a two-electron process is strongly influenced via dynamical electron correlation.

[1]E-mail: dornalex@mpi-hd.mpg.de

Even more compelling is the observation, that this alignment sensitivity decreases as the photon energy increases. It demonstrates that this effect is not enforced by symmetry, but rather is a subtle dynamical correlation which seems to be more effective towards the double ionization threshold.

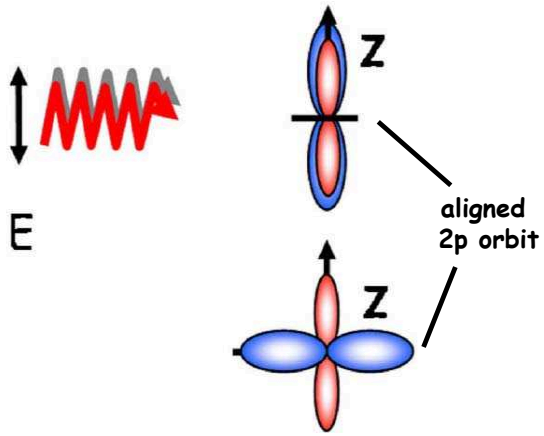

Fig. 1. Schematic of the DPI process, showing that the lithium target is initially prepared with different spatial alignments of the laser excited $nl = 2p$ orbital (blue lobes) relative to the indicated FEL polarization (E), and the dipole emission pattern of the ionized $1s$ electron (red lobes).

In future, combining the upcoming Stanford Linac Coherent Light Source (LCLS) with MOTREMI, will enable to trace the non-linear correlated many-electron quantum dynamics, e.g. in sodium atoms. This novel super-brilliant x-ray source providing photon energies in the keV regime will allow to investigate many phenomena as multiple photon absorption, electron delocalization, and ultra-fast electronic rearrangement of the electronic shell.

Controlling the Vibrational and Dissociation Dynamics of the Hydrogen Molecular Ion with Intense Infrared Laser Pulses

T. Niederhausen[*,1], **U. Thumm**[†2], **F. Martín**[*,3],

[*]Departamento de Química C-9, Universidad Autónoma de Madrid, 28049 Madrid, Spain
[†]James R. Macdonald Laboratory, Kansas State University, Manhattan, KS 66506-2604, USA

Synopsis Using intense infrared laser pulses, we provide theoretical results for controlling the bound vibrational dynamics, the dissociation process and ionization of the hydrogen molecular ions H_2^+ and D_2^+.

The time–resolved imaging of the vibrational dynamics of the hydrogenic molecular ions H_2^+ and D_2^+ has seen great interest over the last decade, and became directly observable in the time domain using ultra–short laser pulses [1]. In particular, the time–dependent kinetic energy release of time–series pump–probe studies has been utilized to reveal intrinsic characteristics of the vibrating wave packet, such as laser induced potential curves, and the vibrational state distribution using internuclear–distant dependent Fourier analysis [2]. Moreover, the addition of one or more precisely timed ultra–short control laser pulses has been shown to be a suitable way to selectively manipulate the vibrational state distribution of the molecular ion and to direct the dissociation pathway [3].

In addition to our previous studies [2, 3] which were limited to the motion of the nuclear wave packet on the coupled $1s\sigma_g^+$ and $1s\sigma_u^+$ adiabatic potential curves of the molecular ion, we now explicitly include all electronic degrees of freedom to account for non Born–Oppenheimer (BO) effects and the electronic interaction with the intense laser field. We restrict the nuclear motion to the internuclear separation and assume alignment of the molecule along the electric field vector of the laser pulse. Taking advantage of the cylindrical symmetry for the electronic motion, we solve the resulting three–dimensional Schrödinger equation on a numerical lattice using the split–operator Crank – Nicolson scheme for the time propagation.

By projecting the propagated wave function $\psi(R,\vec{r},t)$ onto the lowest few eigenvectors $\psi_\nu(R,\vec{r})$ of the full Hamiltonian after the external interaction has stopped $t > t_0$, we obtain the probabilities

$$P_\nu(t) = \Big| \langle \psi_\nu(R,\vec{r}) | \psi(R,\vec{r},t) \rangle \Big|^2,$$

of finding the system in the ν-th bound molecular state (i.e. a non-BO state, described by the combined nuclear and electronic motion). The Fourier transform of the autocorrelation function

$$a(t) = \Big| \langle \psi(R,\vec{r},t_0) | \psi(R,\vec{r},t) \rangle \Big|^2,$$

for $t > t_0$ provides the kinetic energy spectrum of the dissociating nuclei and the ejected photoelectrons [4].

We show results for a series of infrared (800 nm), intense ($\sim 10^{14}$ W/cm^2), femtosecond laser pulses. The first pulse launches a vibrational wave packet from the neutral molecule, and the precise timing of the subsequent control laser pulses allows for the directed manipulation of the bound vibrational state composition and the dissociation dynamics of the ion. We will address the influence of the laser parameters (wavelength, intensity, pulse length) on the extent of controlling the vibrational dynamics of the ion, and compare with previous model calculations [3].

References

[1] Th. Ergler *et al.*, Phys. Rev. Lett. **97**, 193001 (2006).

[2] B. Feuerstein *et al.*, Phys. Rev. Lett. **99**, 153002 (2007); U. Thumm, T. Niederhausen, and B. Feuerstein, Phys. Rev. A **77**, 063401 (2008).

[3] T. Niederhausen and U. Thumm, Phys. Rev. A **77**, 013407 (2008).

[4] L. B. Madsen *et al.*, Phys. Rev. A **76**, 063407 (2007).

[1]E-mail: thomas.niederhausen@uam.es
[2]E-mail: thumm@phys.ksu.edu
[3]E-mail: fernando.martin@uam.es

Two-center interference and nuclear motion effects in molecular harmonic generation

Ciprian C. Chirilă[*,†] [1], **Manfred Lein**[*,†]

[*]University of Kassel, Institute of Physics, Heinrich-Plett Straße 40, 34132 Kassel, Germany
[†]Leibniz Universität Hannover, Institut für Theoretische Physik, Appelstraße 2, 30167 Hannover, Germany

Synopsis The momentum spread of the returning electron in molecular high-harmonic generation (HHG) influences the harmonic phase near the two-center interference minimum [1]. We investigate this effect using the strong-field approximation. Furthermore, we study effects of nuclear motion by simulating HHG in one-dimensional vibrating H_2 molecules irradiated by laser pulses with different wavelengths. The presence of two-center interference is confirmed. We show that the ratio of harmonic signals from the isotope pair H_2/D_2 can be satisfactorily reproduced by a simple semiclassical model [2]. The validity of the one-electron picture in the two wavelength regimes is established.

Atoms or molecules irradiated by intense laser fields undergo highly nonlinear processes that result in high-order harmonic generation (HHG) in the extreme ultraviolet (XUV) range. The physical picture is well explained by the three-step model [3]: laser-induced ionization takes place, followed by the active electron being accelerated by the laser field. In the final step, the electron returns to the atomic/molecular core where it recombines and releases an XUV photon. HHG from molecules is particularly interesting due to the presence of additional degrees of freedom compared to atoms: the multi-center nature, the nuclear vibration, or the molecular rotation.

In the usual picture of the HHG process, the harmonic frequency determines the momentum of the returning electron. Due to the multi-center nature of the molecule, under certain conditions, destructive interference takes place [1].

Around the minimum, the harmonic phase exhibits a jump, but this rapid variation has a certain width. We study the influence of the momentum spread of the returning electron on this width. Within the usual strong-field approximation model [4], the returning electron is described as a plane wave. The recombination matrix element is zero at the two-center interference minimum, implying a phase jump.

However, taking into account the momentum spread can explain the smoothness of the phase variation. The predicted width is bigger than that due to Coulombic effects in the case of a returning electron with fixed momentum.

We solve the time-dependent Schrödinger equation fully numerically for a one-dimensional vibrating H_2 molecule in a strong laser field. To emphasise the effects of the nuclear vibration, we calculate the ratio of the harmonic signals for the D_2/H_2 isotope pair. We employ 800 nm and 1500 laser wavelength.

The ratio clearly shows the two-center interference effect [1]. Moreover, the ratio is satisfactorily predicted at both wavelengths by an intuitive semiclassical model [2] based on classical trajectories and the vibrational wave-packet motion in the molecular ion.

We show that HHG at 800 nm is in essence a one-electron process. In contrast, for 1500 nm wavelength, the interaction of both electrons needs to be taken into account, the single-active electron picture becoming inadequate.

References

[1] M. Lein *et al.*, Phys. Rev. Lett. **81**, 183903 (2002).

[2] Supporting online material, S. Baker *et al.*, Science **312**, 424 (2006).

[3] P. B. Corkum, Phys. Rev. Lett **71**, 1994 (1993).

[4] M. Lewenstein *et al.*, Phs. Rev. A **49**, 2117 (1994).

[1]E-mail: chirila@itp.uni-hannover.de

Highlighting the role of dipole matrix elements in strong field molecular dissociation: vibrational suppression in H_2^+

M. Zohrabi, F. Anis, J. McKenna, B. Gaire, Nora G. Johnson, K. D. Carnes, B. D. Esry and I. Ben-Itzhak [1]

J R Macdonald Laboratory, Physics Department, Kansas State University, Manhattan, KS, 66506, USA

Synopsis H_2^+ in an intense laser field shows stabilization against dissociation. We show that this stabilization can trivially be caused by the dipole matrix element coupling, without the need to summon other complex strong-field mechanisms such as vibrational trapping.

Typically, high vibrational (v) states of H_2^+ dissociate easily when exposed to an intense laser field by the absorption of one photon. Calculations, however, indicate that under the right laser conditions H_2^+ displays a counterintuitive stabilization against dissociation, e.g. [1]. A mechanism used to explain this stabilization phenomenon is vibrational trapping where an H_2^+ wavepacket is momentarily trapped in a laser-induced potential well — sheltering the H_2^+ population from dissociation.

At this conference we raise awareness of an alternative source of dissociation suppression, resulting from merely the amplitude of the H_2^+ dipole matrix elements that show a strong v dependence. Importantly, we find that the dipole matrix elements can explain some stabilization phenomena that had previously been interpreted by invoking the elaborate trapping mechanism.

Figure 1 demonstrates the H_2^+ suppression from its dipole matrix elements. Panel (a) shows the H_2^+ dissociation probability P_D for each v state calculated by solving the three-dimensional time-dependent Schrödinger equation (TDSE) for 45 fs, 4×10^{12} W/cm^2 pulses at 395 nm. For comparison the result from first order time-dependent perturbation theory (scaled) is also shown. Clear dips in P_D are observed for v=7, 9 and 10. These dips appear in the Franck-Condon averaged kinetic energy release (KER) distribution in Fig. 1(b) near 2.1, 2.4 and 2.6 eV, respectively.

Using a coincidence three-dimensional momentum imaging technique that we have developed in conjunction with a crossed laser–ion-beam experimental setup, we are able to observe this suppression effect as evident in the experimental KER distribution in Fig. 1(d), for 40 fs, 3×10^{13} W/cm^2, 395 nm pulses. By a fitting procedure, we retrieve the relative $P_D(v)$ values as plotted in Fig. 1(c) and obtain qualitative agreement with the theory, shown in Fig. 1(a), confirming the role of the H_2^+ dipole matrix element suppression in its intense-field dynamics.

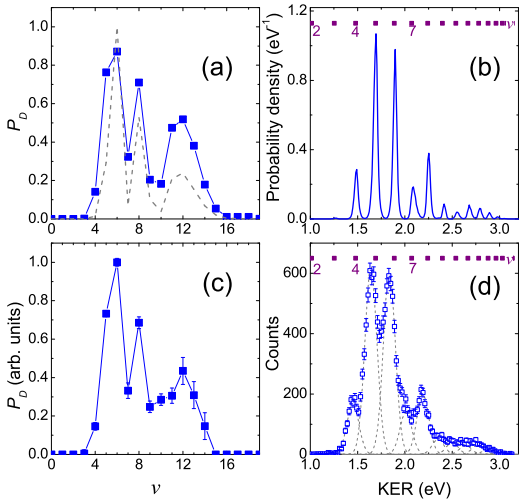

Fig. 1. (a) Calculated $P_D(v)$ of H_2^+ (points: TDSE calculation; dashed curve: perturbation theory), and (b) corresponding Franck-Condon averaged KER distribution. (c,d) same as (a,b) but experimental. For laser conditions, see text.

This work was supported by the Chemical Sciences, Geosciences, and Biosciences Division, Office of Basic Energy Sciences, Office of Science, U.S. Department of Energy.

References

[1] A. Giusti-Suzor and F. H. Mies, Phys. Rev. Lett. **68**, 3869 (1992)

[1] E-mail: ibi@phys.ksu.edu

Strong-field dynamics of a one-dimensional H_2^+/H_2 model molecule

C. B. Madsen[*,†,1], **F. Anis**[†], **J. J. Hua**[†] **and B. D. Esry**[†,2]

[*]Lundbeck Foundation Theoretical Center for Quantum System Research, Department of Physics and Astronomy, University of Aarhus, 8000 Aarhus C, Denmark

[†]J. R. Macdonald Laboratory, Kansas State University, Manhattan, KS, 66506-2604, USA

Synopsis We investigate the dynamics of one-dimensional (1D) H_2^+ and H_2 model molecules in a strong laser field. In the case of H_2^+ we produce momentum distributions to compare with state-of-the-art experiments that resolve the kinetic energy release (KER) spectra. For H_2 our main objective is to study the validity of various approximations, employed in three-dimensional (3D) calculations, by comparing our full 1D model to the 1D analogs of such approximations.

Technological advances have enabled experimentalists to measure 3D momentum distribution of both electrons and ions for ionization of molecules by short instense laser pulses. It remains a challenge, however, to perform theoretical calculations for ionization of even the simplest molecule, H_2^+. Despite several results on the solution of the time-dependent Schrödinger equation (TDSE) within reduced dimensionality models, the calculation of physical observables such as energy or momentum distributions has rarely been accomplished. To address this point, we resolve the previously presented [1] total energy spectra (Fig. 1) by calculating accurate momentum distributions for $p + p + e$.

To investigate the dynamics of H_2^+ in a strong laser field, we use a 1D model with a soft-core Coulomb interaction between the charged particles. We take the soft-core to be a function of the internuclear distance, so that the model system reproduces the true ground state Born-Oppenheimer (BO) potential curve. By comparing our results for dissociation to full 3D calculations, we can estimate to what extent the parametrized soft-core potential actually provides an improvement over the usual 1D model Coulomb potential with fixed soft-core parameters.

For the treatment of H_2, approximations such as the BO approximation, reduced dimensionality for the electrons and the single-active-electron approximation are tested. By generalizing our parametrized soft-core potential to the case of H_2 [2], we will investigate the validity of the various approximate treatments of ionization of H_2 in 3D by comparing the 1D analogs with our full 1D H_2 solution. Also, the restriction to 1D allows us to include all electronic and nuclear degrees of freedom, and, thus, to study the interplay between vibrational motion and single or double ionization.

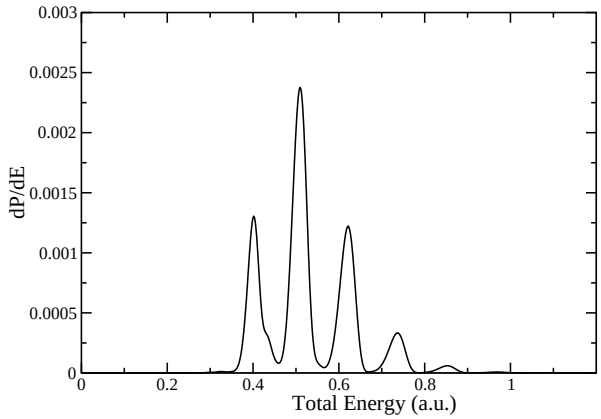

Fig. 1. The total ionization probability for H_2^+ as a function of the total energy (electron plus nuclei) for a 400 nm, 5 fs laser with peak intensity 10^{14} W/cm^2.

This work is supported by the Chemical Sciences, Geosciences, and Biosciences Division, Office of Basic Energy Sciences, Office of Science, U.S. Department of Energy.

References

[1] J. J. Hua and B. D. Esry, Bull. Am. Phys. Soc. **52**, 47 (2007)

[2] S. Saugout et al., Phys. Rev. A **98**, 253003 (2007)

[3] V. Roudnev and B. D. Esry, Phys. Rev. A **71**, 013411 (2005)

[4] M. Lein et al., Phys. Rev. A **65**, 033403 (2002)

[1]E-mail: cbm@phys.au.dk
[2]E-mail: esry@phys.ksu.edu

Strong-field ionization of aligned molecules

M. Abu-samha[*, 1], **L. B. Madsen**[† 2],

The Lundbeck Foundation Theoretical Center for Quantum System Research,
Department of Physics and Astronomy, Aarhus University, 8000 Aarhus C, Denmark.

Synopsis A framework for studying strong-field ionization of aligned molecules is presented, and alignment-dependent ionization yields are computed for CO_2 and CS_2. Our calculations are in unprecedented agreement with recent experiments, and explain the breakdown of the molecular tunnelling theory and strong-field approximation.

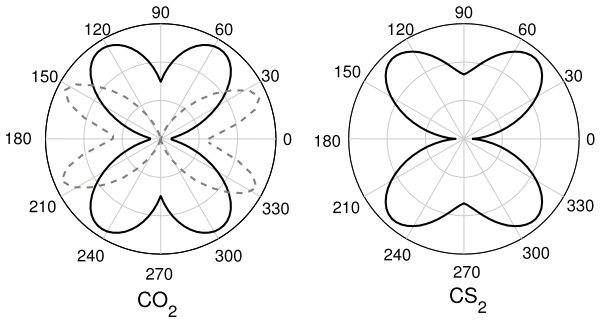

Fig. 1. Ionization yields as a function of the angle β for CO_2 and CS_2. The solid (dashed) line denotes our TDSE (MO-ADK) calculations.

Theoretical studies of strong-field ionization of molecules are impeded by the complexity of the molecular electronic structure. Up till now, full *ab initio* calculations of the alignment-dependent ionization are available only for H_2^+ and H_2. For larger molecules, despite a tremendous amount of experiments, no *ab initio* calculations are available, and the most widely used approaches to explain strong-field processes are the molecular tunneling theory and strong-field approximation. Calculations of alignment-dependent ionization yields based on these theories fail to explain recent experiments: Tunneling theory and strong-field approximation predict the ionization yield to follow the electron density of the initial electronic state, in contrast with observations for the CO_2 molecule. [1]

In [2], we use *ab initio* theory within the single-active electron approximation to investigate the response of polyatomic molecules to intense femtosecond laser pulses. Our approach is grid based, which is the most widely used approach in strong-field physics, and takes input potentials from standard quantum chemistry codes. We only consider the dynamics of the outermost electron (the HOMO orbital): the remaining electrons are accounted for by an effective potential.

The computed ionization yields are shown in Fig. 1 for CO_2 and CS_2 as a function of the angle β. The orientation-dependencies of ionization are generally similar for the two molecules. For CO_2 and CS_2, the ionization yields are largest at $54\pm3°$ and $48\pm3°$, respectively. These results are in unprecedented agreement with recent experiments [1], which predict the ionization yields to peak at about 46°. Our approach is clearly superior to the tunneling theory (cf. the figure) and the strong-field approximation (results not shown here) which predict the ionization yields for CO_2 to peak at about 25°.

References

[1] D. Pavičić, K. F. Lee, D. M. Rayner, P. B. Corkum, and D. M. Villeneuve, Phys. Rev. Lett. **98**, 243001 (2007).

[2] M. Abu-samha and L. B. Madsen (Submitted for publication).

[1]E-mail: mahmoud@phys.au.dk
[2]E-mail: bojer@phys.au.dk

Ionization, dissociation, and Coulomb explosion of H_2 in intense laser fields: A theoretical study based on moving-grid approach in phase space

Zhongyuan Zhou[1] **and Shih-I Chu**[2]

Department of Chemistry, University of Kansas, Lawrence, KS, 66045, USA

Synopsis: A moving-grid approach based on coupled coherent states and classical trajectories is developed for the study of dynamics of polyatomic molecules in intense laser fields. In this approach, the initial state and trajectories are determined by solving the imaginary time-dependent Schrödinger equation using diffusion Monte Carlo method. The wave function is then calculated by propagating the initial state on the moving grids guided by the classical trajectories. This approach has been applied to study ionization, dissociation, and Coulomb explosion of H_2 in intense laser fields as a demonstration.

Ab initio calculation based on fully quantum mechanical approach is still a challenge for the study of dynamics of polyatomic molecules in intense laser fields due basically to the huge numbers of configurations involved. This difficulty may be conquered by using a moving-grid approach based on couple coherent states in phase space. This approach has been applied to the study of double ionization of He in strong laser field [1]. In this paper we extend the moving-grid approach to the polyatomic molecules interacting with intense laser fields. As a demonstration, we apply the approach to explore ionization, dissociation, and Coulomb explosion of H_2 in intense laser fields.

The moving-grid approach characterizes a quantum system in phase space with coherent-state representation (CSR) wave functions [2] that depend on classical trajectories represented by coordinates and momenta. The basic equation of the moving-grid approach is an integro-differential equation which is derived from the time-dependent Schrödinger equation by expanding the wave function in coherent states and deliberating the evolution of trajectories (moving grids). The trajectories are determined by Hamiltonian canonical equation with quantum corrections.

The CSR wave functions are calculated by solving the basic integro-differential equation together with the Hamiltonian canonical equation for the moving grids. The initial CSR wave function and initial values of trajectories are estimated and optimized simultaneously by the solution of imaginary time-dependent Schrödinger equation with diffusion Monte Carlo method [3,4]. The spin symmetry of the initial CSR wave function is taken into account by using symmetrized and antisymmetrized coherent states [4].

To investigate the full dynamics of H_2 in intense laser fields, we consider both electron and nucleus motions. The electron motion is described by the CSR wave functions in the moving-grid approach while the nucleus motion is depicted by the classical dynamics. In CSR, the singularities of Coulombic potentials of electrons and nuclei are removed completely [1,4]. The CSR wave functions of electrons are computed under the consideration of the nuclear motion. The probabilities of ionization, dissociation, and Coulomb explosion of H_2 are then calculated for different laser intensities and frequencies with different numbers of trajectories. The results change with the number of trajectories. The scaling rules of Monte Carlo method are used to estimate the final results. Our results are in well qualitative agreement with available experimental and other theoretical results.

References

[1] D.V. Shalashilin, M.S. Child, and A. Kirrander, *Chem. Phys.* **347,** 257 (2008).
[2] D.V. Shalashilin and M.S. Child, *Chem. Phys.* **304,** 103 (2004).
[3] I. Kosztin, B. Faber, and K. Schulten, *Am. J. Phys.* **64,** 633 (1996).
[4] D.V. Shalashilin and M.S. Child, *J. Chem. Phys.* **122,** 224108 (2005); **122,** 224109 (2005).

[1] E-mail: zvzhou@ku.edu
[2] E-mail: sichu@ku.edu

Dynamic Stark effect and the Coulomb-Volkov approximation

V D Rodríguez[†1] **and M G Bustamante**[†2]

[†]Departamento de Física, FCEyN, Universidad de Buenos Aires, 1428 Buenos Aires, Argentina

Synopsis A modified Coulomb-Volkov theory is used to study the interaction of intense laser pulses with atomic Hydrogen. Photon energy greater than the ionization potential and non-perturbative conditions are considered. The dynamical Stark effect is accounted by introducing the initial state coupling to the remaining discrete and continuum atomic spectrum. Both the Stark shift and the decay of the initial state are studied. The ionization spectra, the Stark shift and the total ionization probability are compared with results obtained from numerical solution of the time dependent Schrödinger equation. Both results agree well.

The above threshold ionization of atomic Hydrogen by ultrashort laser pulses is studied. We consider the case in which the photon energy is greater than the ionization potential. Under perturbative conditions, the Coulomb-Volkov ($CV2^-$) theory provides a good description of the multiphoton ionization spectrum [1]. Continuum-continuum coupling is already included in the $CV2^-$ theory by using the Coulomb-Volkov wave function for the final state. However, non-perturbative conditions require introducing the coupling of the initial state with the discrete and continuous part of the atomic spectrum. Thus, the trial initial state wave function here proposed accounts for both the decay of the initial state and the Stark shift of its energy level. The ionization spectra, the initial state Stark shift and the total ionization probability are analyzed.

In the Schrödinger picture the transition amplitude from the initial state i at time $t = 0$ to the final state f at time $t = \tau$ may be approximated by the Demkov variational expression for the transition amplitude. The final state is represented by the Coulomb-Volkov wave function while the initial is approximated by

$$\chi_i^+(\overrightarrow{r}, t) = a_{1s}^{DC}(t)\varphi_{1s}(\overrightarrow{r}) \exp(-i\epsilon_{1s}t), \qquad (1)$$

where the amplitude of the state is obtained from the solution of the model's integro-differential equation. Figure 1 shows in a) the Stark shift of the first ATI peak of the spectrum and in b) the total probability of ionization, both as a function of the laser electric field intensity. It can be noticed that the present model (CV2-DC) is in good agreement with the results of the TDSE obtained using the Qprop code [3]. Results using reference [2] are shown as upper triangles. The model introduced in [2] has been improved in this work. First, the integro-differential equation arising from the coupling to the continuum is solved exactly. Second, the coupling to the discrete spectrum is accounted for. This is essential to the correct ATI peaks description. It is not necessary to suppress the ponderomotive potential to explain the ATI peaks position.

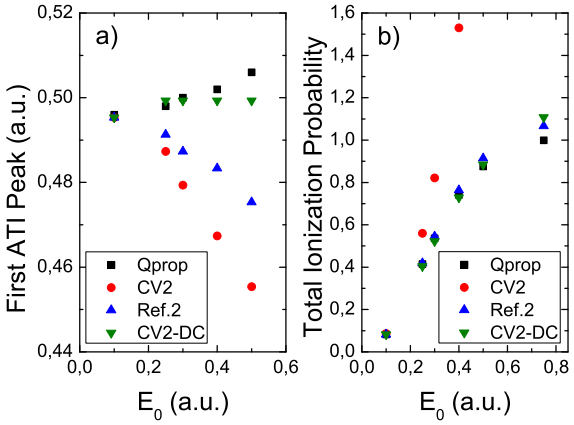

Fig. 1. a) First ATI peak energy position, and b) Total ionization probability as a function of the laser electric field amplitude. Laser pulse duration and frequency are 20 cycles and 1 a.u., respectively.

References

[1] V. D. Rodríguez, E. Cormier, and R. Gayet, *Phys. Rev.* A **69**, 053402 (2004).

[2] R. Gayet, *J. Phys. B: At. Mol. Opt. Phys.* **38**, 3905-3916 (2005).

[3] D. Bauer and P. Koval, *Comput. Phys. Comm.*, **174** 396-421 (2006)

[1]E-mail: vladimir@df.uba.ar
[2]E-mail: 6bustamante@gmail.com

Multiple orbital contribution in multiphoton ionization of H_2O in intense ultrafast laser fields

Sang-Kil Son[*] [1] **and Shih-I Chu**[*†] [2]

[*]Dept. of Chemistry, University of Kansas, Lawrence, KS 66045, USA

[†]Center for Quantum Science and Engineering, Dept. of Physics, National Taiwan University, Taipei, Taiwan

Synopsis We present all-electron time-dependent density-functional theory (TDDFT) investigation of multiphoton ionization (MPI) of H_2O in intense ultrafast linearly-polarzied laser pulses with arbitrary molecular orientation. A new time-dependnet Voronoi-cell finite difference method featuring highly adaptive molecular grids and an efficient time propagator is applied for accurate TDDFT solutions, taking into account the detailed electronic structure and responses in multiple orbital dynamics. Our results demonstrate that the inner orbital dominantly contributes to the overall orientation dependence of H_2O MPI.

The study of MPI of molecules in intense ultrafast laser fields is a subject of much current interest in strong-field molecular physics. Most theoretical studies of MPI today are based on approximate models that usually consider the highest occupied molecular orbital (HOMO) only and neglect multi-electron effects from multiple orbitals. Recently, it has been reported that significant discrepancy exists between experiments and approximate models for the orientation dependence of CO_2 MPI [1]. Furthermore, contribution of lower-lying orbitals below HOMO in high harmonic generation of N_2 has been observed [2]. Thus, it is a timely and important task to develop more detailed and accurate theoretical description of strong-field electronic dynamics.

We recently develop a new grid-based time-dependent Voronoi-cell finite difference method [3] to accurately solve TDDFT calculations for polyatomic molecules. In contrast to the ordinary finite difference method with regular uniform grids, the new method can achieve highly adaptive molecular grids with the help of geometrical flexibility of the Voronoi diagram, and can provide an efficient time-propagation method of the electronic density. With this new method, we first investigate strong-field electronic dynamics of polyatomic molecules including multi-electron effects such as electron correlation effects and multiple orbital contribution.

We present all-electron TDDFT study of the orientation dependence of H_2O MPI in intense ultrafast laser fields. Our results reveal that the orientation dependence is reflected by individual orbital symmetry. In particular, contribution from the inner orbital below HOMO (HOMO−1) becomes dominant in the overall pattern of the orientation dependence, when the orientation angle is varying in a specific direction with respect to H_2O [Fig. 1]. This interesting prediction emphasizes importance of multiple orbital contribution in molecular imaging and tomography.

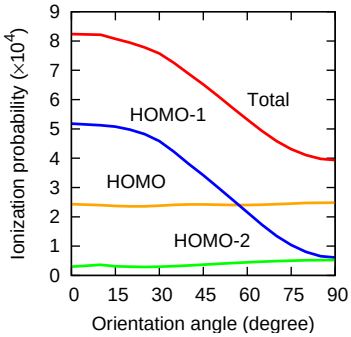

Fig. 1. Orientation dependence of individual ionization probabilities of H_2O with the peak intensity 5×10^{13} W/cm^2 and frequency 800 nm.

This work is partially supported by U.S. Department of Energy, U.S. National Science Foundation, National Science Council of Taiwan, and National Taiwan University.

References

[1] D. Pavičić, K. F. Lee, D. M. Rayner, P. B. Corkum, and D. M. Villeneuve, Phys. Rev. Lett. **98**, 243001 (2007).

[2] B. K. McFarland, J. P. Farrell, P. H. Bucksbaum, and M. Gühr, Science **322**, 1232 (2008).

[3] S.-K. Son and S. I. Chu, Chem. Phys. (submitted).

[1]E-mail: sangkil@ku.edu

[2]E-mail: sichu@ku.edu

The Magnus expansion for laser-matter interaction

Darko Dimitrovski[*,1], **Morten Foerre**[†], **Michael Klaiber**[‡], **Lars B. Madsen**[*] **and John S. Briggs**[‡]

[*]Lundbeck Foundation Theoretical Center for Quantum System Research, Department of Physics and Astronomy, Aarhus University, 8000 Aarhus C, Denmark

[†] Department of Physics and Technology, University of Bergen, 5007 Bergen, Norway

[‡]Theoretical Quantum Dynamics, University of Freiburg, Hermann-Herder Strasse 3 D-79104, Freiburg, Germany

Synopsis The interaction of an atom with a short, intense few-cycle pulse *including* nondipole effects is described by the Magnus expansion of the time-evolution operator. The time-evolution operator obtained in this approach is particularly simple involving position and momentum shifts of the laser field and the work done by the potential. The analytical Magnus expansion results agree excellently with numerical *ab initio* results.

The process of strong-field laser-matter interaction is highly nonlinear and, as such introduces theoretical and in particular computational challenges. However, at short wavelengths for atoms in their ground states or at ~ 800 nm for atoms in their low-lying Rydberg states the dynamics profoundly differs [1, 2]. In such cases, as we show here, a unitary approximation based on the Magnus expansion [3] of the time-evolution operator becomes appropriate.

In this contribution we

- give a recipe for the calculation of transition probabilities based on a systematic application of the Magnus expansion in powers of the pulse duration in dipole approximation and including nondipole effects,
- formulate the Magnus expansion for the calculation of *time-resolved* transition probabilities under the action of short laser pulses in dipole approximation, and
- set the limits of applicability and establish the connection of this approach to existing theoretical methods.

The main result is an analytic approximation to the time-evolution operator,

$$U(T,0) \approx U_0(T,T/2)e^{-iD(T)}e^{-iN(T)}U_0(T/2,0),$$

with T pulse duration, $U_0(t,t') = \exp(-iH_0(t-t'))$, $D(T)$ is operator summarizing dipole effects and $N(T)$ includes the nondipole effects. The operator $D(T)$ depends on the laser pulse type [1] and $N(t)$ amounts to shifting of the wavefunction in the propagation direction irrespective of the pulse type (see Fig. 1) [2].

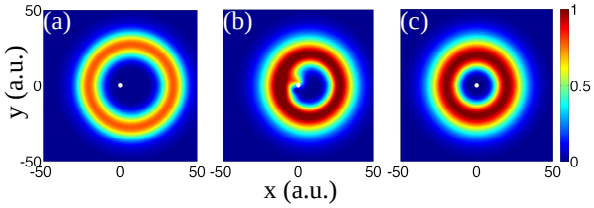

Fig. 1. Electron density in the $z = 0$ plane.; (a) obtained numerically; (b) obtained by backpropagating (a) in the field-free Hamiltonian for half pulse duration; (c) of the initial state $|n = 5, l = 4, m = 4\rangle$. The laser pulse at 400 nm propagates in x- and is polarized in z-direction (from [2]).

This analytic theory, easily extendable to a many-electron case, paves the way for controllable dipole- and nondipole-induced wavepacket shifting including ultrafast population transfer.

References

[1] M. Klaiber, D. Dimitrovski, and J. S. Briggs, Phys. Rev. A **79**, 043402 (2009).

[2] D. Dimitrovski, M. Førre, and L. B. Madsen (submitted).

[3] W. Magnus, Commun. Pure Appl. Math. **7**, 649 (1954).

[1]E-mail: darkod@phys.au.dk

Strong field double ionization of H_2 : The phase space perspective

F. Mauger[a,b 1] **C. Chandre**[b 2] **T. Uzer**[c 3]

[a] Ecole Centrale de Marseille, Technopôle de Château-Gombert,
38 rue Frédéric Joliot Curie F-13451 Marseille Cedex 20, France
[b] Centre de Physique Théorique, CNRS – Aix-Marseille Universités,
Campus de Luminy, case 907, F-13288 Marseille cedex 09, France
[c] School of Physics, Georgia Institute of Technology, Atlanta, GA 30332-0430, USA

Synopsis Composed of both sequential and nonsequential process, the double ionization probability of the H_2 molecule in strong laser pulses takes the form of a "knee" as a function of the intensity of the pulse. We identify the organizing structures that regulate the ionization process. Using finite-time Lyapunov maps, laminar plots, and periodic orbits, we derive reduced Hamiltonian models which help us inferring the classical mechanisms of sequential and nonsequential double ionization. Phase-space structures that regulate atomic double ionization are identified allowing verifiable predictions on the characteristic features of the "knee", a hallmark of the nonsequential process.

One of the most striking surprises of recent years in intense laser-matter interactions has come from multiple ionization by intense short laser pulses: Correlated (nonsequential) double ionization rates were found to be several orders of magnitude higher than the uncorrelated sequential mechanism allows. This discrepancy has made the characteristic "knee" shape in the double ionization yield versus intensity plot into one of the most dramatic manifestations of electron-electron correlation in nature. The precise mechanism that makes correlation so effective is far from settled. Different scenarios have been proposed to explain the mechanism behind ionization and have been confronted with experiments, the recollision scenario, in which the ionized electron is hurled back at the ion core by the laser, being in best accord with experiments.

The characteristic features of double ionization have been reproduced using classical trajectories and this success was ascribed to the paramount role of correlation. Indeed, entirely classical interactions turn out to be adequate to generate the strong two-electron correlation needed for double ionization.

We consider the double ionization of the molecule H_2 where the two nuclei are fixed. We complement [1] the well-known recollision scenario by identifying the organizing principles which explain the statistical properties of the classical trajectories such as ionization probabilities :

- Periodic orbits which organize the motion
- Identification of an inner and an outer electron
- Reduced Hamiltonians for each electron
- Finite time Lyapunov maps (see Fig. 1) and laminar plots
- Prediction of the maximum of nonsequential double ionization

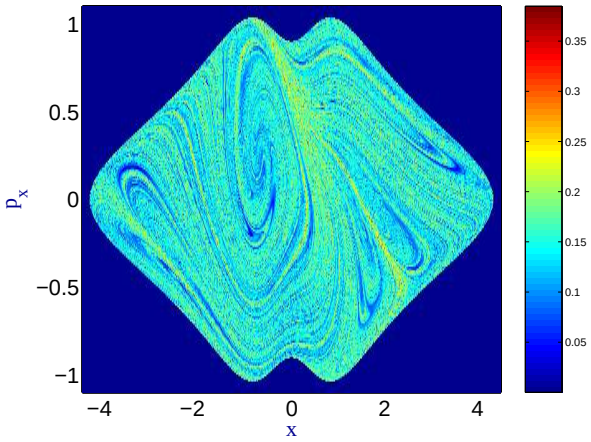

Fig. 2. Finite time Lyapunov map without the field at time $t = 50$ a.u. in the plane (x, p_x) with $y = 0$.

References

[1] F. Mauger, C. Chandre, and T. Uzer, Phys. Rev. Lett., to appear, 2009.

[1] E-mail: mauger@cpt.univ-mrs.fr
[2] E-mail: chandre@cpt.univ-mrs.fr
[3] E-mail: trugay.uzer@physics.gatech.edu

Unitary model for the ionization of atoms of hydrogen by an intense laser pulse

V D Rodríguez[†] [1] **and M G Bustamante**[†] [2]

[†]Departamento de Física, FCEyN, Universidad de Buenos Aires, 1428 Buenos Aires, Argentina

Synopsis A unitary model describing the electronic transitions in an atom subject to a laser pulse is proposed. The model include the initial state coupled with both the discrete and the continuum spectrum. Continuum-continuum transitions are neglected. The model lead to a single integro-differential equation for the initial state amplitude which is solved numerically. We compare our results with TDSE simulations for hydrogen atoms.

In recent years a variational method for describing laser-atom interactions has been proposed. The so called modified Coulomb-Volkov (MCV2$^-$) theoretical approximation is based on this two front approach to provide the ionization amplitudes for atomic multiphoton ionization [1]. For the final state, the Coulumb-Volkov wave function is used. This wave function accounts for continuum-continuum coupling. For the initial state, previous options were either the simple unperturbed wave function or some expansions in terms of intermediate transient states [1]. For non-perturbative situations, the initial state decay should be considered. In this work we introduced a model accounting for full initial state coupling to the continuum while neglecting further continuum-continuum transitions. The model also consider transitions between initial state and other discrete states. Other discrete-discrete or discrete-continuum transitions are neglected. The present model leads to a single integro-differential equation for the initial state amplitude. This equation is easily solved (see [2]). We have analytically demonstrated that the sum of all transition probabilities is unity, *i.e.*, the model is unitary. As a test for the model goodness we show in Figure 1 transition probabilities of Hydrogen under a 20 cycles XUV laser pulse (ω=1 a.u.). Two laser intensities are examined, E_0=0.2 a.u. (1.4×10^{14} W/cm^2) and E_0=0.4 a.u. (5.6×10^{14} W/cm^2). The model results for surviving probability as function of time is compared with full time dependent Schrdinger equation simulation performed with the Qprop code [3]. The comparison is rather good and it is meaningful for times t_i when the vector potential $\vec{A}(t_i)$ is null. For the larger intensity we observe a slight departure between both results. We have been able to obtain a time-dependent ionization probability estimation from the mean energy provided by the Qprop code [3]. This ionization probability is also in good agreement with our model results, specially for the lower intensity here analyzed. In the same figure the sum of transition probabilities to the excited states is displayed. These probabilities while small are important to fulfill the unitary property.

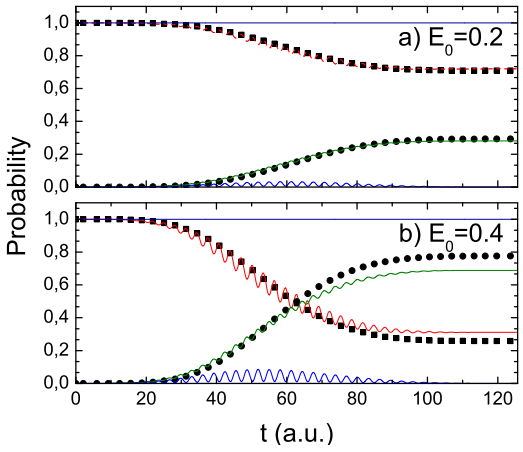

Fig. 1. Transition probabilities as a function of time. Symbols, Qprop: squares, survival probability; circles, ionization probability. Curves, model results. Lower curves, total excitation probability to bound states.

References

[1] V D Rodríguez, E Cormier y R Gayet 2004 *Phys. Rev.* A **69** 053402.

[2] A. Goldfine, *Mathematics of Computation*, Vol. 31, No. 139, 691-707 (1977).

[3] D. Bauer and P. Koval, *Comput. Phys. Comm.*, **174** 396-421 (2006).

[1]E-mail: vladimir@df.uba.ar
[2]E-mail: 6bustamante@gmail.com

Tomographic reconstruction of the 3-D momentum distribution in velocity map imaging experiments

C Smeenk[*,1], **L Arissian**[*,†], **A Staudte**[*], **D M Villeneuve**[*] **and P B Corkum**[*]

[*] Joint Laboratory for Attosecond Science, University of Ottawa and National Research Council, 100 Sussex Drive, Ottawa, Canada

[†] Department of Physics, Texas A & M University, College Station, USA

Synopsis We apply tomography, a general method for reconstructing 3-D distributions from multiple projections, to reconstruct the momentum distribution of electrons produced by photoionization. The projections are obtained by rotating the electron distribution via the polarization of the ionizing laser beam and recording a momentum spectrum at each angle with a 2-D velocity map imaging spectrometer. For linearly polarized light the tomographic reconstruction agrees with the distribution obtained using an Abel inversion. Electron tomography, which can be applied to any polarization, will simplify the technology of electron imaging. Our method can be directly generalized to other charged particles.

In velocity map imaging experiments, an inhomogeneous electric field is used to to project the velocity vector of charged particles into the 2-D plane of a detector. Since one component of the velocity vector is integrated over by the spectrometer's DC electric field, this component is not observable unless additional information is provided such as (a) symmetry assumptions, or (b) measurements from multiple directions. The former is a condition for Abel inversion [1] and allows the inversion of a single projection. The latter is a requirement for tomographic inversion [2] and is a more general approach.

We present results of a general method to measure the complete three-dimensional momentum distribution of charged particles in a velocity map imaging spectrometer. The method requires no knowledge of the symmetry of the distribution. It can be applied to any laser polarization. This means that 3-D momentum distributions can be obtained for any photoionization or photofragment experiment involving charged particles. As in all tomographic methods, multiple projections of the 3-D distribution are required. The projections are obtained by placing a half wave plate in the ionizing laser beam and recording spectra for each angle of the wave plate. Using multiphoton ionization of argon as an example, we confirm that the retrieved image agrees with those obtained with an Abel inversion for the case where an Abel inversion is possible. We present 3-D distributions of the electron momentum distribution created in linearly and elliptically ($E_1/E_2 = 0.89$) polarized light.

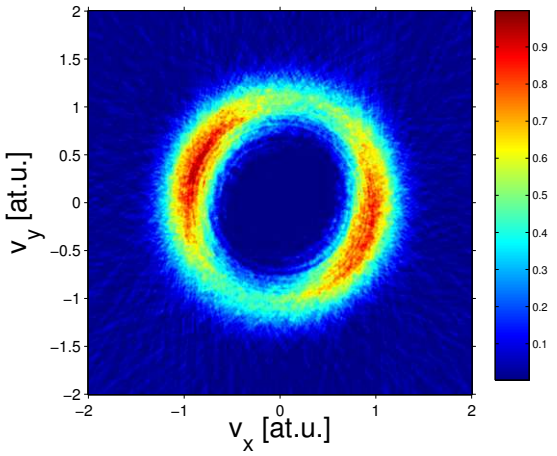

Fig. 1. Reconstructed electron velocity distribution in the plane of laser polarization. The color code represents the probability to measure an electron at a particular momentum.

References

[1] Dribinski, V, Ossadtchi, A, Mandelshtam, V and Reisler, H, Rev. Sci. Instr., **73**, 7, 2634-2642 (2002)

[2] Kak, A and Slaney, M, *Principles of Computerized Tomographic Imaging*, IEEE Press, 1988

[1] E-mail: christopher.smeenk@nrc.ca

Strong-field electron spectra of rare gas atoms in the rescattering region: channel closing and a simulation of the experiment

D. B. Milošević[‡,§] [1], W. Becker[§], M. Okunishi[*], G. Prümper[*], K. Shimada[*], and K. Ueda[*]

[‡]Faculty of Science, Zmaja od Bosne 35, University of Sarajevo, 71000 Sarajevo, Bosnia and Herzegovina
[§]Max-Born-Institut, Max-Born-Strasse 2a, 12489 Berlin, Germany
[*]Institute of Multidisciplinary Research for Advanced Materials, Tohoku University, Sendai 980-8577, Japan

Synopsis We report experimental photoelectron spectra of Ne, Ar, Kr, and Xe in intense laser fields. These results are simulated using the low-frequency approximation for high-order above-threshold ionization. Resonant-like structures, observed both in the experiment and simulation, are analyzed.

In recent years femtosecond infrared lasers with peak intensity in the TW to PW cm^{-2} range have become widely available. When such intense laser pulses are irradiated on atoms, interesting nonlinear phenomena such as high-order above-threshold-ionization (HATI) occur. It had been shown that HATI is due to the elastic scattering of the returning electrons into the backward directions by the target ion. Theoretical considerations for longer pulses have shown that resonantlike enhancements should appear for higher energy electrons. They have been interpreted in terms of channel closings and it has been shown that these enhancements result from constructive interference of a large number of long orbits of the returning electron [1].

The resonantlike enhancement has been observed [2], but a detailed comparison between the theory and experiment is still missing. We report here experimental HATI spectra of rare gas atoms (Ne, Ar, Kr, and Xe) recorded at 800 nm, with pulse width of 100 fs and laser power densities in the region $0.5 - 3.2 \times 10^{14}$ W/cm^2. These results are simulated using recently introduced low-frequency approximation for HATI [3], modified to include the laser dressing of the bound state. An example of this simulation is shown in Fig. 1. The spectra for energies below $4U_p$ in simulation are denoted by dashed line since in this region the spectrum is dominated by the direct electrons while our simulation includes only the rescattered electrons.

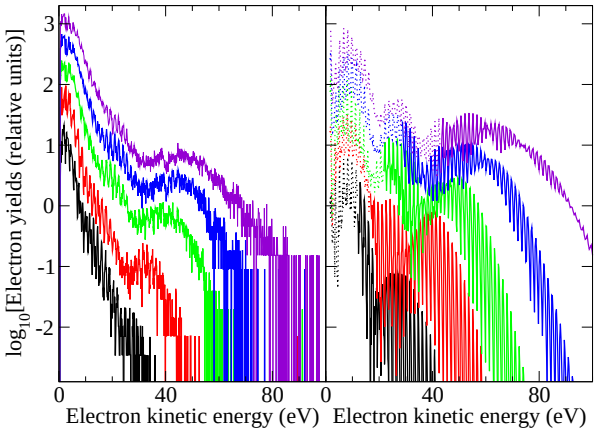

Fig. 1. Electron energy spectra in direction of the polarization axis of linearly polarized 800 nm laser pulse at several laser intensities $I \times 10^{14}$ W/cm^2, where: $I = 0.5$ (bottom, black curve), 0.7 (red), 0.9 (green), 1.2 (blue), and 1.8 (top, violet). Left panel: experiment. Right panel: simulation.

References

[1] D. B. Milošević, E. Hasović, M. Busuladžić, A. Gazibegović-Busuladžić, and W. Becker, Phys. Rev. A **76**, 053410 (2007).

[2] M. P. Hertlein, P. H. Bucksbaum, and H. G. Muller, J. Phys. B **30**, L197 (1997).

[3] A. Čerkić, E. Hasović, D. B. Milošević, and W. Becker, Phys. Rev. A **79**, 033413 (2009).

[1] E-mail: milo@bih.net.ba

Attosecond soft X-ray pulses : From XUV attosecond pulse control by aperiodic multilayer optics to localized surface plasmon field dynamics

Michael Hofstetter[1], Casey Chew[1], Jingquan Lin[1], Nils Weber[2], Matthias Escher[2], Michael Merkel[2], Ulf Kleineberg[1]

[1]Ludwig-Maximilians University Munich, Faculty of Physics, D- 85748 Garching, Germany
[2]Focus GmbH ,D-65510 Hünstetten-Kesselbach, Germany

Synopsis XUV multilayer mirrors serve as powerful reflective optics to control the spectrum and phase of attoseocnd HHG pulses which is an important requirement for measuring time-resolved photoelectron emission dynamics from solid surfaces and nanostructures. Based on a time-of-flight photoelectron emission microscope, a new experiment for spatial and temporal characterization of photoelectron dynamics and localized surface plasmon fields is presented.

Attosecond soft X-ray pulses from High Harmonic Generation filtered by bandwidth and phase optimized multilayer soft X-ray mirrors serve as a powerful light source for XUV pulses with pulse duration less than 100 attoseconds [1]. Besides the HHG generation process, subsequent spectral filters and optics play an important role for the spectral and temporal properties of the XUV pulses in the experiment. Multilayer mirrors are powerful optical elements to control the spectrum and the phase of the reflected pulses resulting in compressed XUV pulses of minimum time duration or chirped XUV pulses of controlled dispersion. We report on our XUV multilayer optics development spanning the photon energy range from the Extreme Ultraviolet (~ 100 eV) to the "water window "soft X-ray range (280-500 eV), which is particularly important for studying in-vitro samples.

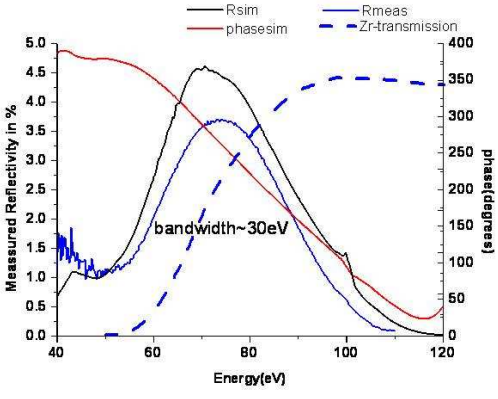

Figure 1. Reflectivity and phase of an attosecond multilayer mirror at 60-90 eV photon energy [1]

In nanoscience, one of important topics is the study and utilization of phenomena that are localized on the nanoscale and ultrafast. The localization length of surface plasmons can be on the order of several nanometers. The relaxation time of surface plasmons is in the 10-100 fs range, allowing coherent control of nanoscale localization with femtosecond laser light. Importantly, collective motion in plasmonic nanosystems unfolds on much shorter, attosecond time scales. Here we propose a principally new approach that will allow one to *directly* measure the spatiotemporal dynamics of the nanolocalized optical fields with ~100 as temporal resolution and nanometer spatial resolution [2]. Measurement of nanolocalized optical fields is interesting from both the fundamental positions and in view of the multiple applications of nanoplasmonics.
First steps towards the experimental realization of an *attosecond nanoplasmonic field microscope*, based on a ToF PEEM with 2PPE excitation or as XUV excitation, are reported [3].

References

[1] E. Goulielmakis, M. Schultze, M. Hofstetter, V.S. Yakovlev, J. Gagnon, M. Uiberacker, A.L. Aquila, E.M. Gullikson, D.T. Attwood, R. Kienberger, F. Krausz, U.Kleineberg. "Single-cycle nonlinear optics", Science **320**, 1614 (2008)

[2] M.I. Stockman, M.F. Kling, U. Kleineberg, F. Krausz; "Attosecond nanoplasmonic field microscope", Nature Photonics **1**, 539 (2007)

[3] Jingquan Lin, N Weber, A Wirth, S Chew, M Escher, M Merkel, Matthias F Kling, Mark I Stockman, Ferenc Krausz and Ulf Kleineberg "TOF-PEEM for ultrahigh spatiotemporal probing of nanoplasmonic optical fields", J. Phys. Cond. Matter (in press, published online May 2009]

Corresponding author : ulf.kleineberg@physik.uni-muenchen.de

White light generation under laser driven avalanche breakdown of air

*Updesh Verma and A. K. Sharma
Center for Energy Studies, Indian Institute of Technology Delhi,
New Delhi-110016, India

Abstract

A theoretical model of avalanche breakdown of air by a Gaussian laser beam and white light generation is developed. An intense laser beam, below the threshold for tunnel ionization heats the seed electrons to high energy that causes avalanche ionization of the air. However, the plasma density has a maximum on axis and falls off with radial coordinates. Such a density profile causes refraction divergence of the beam. However, temporal evolution of plasma density causes self phase modulation of the laser pulse causing frequency broadening of the pulse. The hot plasma thus produced causes strong spectral emission in the visible.

*updeshv@gmail.com, updesh.verma@mail2.iitd.ac.in

Tunable THz Generation by Short Laser Pulses

Anil K Malik and Hitendra K Malik
Department of Physics, Indian Institute of Technology Delhi, New Delhi – 110 016, INDIA

A theoretical and simulation study has been done for THz generation by direct conversion of an ultra short laser pulse into terahertz radiations. In our mechanism we use two very short laser pulses (one is circularly polarized and other is linearly polarized with same frequency while different amplitude and phases) focused on a gas which tunnel ionizes the gas. The conversion is due to ionization induced excitation in presence of static magnetic field and subsequent transverse transient current because of the presence of residual momentum after passing the laser pulse. Due to this oscillatory current THz radiation is emitted. The directionality of the emitted THz radiation is observed to be controlled by the phase difference of incident fs laser pulses. This mechanism is observed to be very efficient and is able to provide THz radiation with high power level of the order of GW.

Collinear generation of few-cycle UV and XUV laser pulses for probing and controlling ultrafast electron dynamics at solid interfaces

Agustin Schiffrin*[,1], Elisabeth Bothschafter[*], Ulrich Graf[*], Eleftherios Goulielmakis[*], Ralph Ernstorfer[*,†], Reinhard Kienberger[*,†] and Ferenc Krausz[*,§]

[*] Max-Planck-Institut für Quantenoptik, Hans-Kopfermann-Strasse 1, D-85748 Garching, Germany
[†] Physik-Department, Technische Universität München, D-85748 Garching, Germany
[§] Department für Physik, Ludwig-Maximilians-Universität, Am Coulombwall 1, D-85748 Garching, Germany

Synopsis: Here we discuss the implementation of the simultaneous collinear production of few-cycle UV and XUV laser pulses by high-harmonic generation of a few-cycle NIR laser pulse in two subsequent noble gas targets. Combining any of the few-cycle XUV, UV and NIR pulses will allow probing and controlling ultrafast electron dynamics in metal and semiconducting interfaces.

The generation of isolated attosecond XUV pulses by means of high-harmonic generation in noble gases with few-cycle NIR laser fields has been established in recent years[1]. Lately, the generation of few-cycle low-order harmonics has been demonstrated: sub-4 fs UV pulses were produced by third and fifth harmonic generation of few-cycle near-infrared (NIR) laser pulses in a noble gas target[2]. Here, we discuss the possibility to implement in an experimental setup the simultaneous generation of low-order harmonics and high-harmonic by two subsequent gas targets in a collinear geometry. Such achievement will enable attosecond pump-probe spectroscopy with any combination of XUV, UV, VIS and NIR few-cycle pulses. Future experiments employing this experimental configuration with such unique laser pulses include probing ultrafast intraband electron dynamics in semiconductors, time-resolving ultrafast electron transfer in organic/condensed matter interfaces, and controlling electronic motion in metal and semiconductor nanostructures with coherent optical fields (see Fig. 1).

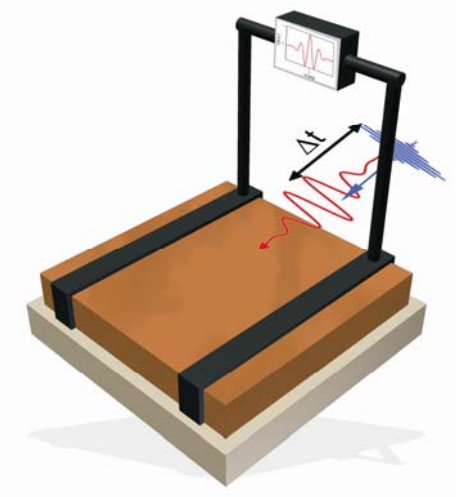

Fig. 1. Schematic of a nanostructured metal-semiconductor interface for the control of photoinduced currents with few-cycle UV and NIR laser pulses.

References

[1] E. Goulielmakis, M. Schultze, M. Hofstetter, et al., Science **320**, 1614 (2008).
[2] U. Graf, M. Fiess, M. Schultze, et al., Optics Express **16**, 18956 (2008).

[1] E-mail: Agustin.Schiffrin@mpq.mpg.de

Photoelectron Angular Distributions at the Ionization of Atoms by Intense Sub-one-cycle Laser Pulses

V.S. Rastunkov[1], **V.P. Krainov**

Moscow Institute of Physics and Technology, 141700 Dolgoprudny, Moscow Region, Russia

Synopsis: The phase sensitivity of the photoelectron angular distributions by intense sub-one-cycle linearly polarized laser pulses has been investigated within the analytic Landau–Dykhne approximation. In both cases of sine and cosine laser pulses most of the electrons are ejected along the polarization axis of the laser field. Nevertheless the electron yield and the electron kinetic energies are much larger for the cosine waveform pulse.

The phase sensitivity of the photoelectron angular distributions by intense sub-one-cycle linearly polarized laser pulses is discussed within the analytic Landau-Dykhne approximation. In the case of many-cycle pulses, for this approximation to be valid it is required that the photon energy $\hbar\omega$ of the laser radiation be small compared to the atomic ionization potential E_i. For sub-one-cycle laser pulses the generalized Keldysh parameter $\gamma = \sqrt{2E_i}\,/F\tau$ depending on the duration of the laser pulse was introduced. The non-relativistic ionization rate is of the form

$$w \sim \exp\left\{-\left(2/\hbar\right)\mathrm{Im}\int_0^{t_0}\left[E\left(t\right)+E_i\right]dt\right\}$$

(with the exponential accuracy).

With the Landau-Dykhne approach, we obtained analytic expressions for the energy spectra.

In the case of sine and cosine waveform laser pulses most of electrons are ejected along the polarization axis of the laser field. But the electron yield and electron kinetic energies are much larger for cosine waveform pulse. We conclude that the carrier-envelope-phase difference is one of the essential control parameters in few-cycle pulses applications and attosecond science.

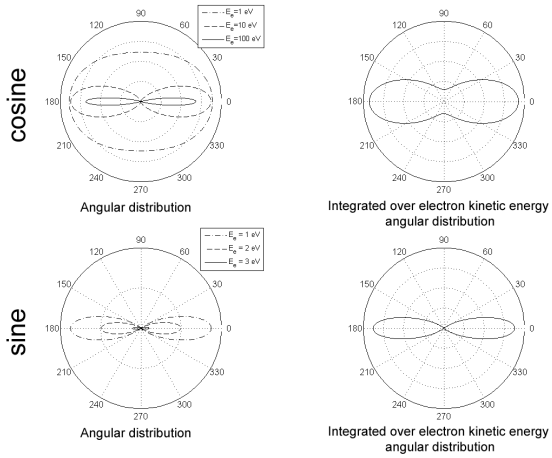

Fig. 1. Some results of numerical calculation.

References

[1] V.S. Rastunkov and V.P. Krainov, *J. Phys. B*: At. Mol. Opt. Phys. **40** (2007) 2277–2290.
[2] V.S. Rastunkov and V.P. Krainov, Proc. of SPIE Vol. 6726, 672649 (2007).
[3] V.S. Rastunkov and V.P. Krainov, *Laser Physics*, **19**, 4 (2009), 813–816.

[1] E-mail: rastunkovvs@mail.ru